2nd Annual Science Day
Faculty of Science-Sohag University

April 19, 2017

Abstract Book for Papers Published by Staff Members of Faculty of Science during 2016

PREFACE

This abstract book is compiled of more than 230 papers published in estimated INTERNATIIONAL journals by Staff members of Faculty of Science, Sohag University during 2016. The book was made on the sidelines of the 2nd Annual Science Day ceremony held on Tuesday, April 19, 2017 at Sohag Faculty of Science under the patronage of Dr. Ayman Abdel-Moneim-the Governor of Sohag, Prof. Dr. Safa Mahmoud Elssayed, President of Sohag University, and Prof. Dr. Ahmed Mohamed Soliman-Dean of Faculty of Science.

Besides emerging the scientific research activities of staff members, the Abstract book as a whole is an important reference of the recent advances in research. Furthermore, the Annual Science Day meeting offers an opportunity for researchers from different departments who work on similar research problems but rarely cross paths, to connect with each other. Science Day event is also a great opportunity to share the value of our research with different sectors of community services.

Congratulations to all who participated, and thanks to everyone made this event such a huge success.

Dean of Faculty of Science
Prof. Dr. Ahmed M. Soliman

Organizing Committee

Prof. Dr. Ahmed M. Soliman	Dean of Faculty of Science
Prof. Dr. Ahmed M. Ahmed Ali	Vice-Dean for Graduate Students & Research Affairs
Prof. Dr. Zakaria A. Mohamed	Botany & Microbiology Department (Chairman)
Prof. Dr. Hazem Elmeshneb	Physics Department
Dr. Alaa Y. Fahmey	Zoology Department
Dr. Mohamed Ismael	Chemistry Department
Dr. Mostafa G. Redwan	Geology Department
Dr. Omar Elhady	Chemistry Department
Dr. Hamdy A. Soliman	Zoology Department
Dr. Naglaa Yousef	Botany & Microbiology Department
Dr. Mahmoud Abdel Aleem Ali	Chemistry Department
Dr. Gamal Ismail	Mathematics & Computer Science Department
Dr. Ahmed M. Abu-Dief	Chemistry Department
Dr. Mohamed Fathy	Physics Department
Dr. Mohamed H. El-Khashab	Geology Department
Dr. Hamdy Hassan	Mathematics & Computer Science Department
Dr. Alaa Elmeshneb	Physics Department
Dr. Mahmoud S. Bakheit	Botany & Microbiology Department

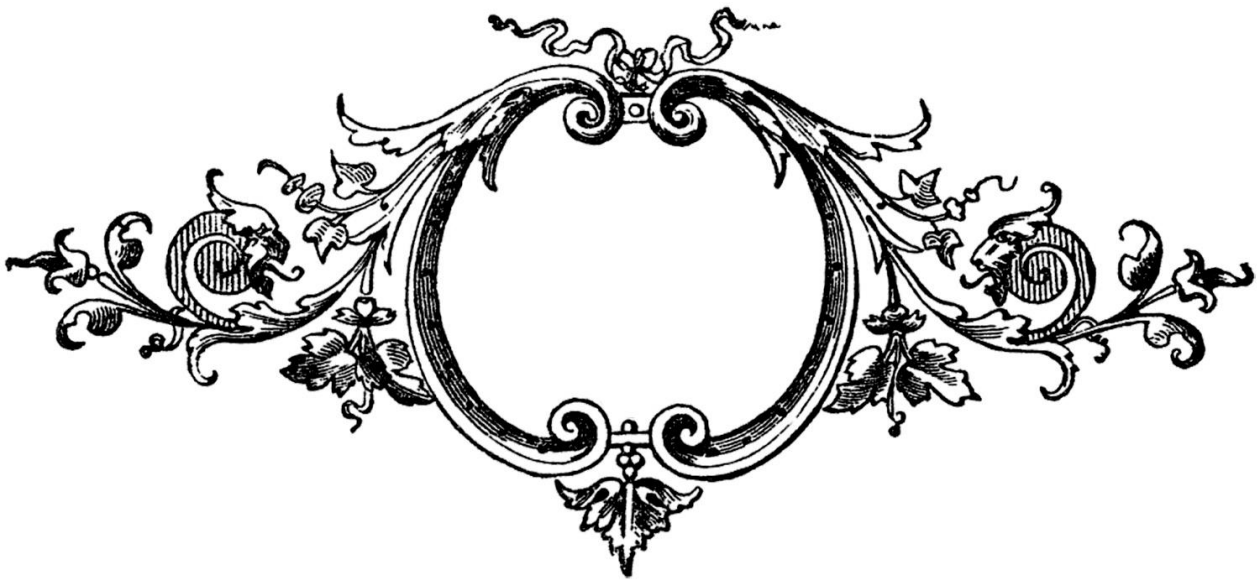

List of Publications

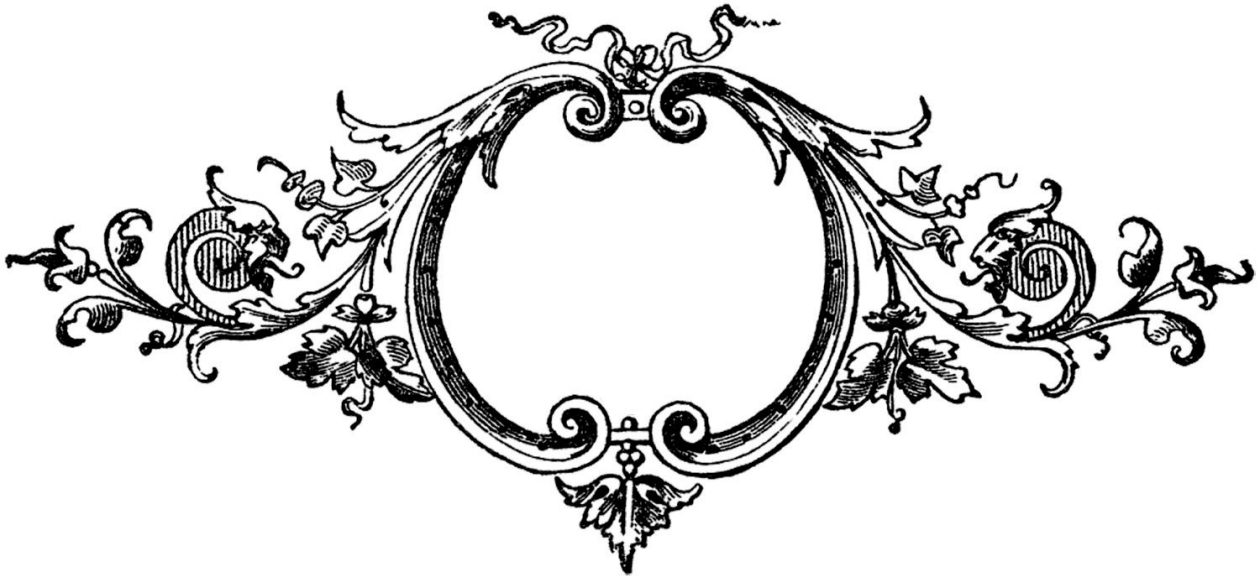

List of papers published by Staff members of Mathematics & Computer Science Department

1	**Shortest Paths Routing Problem In Manets** *Hamdy H. El Sayed*
2	**Performance Analysis of Medical Image Compression Using Various Wavelet Techniques** *Torki Altameem, Osama Alfarraj, E. A. Zanaty, Amr Tolba, Sherif M. Ibrahim*
3	**Surface-Surface Tissue Reconstruction and Visualization for the Magnetic Resonance Imaging or Tomography Imaging Engineering Design** *E. A. Zanaty, Walla M. Abdelhafiz*
4	**A Performance Study of Classical Techniques for Medical Image Segmentation** *Ahmed S. Ghiduk, E. A. Zanaty*
5	**Modified Fuzzy C-Means for Segmenting Magnetic Resonance Images (MRIs)** *Ahmed S. Ghiduk, E. A. Zanaty*
6	**Image Encryption using Chaos-Driven Elliptic Curve Pseudo-Random Number Generators** *Omar Reyad, Zbigniew Kotulski , W. M. Abd-Elhafiez*
7	**A Hybrid Cascade Approach for Human Skin Segmentation** *Samy Bakheet, Ayoub Al-Hamadi*
8	**A Discriminative Framework for Action Recognition Using f-HOL Features** *Samy Bakheet, Ayoub Al-Hamadi*
9	**New Efficient Method for Coding Color Images** *Walaa M. Abd-Elhafiez, Essam O. Abdel-Rahman*
10	**Pseudo-random Sequence Generation from Elliptic Curves over a Finite Field of Characteristic 2** *Omar Reyad, Zbigniew Kotulski*
11	**Face Identification System in Video** *Mohamed Heshmet, Walaa M. Abd-Elhafiez, Moheb Girgis, Seham Elaw*
12	**Estimation for the exponentiated Weibull model with adaptive Type-II progressive censored schemes** *Mashail M. AL Sobhi, Ahmed A. Soliman*
13	**Cells distribution in the modeling of fibrosis, Comment on "Towards a unified approach in the modeling of fibrosis: A review with research perspectives" by Martine Ben Amar and Carlo Bianca** *Mahmoud Abdel-Aty*
14	**New Perspectives on Nonlinear Multi-Atoms Interacting with a Cavity Field** *Y. S. El-Saman, S. Abdel-Khalek, A. Badawi, M. Abdel-Aty*
15	**Theorems on q-Frobenius-Euler polynomials under Sym (4)** *Serkan Araci, Ugur Duran, Mehmet Acikgoz, Mahmoud Abdel-Aty*
16	**Nonclassical properties and purity of a qubit system in photon-added squeezed thermal states with time-dependent coupling effect** *K. Berrada, S. Abdel-Khalek*
17	**New features of the stationary and moving atom-atom entanglement** *S. Abdel-Khalek, S.H.A. Halawani*
18	**Erratum to „„Effect of the time-dependent coupling on a superconducting qubit-field system under decoherence: Entanglement and Wehrl entropy""** *S. Abdel-Khalek, K. Berrada, H. Eleuch*
19	**Entanglement and Statistical Properties of a System Consisting of Three-Level Atom Interacting with a Nonlinear Kerr Medium Field** *S. Abdel- Khalek, M.A. Al-Rajhi, K. Berrada*
20	**Numerical Study of Some Statistical Quantities for Quantum Systems under Damping Effects** *K. J. M. Abu Alnaj, S. E. Waheed, S. Abdel-Khalek*
21	**Information dynamics for a non-degenerate two-photon JC model in phase damping cavity** *K. Berrada, S. Abdel-Khalek*

22	**Dynamics of Correlations in the Presences of Intrinsic Decoherence** *Nour Zidan*
23	**On Fuzzy Soft Irresolute Functions** *S. E. Abbas, E. El-sanowsy, A. Atef*
24	**(r,s)-(τ_{12},τ_{12}^{*})-θ-Generalized double fuzzy closed Sets in bitopological spaces** *E. ElSanousy*
25	**Spacelike and timelike admissible Smarandache curves in pseudo-Galilean space** *M. Khalifa Saad*
26	**Decomposition of bilinear forms as sums of bounded forms** *Mohamed Elmursi*
27	**An Analytical Technique for Solving Nonlinear Oscillators of the Motion of a Rigid Rod Rocking Bock and Tapered Beams** *G. M. Ismail*
28	**Analytical solution of strongly nonlinear Duffing oscillators** *A. M. El-Nagger, G. M. Ismail*
29	**Periodic Solutions of the Duffing Harmonic Oscillator by He's Energy Balance Method** *A. M. El-Nagger, G. M. Ismail*
30	**Random fixed point theorems with an application to a random nonlinear integral equation** *R. A. Rashwan, H. A. Hammad*
31	**Random Common Fixed Point Theorem for Random Weakly Subsequentially Conti nuous Generalized Contractions with Application** Rashwan. A. Rashwan, Hammad. A. Hammad
32	**Rotational effect on Rayleigh, Love and Stoneley waves in non-homogeneous fibre-reinforced anisotropic general viscoelastic media of higher order** *S.M. Abo-Dahab, A.M. Abd-Alla, Aftab Khan*
33	**Effect of the Rotation on a Non-Homogeneous Infinite Elastic Cylinder of Orthotropic Material with Magnetic Field** *A.M. Abd-Alla, S.M. Abo-Dahab, Hind A. Alotaibi*
34	**Green Lindsay model on reflection and refraction of p- and SV-waves at interface between solid-liquid media presence in magnetic field and initial stress** *S.M. Abo-Dahab, A.M. Abd-Alla*
35	**SV-waves incidence at interface between solid-liquid media under magnetic field, initial stress and two thermal relaxation times** *S.M. Abo-Dahab, A.M. Abd-Alla, M Marin*
36	**Rotation effect on peristaltic transport of a Jeffrey fluid in an asymmetric channel with gravity field** *A.M. Abd-Alla, S.M. Abo-Dahab*
37	**SV-waves incidence at interface between solid-liquid media under Electromagnetic field and initial stress in the context of three thermoelastic theories** *A. M. Abd-Alla, S. M. Abo-Dahab, A. A. Kilany*
38	**Reflection of Plane Waves from Electro-magneto-thermoelastic Half-space with a Dual-Phase-Lag Model** *A. M. Abd-Alla, Mohamed I. A. Othman, S. M. Abo-Dahab*
39	**Bayesian Estimation of Exponentiated Weibull Distribution Under Partially Acceleration Life Tests** *Mashail M. AL Sobhi, Ahmed A. Soliman, Abd EL-Baset A. Ahmad, Ahmed A. Soliman, Manal M. Yousef*
40	**Bayesian estimation of P[Y < X] Based on Record V alues from the Lomax Distribution and MCMC Technique** *M. A. W Mahmoud, R. M. El-Sagheer, A. A . Soliman, A. H. Abd Ellah*

List of papers published by Staff members of Physics Department

1	**Properties of TiAlN coating deposited by MPIIID on TiN substrates** *F. M. El-Hossary, A. M. Abd El-Rahman, M. Raaif, D. A. Ghareeb*
2	**Counting of the Fusion Neutron Yield from the Pulse Height of Time-Of-Flight Spectrometer involves Ultrafast Timing/Counting Plastic Scintillator** *A. Youssef*
3	**Counting of ultraintense laser-driven neutrons from the pulse height of time-of-flight detector includes ultrafast timing plastic scintillator** *A. Youssef*
4	**Achievement of laser fusion with high energy efficiency using a mixture of D and T ions** *A. Youssef, M. Haparir*
5	**Synthesis, characterization and low field magnetotransport of $Nd_{0.6}Sr_{0.4}MnO_3/CrO_3$ composite** *A. M. Ahmed, H. F. Mohamed, A. K. Diab, Sara A. Mohamed*
6	**Annealing temperature effect on magnetic and magnetocaloric properties of manganites** *Abd El-Moez A. Mohamed, V. Vega, M. Ipatov, A. M. Ahmed, B. Hernando*
7	**The annealing influence onto the electrical and magnetic behavior of magnetoresistive/insulator system** *A. M. Ahmed, Abd El-Mo'ez A. Mohamed, H. F. Mohamed, A. K. Diab, Aml M. Mohamed, A. E. A. Mazen*
8	**Magnetocaloric-transport properties correlation in doped manganites** *Abd El-Moez A. Mohamed, B. Hernando, A. M. Ahmed*
9	**Magnetoresistive properties of Ni-doped $La_{0.7}Sr_{0.3}MnO_3$ Manganites** *Ahmed Mohamed Ahmed, Abd El-Moez Ahmed Mohamed, Medhat Abdelrady Abdellateef, Hassan Ahmed Abd El-Ghanny*
10	**Tuning magnetoresistive and magnetocaloric properties via grain boundaries engineering in granular manganites** *Abd El-Moez A. Mohamed, Mohamed A. Mohamed, V. Vega, B. Hernando, A. M. Ahmed*
11	**Influence of heat treatment on the magnetic and magnetocaloric properties in $Nd_{0.6}Sr_{0.4}MnO_3$ compound** *A. M. Ahmed, H. F. Mohamed, A. K. Diab, Sara A. Mohamed, S. García-Granda, D. Martínez-Blanco*
12	**Magnetoresistive and magnetocaloric response of manganite/insulator system** *Abd El-Moez A. Mohamed, V. Vega, M. Ipatov, A. M. Ahmed, B. Hernando*
13	**Effect of Annealing Temperature on Electrical and Magnetic Properties of $(Nd_{0.6}Sr_{0.4}MnO_3)_{1-x}/(CrO_3)_x$** *A. M. Ahmed, A. K. Diab, H. F. Mohamed, Sara A. Mohamed*
14	**Improvement of Corrosion resistance of NiTiorthopedic materials by inductively radio frequency plasma** *F. M. El-Hossary, S. M. KHALIL, M. A. Kassem, M. Abd EL Lateef, Kh. Lotfy*
15	**Effect of Fe doping on the electrical and magnetic properties of $Sn_{1-x}Fe_xO_2$ nanoparticles** *Saleh A. Saleh, Ahmed M. Abdel Hakeem, Eslam M.M. Ibrahim*
16	**The Effect of Radio Frequency Plasma Nitriding on Biocompatibility of Nickel-Titanium Shape Memory Alloy** *F. M. El-Hossary, S. M. KHALIL, M. A. Kassem, M. Abd EL Lateef, Doha. S. Mohamed, Kh. Lotfy*
17	**Photoproduction of π_0-Mesons from the Nucleon and Deuteron** *Eed M. Darwish, A. Hemmdan, N.T. El-Shamy*
18	**Influence of the Choice of NN Potential Model on $\gamma d \rightarrow \pi_0 d$ Observables near η-Threshold** *Eed M. Darwish*
19	**Thin film CdS/CdTe and CdS/PbS photovoltaic solar cells** *H. A. Mohamed*
20	**Influence of sodium doping on the electrical and magnetic properties of $La_{0.90}Li_{0.10}MnO_3$ manganites** *H. F. Mohamed*
21	**Asymmetric Nuclear Matter and Neutron Star Properties within Extended Brueckner Theory** *Khaled S. A. Hassaneen*
22	**The Thermal Properties of Asymmetric Nuclear Matter within the Extended Brueckner-Hartree- Fock Approach** *Khaled S. A. Hassaneen*

23	**Theoretical study of the $SrLi^+$ molecular ion:structural, electronic and dipolar properties** *Soulef Jellali, Héla Habli, Leila Mejrissi, Mahmoud Mohery, Brahim Oujia, Florent Xavier Gadéa*
24	**Structural and optical characterization of Sb-doped ZnO co-sputtered thin films** *M. M. Abd El-Raheem, S. A. Amin, M. A. Alharbi, A. M. Badawi*
25	**Daily variation of radon gas and its short-lived progeny concentration near ground level and estimation of aerosol residence time** *M. Mohery, A. M. Abdallah, A. Ali, S. S. Baz*
26	**Optical characteristics of transparent samarium oxide thin films deposited by the radio frequency sputtering technique** *A. A. Atta, M. M. EL-Nahass, Khaled M. Elsabawy, M. M. Abd El-Raheem, A. M. Hassanien, A. Ahuthali, Ali Bbadawi, Amar Merazga*
27	**Effect of gas pressure and film thickness on the optical constants of transparent conducting oxide based on zinc oxide** *M. M. Abd El-Raheem, A, K. Diab, Abdullah Alhuthali, Ateyyah M. Al-Baradi*
28	**Influence of Cu doping on structural, morphological, photoluminescence, and electrical properties of ZnO nanostructures synthesized by ice-bath assisted sonochemical method** *A.A. Othman, Manar A. Ali, E.M.M. Ibrahim, M.A. Osman*
29	**Study of Plasma Formation in Potassium Vapor Excited by Nanosecond Resonant Laser Pulses** *M. A. Mahmoud, E. Sultan, Asmaa Gamal*
30	**Effect of Calcination Temperature on Magnetic Properties of $BiFeO_3$ Nanoparticles Prepared By Sol-Gel Method** *E. M. M. Ibrahim , G. Farghal, Mai M. Khalaf , Hany M. Abd El-Lateef*
31	**Sonochemically Synthesized ZnO Nanosheets and Nanorods: Annealing Temperature Effects on the Structure, and Optical properties** *A. Othman, M. A. Osman, E.M.M. Ibrahim, Manar A. Ali*
32	**Optical and electrical properties of hydrothermally prepared CdTe nanowires** *N. M. A. Hadia, M. A. Awad, S. H. Mohamed, E. M. M. Ibrahim*
33	**The synthesis of $Bi_2(TeSe)_3$ nanoparticles for clean energy production: Effect of the synthesis conditions** *M. A. A. Mohamed, E. M. M. Ibrahim, H. M. Ali, M. M. Wakkad*
34	**Magnetic Nanoparticles for Cancer Therapy: Facile Synthesis Techniques and Desired Properties** *E. M. M. Ibrahim, G. Farghal, M. Mostafa, H. Abdelateef, S. Hampel, V. Khavrus, C. Täschner, A. Leonhardt, B. Büchner*
35	**Study of Electron Energy Distribution Function (EEDF) in Potassium Vapor Excited By Nanosecond Laser Pulses** *M. A. Mahmoud, Emad Sultan, Asmaa Gamal*
36	**Structural and Optical Properties of Nanostructured Fe-Doped SnO_2** *S. A. Saleh, A. A. Ibrahim, S. H. Mohamed*
37	**Analysis Slow Particle Emitted $_{24}$Mg with Emulsion Interactions at Relativistic Energies** *A. Abd El-Daiem, A. E. Elmeshneb*
38	**Electrical and magnetic transportin Strontium doped Europium Ferrimanganites** *I. A. Abdel-Latif, Mahrous R. Ahmed, I. A. Al-Omari, A. Sellai*
39	**Thickness-dependent dispersion parameters, energy gap and nonlinear refractive index of ZnSe thin films** *Deo Prakash, E. R. Shaaban, M. Shapaan, S. H. Mohamed, A. A. Othman, K. D. Verma*
40	**Hardening of the soft phonon in bulk $SrTiO_3$ interfaced with $LaAlO_3$ and $SrRuO_3$** *A. Nucara, M. Ortolani, L. Baldassarre,W. S. Mohamed, U. Schade, D. Winkler, A. Khare, F. Miletto Granozio, P. Calvani*
41	**Complete Destruction of Ag Br Emulsion Nuclei BY_{28}Si Ions with 4.5 GeV/Nucleon Energy** *A. Abd EL-Daiem*

List of papers published by Staff members of Chemistry Department

1	**Effect of ammonium groups on the properties of anion conductive membranes based on partiallyfluorinated aromatic polymers** *Ahmed Mohamed Ahmed Mahmoud, Ahmed Mohamed Mohamed El-Saghier, Kenji Miyatake*
2	**One-pot Synthesis and An Antibacterial Activity of 2-(2-hydroxyphenyl)-4-oxothiazolidin-3-yl)alkyl/ phenylthiazolidin-4-one Derivatives and Reaction with Aromatic Aldehydes** *Ahmed Mohamed Mohamed El-Saghier, NaglaaFawzyHassaMahmoud*
3	**Utilization of 2-Ylidene-4-thiazolidinones in Synthesis of Heterocyclic Compounds Part (II): Transformation of (4-Oxo-3-phenyl-1,3-thiazolidin-2-ylidene)malononitrile to 3-Aminothiophene Derivatives** *M. F. Farhat, M. A. Makhlouf, A. B. El-Mezoughi, A. M. El-Saghier*
4	**Evaluation of Antidiabetic Activity of *Ipomoea Aquatica* Fractions in Streptozotocin Induced Diabetic in Male Rat Model** *Nagwa El-Sawi, Mahmoud Hefny Gad, MadehaNooh Al-Seeni, Sabry Younes, El-Mewafy El-Ghadban, Soad Shaker Ali*
5	**Relationship of C-Reactive Proteins with Oxidative Stress and Obesity in Type 2 Diabetic Subjects** *Nagwa M. Elsawi, Hossam El-Din M. Omar, Ali Taha A. Hassan, Amira M. Ahmed*
6	**Highly sensitive determination of atropine using cobalt oxide nanostructures: Influence of functional groups on the signal sensitivity** *Soomro R. A., Nafady A., Hallam K. R., Jawaid S., Al Enizi A., Sherazi S. T. H., Sirajuddinb Ibupoto Z. H., Willander M.*
7	**Assessment of Lycium Barbarum for detoxification of Patulin toxin and their effects on rat serum globulin** *Nagwa M. El-Sawi, Asma S. Abdo, M.A.A. Mohamed, H. Salah, MadehaN. Al Seni, M. T. El-Wassimy*
8	**Selective synthesis of monosubstituted p-tert-butylthiacalix[4]arene under phase transfer catalysis** *Omran A. Omran*
9	**Fabrication and applications of potentiometric sensors based on p-tert-butylthiacalix[4]arene comprising two triazole rings ionophore for silver io n detection** *Omran A. Omran, Fadl A. Elgendy, Ayman Nafady*
10	**Electrochemical behavior of antioxidants: Part 3. Electrochemical studies of caffeic Acid DNA interaction and DNA/carbon nanotube biosensor for DNA damage and protection** *Refat Abdel-Hamid, Emad F. Newair*
11	**Synthesis and Reactivity of Enaminones: Synthesis of Some 1,3,4- Thiadiazole Linked to Pyrazole, Pyridine, Benzimidazolopyrimidine, Pyrazolopyrimidine, Pyrazolotriazine and Triazolotriazine Derivatives** *Mohamed A. Raslan, Omran A. Omran*
12	**N,N,N-Triethylethanaminium 5,11,17,23-tetra-tert-butyl-25 [(ethoxycarbonyl)methoxy]-26,28-dihy-droxy-27-oxido-2,8,14,20 tetrathiacalix[4]arene: a molecular salt** *Joel T. Mague, Mehmet Akkurt, Shaaban K. Mohamed, Omran A. Omran, Mustafa R. Albayati*
13	**N,N,N-Triethylethanaminium 5,11,17,23-tetra-tert-butyl-25-cyanomethoxy-26,28-dihydroxy-27-oxido- 2,8,14,20-tetrathiacalix[4]arene: a molecular salt** *Omran A. Omran, Joel T. Mague, Shaaban K. Mohamed, Mehmet Akkurt, Alaa F. Mohamed*
14	**Synthesis and antibacterial activity of some new 4-anilino-5-phenyl-4*H*-1,2,4-triazole-3- thiol derivatives** *Abd El-Badih A.G. Ghattas, Hassan M. Moustafa, Elsayed A.A. Hassanein, Bahgat R.M. Hussein*
15	**Cobalt(III)-porphyrin complex (CoTCPP) as an efficient and recyclable homogeneous catalyst for the synthesis of tryptanthrinin aqueous media** *Mahmoud Abd El Aleem Ali Ali El-Remaily, O. M. Elhady*
16	**A robust synthesis and characterization of superparamagnetic $CoFe_2O_4$ nanoparticles as an efficient and reusable catalyst for green synthesis of some heterocyclic rings** *Mahmoud Abd El Aleem Ali El-Remaily, Ahmed M. Abu-Dief, Rafat M. El-Khatib*

17	**Synthesis and Antimicrobial Screening of Fused Heterocyclic Pyridines** *Mahmoud A. A. El-Remaily, O. M. Elhady, Eman M. M. Abdel-Raheem*
18	**Divinyl Sulfone Cross-Linked b-Cyclodextrin Polymer as Newand Effective Corrosion Inhibitor for Zn Anode in 3.5 M KOH** *Hany M. Abd El-Lateef, Mahmoud Abd El Aleem Ali Ali Elremaily*
19	**Epichlorohydrin cross-linked β-cyclodextrin:an environmental method for the synthesis of 2-arylbenzothiazoles derivatives in water** *Mahmoud Abd El Aleem Ali Ali El-Remaily, Ahmed M. M. Soliman*
20	**Synthesis and in vitro Antibacterial Activity of Some Novel Fused Pyridopyrimidine Derivatives** *Mahmoud Abd El Aleem Ali Ali El-Remaily, O. M. El Hady, H. Salah Abo Zaid, E. M. M. Abd El-Raheem*
21	**Design, Synthesis and Hypolipidemic Activity of Novel Hydrazones of Nicotinic acid Hydrazide** *Moustafa O. Aboelez, Omar M. Elhady, Montaser S. A. Shaykoon, Mai E.Shoman, Sanaa A. Ahmed, Gamal ElDin A. Abuo-Rahma*
22	**Mimic Analogues and their Toxicological Aspects on *Spodoptera littoralis* (Boisd.)** *M. T. M. El-Wassimy, Erian. S. Mansour, Omar M. Elhady, Ali M. Drar*
23	**Synthesis of Novel Fused Heterocycles Based on 6-Amino-4-phenyl-2-thioxo-1,2-dihydropyridine-3,5-dicarbonitrile** *H. Abdel-Ghany, A. M. El-Sayed, A. A. Amer, A. M. Ahmed*
24	**Synthesis, structure elucidation, biological screening, molecular modeling and DNA binding of some Cu(II) chelates incorporating imines derived from amino acids** *Laila H. Abdel-Rahman, Ahmed M. Abu-Dief, Mohammed Ismael, Mounir A.A. Mohamed, Nahla Ali Hashem*
25	**A Biocatalytic Aza-Achmatowicz Reaction** *Fernández-Fueyo E., Younes S. H. H., Van Rootselaar S., Aben R. W. M., Renirie R., Wever R., Holtmann D., Rutjes F. P. J. T., Hollmann, F.*
26	**4-Toluenesulfonamide as a Building Block for Synthesis of Novel Triazepines, Pyrimidines, and Azoles** *A. Khodairy, Ali M. Ali, M. T. El-Wassimy*
27	**Synthesis of 3-Pyrazolyl-1,2,4-Triazoles via One-Pot Multicomponent Reaction in Phosphoric Acid** *Amer A.A., Moustafa A.H.*
28	**Triclinic and monoclinic polymorphs of meso-(E,E)-1,1'-[1,2-bis(4-chlorophenyl)ethane-1,2-diyl]bis(phenyldiazene): The high-yield synthesis of an unexpected product, concomitant polymorphism and configurational disorder** *Mohamed S. K., Younes S. H. H., Abdel-Raheem E. M. M., Horton P. N., Akkurt M., Glidewell C.*
29	**New Heterocyclic Compounds Derived from 4,6-Diamino-3-cyano-2-methylthiopyridine and their Biological Activity** *Ghattas A. E.-B. A. G., Khodairy A., Moustafa H. M., Hussein B. R. M.*
30	**Functionalization of Magnetic Nano Particles: Synthesis, Characterization and Their Application in Water Purification** *Ahmed M. Abu-Dief, Samar Kamel Hamdan*
31	**4-Hydroxy-1-phenylquinolin-2(1H)-one in One-pot Synthesis of Pyrimidoquinolines and Related Compounds under Microwave Irradiation and Conventional Conditions** *Mourad A. -F. E., Amer A. A., El-Shaieb K. M., Ali A. M., Aly A. A.*
32	**Synthesis of novel coumarin derivatives based on 6-aminocoumarin, kinetic inspection of base hydrolysis, and spectrophotometric tracer of intermediate progress** *Abd Allah O. A. E. A., Nassr L. A.-M. E.*
33	**Porous $LaFeO_3$/Silica Nanocomposites via Sol-Gel Mixing Involving Citric Acid** *Khalil K. M. S., Elhamdy W. A., Said A. E.-A. A., Elsamahy A. A.*
34	**Magnetic $NiFe_2O_4$ nanoparticles: efficient, heterogeneous and reusable catalyst for synthesis of acetylferrocene chalcones and their anti-tumour activity** *Ahmed M. Abu-Dief, Ibrahim F. Nassar, Wafaa H. Elsayed*

35	**Some new nano-sized Fe(II), Cd(II) and Zn(II) Schiff base complexes as precursor for metal oxides: Sonochemical synthesis, characterization, DNA interaction, in vitro antimicrobial and anticancer activities** *Laila H. Abdel-Rahman, Ahmed M. Abu-Dief, Rafat M. El-Khatib, Shimaa Mahdy Abdel-Fatah*
36	**Some New Nano-sized Mononuclear Cu(II) Schiff Base Complexes: Design, Characterization, Molecular Modeling and Catalytic Potentials in Benzyl Alcohol Oxidation** *Laila H. Abdel-Rahman, Ahmed M. Abu-Dief, Mohamed Shaker S. Adam, Samar Kamel Hamdan*
37	**Artificial Macrocycles by Ugi Reaction and Passerini Ring Closure** *Abdelraheem E. M. M., Kurpiewska K., Kalinowska-Tłuścik J., Dömling A.*
38	**Some new nano-sized Cr(III), Fe(II), Co(II), and Ni(II) complexes incorporating 2-((E)-(pyridine-2-ylimino) methyl) napthalen-1-olligand: Structural characterization, electrochemical, antioxidant, antimicrobial, antiviral assessment and DNA interaction** *Laila H. Abdel-Rahman, Ahmed M. Abu-Dief, Emad F. Newair, Samar Kamel Hamdan*
39	**New Cd(II), Mn(II) and Ag(I) Schiff Base Complexes : Synthesis, Characterization, DNA Binding and Antimicrobial Activity** *Laila H. Abdel-Rahman, Ahmed M. Abu-Dief, Rafat M. El-Khatib, Shimaa Mahdy Abdel-Fatah, Amin Abdou Seleem*
40	**Nano Sized Moringa oleifera an Effective Strategy for Pb(II) ions Removal from Aqueous Solution** *Laila H. Abdel-Rahman, Ahmed M. Abu-Dief, M. A. Abd- El Sayed, Mallak Megalea Zikry*
41	**Effect of chromium substitution on the structural and magnetic properties of nanocrystalline zinc ferrite** *Ahmed M. Abu-Dief, Mohammed S.M. Abdelbaky, David Martínez-Blanco, Zakariae Amghouz, Santigo García-Granda*
42	**Sonochemical synthesis, DNA binding, antimicrobial evaluation and in vitro anticancer activity of three new nano-sized Cu(II), Co(II) and Ni(II) chelates based on tri-dentate NOO imine ligands as precursors for metal oxides** *Laila H. Abdel-Rahman, Ahmed M. Abu-Dief, Rafat M. El-Khatib, Shimaa Mahdy Abdel-Fatah*
43	**Removal of Toxic Pb(II) Ions from Aqueous Solution by Nano Sized Flamboyant Pod (*Delonix regia*)** *Laila H Abdel-Rahman, Badriah SF Al-Farhan, Ahmed M Abu-Dief, Mallak Megalea Zikry*
44	**One-Pot Multicomponent Synthesis of Novel 2 Tosyloxyphenyl-pyrans under Green and Conventional Condition with Anti-inflammatory Activity** *Khodairy A., Ali A. M., Aboelez M. O., El-Wassimy M. T.*
45	**Reactivity tracers of the hydrolysis of Fe(II)-bis(salicylidene) complexes: Initial –transition states analysis and enhanced impact of tensides on the kinetic trends** *Lobna Abddel-Mohsen E. Nassr*
46	**Oxidation efficiencies of high spin Fe(II)-azo amino acid complexes by potassium peroxydisulfate. Initial state-transition state solvation effects** *M. S. S. Adam, U. El-Ayaan, A. D. M. Mohamad*
47	**Pyrido-anellated 1,3-azaphospholes-current state and future challenges** *M. S. S. Adam, M. Ghalib, G. J. Palm, P. G. Jones, J. W. Heinicke*
48	**3*H*-1,3-Azaphospholo[4,5-*b*]pyridines - novel heterocyclic P,N-bridging or hybrid ligands: Synthesis and first d^8-transition metal complexes** *M. S. S. Adam, M. K. Kindermann, P. G. Jones, J. W. Heinicke*
49	**Voltammetric determination of polyphenolic content in pomegranate juice using a poly(gallic acid)/multiwalled carbon nanotube modified electrode** *Abdel-Hamid R., Newair E. F.*
50	**Mechanism of Chicoric Acid Electrochemical Oxidation and Identification of Oxidation Products by Liquid Chromatography and Mass Spectrometry** *Newair E. F., Abdel-Hamid R., Paul A. Kilmartin*

51	**Electroanalytical Determination of Luteolin in Peanut Hulls Using Carbon Blac k Modified Glassy Carbon Electrode** *Newair E. F., Abdel-Hamid R., François Garcia*
52	**Synthesis and evaluation of novel series of Schiff base cationic surfactants as corrosion inhibitors for carbon steel in acidic/chloride media: experimental and theoretical investigations** *Hany M. Abd El-Lateef , Ahmed H. Tantawy*
53	**Corrosion protection of mild steel by coating with TiO_2 thin films co- doped with NiO and ZrO_2 in acidic chloride environments** *Mai M. Khalaf, Hany M. Abd El-Lateef*
54	**Empirical and Theoretical Calculations for Corrosion Inhibition of Carbon Steel C1018 in Acidic Solutions Using Some Selected Fatty Acid Surfactants** *Hany M. Abd El-Lateef, Mohamed Ismael, Ahmed H. Tantawy*
55	**Empirical and quantum chemical studies on the corrosion inhibition performance of some novel synthesized cationic gemini surfactants on carbon steel pipelines in acid pickling processes** *Hany M. Abd El-Lateef, Mohamed A. Abo-Riya, Ahmed H. Tantawy*
56	**Modification of Hematite Photoanode with Cobalt Based Oxygen Evolution Catalyst via Bifunctional Linker Approach for EfficientWater Splitting** *Amira Y. Ahmed, Mahmoud G. Ahmed, Tarek A. Kandiel*
57	**Solvent-induced deposition of Cu-Ga-In-S nanocrystals onto a titanium dioxide surface for visible-light-driven photocatalytic hydrogen production** *Tarek A. Kandiel, Kazuhiro Takanabe*
58	**TiO_2(B)/anatase heterostructure nanofibers decorated with anatase nanoparticles as efficient photocatalysts for methanol oxidation** *Tarek A. Kandiel, Amira Y. Ahmed, Detlef Bahnemann*
59	**Visible light driven hydrogen evolution with a noble metal free $CuGa_2In_3S_8$ nanoparticle system in water** *Tarek A. Kandiel, Georgina A. M. Hutton, Erwin Reisner*
60	**Photocatalytic hydrogen production from biomass-derived compounds: A case study of citric acid** *Ayad F. Alkaim, Tarek A. Kandiel, Ralf Dillert, Detlef W. Bahnemann*
61	**Photo and electrical peculiarities of the nanostructured glass/ITO/AAO and glass/ITO/CdS systems** *Sh. O. Eminov, D. B. Tagiyev, A. Sh. Aliyev, N. Sh. Soltanova, J. A. Guliyev, Kh. D. Jalilova, N. J. Ismayilov, I. S. Hasanov, A. A. Rajabli, G. Kh. Mamedova, I. I. Gurbanov, Mahmoud Elrouby*
62	**Self-assembly of porous copper oxide hierarchical nanostructures for selective determinations of glucose and ascorbic acid** *Bahaa G. Mahmoud, Mohamed Khairy, Farouk A. Rashwan, Christopher W. Foster, Craig E. Banks*
63	**Electrochemical Fabrication and Characterization of Corrosion-Resistant, Ternary, Lead-Based Alloys as a New Material for Steel Surface Protection** *A. Sh. Aliyev, H. M. Tahirli, Mahmoud Elrouby, N. Sh. Soltanova, D. B. Tagiev*
64	**Revealing the mechanism, degradation pathways and kinetics of UV_{254nm}/H_2O_2-baseddegradation of model active sunscreen ingredient PBSA** *Wael H. M. Abdelraheem, Xuexiang He, Zanaty R. Komy, Nabawia M. Ismail, Dionysios D. Dionysiou*
65	**A natural clayey adsorbent for selective removal of lead from aqueous solutions** *Ali Sdiri, Mohamed Khairy, Samir Bouaziz, Sherif El-Safty*
66	**Ceria-zirconia modified MnOx catalysts for gaseous elemental mercury oxidation and adsorption** *Deshetti Jampaiah, Samuel J. Ippolito, Ylias M. Sabri, James Tardio, P. R. Selvakannan, Ayman Nafady, Benjaram M. Reddy, Suresh K. Bhargava*
67	**Natural betanin dye extracted from bougainvillea flowers for the naked-eye detection of copper ions in water samples** *Mohamed Khairy, Mohamed Ismael, Rafat M. El-Khatib, Mostafa Abdelnaeemb, Mariam Khalaf*
68	**The Path Towards Healthier Societies, Environments & Economies: A Broader Perspective for Sustainable Engineered Nanomaterials** *Thabet Tolaymat, Wael Abdelraheem, Amro El Badawy, Dionysios D. Dionysiou, Ash M. Genaidy*

69	**Evaluation of serum cortisol, growth and thyroid hormones and its relation with lipolysis in non-diabetic obese and diabetic obese subjects attending Sohag Governorate, Egypt** *Ali Taha A. Hassan, Hossam El-Din M. Omar, Nagwa M. Elsawi, Amira M. Ahmed*
70	**Preferential synthesis of highly conducting Tl(TCNQ) phase II nanorod networks via electrochemically driven TCNQ/Tl(TCNQ) solid-solid phase transformation** *Nafady A., Sabri Y. M., Kandjani A. E., Alsalme A. M., Bond A. M., Bhargava S.*
71	**Potentiometric and computational studies of Cobalt, nickel and copper complexes with bipyridyl and dl-2-amino-N-hydroxy-n-butanamide in aqueous solution** *Laila H. Abdel Rahman, Badriah S.F Al Farhan, Mohamed Ismael*
72	**Ascorbic Acid Assisted Synthesis of Cobalt Oxide Nanostructures, Their Electrochemical Sensing Application for the Sensitive Determination of Hydrazine** *Tahira A., Nafady A., Baloach Q., Sirajuddin, Sherazi S. T. H., Shaikh T., Arain M., Willander M., Ibupoto Z. H.*
73	**The synthesis of new nanostructures of CuO using ascorbic acid as growth directing agent and their sensitive electrochemical detection of hydrazine** *Tahira A., Nafady A., Arain M., Sirajuddin, Sherazi S. T. H., Shaikh T., Baloach Q., Willander M., Ibupoto Z. H.*
74	**Copper Oxide Microstructures with Hemisphere Pineapple Morphology for Selective Amperometric Determination of Vitamin C (L-ascorbic Acid) in Human Fluids** *Mohamed Khairy, Bahaa G. Mahmoud*
75	**Simpler and highly sensitive enzyme-free sensing of urea via NiO nanostructures modified electrode** *Arain, M., Nafady, A., Sirajuddin, Ibupoto Z. H., Hussain Sherazi S. T., Shaikh T., Khan H., Alsalme A., Niaz A., Willander M.*
76	**Cefuroxime derived copper nanoparticles and their application as a colorimetric sensor for trace level detection of picric acid** *Hussain M., Nafady A., Sirajuddin, Hussain Sherazi S. T., Shah M. R., Alsalme A., Kalhoro M. S., Mahesar S. A., Siddiqui S.*
77	**Design and control of Lewis acid sites in Sn-substituted microporous architectures** *Khaled M. H. Mohammed, Arunabhiram Chutia, June Callison, Peter P. Wells, Emma K. Gibson, Andrew M. Beale, C. Richard A. Catlow, Robert Raja*
78	**Effect of phosphoric acid concentration on conductivity of anodic passive film formed on surface of lead-indium alloy** *Abdel-Rahman El-Sayed, Hossnia S. Mohran, Hoda Abdel Shafy Shilkamy*
79	**Iminophosphoranes in Heterocyclic Synthesis: A FacileSynthesis of Pyrido[4,3-D]Pyrimidine andPyrido [4,3D][1,3]Oxazine Derivatives viaIntermolecularaza-Wittig Reactions** *Omran A. Omran, Samia M. Sayed, Mohamed A. Raslan*
80	**Designing CuO_x Nanoparticle-Decorated CeO_2 Nanocubes for Catalytic Soot Oxidation: Role of the Nanointerface in the Catalytic Performance of Heterostructured Nanomaterials** *Putla Sudarsanam, Brendan Hillary, Baithy Mallesham, Bolla Govinda Rao, Mohamad Hassan Amin, Ayman Nafady, Ali M. Alsalme, B. Mahipal Reddy, Suresh K. Bhargava*
81	**Effect of preparation conditions on structural and catalytic properties of lithium zirconate** *Katabathini Narasimharao, Tarek T. Ali*
82	**In situ spectroscopic investigations of MoO_x/Fe_2O_3 catalysts for the selective oxidation of methanol** *Catherine Brookes, Michael Bowker, Emma K. Gibson, Diego Gianolio, Khaled M. H. Mohammed, Stephen Parry, Scott M. Rogers, Ian P. Silverwood, Peter P. Wells*
83	**Electrochemical behaviour of antioxidants: Part 2. Electrochemical oxidation mechanism of quercetin at glassy carbon electrode modified with multi-wall carbon nanotubes** *Refat Abdel-Hamid, Emad F. Newair*
84	**Evaluation of copper speciation in the extract of Eichhornia crassipes using reverse and forward/CLE voltammetric titrations** *Wael H.M. Abdelraheem, Mostafa K.M. Rabia, Nabawia M. Ismail*

85	**Photocatalytic degradation of p-nitrophenol in aqueous suspension by using Graphene/ZrO_2 catalysts** *Basahel Sulaiman N., Mokhtar Mohamed, Alsharaeh Edreese H., Ali Tarek T., Mahmoud Hatem A., Narasimharao Katabathini*
86	**Physico-chemical and catalytic properties of mesoporous CuO-ZrO_2 catalysts** *Sulaiman N. Basahel, Mohamed Mokhtar, Edreese H. Alsharaeh, Tarek T. Ali, Hatem A. Mahmoud, Katabathini Narasimharao*
87	**Sol-gel Derived Mixed Oxide Zirconia: Titania Green Heterogeneous Catalysts and Their Performance in Acridine Derivatives Synthesis** *Mai M. Khalaf, Antar A. Abdelhamid*
88	**Synergistic effect of polyethylene glycols and rare earth Ce^{4+} on the corrosion inhibition of carbon steel in sulfuric acid solution: electrochemical, computational, and surface morphology studies** *Hany M. Abd El-Lateef*
89	**Physical-chemical study for the treatment of Iron and Manganese in ground water** *M. K. Moustsfa, M. A. Hussien, M.E. Mohamed, A.A. Mohamed*
90	**Physico-Chemical Studies on Treatment of some Divalent Elements in Ground Water** *M. K. Moustsfa, M. A. Hussien, M.E. Mohamed, A.A. Mohamed*

List of papers published by Staff members of Botany&Microbilogy Department

1	**Cyanobacterial Toxins in Water Sources and Their Impacts on Human Health** *Z. Mohamed*
2	**Breakthrough of *Oscillatoria limnetica* and microcystin toxins into drinking water treatment plants - Examples from the Nile River, Egypt** *Mohamed Z. A.*
3	**Harmful cyanobacteria and their cyanotoxins in Egyptian fresh waters-state of knowledge and research needs** *Mohamed Z. A.*
4	**Occurrence of toxic cyanobacteria and microcystin toxin in domestic water storage reservoirs, Egypt** *Mohamed Z. A., Deyab M. A., Abou-Dobara M. I., El-Raghi W. M.*
5	**Photosynthesis, antioxidant status and gas-exchange are altered by glyphosate application in peanut leaves** *Radwan D. E. M. , Fayez K. A.*
6	**Impact of greenhouse environmental factors and fungicide Trinol (triadimend) treatment on berry leaves infected with powdery mildew (*Uncinula necator* (Schwein.) Burrill: Role of host antioxidant systems against pathogen infection** *Khalaf A Fayez, Yassin M Al-Sodany, Alaa Abouzaid*
7	**Isolation of *Bdellovibrio* sp. from Wastewater and Their Potential Application in Control of *Salmonella paratyphi* in Water** *El-Shanshoury A. E.-R. R., Abo-Amer A. E., Alzahrani O. M.*
8	**Mycobiota of Oil-Contaminated Soil Samples and Their Abilities for Dibenzothiophene Desulfurization** *Gherbawy Y., El-Deeb B., Hazzani A. A., Maher A., Shehata A.*
9	**The genus Lolia from freshwater habitats in Egypt with one new species** *Abdel-Aziz F. A.*
10	**Comparative anatomy of stems and leaves of plectranthus L. (Lamiaceae) in Saudi Arabia and systematic implications** *Khalik, K.N.A., Karakish, E.A.*
11	**Two new species of Kallichroma (Bionectriaceae, Hypocreales) from Saudi Arabian mangroves** *Abdel-Wahab M. A., Bahkali A. H., Jones E. B. G., Elgorban A. M., Abdel-Aziz F. A., Hodhod M. S., Al-Hebshi M.O.*
12	**Two new cheirosporous asexual taxa (Dictyosporiaceae, Pleosporales, Dothideomycetes) from freshwater habitats in Egypt** *Abdel-Aziz FA*
13	**Seed morphology and surface microstructure of the genus 'Plectranthus' L. (Lamiaceae) in Arabian Peninsula highlighting on their systematic implications** *Khalik, Kadry Abdel*
14	**Growth and Physiological Response of Some Cultivated Species Under Allelopathic Stress of Calotropis Procera (Aiton)** *A. A. El-Khatib, N. A. Barakat, Heba Nazeir*
15	**A new species of Plectranthus (Lamiaceae) from Saudi Arabia** *Khalik K. Abdel*
16	**Evaluation of silver nanoparticles for the control of Phragmidium species in vitro and taif'rose rust disease in field** *Gado E. A. M., El-Deeb B., Ali, E. F., Mostafa N. Y., Bazaid S.A*

17	**Diagnosis of pulmonary tuberculosis and detection of resistance to rifampin and isoniazid through direct molecular methods in stool samples** *Al Yousef S. A., Ali AbdelRahim K. A., Ahmed A. O., Almaary K. S., Mohamed A. M. A.*
18	**Antimicrobial activity of silver and gold nanoparticles biosynthesized using ginger extract** *El-Deeb B., Elhariry H., Mostafa N. Y.*
19	**A Systematic Revision of the Genus Plectranthus L. (Lamiaceae) in Saudi Arabia Based on Morphological, Palynological, and Micromorphological Characters of Trichomes** *Kadry N. Abdel Khalik*
20	**Recommendations for competing sexual-asexually typified generic names in Sordariomycetes (except Diaporthales, Hypocreales, and Magnaporthales)** *Réblová M., Miller, A.N., Rossman, A.Y., Seifert, K.A., Crous, P.W., Hawksworth, D.L., Abdel-Wahab, M.A., Cannon, P.F., Daranagama, D.A., Wilhelm De Beer, Z., Huang, S.-K., Hyde, K.D., Jayawardena, R., Jaklitsch, W., Gareth Jones, E.B., Ju, Y.-M., Judith, C, Maharachchikumbura S.S.N., Pang, K.-L., Petrini, L.E., Raja, H.A., Romero, A.I., Shearer, C., Senanayake, I.C., Voglmayr, H., Weir, B.S.,Wijayawarden, N.N.*
21	**Families of Sordariomycetes** *Maharachchikumbura S.S.N., Hyde K.D., Jones E.B.G., McKenzie E.H.C., Bhat J.D., Dayarathne M.C., Huang S.K., Norphanphoun C., Senanayake I.C., Perera R.H., Shang Q.J., Xiao Y., D'souza M.J., Hongsanan S., Jayawardena R.S., Daranagama D., Konta S., Goonasekara I.D., Zhuang W.Y., Jeewon R., Alan J. L. Phillips, Abdel-Wahab M.A., Al-SadiAli A.M., Bahkali A.H., Boonmee S., Boonyuen N., Cheewangkoon R., Asha J. Dissanayake Jichuan Kang Qi-Rui Li, Liu J.K., Liu X.Z., Liu Z.Y., Luangsa-ard J.J., Pang K.L., Phookamsak R., Promputtha I., Suetrong S., Stadler M., Wen T., Wijayawardene N.N.*
22	**Freshwater fungi from the River Nile, Sohag, Egypt** *Abdel-Aziz F A*
23	**Mycotoxins production by Aspergillus ostianus Wehmer and using phytochemicals as control agent** *Saber S M, Youssef M S, Arafa R F, Hassane A M A*
24	**Differential tolerance to high salt with regard to cell growth and superoxide dismutase (SOD) activity in calluses of the halophyte Suaeda maritima from Japan and Egypt** *Elsayed Mohamed, Ryuya Matsuda, Ahmed A El-khatib, Katsuaki Takechi, Hiroyoshi Takano, Susumu Takio*
25	**Fungal diversity notes 253-366: taxonomic and phylogenetic contributions to fungal taxa** *Li GJ, Hyde KD, Zhao RL, Hongsanan S, Abdel-Aziz FA, Abdel-Wahab MA, Alvarado P, Alves-Silva G, Ammirati JF, Ariyawansa HA, Baghela A, Bahkali AH, Beug M, Bhat DJ, Dimitar Bojantchev D, Boonpratuang T, Bulgakov TS, Camporesi E, Boro MC, Ceska O, Chakraborty D, Chen JJ, Chethana KWT, Chomnunti P, Consiglio G, Cui BK, Dai DQ, Dai YC, Daranagama DA, Das K, Dayarathne MC, De Crop E, De Oliveira RJV, de Souza CAF, de Souza JI, Dentinger BTM, Dissanayake AJ, Doilom M, Drechsler-Santos ER, Ghobad- Nejhad M, Gilmore SP, Góes-Neto A, Gorczak M, Haitjema CH, Hapuarachchi KK, Hashimoto A, He MQ, Henske JK, Hirayama K, Iribarren MJ, Jayasiri SC, Jayawardena RS, Sun Jeong Jeon, Gustavo H Jerônimo, Ana L Jesus, EB Gareth Jones, Ji Chuan Kang, Karunarathna SC, Kirk PM, Konta S, Kuhnert E, Langer E, Lee HS, Lee HB, Li WJ, Li XH, Liimatainen K, Lima DX, Lin CG, Liu JK, Liu XZ, Liu ZY, Luangsaard JJ, Lücking R, Lumbsch HT, Lumyong S, Leaño EM, Marano AV, Matsumura M, McKenzie EHC, Mongkolsamrit S, Mortimer PE, Nguyen TTT, Niskanen T, Norphanphoun C, O'Malley MA, Parnmen S, Pawłowska J, Perera RH, Phookamsak R, Phukhamsakda C, Pires-Zottarelli CLA, Raspé O, Reck MA, Rocha SCO, de Santiago ALCMA, Senanayake IC, Setti L, Shang QJ, Singh SK, Sir EB, Solomon KV, Song J, Srikitikulchai P, Stadler M, Suetrong S, Takahashi H, Takahashi T, Tanaka K, Tang LP, Thambugala KM, Thanakitpipattana D, Theodorou MK, Thongbai B, Thummarukcharoen T, Tian Q, Tibpromma S, Verbeken A, Vizzini A, Vlasák J, Voigt K, Wanasinghe DN, Wang Y, Weerakoon G, Wen HA, Wen TC, Wijayawardene NN, Wongkanoun S, Wrzosek M, Xiao YP, Xu JC, Yan JY, Yang J, Yang SD, Hu Y, Zhang JF, Zhao J, Zhou LW, Peršoh D, Phillips AJL, Maharachchikumbura SSN*

26	**Fungal diversity notes 367-492: taxonomic and phylogenetic contributions to fungal taxa** *Kevin D. Hyde, Sinang Hongsanan, Rajesh Jeewon , D. Jayarama Bhat, Eric H. C. McKenzie, E. B. Gareth Jones, Rungtiwa Phookamsak, Hiran A. Ariyawansa, Ali H. Bahkali, Saranyaphat Boonmee, Qi Zhao, Faten A .Abdel-Aziz, Mohamed A. Abdel-Wahab, Supharat Banmai, Putarak Chomnunti, Bao-Kai Cui, Dinushani A. Daranagama, Kanad Das, Monika C. Dayarathne, Nimali I. de Silva, Asha J. Dissanayake, Mingkwan Doilom , Anusha H. Ekanayaka, Tatiana Baptista Gibertoni, Aristóteles Góes-Neto , Shi-Ke Huang, Subashini C. Jayasiri, Ruvishika S. Jayawardena, Sirinapa Konta, Hyang Burm Lee, Wen-Jing Li, Chuan-Gen Lin, Jian-Kui Liu, Yong-Zhong Lu, Zong-Long Luo, Ishara S. Manawasinghe, Patinjareveettil Manimohan, Ausana Mapook, Tuula Niskanen, Chada Norphanphoun, Moslem Papizadeh, Rekhani H. Perera, Chayanard Phukhamsakda, Christian Richter, André L. C. M. A. de Santiago, E. Ricardo Drechsler-Santos, Indunil C Senanayake, Kazuaki Tanaka, T. M. D. S. Tennakoon, Kasun M. Thambugala, Qing Tian, Saowaluck Tibpromma, Benjarong Thongbai, Alfredo Vizzini, Dhanushka N. Wanasinghe, Nalin N. Wijayawardene, Haixia Wu, Jing Yang, Xiang-Yu Zeng, Huang Zhang, Jin-Feng Zhang, Timur S. Bulgakov, Erio Camporesi, Mohammad A. Amoozegar, Lidia Silva Araujo-Neta, Joseph F. Ammirati, Abhishek Baghela, R. P. Bhatt, Dimitar Bojantchev, Bart Buyck, Gladstone Alves da Silva, Catarina Letícia Ferreira de Lima, Rafael José Vilela de Oliveira, Carlos Alberto Fragoso de Souza, Yu-Cheng Dai, Bálint Dima, T.T. Duong, Enrico Ercole, Fernando Mafalda-Freire, Aniket Ghosh, Akira Hashimoto, Sutakorn Kamolhan, Ji-Chuan Kang, Samantha C. Karunarathna, Thilini Chethana, Paul M. Kirk, Ilkka Kytövuori, Angela Lantieri, Kare Liimatainen, Zuo Yi Liu, Xing-Zhong Liu, Robert Lücking, Gianfranco Medardi, Peter E. Mortimer, Thi Thuong Thuong Nguyen, K. N. Anil Raj, Mateus A. Reck, Saisamorn Lumyong, Seyed Abolhassan Shahzadeh-Fazeli, Marc Stadler, Mohammad Reza Soudi, Hong-Yan Su, Takumasa Takahashi, Narumon Tangthirasunun, Priyanka Uniyal, Yong Wang, Ting Chi Wen, Jian-Chu Xu ,Zhongkai Zhang, Yongchan Zhao, Jun-Liang Zhou, Lin Zhu, Itthayakorn Promputtha, Saisamorn Lumyong*

List of papers published by Staff members of Zoology Department

1	**Cistrome Analysis of Glucocorticoid Receptor Activity in Bronchial Epithelial Cells Defines Novel Mechanisms of Steroid Efficacy** *Vineela Kadiyala, Sarah K. Sasse, M. Omar Altonsy, Tzu L. Phang, Anthony N. Gerber*
2	**Diallyl disulfide protects against rectal cancer in vivo model of male rabbits: II-Analysis of histological and cytogenetic variations** *Tito N. Habib, Mohammed O. Altonsy, Soheir A. Abd El-Raheem, Yassmin R. Bakeer*
3	**Survivin as a Novel Biomarker in the Pathogenesis of Acne Vulgaris and Its Correlation to Insulin-Like Growth Factor-I** *Hanan A. Assaf, Wafaa M. Abdel-Maged, Bakheet E. M. Elsadek, Mohammed H. Hassan, Mohamed A. Adly, Soher A. Ali*
4	**Effects of seasonal acclimatization on temperature-dependence of cardiac excitability in the roach, Rutilus rutilus** *A. Badr, M.F. El-Sayed, M. Vornanen*
5	**Establishment of hepatitis model in rat liver induced by injecting extracted DNA: Histopathological study** *Ahmed S. Ibraheem, Mohamed F. El-Sayed, Heba A. Khalil*
6	**Ameliorative effect of antioxidants (vitamins C and E) against abamectin toxicity in liver, kidney and testis of male albino rats** *B. Wilson Magdy, F. El_sayed Mohamed, A. Seleem Amin, S. Sarhan Rana*
7	**Single or combined cadmium and aluminum intoxication of mice liver and kidney with possible effect of zinc** *Ahmed S. Ibraheem, Amin A. Seleem, Mohamed F. El-Sayed, Basma H. Hamad*
8	**Comparative histopathological and histochemical abnormalities induced by the posterior salivary gland and ink sac extracts of Octopus vulgaris into mice** *Alaa Y. Moustafa, Aziz waad*
9	**Immunotoxicity of acid secretion produced by Berthellinacitrina (Mollusca: Heterobranchia) in mice spleen: Histological and Immunohistochemical study** *Aziz Awaad, Alaa Y. Moustafa*
10	**A review of the genus Berthellina (Mollusca: Heterobranchia: Pleurobranchidae) in the Red Sea based on molecular and anatomical data** *Alaa Y. Moustafa, Haleh Golestani, Ángel Valdés*
11	**Reproductive Cycle, Gametogenesis and Embryonic Development of Nitiateretiuscula (Bivaliva : Unionidae), from the River Nile, at Sohag Governorate, Egypt** *Fathey E. Soliman; Alaa Y. Moustafa; Tarek G. Ismail, Olfat T. Mohamed*
12	**Drosophila melanogaster as a suitable in vivo model to determine potential side effects of nanomaterials: A review** *Alaraby M, Annangi B, Marcos R, Hernández A*
13	**New insights in the acute toxic/genotoxic effects of CuO nanoparticles in the in vivo Drosophila model** *Alaraby M, Hernández A, Marcos R*
14	**Impact of nematode helminthes on metal concentrations in the muscles of Koshar fish, Epinephelussummana, in Jeddah, Saudi Arabia** *A. H. Hassan, N. A. Al-Zanbagia, E. A. Al-Nabatic*
15	**Buccal deformities in chironomid larvae (Diptera: Chironomidae) as an indicator Risk Assessment and Anthropogenic stresses of pollution in fresh water of the River Nile, Sohag Governorate, Egypt. Available from** *Fatma K. Adham, Azza M. Khedre, Tarek G. Ismail, Mohamed El Araby, Shahenda A. A. Abu ElEla, Wael M. ElSayed*

16	**Histopathological study on rodent small intestine infected with an adult tapeworm, *Hymenolepis diminuta* recorded at Sohag, Egypt** *Ramadan S. A., Hassan A. H., Asran A. A., Abd Elgwad E. F.*
17	**Histopathological changes of rodent liver infected with a larval cestodes recorded at Sohag, Egypt** *Ramadan S. A., Hassan A. H., Asran A. A., Abd Elgwad E. F.*
18	**Effect of maternal caffeine and retinoic acid intake on liverduring pre- and postnatal development of mice, musmusculus** *Fakhr El-Din M. Lashein, Amin A. Seleem, Abeer A. Ahmed*
19	**Effect of verapamil on some of the pro- and apoptotic factors during prenatal retinal differentiation of mice, Musmusculus** *Amin AbdouSeleem, Fakhr El-Din M. Lashein*
20	**Effect of caffeine and retinoic acid on skeletonof mice embryos** *Fakhr El-Din M. Lashein, Amin A. Seleem, Abeer A. Ahmed*

List of papers published by Staff members of Geology Department

1	**Carbonate platform facies development of the Turonian Wata Formation in central and eastern Sinai, Egypt** *Khalifa M. A., Farouk S., Hassan A. M.*
2	**New simulation technique to estimate the hydrocarbon type for the two untested members of Belayim Formation in the absence of pressure data, Badri Field, Gulf of Suez, Egypt** *Abudeif A. M., Attia M. M., Radwan A. E.*
3	**Natural and human-induced sinkhole hazards in Saudi Arabia: distribution, investigation, causes and impacts** *Ahmed M. Youssef, Hasan M. Al-Harbi, Francisco Gutiérrez, Yasser A. Zabramwi, Ali B. Bulkhi, Saeed A. Zahrani, Alaa M. Bahamil, Ahmed J. Zahrani, Zaam A. Otaibi, Bosy A. El-Haddad*
4	**Petrophysical and petrographic evaluation of Sidri Member of Belayim Formation, Badri field, Gulf of Suez, Egypt** *Abudeif A. M., Attia M. M., Radwan A. E.*
5	**Human-Induced Geo-Hazards in the Kingdom of Saudi Arabia: Distribution, Investigation, Causes and Impacts** *Ahmed M. Youssef, Hasan M. Al-Harbi, Yasser A. Zabramwi, Bosy A. El-Haddad*
6	**Comparison of four kernel functions used in support vector machines for landslide susceptibility mapping: a case study at Suichuan area (China)** *Hong H., Pradhan B., Bui D. T., Xu C., Youssef A. M., Chen W.*
7	**Landslide susceptibility mapping using random forest, boosted regression tree, classification and regression tree, and general linear models and comparison of their performance at Wadi Tayyah Basin, Asir Region, Saudi Arabia** *Youssef A. M., Pourghasemi H. R., Pourtaghi Z. S., Al-Katheeri M. M.*
8	**Debris flow impact assessment along the Al-Raith Road, Kingdom of Saudi Arabia, using remote sensing data and field investigations** *Youssef A. M., Al-Kathery M., Pradhan B., El-Sahly T.*
9	**Analysis on causes of flash flood in Jeddah city (Kingdom of Saudi Arabia) of 2009 and 2011 using multi-sensor remote sensing data and GIS** *Youssef A. M., Sefry S. A., Pradhan B., Alfadail E. A.*
10	**Effect of water–rock interaction processes on the hydrogeochemistry of groundwater west of Sohag area, Egypt** *Redwan M., Abdel Moneim A. A., Amra M. A.*
11	**Flash flood susceptibility assessment in Jeddah city (Kingdom of Saudi Arabia) using bivariate and multivariate statistical models** *Youssef A. M., Pradhan B., Sefry S. A.*
12	**Using Na/K Ratios to Identify the Potential Impacts of Sewage Effluent on Groundwater Quality in Sohag, Egypt** *Redwan M., Abdel Moneim A.A.*
13	**Factors controlling groundwater hydrogeochemistry in the area west of Tahta, Sohag, Upper Egypt** *Redwan M., Abdel Moneim A. A.*
14	**Landslide susceptibility maps using different probabilistic and bivariate statistical models and comparison of their performance at Wadi Itwad Basin, Asir Region, Saudi Arabia** *Youssef A. M., Pourghasemi H. R., El-Haddad B. A., Dhahry B.K.*
15	**Seasonal variation and enrichment of metals in sediments of Rosetta branch, Nile River, Egypt** *Redwan M., Elhaddad E.*
16	**Groundwater Management at West El-Minia Desert Area, Egypt Using Numerical Modeling** *Ahmed A. Abdel Moneim, José Paulino Fernández-Álvarez, Elsayed M. Abu El Ella, Ahmed M. Masoud*

17	**Experimental study on the utilization of dune sands as a construction material in the area between Jeddah and Mecca, Western Saudi Arabia** *Abu Seif E.-S. S., Sonbul A. R., Hakami B. A. H., El-Sawy E. K.*
18	**Evaluation of geotechnical properties of Cretaceous sandstone, Western Desert, Egypt** *Seif E.-S. S. A.*
19	**Geochemistry and spatial distribution of selected heavy metals in surface soil of Sohag, Egypt: a multivariate statistical and GIS approach** *Ali M. H., Mustafa A.-R. A., El-Sheikh A. A.*
20	**Genesis and petrology of Late Neoproterozoic pegmatites and aplites associated with the taba metamorphic complex in southern Sinai, Egypt** *Abdelfadil K. M., Asimow P. D., Azer M. K., Gahlan H. A.*

Number of published papers by staff members of Faculty of Science during 2016

Department	Number
Mathematics	40
Physics	41
Chemistry	90
Botany & Microbiology	26
Zoology	20
Geology	20
Total	237

- **Collaborative research publications include:**
  Chemistry Department publishes three articles in collaboration with Physics, Botany Departments.

Mathematics

Shortest Paths Routing Problem in MANETs

Hamdy H. El-Sayed
Mathematics Department, Faculty of Science, Sohag University, Egypt

The need for communication services is rapidly increasing, because the mobile communication service is synonymous with an ideal communication style realizing communication anytime, anywhere and with anyone. The availability of a path depends on the number of links and the reliability of each link forming the path. Many routing metrics in terms of number of links have been proposed, such as the shortest path routing. Shortest path routing selects a path having minimum cost to forward the data to the destination node. Shortest path routing algorithm selection depends on direct traffic form source to destination, maximizing the network performance and minimizing the cost. Performance of the network can be enhanced through shortest path routing but it also depends upon the functionality of the routing protocol and the parameters that are selected for the shortest path routing. The primary goal of such an ad hoc network routing protocol is correct and efficient route establishment between a pair of nodes so that messages may be delivered in a timely manner. Route construction should be done with a minimum of cost, overhead and bandwidth consumption. Some of researchers explored the concept of shortest path routing over ad hoc network. Each one uses his own parameters with different topology. No one uses all parameters. In this paper, we will discuss the solutions ideas that have been proposed by them.

Appl. Math. Inf. Sci., 10 (5) (2016) 1885-1891

Performance Analysis of Medical Image Compression Using Various Wavelet Techniques

Torki Altameem[1], Osama Alfarraj[1*], E. A. Zanaty[2], Amr Tolba[13], and Sherif M. Ibrahim[4]
[1]*Riyadh Community College, King Saud University, Riyadh, Saudi Arabia*
[2]*Faculty of Science, Sohag University, Egypt*
[3]*Faculty of Science, Menoufia University, Menoufia, Egypt*
[4]*Faculty of Science, SV University, Qena, Egypt*

Medical image compressions allow large volume data to be kept in an exceedingly quantity of disk and to move towards complete film-less imaging. Also, the image compression process minimizes the time while download or sent the image from the internet. For that, several wavelets are used for image compression, which composed of multi-resolution based function. The choice of the suitable wavelet technique depends on the image content and there is no universal technique for all images. This paper addresses the problem of compressing the images, especially to determine whether the wavelet technique can obtain stable and accurate results for medical image compression. We analyze most wavelet techniques like: Haar, Daubechie, Biorthogonal, Coiflet, Symlets, 5/3 and 9/7 lifting technique for image compression. Then the performance of these techniques are evaluated by the Peak Signal to Noise Ratio (PSNR), Transforming Time (T), Encoding time, Decoding time, Compression Time (CT) and Mean Square Error value (MSE). The studied wavelets are applied to the challenge medical images likes: magnetic resonance (MRI) for posterior cruciate ligament, computer tomography (CT) of the brain and retina; with varying size images to prove their efficiency. A direct benefit of this study is being able to determine the most suitable wavelet techniques for given application medical images.

J Medical Imaging and Health Informatics, 6 (2016 1-11

Surface-Surface Tissue Reconstruction and Visualization for the Magnetic Resonance Imaging or Tomography Imaging Engineering Design

Torki Altameem[1], E. A. Zanaty[2], Amr Tolba[1,3], Ayam Asaad[4]

[1]Riyadh Community Collage, King Saud University,Riyadh, KSA

[2]Faculty of Science, Sohag University, Egypt

[3]Faculty of Science, Menoufia University, Menoufia, Egypt

[4]Faculty of Science, Al-Azhar University, Assuit, Egypt

This paper presents a surface–surface tissue reconstruction and visualization algorithms of the magnetic resonance or tomography imaging (MRI/CT) for the practical applications to assist in engineering design and diagnostic diseases. The proposed algorithm starts by feeding MRI/CT images slice by slice, applying the region growing segmentation processes and 3D surface reconstruction. An *automatic region growing (ARG)* process has been proposed in the new framework, and the core of ARG contains a local search algorithm and homogeneity criterions. The initial seeds are obtained by using the local search algorithm while the homogeneity criterion values are selected as a probability function of image pixels. The ARG is used to segment an image into multiple surfaces (2D imaging planes). The surface–surface method is provided to create volume imaging based on marching cube algorithm which is used to obtain vertices and triangulation from segmentation tissue. Due to the diversity of algorithms at reconstruction processes, the resulting surfaces of marching cube need to be smooth and accurate. Therefore, a mean filtering smoothing technique has been applied to smooth the surfaces of tissues for accurate 3D tissue reconstruction. The visualization process is applied to these vertices and triangulations in order to get more accurate 3D reconstruction view of the MRI/CT images. The proposed algorithms are applied to MRI/CT images to prove their efficiency and the assessment of the obtained results is judged visually.

J Medical Imaging and Health Informatics, 6 (2016) 1-11

A Performance Study of Classical Techniques for Medical Image Segmentation

E. A. Zanaty, Walla M. Abdelhafiz

Mathematical Department, Faculty of Science, Sohag University, Sohag, Egypt

In this paper, we compare the performance of key classical and clustering techniques for image segmentation when they are applied on medical data. These methods are applied on two different sets: reference images (RI), for objective evaluation based on estimation of segmentation accuracy and time, and non reference images (NRI), for objective evaluation based on combined judgment of opinions of specialists. A direct benefit of this study is being able to determine the most suitable segmentation techniques for given application medical images.

JIMDP, 1 (2) (2016) 33-47

Modified Fuzzy C-Means for Segmenting Magnetic Resonance Images (MRIs)

Ahmed S. Ghiduk[1], E. A. Zanaty[2]
[1]*Faculty of Science, Beni-Suef University, Egypt*
[2]*Mathematical Department, Faculty of Science, Sohag University, Sohag, Egypt*

In this paper, a new modified fuzzy c-means algorithm is presented that could improve the medical image segmentation. The proposed algorithm is realized by modifying the objective function of the conventional FCM algorithm with a flexible penalty. This penalty is based on a data shape and data size used for the generation of fuzzy terms. The complexity of the proposed algorithm is reduced using initial seed information into the objective function instead of whole data set. The performance of the proposed algorithm is tested on noisy real images. The results of the conducted experiments show that the efficiency of the proposed method in preserving the regions homogeneity and its robustness in segmenting noisy images is better than other FCM-based methods.

JIMDP, 1 (2) (2016) 48-58

Image Encryption using Chaos-Driven Elliptic Curve Pseudo-Random Number Generators

Omar Reyad[1,2,*], Zbigniew Kotulski [1], W. M. Abd-Elhafiez[2]
[1]Faculty of Electronics and Information Technology, Warsaw University of Technology, Poland
[2] Faculty of Science, Sohag University, Egypt

Pseudo-random number sequences which using the form of elliptic curves can be generated efficiently in software or hardware by the same methods that are used for the implementation of elliptic curve (EC) public-key cryptosystems. In this paper, we proposed a secure image encryption scheme using key sequences generated from Chaos-Driven Elliptic Curve Pseudo-random Number Generator (C-D ECPRNG). This key sequences derived from random sequences based on EC points operations driven by a chaotic map. These constructions improve randomness properties of the generated sequences since it combines good statistical properties of an ECPRNG and a Chaotic Pseudo-random Number Generator (CPRNG). Entropy analysis of two test images shows that randomness of the ciphered images with the proposed key schemes are more random than in case of the ECPRNG without modulation by a chaotic map. Statistical and differential analysis demonstrate that the proposed schemes have adequate security for the confidentiality of digital images and the encryption is efficient compared to other competitive algorithms.

Appl. Math. Inf. Sci., 10 (4) (2016) 1283-1292

A Hybrid Cascade Approach for Human Skin Segmentation

Samy Bakheet[1,2,*], **Ayoub Al-Hamadi**[2]

[1]*Department of Mathematics & Computer Science, Faculty of Science, Sohag University, Egypt*

[2]*Institute for Information Technology and Communications, Otto-von-Guericke-University Magdeburg, P.O.Box 4120, 39016 Magdeburg, Germany*

Human skin segmentation is fundamental to a wide range of computer vision applications ranging from face recognition, facial expression recognition and gesture analysis to various human computer interaction domains. In this paper, we propose a multistage skin segmentation method built as a cascade of a nonparametric generic model and an adaBoost classifier. Several entities are used to train the adaBoost classifier. Feature vectors fed into the ada Boost contain color information from two different color spaces. Extensive experiments are conducted on two datasets in order to evaluate the performance of the approach. The various results obtained show that the proposed method is a promising approach and it successfully achieves high quality segmentation, while concurrently retaining reasonably low false alarm rates. The comparison of the proposed method with related state-of-the-art competitors reveals the superiority and effectiveness of the proposed method, while maintaining real-time performance.

British Journal of Mathematics & Computer Science, 17 (6) (2016) 1-14

A Discriminative Framework for Action Recognition Using f-HOL Features

Samy Bakheet[1,*], **Ayoub Al-Hamadi**[2]

[1]Department of Math and Computer Science, Faculty of Science, Sohag University, 82524 Sohag, Egypt

[2]Institute for Information Technology and Communications, Otto-von-Guericke-University Magdeburg, P.O. Box 4120, 39016 Magdeburg, Germany

Inspired by the overwhelming success of Histogram of Oriented Gradients (HOG) features in many vision tasks, in this paper, we present an innovative compact feature descriptor called fuzzy Histogram of Oriented Lines (f-HOL) for action recognition, which is a distinct variant of the HOG feature descriptor. The intuitive idea of these features is based on the observation that the slide area of the human body skeleton can be viewed as a spatiotemporal 3D surface, when observing a certain action being performed in a video. The f-HOL descriptor possesses an immense competitive advantage, not only of being quite robust to small geometric transformations where the small translation and rotations make no large fluctuations in histogram values, but also of not being very sensitive under varying illumination conditions. The extracted features are then fed into a discriminative conditional model based on Latent-Dynamic Conditional random fields (LDCRFs) to learn to recognize actions from video frames. When tested on the benchmark Weizmann dataset, the proposed framework substantially supersedes most existing state-of-the-art approaches, achieving an overall recognition rate of 98.2%. Furthermore, due to its low computational demands, the framework is properly amenable for integration into real-time applications.

Information, 7 (4) (2016) 7040068-14

New Efficient Method for Coding Color Images

Walaa M. Abd-Elhafiez[1,2,*], Essam O. Abdel-Rahman[3,4]
[1]Mathematical and Computer Science Department, Faculty of Science, Sohag University, Egypt
[2]College of Computer Science and Information Systems, Jazan University, Jazan, KSA
[3]College of Science and Computer Engineering, Yanbu Branch, Taibah University, Yanbu, KSA
[4]Computer Science Department, Faculty of Computers and Information, Minia University, Egypt

In this paper a novel color image compression technique for efficient storage and delivery of data is proposed. The proposed compression technique started by RGB to YCbCr color transformation process. Secondly, the canny edge detection is used to classify the blocks into edge and non-edge block. Each color component Y, Cb, and Cr compressed by discrete cosine transform (DCT) process, quantizing and coding step by step using adaptive arithmetic coding. Our technique is concerned with the compression ratio, bits per pixel and peak signal to noise ratio, and produc better results than JPEG and more recent published schemes (like, CBDCT-CABS and MHC). The provided experimental results illustrate the proposed technique is efficient and feasible in terms of compression ratio, bits per pixel and peak signal to noise ratio.

Appl. Math. Inf. Sci., 10 (5) (2016) 1885-1891

Pseudo-random Sequence Generation from Elliptic Curves over a Finite Field of Characteristic 2

Omar Reyad, Zbigniew Kotulski
Warsaw University of Technology. Warsaw, Poland

In this paper, the randomness of binary sequences generated from elliptic curves over a finite field of characteristic 2 is studied. A scheme of construction based on the Chaos Driven Elliptic Curve Pseudo-random Number Generator (C-D ECPRNG) is proposed. The generators based of this scheme are verified by using tests from the NIST Statistical Test Suite to analyze their statistical properties. An elliptic curve used in the numerical example is defined over F28. The investigations which made for the generated series of two output sequences of the lengths of 210 and 220 bits shown that 14 generators working according to our general scheme exhibit good randomness properties. Next, the binary sequences generated by these 14 schemes were used for encrypting a 256 × 256 grayscale Lena image as an application example and the security analysis of the ciphered images was carried out.

Proceeding of the Federated Conference on Computer Science and information Systems, 8 (2016) 991-998

Face Identification System in Video

Mohamed Heshmet[1], Walaa M. Abd-Elhafiez[1], Moheb Girgis[2], Seham Elaw[1]

[1]*Mathematical and Computer Science Department, Faculty of Science, Sohag University, Egypt*

[2]*Department of Computer Science, Faculty of Science, Minia University, El-Minia, Egypt*

This paper provides a simple and efficient method to detect human faces in videos and recognize persons within the video according to a preset database of known persons. The proposed system consists of three main steps. The first step is skin-like regions detection in CIE-Luv color space. The second step is face detection based on skin-like regions, contour detection and geometrical properties such as face shape. The third step is face verification, in which, each face is compared with a gallery of known faces and the location of the best matched one is returned. Face verification step uses variance formula and skin to non-skin percentage in each facial feature to compare the test face and the faces images in the known database. The proposed system was tested on many different videos with different number of persons in the video. The detected faces are compared with a preset database of known images. Experimental results show that the proposed system is efficient enough to detect faces in different lighting conditions, head pose and face expressions. The results of verification step show that the proposed system is able to retrieve faces from a database with good accuracy in a reasonable computational time compared with classical method, variance estimation method and facial extraction method.

11th International Conference on Computer Engineering & Systems, Cairo, (2016) 147-154

Estimation for the exponentiated Weibull model with adaptive Type-II progressive censored schemes

Mashail M. AL Sobhi[a] and Ahmed A. Soliman[b,c]

[a]*Mathematics Department, Umm-Al-Qura University, Makkah, Saudi Arabia*

[b]*Mathematics Department, Islamic University, Madina, Saudi Arabia*

[c]*Department of Mathematics, Faculty of Science, Sohag University, Sohag, 82524, Egypt*

In reliability and life testing experiments, the censoring scheme which can balance between the total time spent for the experiment, the number of units used and the efficiency of statistical inference based on the results of the experiment is desirable. An adaptive Type-II progressive censoring schemes have been shown to be useful in this case. This article deals with the problem of estimating parameters, reliability and hazard functions of the two-parameter exponentiated Weibull distribution, under adaptive progressive Type II censoring samples using Bayesian and non-Bayesian approaches. Maximum likelihood estimates (M LEs) are proposed for unknown quantities. The asymptotic normality of the MLEs are used to compute the approximate confidence intervals for these quantities, parametric bootstrap confidence intervals are also constructed. Markov Chain Monte Carlo (MCMC) samples using importance sampling scheme are used to produce the Bayes estimates and the credible intervals for the unknown quantities. A real-life data-set is analyzed to illustrate the proposed methods of estimation. Finally, results from simulation studies assessing the performance of the maximum likelihood and Bayes estimators are discussed.

Applied Mathematical Modelling 40, (2016) 1180-1192

Cells distribution in the modeling of fibrosis, Comment on "Towards a unified approach in the modeling of fibrosis: A review with research perspectives" by Martine Ben Amar and Carlo Bianca

Mahmoud Abdel-Aty
University of Science and Technology, Zewail City, 6th of October, Giza, Egypt
Mathematics Department, Faculty of Science, Sohag University, Egypt

The modeling of a complex system requires the analysis of all microscopic constituents and in particular of their interactions [1]. The interest in this research field has increased considering also recent developments in the informa-tion sciences. However interaction among scholars working in various fields of the applied sciences can be considered the true motor for the definition of a general framework for the analysis of complex systems. In particular biological systems constitute the platform where many scientists have decided to collaborate in order to gain a global description of the system. Among others, cancer–immune system competition (see [2]and the review papers [3,4]) hasattracted much attention.

Physics of Life Reviews, 17 (2016) 86-87

New Perspectives on Nonlinear Multi-Atoms Interacting with a Cavity Field

Y. S. El-Saman[1], S. Abdel-Khalek[1,2], A. Badawi[3] and M. Abdel-Aty[3]
[1]Department of Mathematics, Faculty of Science, Sohag University, Egypt
[2]The Abdus Salam International Centre for Theoretical Physics, Trieste, Italy
[3]University of Science and Technology, Zayed City, 12588 Giza, Egypt

We investigate the entanglement dynamics of two two-level atoms interacting with a quantized cavity field, considering the level shifts produced by the Stark effect. We perform comparisons of the entanglement evolution of this system when the cavity is filled with a Kerr-like medium. The presence of entanglement sudden death and sudden birth using extended Werner-like states is observed. Entanglement is guaranteed to survive and can be easily adapted to allow for periodic behavior. The similar dynamic relations between both the Kerr-like medium and the Stark-shift models are shown.

Appl. Math. Inf. Sci. 10, No. 2 (2016) 421-429

Theorems on q-Frobenius-Euler polynomials under Sym (4)

Serkan Araci[1], Ugur Duran[2], Mehmet Acikgoz[3], and Mahmoud Abdel-Aty[4]

[1]*Department of Economics, Faculty of Economics, Administrative and Social Science, Hasan Kalyoncu University, TR-27410 Gaziantep, Turkey*

[2]*Department of Mathematics, Faculty of Science and Arts, University of Gaziantep, TR-27310 Gaziantep, Turkey*

[3]*Department of Mathematics, Faculty of Science and Arts, University of Gaziantep, TR-27310 Gaziantep, Turkey*

[4]*University of Science and Technology, Zewail City of Science and Technology, Cairo, Egypt*

In this paper, we perform a further investigation for the q-Frobenius-Euler polynomials, and we establish some new symmetric identities which are derived from the fermionic p-adic integral on Z_p. The results derived here are corresponding formulas involving symmetric group of degree four.

Utilitas Mathematica 101 (2016) 129-137

Nonclassical properties and purity of a qubit system in photon-added squeezed thermal states with time-dependent coupling effect

K. Berrada[a,b], S. Abdel-Khalek[b,c]

[a]*Al Imam Mohammad Ibn Saud Islamic University (IMSIU), College of Science, Department of Physics, Riyadh, Saudi Arabia*

[b]*The Abdus Salam International Centre for Theoretical Physics, Strada Costiera 11, Miramare-Trieste, Italy*

[c]*Mathematics Department, Faculty of Science, Sohag University, Sohag, Egypt*

The degree of purity and nonclassical properties for a two-level system interacting with a photon-added squeezed thermal field (PASTF) are described in terms of the physical parameters involved in the whole system state with and without time-dependent coupling effect. Specially, we investigate the influence of the squeezed parameter and photon-added number on the behavior of the linear entropy and the Mandel's parameter. We find that for each value of the photon-added number, there exist critical value of the squeezed parameter for which the linear entropy is maximal and the statistical properties get farther from the trivial case. Moreover, we show that the presence of the time-dependent coupling effect may increase the periodicity time and lead to quench oscillations of the Mandel's parameter during the evolution. Finally, we exploit an interesting relationship between the linear entropy and the Mandel's parameter in terms of the physical parameters.

Physica E, 84 (2016) 361-366

New features of the stationary and moving atom-atom entanglement

S. Abdel-Khalek[a,b,c], S.H.A. Halawani[b]
[a]*Mathematics Department, Faculty ofScience, Sohag University, Sohag, Egypt*
[b]*Mathematics Department, Faculty ofScience, TaifUniversity, Taif, Saudi Arabia*
[c]*The Abdus Salam ICTP, Strada Costiera 11, Miramare-Trieste, Italy*

In this paper, we introduce useful scheme of the atom–atom interaction in the case of absence and presence ofthe atomic motion effect. The quantum entanglement between the two two-level atoms based on concurrence quantifier will be investigated. The dependence atom–atom entanglement on the different system parameters will be examined. Moreover, the influence ofthe atomic motion and initial state setting on the dynamical behavior ofthe entanglement between two atoms will be discussed. Furthermore, we have explored some important phenomena related to the entanglement between two atoms such as entanglement sudden death (ESD) and entanglement sudden birth (ESB). Finally, we have obtained a high amount ofthe atom–atom entanglement by a proper choice ofthe system parameters in the case of stationary and moving atoms.

Optik, 127 (2016) 9020-9025

Erratum to ‘‘Effect of the time-dependent coupling on a superconducting qubit-field system under decoherence: Entanglement and Wehrl entropy’’

S. Abdel-Khalek[a,b], K. Berrada[b,c], H. Eleuch[d,e]
[a]*Mathematics Department, Faculty of Science, Sohag University, 82524 Sohag, Egypt*
[b]*The Abdus Salam International Centre for Theoretical Physics, Strada Costiera 11, Miramare-Trieste, Italy*
[c]*Al Imam Mohammad Ibn Saud Islamic University (IMSIU), College of Science, Department of Physics, Riyadh, Saudi Arabia*
[d]*Department of Physics, McGill University, 3600 rue University, Montreal, QC, H3A 2T8, Canada*
[e]*Department of Physics, Université de Montréal, 2900 boul. douard-Montpetit, Montreal, QC, H3T 1J4, Canada*

The dynamics of a superconducting (SC) qubit interacting with a field under decoherence with and without time-dependent coupling effect is analyzed. Quantum features like the collapse revivals for the dynamics of population inversion, sudden birth and sudden death of entanglement, and statistical properties are investigated under the phase damping effect. Analytic results for certain parametric conditions are obtained. We analyze the influence of decoherence on the negativity and Wehrl entropy for different values of the physical parameters. We also explore an interesting relation between the SC-field entanglement and Wehrl entropy behavior during the time evolution. We show that the amount of SC-field entanglement can be enhanced as the field tends to be more classical. The studied model of SC-field system with the time-dependent coupling has high practical importance

Annals of Physics, 361 (2016) 564-565.

Entanglement and Statistical Properties of a System Consisting of Three-Level Atom Interacting with a Nonlinear Kerr Medium Field

S. Abdel- Khalek[a,b,c], M.A. Al-Rajhi[d] and K. Berrada[a,d]

[a]The Abdus Salam International Centre for Theoretical Physics, Strada Costiera 11, Miramare-Trieste, Italy

[b]Mathematics Department, Faculty of Science, Sohag University, Sohag, Egypt

[c]Mathematics Department, Faculty of Science, Taif University, Taif, Saudi Arabia

[d]Al Imam Mohammad Ibn Saud Islamic University (IMSIU), College of Science, Department of Physics, Riyadh, Saudi Arabia

In this paper, we present a proper quantum system to perform different tasks of quantum information processing with optimal conditions. We study the populations, entanglement, and nonclassical properties of a system consisting of three level atom interacting with a nonlinear Kerr medi um field constructed in the framework of generalized Heisenberg algebra. We quantify these quantities in terms of different parameters involved in the whole system considering the case of moving and stationary atom in the real experimental meaning of the coupling constant. The nonlinearity introduced by th ese kinds of fields play a useful role to create high amount of entanglement during the time evolution. Interestingly, the relationship between the degree of nonlinearity and robust of entanglement is explored in this present model.

Acta Physica Polonica A 129 (2016), 1083-1088

Numerical Study of Some Statistical Quantities for Quantum Systems under Damping Effects

K. J. M. Abu Alnaj[1], S. E. Waheed[1,2], and S. Abdel-Khalek[1,3]

[1]*Mathematics Department, Faculty of Science, Taif University Taif, Saudi Arabia*

[2]*Mathematics department, Faculty of Science, Benha University Benha, Egypt*

[3]*Mathematics department, Faculty of Science, Sohag University Sohag, Egypt*

In this paper, we present a p000 We present a model of interaction between a four-level atom and the cavity field initially prepared in the coherent state in the presence of the phase damping effect. We discuss the atom–field entanglement and statistical properties under the damping effect in view of numerical calculations. We use the Mandel parameter as a quantifier of the statistical properties of the field; moreover, we study the different effects of the collective parameters in the master equation on the dynamical behavior of the field statistical properties and the entanglement measured by the negativity. Finally, we explore the link between the entanglement and statistical properties in view of the numerical results during the time evolution.

Journal of Russian Laser Research, 37 (3) (2016) 219-226

Information dynamics for a non-degenerate two-photon JC model in phase damping cavity

K. Berrada[a,b], S. Abdel-Khalek[b,c]
[a]Al Imam Mohammad Ibn Saud Islamic University (IMSIU), College of Science, Department of Physics, Riyadh, Saudi Arabia
[b]The Abdus Salam International Centre for Theoretical Physics, Strada Costiera 11, Miramare-Trieste, Italy
[c]Mathematics Department, Faculty of Science, Sohag University, Sohag, Egypt

The degree of purity and nonclassical properties for a two-level system interacting with a photon-added squeezed thermal field (PASTF) are described in terms of the physical parameters involved in the whole system state with and without time-dependent coupling effect. Specially, we investigate the influence of the squeezed parameter and photon-added number on the behavior of the linear entropy and the Mandel's parameter. We find that for each value of the photon-added number, there exist critical value of the squeezed parameter for which the linear entropy is maximal and the statistical properties get farther from the trivial case. Moreover, we show that the presence of the time-dependent coupling effect may increase the periodicity time and lead to quench oscillations of the Mandel's parameter during the evolution. Finally, we exploit an interesting relationship between the linear entropy and the Mandel's parameter in terms of the physical parameters.

Physica E, 84 (2016) 361-366

Dynamics of Correlations in the Presences of Intrinsic Decoherence

Nour Zidan
Department of Mathematics, Faculty of Science, Sohag University, Sohag, 82524, Egypt

The dynamics of a mixed spin system governed by XXZ model in additional to an intrinsic decoherence is investigated. The behavior of quantum correlation and the degree of entanglement between the two subsystems is quantified by using measurement-induced disturbance and the negativity, respectively. It is shown that, the phenomena of long-lived entanglement appears for larger values of intrinsic decoherence parameters. The degree of entanglement and quantum correlation depend on the dimensions of subsystems which are pass through the external field and the initial states setting. We show that the negativity for some initial classes is more robust than the measurement-induced disturbance, while for some other initial classes the quantum correlations are more robust than entanglement.

International Journal of Theoretical Physics 55, (2016) 1274-1284

On Fuzzy Soft Irresolute Functions

S. E. Abbas[a,b], E. El-sanowsy[b], A. Atef[c]

[a]*Department of Mathematics, Faculty of Science, Jazan University, Saudi-Arabia*

[b]*Department of Mathematics, Faculty of Science, Sohag 82524, Egypt*

[c]*Preparatory Year Deanship, King Saud University, Saudi-Arabia.*

In this paper, semi-open and semi-closed sets on a fuzzy soft topological space in Sostak sense are introduced and some properties have been studied. Fuzzy soft semiclosure and fuzzy soft semi-interior operators are introduced and studied. Also, semicontinuous, semi-open, semi-closed and irresolute fuzzy soft functions on a fuzzy soft topological space are introduced and characterized.

The Journal of Fuzzy Mathematics, 24 (2016) 465-482

(r,s)-$(\tau_{12},\tau_{12}^{*})$-θ-Generalized double fuzzy closed Sets in bitopological spaces

E. El-Sanousy

Department of Mathematics, Faculty of Science, Sohag University, Sohag, 82524, Egypt

In this paper, we introduce the notion of $(r,s)=(i,j)-\theta$ generalized double fuzzy closed sets in double fuzzy bitopological spaces. A new θ-double fuzzy closure C_{12}^{θ} on double fuzzy bitopological spaces by using double supra fuzzy topological spaces are defined. Furthermore, generalized double fuzzy θ-continuous (resp. irresolute) and double fuzzy strongly θ-continuous mappings are introduced and some of their properties studied.

Journal of the Egyptian Mathematical Society, 24 (2016) 574-581

Spacelike and timelike admissible Smarandache curves in pseudo-Galilean space

M. Khalifa Saad
Math. Dept., Faculty ofScience, Islamic University in Madinah, Saudi Arabia
Math. Dept., Faculty ofScience, Sohag University, 82524 Sohag, Egypt

In this paper, we study space and timelike admissible Smarandache curves in the pseudo-Galilean space G_1^3. Also, we obtain Smarandache curves of the position vector of space and timelike arbitrary curve with some of its special curves. Finally, we defray and illustrate some examples to confirm our main results.

Journal of the Egyptian Mathematical Society, 24 (2016), 416-423

Decomposition of bilinear forms as sums of bounded forms

Mohamed Elmursi
Department of Mathematics, Faculty of Science, Sohag University, Sohag, 82524, Egypt

The problem of decomposition of bilinear forms which satisfy a certain condition has been studied by many authors by example in [Hag]: Let H and K be Hilbert spaces and let A, C ∈ B(H), B, D ∈ B(K). Assume that u : H × K → C a bilinear form satisfies

$$|u(x,y)| \le \|Ax\|\|By\| + \|Cx\|\|Dy\|$$

for all x ∈ H and y ∈ K. Then u can be decomposed as a sum of two bilinear forms

$$u = u_1 + u_2$$

where,

$$|u_1(x,y)| \le \|Ax\|\|By\|, |u_2(x,y)| \le \|Cx\|\|Dy\|, \forall x \in H, y \in K.$$

U. Haagerup conjectured that an analogous decomposition as a sum of bounded bilinear forms is not always possible for more than two terms. The aim of current paper is to investigate this problem. In the finite dimensional case, we give a necessary and sufficient criterion for such a decomposition. Finally, we use this criterion to give an example of a sesquilinear form u, even on a two-dimensional Hilbert space, which is majorized by the sum of the moduli of three bounded forms b_1, b_2 and b_3, but can not be decomposed as a sum of three sesquilinear forms u_i where each u_i is majorized by the corresponding $|b_i|$.

J. Operator theory, 75 (2016) 319-336

An Analytical Technique for Solving Nonlinear Oscillators of the Motion of a Rigid Rod Rocking Bock and Tapered Beams

G. M. Ismail
[b]*Department of Mathematics, Faculty of Science, Sohag University, Sohag, 82524, Egypt*

In this paper, a new analytical approach has been presented for solving strongly nonlinear oscillator problems. Iteration perturbation method leads us to high accurate solution. Two different high nonlinear examples are also presented to show the application and accuracy of the presented method. The results are compared with analytical methods and with the numerical solution using Runge-Kutta method in different figures. It has been shown that the iteration perturbation approach doesn't need any small perturbation and is accurate for nonlinear oscillator equations.

Journal of Applied and Computational Mechanics, 2 (2016) 29-34

Analytical solution of strongly nonlinear Duffing oscillators

A. M. El-Nagger[a], G. M. Ismail[b]
[a]*Department of Mathematics, Faculty of Science, Benha University Benha, 13518, Egypt*
[b]*Department of Mathematics, Faculty of Science, Sohag University, Sohag, 82524, Egypt*

In this paper, a new perturbation technique is employed to solve strongly nonlinear Duffing oscillators, in which a new parameter $\alpha = \alpha(\varepsilon)$ is defined such that the value of α is always small regardless of the magnitude of the original parameter ε. Therefore, the strongly nonlinear Duffing oscillators with large parameter ε are transformed into a small parameter system with respect to α. Approximate solution obtained by the present method is compared with the solution of energy balance method, homotopy perturbation method, global error minimization method and lastly numerical solution. We observe from the results that this method is very simple, easy to apply, and gives a very good accuracy not only for small parameter ε but also for large values of ε.

Alexandria Engineering Journal, 55 (2016) 1581-1585

Periodic Solutions of the Duffing Harmonic Oscillator by He's Energy Balance Method

A. M. El-Nagger[a], G. M. Ismail[b]
[a]*Department of Mathematics, Faculty of Science, Benha University Benha, 13518, Egypt*
[b]Department of Mathematics, Faculty of Science, Sohag University, Sohag, 82524, Egypt

Duffing harmonic oscillator is a common model for nonlinear phenomena in science and engineering. This paper presents He´s Energy Balance Method (EBM) for solving nonlinear differential equations. Two strong nonlinear cases have been studied analytically. Analytical results of the EBM are compared with the solutions obtained by using He´s Frequency Amplitude Formulation (FAF) and numerical solutions using Runge-Kutta method. The results show the presented method is potentially to solve high nonlinear oscillator equations.

Journal of Applied and Computational Mechanics, 2 (2016) 35-41

Random fixed point theorems with an application to a random nonlinear integral equation

R. A. Rashwan[a], H. A. Hammad[b]

[a]*Department of Mathematics, Faculty of Science, Assuit University, Assuit 71516, Egypt*
[b]*Department of Mathematics, Faculty of Science, Sohag University, Sohag 82524, Egypt*

In this paper, stochastic generalizations of some fixed point for operators satisfying random contractively generalized hybrid and some other contractive condition have been proved. We discuss also the existence of a solution to a nonlinear random integral equation.

Journal of Linear and Topological Algebra, 5 (2016) 119-133

Random Common Fixed Point Theorem for Random Weakly Subsequentially Continuous Generalized Contractions with Application

Rashwan. A. Rashwan[a], Hammad. A. Hammad[b]

[a]Department of Mathematics, Faculty of Science, Assuit University, Assuit 71516, Egypt

[b]Department of Mathematics, Faculty of Science, Sohag University, Sohag 82524, Egypt

In this paper, we prove random common fixed point theorem for two pairs of random self mappings under a generalized contractive condition using subsequential continuity with compatibility of type (E). An example is given to justify our theorem. Our results in randomness extend and improve the results of S. Beloul [4]. Finally, we give an application to discuss the existence of a solution of random Hammerstein integral equations.

International Journal of Pure and Applied Mathematics, 109 (2016) 813-826

Rotational effect on Rayleigh, Love and Stoneley waves in non-homogeneous fibre-reinforced anisotropic general viscoelastic media of higher order

S.M. Abo-Dahab[1,2], A.M. Abd-Alla[1,3,*], Aftab Khan[4]

[1]Mathematics Department, Faculty of Science, Taif University 888, Saudi Arabia

[2]Mathematics Department, Faculty of Science, SVU, Qena 83523, Egypt

[3]Mathematics Department, Faculty of Science, Sohag University, Egypt

[4]Department of Mathematics, COMSATS, Institute of Information, Park Road, Chakshahzad, Islamabad, Pakistan

In this paper, we investigated the propagation of surface waves in a nonhomogeneous rotating fibre-reinforced viscoelastic anisotropic media of higher order of nth order including time rate of strain. The general surface wave speed is derived to study the effect of rotation on surface waves. Particular cases for Stoneley, Love and Rayleigh waves are discussed. The results obtained in this investigation are more general in the sense that some earlier published results are obtained from our result as special cases. Also results for homogeneous media can be deduced from this investigation. For order zero our results are well agreed to fibre-reinforced materials. Also by neglecting the reinforced elastic parameters, the results reduce to well known isotropic medium. It is also observed that, surface waves cannot propagate in a fast rotating medium. Comparison was made with the results obtained in the presence and absence of rotation and parameters for fibre-reinforced of the material medium Numerical results are given and illustrated graphically. The results indicate that the effect of rotation and parameters for fibre-reinforced of the material are very pronounced.

Structural Engineering and Mechanics, 58, (2016) 181-197.

Effect of the Rotation on a Non-Homogeneous Infinite Elastic Cylinder of Orthotropic Material with Magnetic Field

A.M. Abd-Alla[1,2,*], S.M. Abo-Dahab[1,3], Hind A. Alotaibi[1]
[1]*Department of Mathematics, Faculty of Science, Taif University 888, Saudi Arabia*
[2]*Department of Mathematics, Faculty of Science, Sohag University, 243, Egypt*
[3]*Department of Mathematics, Faculty of Science, South Valley University, Qena 83523, Egypt*

The present investigation is concerned with a study effect of non-homogeneous and magnetic field in rotating orthotropic infinite elastic circular cylinder subjected to certain boundary conditions. Closed form solutions are obtained for rotating orthotropic elastic cylinder and magnetic field with constant thickness for three cases: (1) a solid cylinder; (2) cylinder with a circular hole at the centre and (3) cylinder mounted on a circular rigid shaft. Analytical expressions for the components of the displacement and the stress in different cases are obtained. The effect of the rotation, magnetic field and non-homogeneity on the displacement and stress are studied. Numerical results are given and illustrated graphically for each case is considered. The effects, rotating, magnetic field and non-homogeneity are discussed. Comparisons are made with the results predicted in the presence and absence of rotation and magnetic field. The results indicate that the effect of the magnetic field, rotation and non-homogeneity are very pronounced.

Journal of Computational and Theoretical Nanoscience, 13, (2016) 4476-4492.

Green Lindsay model on reflection and refraction of p- and SV-waves at interface between solid-liquid media presence in magnetic field and initial stress

S.M. Abo-Dahab[1,2], A.M. Abd-Alla[1,3,*]
[1]*Department of Mathematics, Faculty of Science, Taif University 888, Saudi Arabia*
[2]*Department of Mathematics, Faculty of Science, South Valley University, Qena 83523, Egypt*
[3]*Department of Mathematics, Faculty of Science, Sohag University, 243, Egypt*

The present investigation is 0000In this paper, the reflection and transmission of thermoelastic wave at a solid-liquid interface in presence of initial stress and magnetic field is investigated in context of GL model. After solving the governing equations, we can find the two reflection and refraction coefficients of incident p-(pressure) and SV- (shear vertical) waves in presence of initial stress and magnetic field. The boundary conditions at the interface that: (i) displacement continuity, (ii) vanishing the tangential displacement, (iii) continuity of normal force per unit initial area, (iv) tangential force per unit initial area must vanish, and (v) continuity of temperature is applied. The appropriate expressions to find the amplitude ratios for the two incidence waves (p- and SV-waves) have been obtained. A numerical example is considered for the reflection and transmitted coefficients of the incident waves, in which we study the effect of initial stresses and magnetic field. The results obtained are presented graphically for the effect of magnetic field and initial stress to display the phenomena physical meaning.

Journal of Vibration and Control, 22, (2016) 2885-2897.

SV-waves incidence at interface between solid-liquid media under magnetic field, initial stress and two thermal relaxation times

S.M. Abo-Dahab[1,2], A.M. Abd-Alla[1,3,*], M Marin[4]
[1]Department of Mathematics, Faculty of Science, Taif University 888, Saudi Arabia
[2]Department of Mathematics, Faculty of Science, South Valley University, Qena 83523, Egypt
[3]Department of Mathematics, Faculty of Science, Sohag University, 243, Egypt
[4]Department of Mathematics, Transilvania University of Brasov, Romania

In this paper we investigated the propagation of SV-waves under effect of the magnetic field, initial stress and two thermal relaxation times. The problem of reflection and transmission of thermoelastic waves at a solid-liquid interface in presence of initial stress and magnetic field has been investigated subjected to certain boundary conditions. The appropriate expressions to find the amplitudes ratios for the incident wave (SV-waves) have been obtained. The reflection and transmitted coefficients for the incident SV-waves are computed numerically, considering the initial stress, relaxation times, and magnetic field effect and presented graphically. The results indicate that the effects of magnetic field, initial stress and two thermal relaxation times are very pronounced.

Journal of Vibration and Control, 22, (2016) 3426-3428.

Rotation effect on peristaltic transport of a Jeffrey fluid in an asymmetric channel with gravity field

A.M. Abd-Alla[a,c,*], S.M. Abo-Dahab[a,b]
[a]Math. Dept., Faculty of Science, Sohag University, Egypt
[b]Math. Dept., Faculty of Science, SVU, Qena 83523, Egypt
[c]Math. Dept., Faculty of Science, Taif University, 888, Saudi Arabia

In this paper, the peristaltic flow of a Jeffrey fluid in an asymmetric rotating channel is studied under long wavelength and low Reynolds number assumptions are investigated. Closed form expressions for the pressure gradient, pressure rise, stream function, axial velocity and shear stress on the channel walls have been computed numerically. The effects of the ratio of relaxation to retardation times, time-mean flow, rotation, the phase angle and the gravity field on the pressure gradient, pressure rise, streamline, axial velocity and shear stress are discussed in detail and shown graphically. The results indicate that the effect of the ratio of relaxation to retardation times, time-mean flow, rotation, the phase angle and the gravitational field are very pronounced in the phenom-ena. Comparison was made with the results obtained in the asymmetric channel and symmetric channel.

Alexandria Engineering Journal 55, (2016), 1725-1735.

SV-waves incidence at interface between solid-liquid media under Electromagnetic field and initial stress in the context of three thermoelastic theories

A. M. Abd-Alla[a,b,*], S. M. Abo-Dahab[a,c], A. A. Kilany[a]
[a]*Department of Mathematics, Faculty of Science, Taif University, Taif, Saudi Arabia;*
[b]*Department of Mathematics, Faculty of Science, Sohag University, Sohag, Egypt;*
[c]*Department of Mathematics, Faculty of Science, South Valley University, Qena, Egypt*

In this article, we studied the propagation of SV-waves under the effect of electromagnetic field and initial stress for three models in thermoelasticity: The couple and Green–Lindsay theories as well as the dual-phase-lag theory. The problem of reflection and transmission of thermoelastic wavesatasolid–liquid interface in the presence of electromagnetic fields and initial stress we investi-gated subjected to certain boundary conditions. The appropriate expressions to find the amplitude ratios of the incident waves (SV-waves) were obtained. The reflection and transmission coefficients for the incident SV-waves were computed numerically. The effect of electric field, magnetic field, and initial stress were illustrated graphically. Comparisons were made with the obtained results in the presence and absence of considered variables and displayed graphically. The results indicate that the e ect of electric field, magnetic field, and initial stress on SV-waves incidence at the interface between solid–liquid media are very pronounced.

Journal of Thermal Stresses, 39, (2016), 960-976.

Reflection of Plane Waves from Electro-magneto-thermoelastic Half-space with a Dual-Phase-Lag Model

A. M. Abd-Alla[1,2,*], Mohamed I. A. Othman[1,3], S. M. Abo-Dahab[1,4]
[1]*Math. Dept., Faculty of Science, Taif University 888, Saudi Arabia*
[2]*Department of Mathematics, Faculty of Science, Sohag University, Egypt*
[3]*Math. Dept., Faculty of Science, Zagazig University, P.O. Box 44519, Zagazig, Egypt*
[4]*Math. Dept., Faculty of Science, South Valley University, Qena 83523, Egypt*

The aim of this paper is to study the reflection of plane harmonic waves from a semi-infinite elastic solid under the effect of magnetic field in a vacuum. The expressions for the reflection coefficients, which are the relations of the amplitudes of the reflected waves to the amplitude of the incident waves, are obtained. Similarly, the reflection coefficient ratio variations with the angle of incident under different conditions are shown graphically. Comparisons are made with the results predicted by the dual-phase-lag model and Lord-Shulman theories in the presence and absence of magnetic field.

Computer Materials and Continua, (2016), 1-17

Bayesian Estimation of Exponentiated Weibull Distribution Under Partially Acceleration Life Tests

Mashail M. AL Sobhi Ahmed A. Soliman Abd EL-Baset A. Ahmad[1], Ahmed A. Soliman[2], Manal M. Yousef[1]

[1]*Department of Statistics, Faculty of Science, Assiut University, Asyut, Egypt*

[2]*Department of Mathematics, Faculty of Science, Sohag University, Sohag, 82524, Egypt*

This paper presents statistical methods for analyzing partially accelerated life test from constant-stress test. The lifetime of items under use condition follows the two-parameter exponentiated Weibull distribution. Based on progressively Type-II censored sample, the classical maximum likelihood method as well as a fully Bayesian method based on Lindley (Trabajos de Estadistica 31:223–237, 1980) approximation form and the Markov chain Monte Carlo technique are developed for inference about model parameters and acceleration factor. Furthermore, approximate confidence intervals and credible intervals are presented. A Monte Carlo simulation is given to study the precision of different estimators..

Bull. Malays. Math. Sci. Soc. 39, (2016), 227-244.

Bayesian estimation of P[Y < X] Based on Record V alues from the Lomax Distribution and MCMC Technique

M. A. W Mahmoud[a], R. M. El-Sagheer[a], A. A . Soliman[b,c], A. H. Abd Ellah[c]

[a] *Department of Statistics, Faculty of Science Al-Azhar University, Cairo, Egypt*

[b]*Mathematics Department, Islamic University, Madina, Saudi Arabia*

[c]*Department of Mathematics, Faculty of Science, Sohag University, Sohag, 82524, Egypt*

In reliability and life testing experime Our interest is in estimating the stress-strength reliability R=P[Y < X], where X and Y follow the Lomax distribution with common scale parameter. We discuss the problem in the situation where the stress measurements and the strength measurements are both in terms of records. Firstly, we obtain the MLE of R in general case (the common scale parameter is unknown). The MLE of the three unknown parameters can be obtained by solving one non-linear equation. We provide a simple fixed point type algorithm to find the MLE. We propose percentile bootstrap confidence intervals of R. A Bayes point estimator of R, and the corresponding credible interval using the MCMC sampling technique have been proposed. Secondly, assuming the common scale parameter is known, the MLE of R is obtained. Using exact distributions of the MLEs of the two unknown parameters, we construct the exact confidence interval of R. In this case, Bayes estimators have been obtained using Lindley's approximations. Analysis of a simulated data set has been presented for illustrative purposes. Finally, the different proposed methods have been compared via Monte Carlo simulation study.

Journal of Modern Applied Statistical Methods 15, (2016), 488-510.

قسم الفيزياء
Physics Department

Physics

قسم الفيزياء
Physics Department

Properties of TiAlN coating deposited by MPIIID on TiN substrates

F. M. El-Hossary, A. M. Abd El-Rahman, M. Raaif, D. A. Ghareeb
Physics Department, Faculty of Science, Sohag University,Sohag 82524, Egypt

Metal plasma immersion ion implantation and deposition (MPIIID) is employed to produce TiAlN hard coatings on Ti substrate. To improve the load-bearing capacity of Ti substrate, nitrogen PIII is used to prepare a bearing TiN layer on Ti-base substrate. The MPIIID process is performed using Ti50:Al50 target for different nitrogen/ argon gas fractions. The effect of N_2/Ar gas ratio on the microstructure, mechanical and tribological properties of TiAlN coatings has been studied. The plastic microhardness of TiAlN increases with increasing the nitrogen gas fraction to reach a maximum value of 30 GPa at 100 % N_2. The plasticity index and the resistance to plastic deformation increase with increasing the nitrogen gas fraction. The wear volume loss of TiAlN coating deposited on TiN substrate decreases by a factor of 10^3 in comparison with pure Ti. Moreover, the friction coefficient decreases from nearly 0.8 for Ti to 0.25 for TiAlN coatings. The enhanced mechanical and tribological properties of the coating are correlated with the formation of TiAlN hard phase. This phase has randomoriented microstructure, finer grain size, high oxidation resistance and residual internal stress. Moreover, the TiN interface acts as a barrier for the motion of dislocations.

Appl. Phys. A (2016) 122:242

Counting of the Fusion Neutron Yield from the Pulse Height of Time-Of-Flight Spectrometer involves Ultrafast Timing/Counting Plastic Scintillator

A. Youssef
Physics Department, Faculty of Science, Hail University, Hail 2440, Saudi Arabi
Physics Department, Faculty of Science, Sohag University, Sohag 82524, Egypt

Neutron yield is considered the crucial factor to judge the successful achieving of Inertial Confinement Fusion (ICF). Plastic scintillators, which are usually used as a part of time-of-flight (TOF) spectrometer, are common detectors for neutron detection and spectroscopy. Here, a comprehensive study including an analytical model for counting the ICF neutrons from the output pulse height of a TOF spectrometer is presented. The number of recoiled protons due to elastic scattering by the neutrons incident on a plastic scintillator is calculated at any neutron energy over the energy range $0.3 < E < 30$ MeV. The total deposited energy due to specific energy loss of the recoiled protons scattered by 2.45 and 14.1 MeV neutrons is computed depending on the neutron number. Next, the fluorescence light energy, the number of photoelectrons, and the current peak (I_{peak}) of the output pulse are calculated for 2.45 and 14.1 MeV neutrons as a function of neutron number. In addition, the average value of I_{peak} produced by an incident neutron with certain energy is calculated and hence the number of the incident neutrons is computed from the I_{peak} value at any neutron energy. The analytical model is valid for counting the neutron yield of both implosion and fast ignition approaches of ICF. The methodology of calculations is suitable for all types of plastic scintillators. The calculated neutron spectra are compared to the available experimental data measured by the ultrafast timing/counting BC-422Q plastic scintillator which is the proper one to detect the ICF neutrons.

International Journal of Physics and Astronomy, 28(1)(2016) 1177.

Counting of ultraintense laser-driven neutrons from the pulse height of time-of-flight detector includes ultrafast timing plastic scintillator

A. Youssef
Physics Department, Faculty of Science, Hail University, Hail 2440, Saudi Arabi
Physics Department, Faculty of Science, Sohag University, Sohag 82524, Egypt

The scintillation process is one of the most important methods available for neutron detection and spectroscopy. The radioactive isotopes used in calibration of the scintillators cannot provide the required accurate measurement of their response. Here, a comprehensive study including a simple model to calculate the scintillation response of plastic scintillators to high fluxes of neutrons produced by the ultraintense lasers is presented. The number of recoiled protons due to elastic scattering by the neutrons incident on a plastic scintillator is calculated at any neutron energy over the energy range 0.3 < E < 30 MeV. The specific energy loss, the light energy, and the range of the recoiled protons are calculated over the same energy range. As well, the current peak of the electrical signal produced by a photomultiplier tube coupled to the scintillator is given as a function of the neutron energy. Counting of the neutrons incident on the scintillator from the current peak is computed depending on the neutron energy over the energy range 0.3 < E < 30 MeV. The calculated spectra are compared with those obtained from calibration for the available experimental data.

Journal of Instrumentation, 11 (2016) P02009.

Achievement of laser fusion with high energy efficiency using a mixture of D and T ions

A. Youssef[1,2], M. Haparir[2]
[1]Physics Department, Faculty of Science, Hail University, Hail 2440, Saudi Arabi
[2]Physics Department, Faculty of Science, Sohag University, Sohag 82524, Egypt

A mixture of deuterium (D) and tritium (T) is the most likely fuel for laser-driven inertial confinement fusion (ICF) reactors and hence DD and DT are the fusion reactions will fire these reactors in the future. Neutrons produced from the two reactions will escape from the burning plasma, in the reactor core, and they are the only products possible to be measured directly. DT/DD neutron ratio is crucial for evaluation of T/D fuel ratio, burn control, tritium cycle and alpha particle self-heating power. To measure this ratio experimentally, the neutron spectra of DD and DT reactions have to be measured separately and simultaneously under high neutron counting with sufficient statistics (typically within 10% error) in a very short time and these issues are mutually contradicted. That is why it is not plausible to measure this high priority ratio for reactor performance accurately. Precise calculations of the DT/DD neutron ratio are needed. Here, we introduce such calculations using a three dimensional (3-D) Monte Carlo code at energies up to 40 MeV (the predicted maximum ion acceleration energy with the available laser systems). In addition, the fusion power ratio of DD and DT reactions is calculated for the same energy range. The study indicates that for a mixture of 50% deuterium and 50% triton, with taking into account the reactions D(d,n)3He and T(d,n)4He, the optimum energy value for achieving the most efficient laser-driven ICF is 0.08 MeV.

Journal of Energy Efficiency,5 (2016) 48-58.

Synthesis, characterization and low field magnetotransport of $Nd_{0.6}Sr_{0.4}MnO_3/CrO_3$ composite

A. M. Ahmed, H. F. Mohamed, A. K. Diab, Sara A. Mohamed
Physics department, Faculty of Science, Sohag University 82524, Sohag, Egypt

$(Nd_{0.6}Sr_{0.4}MnO_3)_{1-x}/(CrO_3)x$with x=0.0–0.030 step 0.005 weight % composites have been prepared by the solid state reaction process. The X-ray and scanning electron microscopic manifest that all composites are a single orthorhombic phase and there are no CrO_3 grains separated from NdSrMnO matrix. The electrical measurements have revealed an increase of resistivity and a decrease of metal semiconductor transition with increasing CrO_3. The composite x=0.025 has largest magnetoresistance nearly one hundred percent at room temperature.

Indian J Phys Received: 16 February 2016 / Accepted: 29 June 2016.

Annealing temperature effect on magnetic and magnetocaloric properties of manganites

Abd El-Moez A. Mohamed[a,b], V. Vega[b, c], M. Ipatov[d], A. M. Ahmed[a], B. Hernando[b]
[a]Physics Department, Faculty of Science, Sohag University, Sohag 82524, Egypt
[b]Physics Department, Faculty of Science, Oviedo University, Oviedo 33007, Spain
[c]Laboratory of Nanoporous Membranes, Oviedo University, Oviedo 33006, Spain
[d]Materials Physics Department, Faculty of Chemistry, Basque Country University, San Sebastian 20018, Spain

In this work, we investigate the effect of annealing process at different temperatures (600 and 800 ^oC) on structural, magnetic and magnetocaloric properties of $La_{0.7}Ba_{0.3}MnO_3/xTiO_2$ system with x =0.04 and 0.06. Crystal structure analysis shows the R-3c rhombohedral symmetry for composites in both annealing temperatures indicating structure stability. Magnetization and coercive field of doped composites increase with increasing annealing temperature, while there is no effect on their Curie temperature (T_c) that remains constant at 348 K due to the TiO_2- $La_{0.7}Ba_{0.3}MnO_3$interaction lack. Increasing annealing temperature is found to be an effective process that can positively affect the magnetocaloric properties. Where, the relative cooling power of doped composites increases from 50 to 62 J/kg for x = 0.04 composite and from 54 to 66 J/kg for x = 0.06 composite with increasing annealing temperature from 600 to 800 ^oC. Moreover, the experimental results of magnetic entropy change have been modulated using Landau theory and the calculations have indicated the negligible contribution of elastic, magnetoelastic and magnetoelectronic coupling in the magnetocaloric properties of $La_{0.7}Ba_{0.3}MnO_3/xTiO_2$ system in both annealing temperatures.

Journal of Alloys and Compounds 665 (2016) 394e403

The annealing influence onto the electrical and magnetic behavior of magnetoresistive/insulator system

A. M. Ahmed, Abd El-Mo'ez A. Mohamed, H. F. Mohamed, A. K. Diab, Aml M. Mohamed, A. E. A. Mazen
Physics department, Faculty of Science, Sohag University 82524, Sohag, Egypt

This investigation is mainly concerned with the effect of annealing temperature (600, 700, 800 and 900 °C) in air for $(La_{0.7}Ba_{0.3}MnO_3)_{1-x}/(NiO)_x$ with x = 0 and x = 0.10 samples. It was shown that the annealing temperature does not affect the structure and parameters of rhombohedral lattice of the samples. However, it is observed that the annealing treatment has a notable effect on the electrical resistivity and the metal-semiconductor transition temperature Tms. Temperature dependent magnetization measurements showed a decrease in Curie temperature T_C with annealing temperature. In the same time, annealing process decreases the magnetoresistance of $La_{0.7}Ba_{0.3}MnO_3$, in contrast to $(La_{0.7}Ba_{0.3}MnO_3)_{0.9}/(NiO)_{0.1}$ composite.

J Low Temperature Physics/Fizika Nizkikh Temperatur, , 42 (9) (2016) 951–958.

Magnetocaloric-transport properties correlation in doped manganites

Abd El-Moez A. Mohamed[a,b], B. Hernando[b], A. M. Ahmed[a]
[a]*Physics Department, Faculty of Science, Sohag University, Sohag 82524,Egypt*
[b]*Physics Department, Faculty of Science, Oviedo University,Oviedo33007,Spain*

This investigation is interested in studying the relation between magnetocaloric effect and transport properties inLa0.7Ba0.3MnO3 manganite compound. The resistivity shows a metal–semiconductor transition at T_{ms} temperature near to its reported Curie temperature (Tc). Magnetic field application decreases resistivity and increases T_{ms} towards higher temperatures. The magnetoresistance shows a peak around Tc and increases in value with the applied magnetic field. A similar behavior has been observed between magnetic entropy change(ΔS), resistivity and magnetoresistance around Tc, this is attributed to the spin order/disorder feature that plays a main role in the magnetocaloric-transport correlation. In spite of this similarity, the correspondence among the experimental ΔS and ΔS based resistivity calculations is missing because of lattice polarons effect on resistivity as a result of the electron–phonon interaction. The magnetocaloric magnetoresistance relation is also studied and results show the contribution of additional factors in the magnetoresistance mechanism other than spin disorder suppression as Jahn– Teller effect and electronic phase separation.

Solid State Communications233(2016)15–17

Magnetoresistive properties of Ni-doped $La_{0.7}Sr_{0.3}MnO_3$ Manganites

Ahmed Mohamed Ahmed, Abd El-Moez Ahmed Mohamed, Medhat Abdelrady Abdellateef, Hassan Ahmed Abd El-Ghanny

$La_{0.7}Sr_{0.3}Mn_{1-x}NixO_3$ (x = 0, 0.025, 0.050 and 0.075) ceramics were prepared by the conventional solid-state reaction method. The partial substitution of Mn by Ni^{2+} Leads to a decrease in cell volume as well as a structural transition from the rhombohedral to the orthorhombic structure. Ni2? doping increases the electrical resistivity, decreases the semiconductor–metal transition temperature (Tms) and relatively enhances the room temperature magnetoresistance (MR), especially in x = 0.025 and around Tms.With respect to conduction mechanism, the small polaron hopping (SPH) and the variable range hopping (VRH) models were used to examine conduction in the semiconducting region.

Rare Met. (2016) 35(7):551–558

Tuning magnetoresistive and magnetocaloric properties via grain boundaries engineering in granular manganites

Abd El-Moez A. Mohamed,[ab] Mohamed A. Mohamed,[c] V. Vega,[b] B. Hernando[b], A. M. Ahmed[a]
[a]Physics Department, Faculty of Science, Sohag University, Sohag 82524, Egypt
[b] Physics Department, Faculty of Science, Oviedo University, Oviedo 33007, Spain
[c]Instituto de Biolog´ıa Molecular y Celular de Plantas, Consejo Superior de Investigaciones Cient´ıcas-Universidad Polit´ecnica de Valencia, Valencia 46022, Spain

In this work, we investigate the effect of interface size on the electrical, magnetoresistive, magnetic and magnetocaloric properties of the $La_{0.7}Ba_{0.3}MnO_3$ (LBMO) manganite compound. This is done by introducing different sizes of secondary phases of Ni and Ag (Ni powder, Ni nanowires, Ag oxide powder and Ag nanoparticles) to the LBMO compound, forming inhomogeneous systems of LBMO/Ni and LBMO/Ag composites. X-Ray diffraction patterns reveal the interaction lack between Ni & Ag interfaces and LBMO compound through the coexistence of their characteristic peaks. This suggests the segregation of these interfaces between LBMO grains, leading to a change in the boundary resistancethat is found to be an interface-size-dependent change. Accordingly, the transport properties of LBMO are changed, where, the resistivity increases and the metal–semiconductor transition temperature decreases with the introduced interfaces. The change in grain boundary resistance enhances the magnetoresistive properties during the promotion of the spin carrier tunnelling process. For instance, the room temperature low field magnetoresistance of the LBMO compound is enhanced from -1.23% to _4.35, -5.25 and -7.9% with the introduction of Ni powder, Ag nanoparticles and Ag oxide powder interfaces, respectively. The dc thermal magnetization measurements show a constant value of the LBMO Curie temperature (T_c) with the introduced interfaces that may be attributed to the complete interaction lack. However, a small decrease is registered in the Tc value of Ni nanowires doped LBMO composite that may be due to the incomplete interaction lack in this composite. Moreover, the magnetocaloric properties of the LBMO compound show a notable enhancement with the introduced interfaces, where its relative cooling power is enhanced from 44 J kg^{-1} to 107, 167, 92 and 94 J $kg^{-1}$with the introduction of Ni powder, Ni nanowires, Ag oxide and Ag nanoparticle interfaces, respectively,at a 3 T applied magnetic field.

RSC Adv., (2016) 6, 77284 (The Royal Society of Chemistry 2016)

Influence of heat treatment on the magnetic and magnetocaloric properties in $Nd_{0.6}Sr_{0.4}MnO_3$ compound

A. M. Ahmed[a], H.F. Mohamed[a], A.K. Diab[a], Sara A. Mohamed[a], S. García-Granda[b], D. Martínez-Blanco[c]

[a]Physics Department, Faculty of Science, Sohag University, 82524, Sohag, Egypt

[b]Departments of Physical and Analytical and Organic and Inorganic Chemistry, University of Oviedo-CINN, 33006, Oviedo, Spain

[c]ServicioCientífico-Tecnico de MedidasMagneticas, University of Oviedo, C/Gonzalo Gutierrez s/n, 33600, Mieres, Asturias, Spain

In the present investigation, the effect of annealing temperature on the structural, electrical transport and the magnetocaloric effect of $Nd_{0.6}Sr_{0.4}MnO_3$manganites have been studied. Rietveld refinement of XRD data reveals that all samples are single phase with a space group (Pnma). Heat treatment enhances the grain size and decreases the porosity. All samples suffer Curie transition from ferromagnetic to paramagnetic. Magnetocaloric parameters have been determined by the analysis of isothermal M (H) curves around Curie temperature (ΔH=2T) for samples. Heat treatment enhances magnetic entropy, which reaches a maximum at T_{an}=900 °C. In addition, the rate cooling power records highest value at T_{an}=700 °C

J. Solid State Sciences 57 (2016) 1- 8.

Magnetoresistive and magnetocaloric response of manganite/insulator system

Abd El-Moez A. Mohamed[a,b], V. Vega[b, c], M. Ipatov[d], A.M. Ahmed[a], B. Hernando[b]

[a]Physics Department, Faculty of Science, Sohag University, Sohag 82524, Egypt b- Physics [b]Department, Faculty of Science, Oviedo University, Oviedo 33007, Spain [c]Laboratory of Nanoporous Membranes, Oviedo University, Oviedo 33006, Spain [d]Materials Physics Department, Faculty of Chemistry, Basque Country University, San Sebastian 20018, Spain

In this work, we have studied structural, electro-magnetic and magnetocaloric properties of $La_{0.7}Ba_{0.3}MnO_3/xTiO_2$ manganite/insulator system with $0 \leq x \leq 0.08$. X-ray diffraction (XRD) shows the coexistence of TiO_2 and La0.7Ba0.3MnO3 phases in doped composites through their characteristic peaks. This reveals their interaction lack preserving the R-3c rhombohedral structure for all composites. Due to interaction lack, TiO_2 is suggested to segregate at grain boundaries weakening grains connectivity and decreasing metal-semiconductor transition temperature (Tms). The segregated TiO_2 hinders conduction between grains leading to carriers tunneling that increases the low field magnetoresistance (LFMR) of $La_{0.7}Ba_{0.3}MnO_3$ from _3% to -3.3, -3.5 and -3.7% for x = 0.02, 0.04 and 0.06 for doped composites. The dc magnetization measurements reveal the constant value of Curie temperature (Tc) and its non impact by doping level referring to the TiO_2-$La_{0.7}Ba_{0.3}MnO_3$ interaction lack. Also, the magnetocaloric properties of La0.7Ba0.3MnO3 are enhanced with TiO_2 doping, where, the relative cooling power (RCP) of La0.7Ba0.3MnO3 has been enhanced from 35 J/kg to 51, 47, 49 and 50 J/ kg for x = 0.02, 0.04, 0.06 and 0.08 composites at 1.5T magnetic field.

Journal of Alloys and Compounds 657 (2016) 495e505

Effect of Annealing Temperature on Electrical and Magnetic Properties of $(Nd_{0.6}Sr_{0.4}MnO_3)_{1-x}/(CrO_3)_x$

A. M. Ahmed, A. K. Diab, H. F. Mohamed and Sara A. Mohamed
Physics department, Faculty of Science, Sohag University, 82524, Sohag, Egypt.

The effect of annealing temperature on structural, electrical and magnetic properties of bulk $(Nd_{0.6}Sr_{0.4}MnO_3)_{0.99}/(CrO_3)_{0.01}$ and $(Nd_{0.6}Sr_{0.4}MnO_3)_{0.98}/(CrO_3)_{0.02}$ compositions are investigated. X-ray diffraction show that $(Nd_{0.6}Sr_{0.4}MnO_3)_{1-x}/(CrO_3)_x$(NSMOC) crystallize in a single-phase rhombohedral structure for the as-prepared and annealed samples. Electrical measurement show a metal-semiconductor transition temperature (Tms) for the two compositions. It is observed that Tms increases with thermal treatment. The magnetoresistance MR has a negative sign and it records the highest value for annealed sample at 800oC for the two compositions. The sign of S is a negative sign for the two compositions. In addition, the calculated Power factor show that the as prepared samples achieve high power factor, therefore our compositions can be considered as the thermoelectric materials.

Int. J. New. Hor. Phys. 3, No. 2, 49-53 (2016)

Improvement of Corrosion resistance of NiTiorthopedic materials by inductively radio frequency plasma

F.M. El-Hossary, S.M. KHALIL, M.A. Kassem, M. Abd EL Lateef, Kh. Lotfy
Physics department, Faculty of Science, Sohag University, 82524, Sohag, Egypt.

Nickel–titanium shape memory alloys (NiTi) are relatively special group of metallic biomaterials. Extraordinary properties of NiTi shape memory alloys are widely employed in medical applications (orthopedics, orthodontics, urology, etc.) owing to their desirable properties, such as superelasticity, relatively low modulus and good corrosion resistance. Furthermore, toxicity and carcinogenesis of Ni ions released from NiTi alloy are very interesting topics. Therefore, it is necessary to produce a surface barrier to impede the out-diffusion of Ni ions from the materials. Inductively coupled radio frequency plasma (ICRFP) was proposed to modify the surface properties. All nitride samples surfaces exhibit outstanding corrosion and Ni out-diffusion resistance. The microstructure of produced layer was analysed by X-ray diffraction. The enhancement of corrosion resistance proved that TiN layers as well as the intermediate Ti2N phase effectively protect surface of the NiTi alloys against nickel ion release.

International Journal for Applied Science, 2 (2016) 23-36.

Effect of Fe doping on the electrical and magnetic properties of $Sn_{1-x}Fe_xO_2$ nanoparticles

Saleh A. Saleh[1,2], Ahmed M. Abdel Hakeem[1,a], Eslam M.M. Ibrahim[1]
[1]*Physics Department, Faculty of Science, Sohag University, 82524 Sohag, Egypt*
[2]*Physics Department, College of Science & Arts, Najran University, P.O. Box 1988 Najran, KSA*

In this work, $Sn_{1-x}Fe_xO_2$ (x = 0.00, 0.02, 0.04, 0.06 and 0.08) nanoparticles have been synthesized using ball-milling method. The average diameter of the nanoparticles decreases from 487 to 216 nm by adding Fe_2O_3 to the tin dioxide. The X-ray diffraction analyses confirms formation of tetragonal structure which is typical feature of SnO_2 compounds. Theoretical density was found to be larger than the corresponding physical one due to the porosity of the materials. The electrical resistivity versus temperature measurements confirm that the undoped and Fe doped SnO_2 nanoparticles are characterized with semiconducting behavior over the whole measurement range of temperature 300–473 K. The magnetic measurements confirm transformation from diamagnetic to ferromagnetic characteristics as Fe doping level reaches x = 0.06.

Eur. Phys. J. Appl. Phys. 73 (2016) 30401.

The Effect of Radio Frequency Plasma Nitriding on Biocompatibility of Nickel-Titanium Shape Memory Alloy

F.M. El-Hossary, S.M. KHALIL, M.A. Kassem, M. Abd EL Lateef, Doha.S.Mohamed, Kh. Lotfy

Nickel-titanium (Ni-Ti) shape memory alloys (SMAs) are attractive materials for orthopedic and dental implants, due to its two intrinsic properties including shape memory effect (SME) and superelasticity (SE), which may not be found in other commonlyused surgical metals. Possible Ni ion release, however, hampers their medical applications, particularly in orthopedic implants where fretting is always expected at the articulating surface. Inductively coupled radio frequency plasma (ICRFP) was employed to alter the surface of equiatomic Ni-Ti discs in order to create a barrier to out-diffusion of Ni ions from the bulk material. The ICRFP experiments were carried out with nitrogen, which promoted the formation of a titanium nitride layer on the surface of the Ni-Ti samples. The present paper explores the biocompatibility and performance of the ICRFP treated and untreated Ni-Ti samples. The results confirm that nitrogen plasma modified Ni-Ti alloys are potentially suitable materials for orthopedics without inducing harmful biological effects.

Journal of Basic and Applied Physics, 5 (2016) 8-20.

Photoproduction of π^0-Mesons from the Nucleon and Deuteron

Eed M. Darwish[1,2], A. Hemmdan[3], N.T. El-Shamy[1,4]
[1]*Physics Department, Faculty of Science, Taibah University, Medinah 41477, Saudi Arabia*
[2]*Physics Department, Faculty of Science, Sohag University, Sohag 82524, Egypt*
[3]*Physics Department, Faculty of Science, Aswan University, Aswan 81528, Egypt*
[4]*Physics Department, Faculty of Girls, Ain Shams University,Cairo 11566, Egypt*

The photoproduction of π^0-mesons from the nucleon and deuteron has been studied for incidents of photon energies up to 1.5 GeV. By using the MAID-2007 model for the process on the nucleon, we predict results for the unpolarized and helicity-dependent total cross sections of the semi-exclusive reaction $\gamma d \rightarrow \pi^0 X$ ($X=np+d$) with the inclusion of rescattering effects. We find that rescattering effects yield a substantially large contribution. The extracted results are compared with the available experimental data and a satisfactory agreement is obtained. In addition, the contribution of $\gamma d \rightarrow \pi^0 X$ ($X=np+d$) to the finite GDH integral has been evaluated by explicit integration up to 1.5 GeV and a total value of 256.96 μb has been obtained. Convergence of the GDH integral has been reached.

Makara Journal of Science,Vol. 20, No. 2 (2016) 55.

Influence of the Choice of *NN* Potential Model on $\gamma d \rightarrow \pi^0 d$ Observables near η-Threshold

Eed M. Darwish[1,2]
[1]*Physics Department, Faculty of Science, Taibah University, Medinah 41477, Saudi Arabia*
[2]*Physics Department, Faculty of Science, Sohag University, Sohag 82524, Egypt*

Influence of the choice of the *NN* potential model governing the deuteron wave function on the observables for coherent π^0-photoproduction on the deuteron near η-threshold is investigated by using a three-body model for the intermediate ηNN system with separable two-body interactions. Results for unpolarized differential cross section and polarization observables are predicted. It is revealed that the choice of the *NN* potential model has a visible effect on the differential cross section and most of the polarization observables, especially in the photon energy range of 600–800 MeV and extreme backward pion angles. We find that the deviation among results obtained by using different deuteron wave functions is quite large. The use of the CD-Bonn *NN* potential for deuteron wave function doubles the differential cross section in this kinematic region. Compared with the experimental data from CLAS collaboration for differential cross section, sizeable discrepancies are found.

Chinese Physics Letters,Vol. 33, No. 4 (2016) 041301.

Thin film CdS/CdTe and CdS/PbS photovoltaic solar cells

H. A. MOHAMED
Faculty of Science, Sohag University, Sohag 82524, Egypt[2]

The current review article has focused on studying the effect of some losses such as the optical and recombination losses on the calculated short-circuit current density, cell efficiency and other cell parameters (such as: fill factor, open-circuit voltage, output power) of CdS/CdTe and CdS/PbS solar cells. The effect of the thickness of front electrode layer, the thickness of window layer (CdS), the thickness of absorber layer (CdTe or PbS), the width of space-charge region, the electron lifetime and the reflectivity from back contact were considered in this study. The optical losses which include the absorption in window layer and front electrode as well as the reflection at various interfaces recorded a value of 23-33% dependence on the thickness and optical properties of the window and front electrode layers. The front surface recombination losses are about 8% depend on the width of space charge region. The back surface recombination losses are mainly depending on the thickness of the absorber layer. The recombination losses in space charge region can be neglected at long electron lifetime of about 10-8 sec. The reflectivity of metallic back contact plays a significant role in enhancing the short current density particularly at low thickness of the absorber layer. The calculated efficiency of CdS/CdTe of 16.5 % agrees with the corresponding experimental values. The maximum efficiency of CdS/PbS of 6.1% is considered greater than those measured experimentally of this type of solar cells.

Journal of Optoelectronics and Advanced Materials, 18(2016) 254

Influence of sodium doping on the electrical and magnetic properties of $La_{0.90}Li_{0.10}MnO_3$ manganites

H. F. Mohamed

Monovalent *perovskite manganites* $La_{0.90}Li_{0.10-x}Na_xMnO_3$ were synthesized by using the solid-state reaction method. The crystal structure analysis presented that the samples are a single-phase rhombohedral ($R\bar{3}c$ R 3 ¯ c) structure with no detectable impurity phases. Magnetic measurement showed a cusp at a certain temperature $T_{C/F}$ that gradually disappeared with adding the Na content. The samples undergo ferromagnetic-paramagnetic transition, accompanying the metal-semiconductor transition at T_{ms}. There is irreversible on low field M $(T)_{ZFC}$and M $(T)_{FC}$ curves which gradual decrease with increasing the Na doping. The resistivity values decreased and the Tms increased as doping of sodium increased. In addition, two-transition temperature Tms appeared just by adding the sodium. In short, the influence of partial substitution of lithium by sodium at A-site cation of lanthanum manganite on its physical properties was studied.

Journal of Magnetism and Magnetic Materials, 424 (15) (2017) 44-52

Asymmetric Nuclear Matter and Neutron Star Properties within Extended Brueckner Theory

Khaled S. A. Hassaneen[1,2]
[1]*Physics department, Faculty of Science, Sohag University, Sohag, Egypt*
[2]*Physics department, Faculty of Science, Taif University, Taif, Saudi Arabia*
E-mail: khs.hassaneen@yahoo.com

Microscopically, the equation of state (EOS) and other properties of asymmetric nuclear matterat zero temperature have been investigated extensively by adopting the non-relativistic Brueckner-Hartree-Fock (BHF) and the extended BHF approaches by using the self-consistent Green's function approach orby including a phenomenological three-body force. Once three-body forces are introduced, the phenomenological saturation point is reproduced and the theory is applied to the study of neutron star properties.We can calculate the total mass and radius for neutron stars using various equations of state at highdensities in *Beta*-equilibrium without hyperons. A comparison with other microscopic predictions based onnon-relativistic and density-dependent relativistic mean field calculations has been done. It is found thatrelativistic EOS yields however larger mass and radius for neutron star than predictions based on non-relativistic approaches. Also the three-body force plays a crucial role to deduce theoretical value of themaximum mass of neutron stars in agreement with recent measurements of neutron star mass.

Accepted in European Physical Journal A

The Thermal Properties of Asymmetric Nuclear Matter within the Extended Brueckner-Hartree-Fock Approach

Khaled S. A. Hassaneen[1,2]
[1]*Physics department, Faculty of Science, Sohag University, Sohag, Egypt*
[2]*Physics department, Faculty of Science, Taif University, Taif, Saudi Arabia*

The single-particle potentials and other properties at absolute zero temperature in isospin asymmetric nuclear matter are investigated in the frame of an extended Brueckner theory. Also thermal quantities are calculated in asymmetric nuclear matter using CD-Bonn potential and the Urbana three-body forces (3BF). Also, the effects of the hole–hole contributions are investigated within the self-consistent Greens function approach. The inclusion of 3BF or the hole–hole contributions improves the predicted saturation property of symmetric nuclear matter within the Brueckner–Hartree–Fock approach and it leads to a significant stiffening of the density dependence of symmetry energy at high densities but the exact saturation point is not reproduced. This is of great importance in astrophysical calculation. A phenomenological term simulating the three-body interaction is introduced to assure the empirical saturation property. The hot properties of asymmetric nuclear matter such as the internal energy and the pressure are analyzed using T^2-approximation method at low temperatures.

Journal of the Physical Society of Japan 86, No.2, 024201

Theoretical study of the $SrLi^+$ molecular ion:structural, electronic and dipolar properties

Soulef Jellali[a], Héla Habli[a], Leila Mejrissi[b], Mahmoud Mohery[c,d,†], Brahim Oujia[c], Florent Xavier Gadéa[e]

[a]*Laboratoire de Physique Quantique, Faculte des Sciences de Monastir, Universite de Monastir, Monastir, Tunisia*

[b]*Department of Physics, Faculty of Science and Arts, King Abdulaziz University , Rabigh, Saudi Arabia*

[c]*Physics Department, Faculty of Science, University of Jeddah , Jeddah, Saudi Arabia;*

[d]*Physics Department, Faculty of Science, Sohag University, Sohag, Egypt*

[e]*Laboratoire de Chimie et Physique Quantique, Universite de Toulouse , Toulouse, France*

The structural and electronic properties of $(SrLi)^+$ molecular ion have been determined by the useof *ab initio* approaches. Potential energy curves (PECs) with their spectroscopic constants (R_e, D_e,ω_e, T_e, B_e and $\omega_e\chi_e$) have been calculated. Also, the vibrational properties and the electric dipolemoments, either permanent (PDM) or transition (TDM) ones, have been investigated and analysed.Large Gaussian basis sets, the full valence configuration interaction (FCI) and the formalism of nonempiricalpseudo-potential including the two approaches, effective core potential (ECP) and corepolarisation potential (CPP), are analysed. Therefore, (SrLi)+ is considered as a two effective electronssystem. Numerous excited states of symmetries $^{1,3}\Sigma^+$, $^{1,3}\Pi$and $^{1,3}\Delta$dissociating below the ionic limit$Sr^{2+}Li^-$have been investigated. This study shows interesting behaviours around the avoided crossingrelated to charge transfer involving important processes in physics and astrophysics such as dynamics,pre-dissociation and inelastic transitions.

Molecular Physics, 114 (20) (2016) 2910-2923

Structural and optical characterization of Sb-doped ZnO co-sputtered thin films

M. M. Abd El-Raheem, S. A. Amin, M. A. Alharbi, and A. M. Badawi

[1]*Faculty of Science, Taif University, Taif 888, Saudi Arabia*

[2]*Faculty of Science, Sohag University, Sohag 82524, Egypt*

This paper reports the structural and optoelectronics properties of prepared pure and Sb-doped ZnO nanoparticles using the co-sputtering technique. The phase purity and crystallite size of synthesized ZnO and Sb-doped nano-sized particles were characterized and examined using X-ray diffraction and scanning electron microscopy. The elemental analysis was examined by using energy-dispersive X-ray spectroscopy (EDX). Optical properties were carried out by employing UV-visible spectroscopy to study the optoelectronic properties of Sb-doped ZnO thin film. These films are highly transparent in the visible region and exhibit a steep absorption edge at 380 nm. The average value of the optical gap belonging to the thin films deposited under different conditions is 3.17 eV. The refractive index (n) behaves as normal dispersion and decreases with increasing both the rate of flow and thickness. The dispersion energy, single oscillator energy, and optical conductivity increase with increasing the rate of flow of argon.

Journal of optical Technology, vol 83 (2916) 375

Daily variation of radon gas and its short-lived progeny concentration near ground level and estimation of aerosol residence time

M. Mohery[1,2], A. M. Abdallah[1], A. Ali[3,4], S. S. Baz[5]
[1]*Physics Department, Faculty of Science, University of Jeddah, Saudi Arabia*
[2]*Physics Department, Faculty of Science, Sohag University, Sohag, Egypt*
[3]*Astronomy Department, Faculty of Science, King Abdulaziz University, Jeddah, Saudi Arabia*
[4]*Astronomy Department, Faculty of Science, Cairo University, Cairo, Egypt*
[5]*Physics Department, Girls Faculty of Science, King Abdulaziz University, Jeddah, Saudi Arabia*

Atmospheric concentrations of radon (^{222}Rn) gas and its short-lived progenies ^{218}Po, ^{214}Pb, and ^{214}Po were continuously monitored every four hours at the ground level in Jeddah city, Kingdom of Saudi Arabia. The measurements were performed three times every week, starting from November 2014 to October 2015. A method of electrostatic precipitation of positively charged ^{218}Po and ^{214}Po by a positive voltage was applied for determining ^{222}Rn gas concentration. The short-lived ^{222}Rn progeny concentration was determined by using a filter holder connected with the alpha-spectrometric technique. The meteorological parameters (relative air humidity, air temperature, and wind speed) were determined during the measurements of ^{222}Rn and its progeny concentrations. ^{222}Rn gas as well as its short-lived progeny concentration displays a daily and seasonal variation with high values in the night and early morning hours as compared to low values at noon and in the afternoon. The observed monthly atmospheric concentrations showed a seasonal trend with the highest values in the autumn/winter season and the lowest values in the spring/summer season. Moreover, and in parallel with alphaspectrometric measurements, a single filter-holder was used to collect air samples. The deposited activities of ^{214}Pb and the long-lived ^{222}Rn daughter ^{210}Pb on the filter were measured with the gamma spectrometric technique. The measured activity concentrations of ^{214}Pb by both techniques were found to be relatively equal largely. The highest mean seasonally activity concentrations of ^{210}Pb were observed in the autumn/winter season while the lowest mean were observed in the spring/summer season. The mean residence time (MRT) of aerosol particles in the atmospheric air could be estimated from the activity ratios of ^{210}Pb/^{214}Pb.

Chin. Phys. B Vol. 25, No. 5 (2016) 050701

Optical characteristics of transparent samarium oxide thin films deposited by the radio-frequency sputtering technique

A. A. Atta, M. M. EL-Nahass, Khaled M. Elsabawy, M. M. Abd El-Raheem, A. M. Hassanien, A. Ahuthali, Ali Bbadawi, Amar Merazga
[1]*Faculty of Science, Taif University, Taif 888, Saudi Arabia*
[2]*Faculty of Science, Sohag University, Sohag 82524, Egypt*

Transparent metal oxide thin films of samarium oxide (Sm2O3) were prepared on pre-cleaned fused optically flat quartz substrates by radio-frequency (RF) sputtering technique. The as-deposited thin films were annealed at different temperatures (873, 973 and 1073 K) for 4 h in air under normal atmospheric pressure. The topological morphology of the film surface was characterized by using atomic force microscopy (AFM). The optical properties of the as-prepared and annealed thin films were studied using their reflectance and transmittance spectra at nearly normal incident light. The estimated direct optical band gap energy (E_{gd}) values were found to increase by increasing the annealing temperatures. The dispersion curves of the refractive index of Sm_{2O3} thin films were found to obey the single oscillator model.

Pramana – J. Phys. (2016) 87:72.

Effect of gas pressure and film thickness on the optical constants of transparent conducting oxide based on zinc oxide

M. M. Abd El-Raheem, A. K. Diab, Abdullah Alhuthali, Ateyyah M. Al-Baradi
[1]*Faculty of Science, Taif University, Taif 888, Saudi Arabia*
[2]*Faculty of Science, Sohag University, Sohag 82524, Egypt*

Thin films of aluminum zinc oxide are prepared using DC magnetron sputtering. It was found that changing the thickness of the film as well as the pressure of argon affect the transmittance, optical gap, width of the band tails of the localized state, refractive index, real and imaginary parts of the dielectric function. The real and imaginary parts of optical conductivity as well as volume and surface energy loss functions are investigated in the light of changing the thickness of the films and argon pressure.

Journal of Optical technology, vol. 83 (2016) 30

Influence of Cu doping on structural, morphological, photoluminescence, and electrical properties of ZnO nanostructures synthesized by ice-bath assisted sonochemical method

A. A. Othman, Manar A. Ali, E. M. M. Ibrahim, M. A. Osman
Faculty of Science, Sohag University, Sohag 82524, Egypt

Cu-doped ZnO ($Zn_{1-x}Cu_xO$, x = 0.0, 0.01, 0.02, 0.03, 0.04, 0.05)nanocrystals were synthesized by ice-bath assistedsonochemical method.X-ray diffraction (XRD) analysis of the undoped and Cu-doped ZnO nanostructuresreveals the formation of ZnO hexagonalwurtzitestructure for all samples, confirming the incorporation of Cu^{2+} ions into ZnO lattice by substitution. Increasing Cu concentration resulted in the contraction of bond length and unit cell volume, whereas, the crystallite size increases by the doping induced grain growth. High-resolution transmission electron microscopy(HRTEM) images show that the morphology of pure and doped samples consists ofa mixtureofnanorods and nanosheets and the growth mechanism was suggested. Theincrease of Cu content leads to the improvement of preferable growth and the increase of both nanorods length and diameter. Analysis of optical absorption spectrashows thatincorporation of Cu ions into ZnO lattice leads to ared shift of the optical band gap from 3.45 eV to 3.35 eV and the excitonic peak from 3.35 to 3.24 eV. Photoluminescence(PL) spectrum of the undoped ZnO nanopowder at excitation wavelength (λ_{ex}) = 325 nm, reveals near band edge UV emission and defect-related blue and green emission, whereas, PL spectrumat λ_{ex} = 380 nm exhibits only defect-relatedgreen and red emission. The incorporation of Cu leads to the quenching of PL intensity due to the increase of nonradiative recombination centers.Direct current (DC) electrical conductivity measurement reveals the presence of different shallow and deep trapping levels. In addition, the increase of electrical conductivity with increasing Cu content in ZnO lattice can be ascribed to the decrease in the activation energy.To explain the mechanism of PL emission and identify different trapping and recombination levels in ZnO nanopowdersan energy band diagrams were suggested.

Journal of Alloys and Compounds 683 (2016) 399-411

Study of Plasma Formation in Potassium Vapor Excited by Nanosecond Resonant Laser Pulses

M. A. Mahmoud, E. Sultan, Asmaa Gamal
Physics department, Faculty of Science, Sohag University, 82524-Sohag, Egypt

We have studied theoreticaly formation of molecular ion K2+ and the atomic ion K+ which are created in laser excited potassium vapor at the first resonance transition, 4S - 4P. A set of rateequations, which describe the temporal variation of which describe the temporal variation of theelectron energy distribution function(EEDF), the electron density, the population density of theexcited states , atomic ion K+ and molecular ion K+2, are solved numerically. The calculations arecarried out at different laser energy and different potassium atomic vapor densities under theexperimental conditions of Amin et al[9]. The numerical calculations show that the competitionbetween photoionization processes and collisional ionization processes for producing the K^+ and K^{2+}.Moreover, the results are found to be consistent with the experimental observations.

ESCAMPIG XXIII Conference, Bratislava, Slovakia, July 12-16, 2016

Effect of Calcination Temperature on Magnetic Properties of $BiFeO_3$ Nanoparticles Prepared By Sol-Gel Method

E. M. M. Ibrahim , G. Farghal, Mai M. Khalaf , Hany M. Abd El-Lateef
Physics department, Faculty of Science, Sohag University, 82524-Sohag, Egypt

In this work, a $BiFeO_3$ nanoparticle was synthesized by sol–gel method followed by calcination at different temperature 300, 400 and 500 ˚C. Effect of calcination temperature on the structure, morphology, electrical and magnetic properties was studied by using x-ray diffraction, scanning electron microscopy, electrical conductivity measurements and vibrating sample magnetometer, respectively. Structural analysis revealed a typical rhombohedral phase of the prepared BiFeO3 nanoparticles. Scanning electron microscope investigations show that the materials are mesoporous nature with average particle size ~ (52) nm. The magnetic measurement shows significant enhancement of the ferromagnetism with the increasing of the calcination temperature which may be mainly attributed to the crystallinity improvement and the change of the oxygen vacancies content. The DC electrical resistivity measurement was carried out by the two-probe method. The temperature dependence of resistivity behavior shows typical semiconductor features for the synthesized nanoparticles.

J. Nano. Adv. Mat. 5, No. 1, 33-39 (2016)

Sonochemically Synthesized ZnO Nanosheets and Nanorods: Annealing Temperature Effects on the Structure, and Optical properties

A. Othman, M. A. Osman, E. M. M. Ibrahim, Manar A. Ali
Physics department, Faculty of Science, Sohag University, 82524-Sohag, Egypt

ZnO nanopowders were successfully synthesized by the ice-bath assisted sonochemical method. The nanopowders were annealed in air for 3 hours at different annealing temperatures (Ta) ranging from 300 to 700 oC. The effect of Ta on the structural and morphological properties was investigated by the x-ray diffraction (XRD) and the transmission electron microscopy (TEM). The optical properties were studied by recording the optical absorption and photoluminescence (PL) spectra. The XRD analysis showed that the thermal annealing leads to an improvement in the crystallinity associated with an increase in the crystallite size as well as an increase in both the Zn-O bond length and unit cell volume. Also, it was found that the increase of Ta results in a shift in the diffraction angle toward lower values associated with a decrease in the micro-strain. The morphological study confirms that the samples are mixtures of nanosheets and nanorods. In addition, the length and diameter of the nanorods increase as the annealing temperature increases. The optical absorption spectra show that the exciton peak of the as-prepared sample is red shifted from 370 to 378 nm by thermal annealing, and the optical band gap decreases from 3.45 to 3.36 eV. The photoluminescence spectra were reordered at an excitation wavelength of 325 nm, and the deconvolution of the spectra reveals four emission bands where the main UV band (at λ = 397 nm) can be attributed to exciton recombination related to near-band-edge. Furthermore, the thermal annealing results in a reduction of the PL intensity of the annealed samples.

Ceramics International 43 (2016) 527-533.

Optical and electrical properties of hydrothermally prepared CdTe nanowires

N. M. A. Hadia, M. A. Awad, S. H. Mohamed, E. M. M. Ibrahim
Physics Department, Faculty of Science, Sohag University, 82524 Sohag, Egypt

The hydrothermal process was used to synthesizeCdTe nanowires (NWs). Various analytical techniques were used to characterize the obtained NWs. The wire diameters were in the range 35 - 60 nm and the lengths were greater than 5 μm. The CdTe NWs had zinc blende crystal structure. The NWs had high uniformity and high yield. FTIR analysis revealed the presence of the characteristic vibrational spectra of oxygen and hydrogen boundedto Cd and Te in CdTe NWs. The optical band gap value was 2.09 eV. The CdTe NWs showed a strong red emission band centered around 620.3 nm. The conductivity measurements were carried out in the temperature range 300 to 500 K and in air atmosphere. Two types of conduction mechanisms were observed with activation energies of 0.27 and 0.17 eV at highand low temperature regions, respectively.These results validate the potential of CdTe NWs for optoelectronic applications.

Applied Physics A, 122 (2016) 889-P6

The synthesis of $Bi_2(TeSe)_3$ nanoparticles for clean energy production: Effect of the synthesis conditions

M. A. A. Mohamed, E. M. M. Ibrahim, H. M. Ali, M. M. Wakkad
Physics Department, Faculty of Science, Sohag University, Sohag 82524, Egypt

Thermoelectric power generators are promising technique for clean energy production. They are used for transforming the waste energy to electricity in environment friendly ways without any noise or pollutants. In this work, Bi2(TeSe)3 nanoparticles (NPs) were successfully prepared via vapor transport technique. The x-ray diffraction (XRD) patterns show that, the NPs crystalize in a rhombohedral structure. Field-emission scanning electron microscope (FE-SEM) investigation reveals that the NPs size depends significantly on the synthesis conditions of flow rate and temperature where it decreases as one or both of them decreases. The photoluminescence spectra were utilized to describe the free carriers transfer between different energy states and hence they were helpful for understanding the electrical conduction mechanisms. The electrical and thermoelectrical properties were measured over a wide range of temperature 300-600 K. The calculated power factor confirms the effect of particle size on the thermoelectric properties of the Bi2(TeSe)3 compounds.

International Conference on Chemical Science & Applications, ICCSA 2016, Alexandria, Egypt

Magnetic Nanoparticles for Cancer Therapy: Facile Synthesis Techniques and Desired Properties

E. M. M. Ibrahim, G. Farghal, M. Mostafa, H. Abdelateef, S. Hampel, V. Khavrus, C. Täschner, A. Leonhardt, B. Büchner
Physics department, Faculty of Science, Sohag University, 82524-Sohag, Egypt

During last decade, magnetic nanoparticles(MNPs) have attracted an increasing interest for many aspects of applications such as biomedicine, chemical technology, magnetic data storage devices, and nanoscale electronics due to their unique chemical and physical properties. In fact, one of the tremendous areas of growth on the research side involves using MNPs for cancer treatment.MNPs with appropriate surface have been successfully applied to deliver therapeutic biomolecules, such as anticancer drugs, antibodies, and siRNA, to target tumour cells and tissues. Also,They can heat up in Ac magnetic fields, thus act as hyperthermia agents. On the other hand, in cancer diagnostic field, MNPs play an important role as MRI contrast enhancement agents. The potential applicability of MNPs in cancer treatments varies widely depending on their magnetic properties and chemical stability. Actually, various factors can tune the magnetism of the MNPs. A main issue is the individual properties of the magnetic nanoparticles including chemical composition, size, and shape. To ensure the safe use in biomedicine, the chemical stability can be achieved by producing magnetic nanocomposites (MCs). In MCs, the MNPs are coated with shells of highly chemical stable materials such as carbon, silica or polymers. The fascinating properties revealed by the MCs are emerged due to the combination of the MNPs and the coating shells: the MCs acquire magnetic functionality such as monitoring, heating, and guiding from the MNPs, while the coating shells improve the chemical stability, chemical functionality, and biocompatibility. This work presents our results of the synthesis of $Mn_{0.5}Zn_{0.5}Fe_2O_4$, $BiFeO_3$ MNPs, and carbon coated Fe, Co, Ni, FeCo, FeNi MNPs. The magnetic properties, heating response in AC magnetic fields for hyperthermia applications and biocompatibility of the synthesized magnetic systems were studied. Various synthesis methods such as chemical precipitation, chemical vapour deposition, plasma enhanced chemical vapor deposition and ball milling were used and reported to show the crucial role of the synthesis technique for tuning the magnetic and chemical stability of the materials. Different rare earth elements were used for doping the magnetic nanoparticles to enhance their magnetic properties.

International Conference on Chemical Science & Applications, ICCSA 2016, Alexandria, Egypt

Study of Electron Energy Distribution Function (EEDF) in Potassium Vapor Excited By Nanosecond Laser Pulses

M. A. Mahmoud, Emad Sultan, Asmaa Gamal
Physics Department, Faculty of Science, Sohag University, Sohag 82524, Egypt

A theoretical model of laser excited potassium vapour induced by nanosecond laser pulses tuned to the firstresonance, 4s-4p and 4p-nl transitions has been studied. All the important collisional ionization, photoionization, electroncollisions and radiative interactions are included in this mode. The numerical model studies the temporal variation of the Electron Energy Distribution Function (EEDF); the dependence of the (EEDF) on potassium vapor density and laser energy;the variation of atomic ion density; molecular ion and electron density. The applied computer simulation model is based onthe numerical solution of a set of rate equations that describe the rate of change of the ground and excited states population, beside the atomic ion K+ density; molecular ion K2+ and electron density formed during the interaction. The calculationsshowed that, the non-equilibrium shape of the electrons occurs due to the relaxation of fast electrons produced by super elasticcollision with residual excited potassium atoms. Also the results showed a competition between the processes reponsible for producing *K*+. Finally, the model may be useful for interesting applications such as laser isotopes separation and alkali lasersystems.

Int. J. New. Hor. Phys, 3 (2016) 65-71.

Structural and Optical Properties of Nanostructured Fe-Doped SnO_2

S.A. Saleh[a;b], A.A. Ibrahim[c], S.H. Mohamed[a]
[a]Physics Department, Faculty of Science, Sohag University, Sohag 82524, Egypt
[b]Physics Department, College of Science and Arts, Najran University, P.O. 1988 Najran, KSA
[c]Chemistry Department, College of Science and Arts, Najran University, P.O. 1988 Najran, KSA

Nanocrystalline $Sn_{1-x}Fe_xO_2$ (where x = 0, 0.01, 0.02, 0.03 and 0.04) powders have been successfully synthesized by the hydrothermal method followed by sintering at 1000 °C for 3 h. The morphology and structure of the samples have been analyzed by FESEM and XRD, respectively. XRD results revealed that all diffraction peaks positions agree well with the reflection of a tetragonal rutile structure of SnO_2 phase without extra peaks. The formation of a tetragonal rutile structure of SnO_2 nanostructures was further supported by Raman spectra. The band gap of Fe-doped SnO_2 nanoparticles was estimated from the diffuse reflectance spectra using Kubelka–Munk function and it was decreasing slightly with the increase of Fe ion concentration from 3.59 to 3.52 eV. The variation in band gap is attributed predominantly to the lattice strain and particle size. The presence of chemical bonding was confirmed by FTIR spectra.

ACTA PHYSICA POLONICA A 129 (2016) 1220-1225.

Analysis Slow Particle Emitted ^{24}Mg with Emulsion Interactions at Relativistic Energies

A. Abd El-Daiem, **A. E. Elmeshneb**
Department of Physics, Faculty of Science, Sohag University, Sohag, Egypt

In this work has been made to study the general characteristics of slow particles produced in the interactions of ^{24}Mg with emulsion at 4.5 A GeV/c to extract the information about the mechanism of particle production. The results have been compared with the experimental results obtained by other workers. The multiplicity distributions of the slow target associated particles (grey, black and heavy tracks) produced by ^{24}Mg- incident with different targets have been studied. Also several types of correlations between them have been investigated. The variation of the produced particles with projectile mass number and target size has been studied.

Journal of Nuclear and Particle Physics

Electrical and magnetic transportin Strontium doped Europium Ferrimanganites

I. A. Abdel-Latif[a,b], Mahrous R. Ahmed \[c,d], I. A. Al-Omari[e], A. Sellai[e]
[a]*Physics Department, College of Science & Arts, Najran University, P. O. 1988, Najran, KSA*
[b]*Reactor Physics Department, NRC, Atomic Energy Authority, Abou Zabaal, Cairo, Egypt*
[c]*Physics Department, Faculty of Science, Sohag University, Sohag 82524, Egypt*
[d]*Physics Department, Aljamoum University College, Um-Elqura University, Makka, Saudi Arabia*
[e]*Physics Department, Faculty of Science, Soltan Qaboos University, P.O. Box 36, Muscatt, Oman*

$Eu_{0.65}Sr_{0.35}Fe_xMn_1xO_3$ (x¼0.1, 0.3 and 0.5) has been prepared using a standard solid state reaction method. The under-investigation compounds is found to crystallize in a single-phase orthorhombic structure in the P_{bnm} space group (62). The adiabatic polaron electronic transfer was obtained for all samples and the activation energy of x¼0.1 sample is equal to 1.013 meV and slightly increase at x¼0.3 (1.289 meV) while is doubled for x¼0.5 to be 2.1065 meV. The magnetization–temperature dependence measurements of $Eu_{0.65}Sr_{0.35}Fe_xMn_1xO_3$ show the ferromagnetic ordering at low iron concentration x¼0.1 and when iron concentration increase to x¼0.5 the noncollinear magnetic ordering (the canted antiferromagnetic) is obtained. The magnetic phase transition (paramagnetic-ferromagnetic transition) in the $Eu_{0.65}Sr_{0.35}Fe_{0.1}Mn_{0.9}O_3$ is observed at T_c of 150 K. For $Eu_{0.65}Sr_{0.35}Fe_{0.5}Mn_{0.5}O_3$ the multi-magnetic phase transition is observed at T_c of 200K and T_N of 430 K. The resistivity at low temperature is measured. Theoretical Calculations using Monte Carlo code have been done. The magnetization as function of temperature has been calculated using Monte Carlo simulations for $Eu_{0.65}Sr_{0.35}Fe_xMn_1xO_3$ (x¼0.0, 0.1, 0,2, 0.3, 0.4 and 0.5). Ising model is a suitable model to study the magnetization for our compounds. The internal energy for x¼0 is the highest value compared with the other x values which have nearly a ground state value equal to 2.7 J.

Journal of Magnetism and Magnetic Materials 420 (2016) 36

Thickness-dependent dispersion parameters, energy gap and nonlinear refractive index of ZnSe thin films

Deo Prakash[a], E.R. Shaaban[b], M. Shapaan[c], S.H. Mohamed[d], A.A. Othman[e], K.D. Verma[f]

[a]School of Computer Science & Engineering, Faculty of Engineering, SMVD University, Kakryal, Katra 182320, J&K, India

[b]Physics Department, Faculty of Science, Al-Azhar University, Assiut 71542, Egypt

[c]Department of Physics, Faculty of Science, Al-Azahar University, Cairo, Egypt

[d]Physics Department, Faculty of Science, Sohag University, 82524 Sohag, Egypt

[e]Physics Department, Faculty of Science, Assiut University, Assiut 71516, Egypt

[f]Material Science Research Laboratory, Department of Physics, S. V. College, Aligarh 202001, India

Zinc selenide (ZnSe) thin films with different thicknesses were evaporated onto glass substrates using the thermal evaporation technique. X-ray diffraction analysis confirmed that both the film and powder have cubic zinc-blende structure. The fundamental optical parameters like absorption coefficient, extinction coefficient and band gap were evaluated in transparent region of transmittance and reflectance spectrum. The optical transition of the films was found to be allowed, where the energy gap increased from 2.576 to 2.702 eV with increasing film thickness. Also, the refractive index value increase with increasing film thickness. The refractive indices evaluated through envelope method were extrapolated by Cauchy dispersion relationship over the whole spectra range. Additionally, the dispersion of refractive index was determined in terms of Wemple-DiDomenico single oscillator model. Third order susceptibility and nonlinear refractive index were determined for different thickness of ZnSe thin films.

Materials Research Bulletin 80 (2016) 120–126

Hardening of the soft phonon in bulk $SrTiO_3$ interfaced with $LaAlO_3$ and $SrRuO_3$

A. Nucara,[1] M. Ortolani,[2] L. Baldassarre,[1] W. S. Mohamed,[2] U. Schade,[3] D. Winkler,[4] A. Khare,[5] F. Miletto Granozio,[5], P. Calvani[1]

[1]CNR-SPIN and Dipartimento di Fisica, Universita di Roma "La Sapienza", P.le A., Roma, Italy

[2]Dipartimento di Fisica, Universita di Roma "La Sapienza", P.le A. Moro 2, I-00185 Roma, Italy

[3]Helmholtz Zentrum Berlin Mat & Energie GmbH, Methods Mat Dev, D-12489 Berlin, Germany

[4]Dept. of Microtechnology & Nanoscience, Chalmers University, S-41296 Gothenburg, Sweden

[5]CNR-SPIN UOS Napoli, Complesso Universitario di Monte Sant'Angelo, Napoli, Italy

The low-temperature softening of the TO1 phonon of $SrTiO_3$ (STO), which determines its incipient ferroelectricity, is known to be partially hindered either in the bulk under strong electric fields, or in thin STO films. Here we show, by terahertz (THz) reflectivity measurements, that a similar effect is produced in bulk STO and at zero static field by ultrathin metallic films on its surface, like a 10-nm-thick film of $SrRuO_3$ (SRO), or the two-dimensional electron system (2DES) present at the interface with $LaAlO_3$. In SRO/STO, the observed hardening is well explained by the depolarizing action of the SRO free electrons which follow adiabatically the ion motion. In LAO/STO, a weaker TO1 hardening could be detected by patterning the 2DES in the form of microstripes and using a polarized THz field parallel (E_{11}) or orthogonal ($E_{\perp}$) to the stripes. At 10 K, when TO1 is excited together with the free electrons by E_{11}, its absorbance is harder by about 7 cm^{-1} than that measured when TO1 is coupled to the plasmon-polariton confined within the stripes, being excited by $E_{\perp}$.

PHYSICAL REVIEW B 93, 224103 (2016)

Complete Destruction of Ag Br Emulsion Nuclei BY^{28}Si Ions with 4.5 GeV/Nucleon Energy

A. Abd EL-Daiem
Physics Department, Faculty of Science, Sohag University, Sohag, Egypt.

The main experimental characteristics (multiplicity characteristics) of secondary particles have been investigated in interactions of ^{28}Si with emulsion at 4.5 GeV/c per nucleon at rest of emulsion, nuclei. The complete destruction of the heavy target nuclei (Ag, Br) has been studied. The average of shower particles $< n_s >$ is weakly dependent on the target mass whereas the average multiplicity of grey particles $< n_g >$ is strongly dependent on it. The correlations between the multiplicities of the charged secondaries at different mass number of the projectile and center-of-mass-available energy are investigated.

Journal of modern physics ,2016,7,1506-1511

Chemistry

Effect of ammonium groups on the properties of anion conductive membranes based on partiallyfluorinated aromatic polymers

Ahmed Mohamed Ahmed Mahmoud, Ahmed Mohamed Mohamed El-Saghier, Kenji Miyatake
Department of Chemistry, Faculty of Sience, Sohage University, Sohag 82524, Egypt

A series of anion exchange membranes (QPE-bl-9) based on a partially fl uorinated hydrophobic segment and oligophenylene as scaffolds for ammonium cations were synthesized to evaluate the effect of the various ammonium groups derived from trimethyl amine (TMA), dimethyl hexyl amine (DMHA), methyl imidazole (MIm), dimethyl imidazole (DMIm), tributyl amine (TBA), and dicyclohexyl methyl amine (DCHMA) on the membrane properties. QPE-bl-9 membranes were well characterized by ^{1}H NMR spectroscopy, in which all the peaks were assigned to the supposed structure. The TEM images of QPE-bl-9 - TMA, - MIm, - DMIm and - DMHA membranes showed small hydrophilic/hydrophobic phase separated morphology (hydrophilic domains 1 - 3 nm). QPE-bl-9 - TMA (1.6 mequiv. G1) exhibited the highest hydroxide ion conductivity (101 mS cm1at 80C) among the tested membranes, followed by QPE-bl-9 - DMHA (62 mS cm 1) and QPE-bl-9 - DMIm (62 mS cm1). The alkaline stability of the membranes was tested in 1 M KOH at 60C for 1000 h. QPE-bl-9 - TMA exhibited the highest retentionof the conductivity (58%), which was higher than that of the Tokuyama A201 anion exchange membrane(29%). The post stability test IR analyses suggested that the major degradation mechanism of the QPE-bl-9 membranes in alkaline solution involved the decomposition of the ammonium groups. The QPE-bl-9 membranes retained their mechanical stability after the stability test, as proved by DMA analyses.
RSC Adv., 6 (2016) 27862-27870

One-pot Synthesis and An Antibacterial Activity of 2-(2-hydroxyphenyl)-4-oxothiazolidin-3-yl)alkyl/ phenylthiazolidin-4-one Derivatives and Reaction with Aromatic Aldehydes

Ahmed Mohamed Mohamed El-Saghier, Naglaa Fawzy Hassan Mahmoud
Department of Chemistry, Faculty of Sience, Sohage University, Sohag 82524, Egypt

Unexpected 2-(2-hydroxyphenyl)-3-(2-(2-hydroxyphenyl)-4-oxothiazolidin-3-yl)alkyl(phenyl)thiazolidin-4-one Derivatives **4a-d** were synthesized via reaction of 3-acetyl cumarin1 with hydrazine hydrate, ethylene diamine, 1,6-diaminohexane or *p*-phenylenediamine to afford the corresponding Schiff bases **3a-d**, which in turn reacted with thioglycolic acid in the presence of anhydrous $ZnCl_2$. Also, compounds 4a-d were prepared in one-pot reaction via reaction of 3-acetylcumarin, diamine and thioglycolic acid in the presence of $ZnCl_2$. 5-Arylidene derivatives **6a-l**were prepared by reaction of **4a-d** with aromatic aldehydes **5a-c**. The structure of the synthesizedcompounds were assigned on the basis of elemental analysis, IR, ^{1}H-NMR and ^{13}C-NMR.
Ciência e TécnicaVitivinícola, 31 (3) (2016) 107-117

Utilization of 2-Ylidene-4-thiazolidinones in Synthesis of Heterocyclic Compounds Part (II): Transformation of (4-Oxo-3-phenyl-1,3-thiazolidin-2-ylidene)malononitrile to 3-Aminothiophene Derivatives

M. F. Farhat, M. A. Makhlouf, A. B. El-Mezoughi, A. M. El-Saghier
Department of Chemistry, Faculty of Sience, Sohage University, Sohag 82524, Egypt

Alkyl 3-aminothiophene carboxylates derivatives **(3a-d)** were prepared via reaction of (4-oxo-3-phenyl-1,3-thiazolidin-2-ylidene)malononotrile**(2)** with alcohols. Compound **3a** was allowed to react with acetic anhydride, chloroacetyl chloride and nitrous acid to afford N,N,N-triacetylthiophene, 3-chloroacetamidothiophene and 3-diazothiophene derivative (**6,7** and **8**) respectively. Compound **8** was allowed to react with sodium azide to afford the 3-azidothiophenederivative **(9)**. On the other hand, 3-amino-2-carboxamidothiophene derivative**(10a-c)** were prepared via reaction of compound **2** with a variety of amines. Compound **10a** was allowed to react with acetic anhydride to afford thieno[2,3-d]oxazinone**(12)**
Asian J. Chem., 28(8) (2016) 1823-1827

Evaluation of Antidiabetic Activity of *Ipomoea Aquatica* Fractions in Streptozotocin Induced Diabetic in Male Rat Model

Nagwa El-Sawi[1], Mahmoud Hefny Gad[2], MadehaNooh Al-Seeni[3], Sabry Younes[1], El-Mewafy El-Ghadban[2], Soad Shaker Ali[3]
[1]Department of Chemistry, Faculty of Science, Sohag University, Sohag, Egypt
[2]Medicinal and Aromatic Plants Research Department, Horticulture Institute, Agriculture Research Center, Dokki, Giza, Egypt
[3]Biochemistry Department, Faculty of Science, King Abdulaziz University, Saudi Arabia
[4]Histology Department, Faculty of Medicine, King Abdoul Aziz University

Ipomoea aquatica (IA) is a common green leafy vegetable consumed in many parts of the world. The plant is considered as a good antidiabetic herbal plant. The present work was designed to investigate the oral hypoglycaemic activity of Ipomeaaquatica fractions in streptozotocin induced diabetic male rats. The male rats with average weight 200-220 g were divided into four groups (n=6), control, diabetic (induced with a single dose of streptozotocin (50 mg/kg body weight), T-1 and T-2 as treated diabetic with the two fractions of Ipomoea aquatica (IA6-1 and IA9-2), respectively. Biochemical evaluation of blood glucose, serum insulin and C-peptide were carried out. Histological examination of islets of Langerhans was done for cellular population changes. The results revealed that the oral consumption of two fractions of I. aquatica for 15 days, effective significantly reduced the fasting blood sugar level of streptozotocin-induced diabetic rats ($p < 0.05$). The percent changes were a 51% and 31% decrease in the serum glucose concentration of the diabetic rats when treated with the plant fractions of IA6-1 and IA9-2, respectively. Most biochemical parameters tested returned to nearly normal levels. Histologically, islets area and normal cell population were preserved in treated animals with superior results in T-1 and T-2 groups. In conclusion, fractions IA6-1 and IA9-2 showed potential antidiabetic effects when given orally to diabetic rats. The mechanism of action requires further investigation using both molecular and immunohistochemical methods investigation of both insulin secreting cells and insulin receptors. Future clinical trials could be tried using volunteers to confirm the present results so could be marketed as a supplement for diabetic patients.
Sohag J. Sci. 1(1) (2016) 7-12

Relationship of C-Reactive Proteins with Oxidative Stress and Obesity in Type 2 Diabetic Subjects

Nagwa M. Elsawi[1],*, Hossam El-Din M. Omar[2], Ali Taha A. Hassan[3], Amira M. Ahmed[1]
[1]*Department of Chemistry, Faculty of Sience, Sohage University, Sohag 82524, Egypt*
[2]*Zoology Department, Faculty of Science, Assiut University, Assiut 71516, Egypt*
[3]*Department of Internal Medicine, Faculty of Medicine, Sohag University,Egypt*

Objective: The present work was aimed to study the correlation between C-reactive proteins as marker of acute phase response, total antioxidants capacity as marker of oxidative stress and blood pictures with the electrophoresis patterns of serum protein in sera of subjects with obese and diabetic obese subjects attending Sohag University Hospital.
J. Pharm. Appl. Chem., 2 (3) (2016) 1-11

Highly sensitive determination of atropine using cobalt oxide nanostructures: Influence of functional groups on the signal sensitivity

Soomro R. A.[ab], Nafady A.[cd], Hallam K. R.[a], Jawaid S.[b], Al Enizi A.[c], Sherazi S. T. H.[b], Sirajuddinb Ibupoto Z. H.[e], Willander M.[f]
[a]*Interface Analysis Centre, School of Physics, University Bristol, Bristol, United Kingdom*
[b]*National Centre of Excellence in Analytical Chemistry, University of Sindh, Jamshoro, Pakistan*
[c]*Department of Chemistry, College of Science, King Saud University, Riyadh, Saudi Arabia*
[d]*Department of Chemistry, Faculty of Science, Sohag University, Sohag, Egypt*
[e]*Dr M.A. Kazi Institute of Chemistry, University of Sindh, Jamshoro, Pakistan*
[f]*Department of Science and Technology, Campus Norrkoping, Linkoping University, Sweden*

This study describes sensitive determination of atropine using glassy carbon electrodes (GCE) modified with Co_3O_4 nanostructures. The as-synthesised nanostructures were grown using cysteine (CYS), glutathione (GSH) and histidine (HYS) as effective templates under hydrothermal action. The obtained morphologies revealed interesting structural features, including both cavity-based and flower-shaped structures. The as-synthesised morphologies were noted to actively participate in electro-catalysis of atropine (AT) drug where GSH-assisted structures exhibited the best signal response in terms of current density and over-potential value. The study also discusses the influence of functional groups on the signal sensitivity of atropine electro-oxidation. The functionalisation was carried with the amino acids originally used as effective templates for the growth of Co_3O_4 nanostructures. The highest increment was obtained when GSH was used as the surface functionalising agent. The GSH-functionalised Co_3O_4-modified electrode was utilised for the electro-chemical sensing of AT in a concentration range of 0.01-0.46 μM. The developed sensor exhibited excellent working linearity (R^2 = 0.999) and signal sensitivity up to 0.001 μM of AT. The noted high sensitivity of the sensor is associated with the synergy of superb surface architectures and favourable interaction facilitating the electron transfer kinetics for the electro-catalytic oxidation of AT. Significantly, the developed sensor demonstrated excellent working capability when used for AT detection in human urine samples with strong anti-interference potential against common co-existing species, such as glucose, fructose, cysteine, uric acid, dopamine and ascorbic acid.
Analytica Chimica Acta, 948 (2016) 30-39

Assessment of Lycium Barbarum for detoxification of Patulin toxin and their effects on rat serum globulin

Nagwa M. El-Sawi[1], Asma S.Abdo[1], M.A.A. Mohamed[1], H.Salah[1], MadehaN.Al Seni[2], Mohamed T. El-Wassimy[1]

[1]Chemistry Department, Faculty of science,Sohag University,Sohag,82524,Egypt
[2]Department of Biochemistry, Faculty of Science, King Abdulaziz University, Jeddah, KSA

The aim of this study was to show the efficiacy of Goji extract on rat serum globulins which treated with patulinmycotoxin. 50 adult albino male rats were divided into 5 groups. Control group was injected subcutaneously daily with distilled water; groups I and II were injected subcutaneously daily with Patulin (0.2 mg/kg/day) for one and two weeks respectively.Group III was treated with an equal dose of patulin for two weeks then injected subcutaneously with Goji extract (2ml/kg /day) for two weeks. Group IV was treated by Goji for two weeks then they were treated with an equal dose of patulin for two weeks.The mean values of albumin level in treated groups with patulin showed highly significant decrease compared with control group. But the mean values of α_1, α_2, β and γ globulins showed highly significant increase in GI and G II compared with control group. However there is no significant change in the mean value of albumin, α_1, α_2, β and γ globulins in G III and G IV compared with the control.

GARJEST, 5(2) (2016) 9-15.

Selective synthesis of monosubstituted p-tert-butylthiacalix[4]arene under phase transfer catalysis

Omran A. Omran

Medical laboratory department, College of Science, Majmaah University, Zulfi, 1712, 11932, Saudi Arabia
Chemistry Department, Faculty of Science, Sohag University, Sohag, 82524, Egypt

Phase transfer catalysis (PTC) technique for lower rim alkylation ofp-tert-butylthiacalix[4]arene (TCA) with diethyl bromomalonate, phenacylbromide, N,N-diethylchloroacetamide, ethyl bromoacetate and chloroacetonitrileusing K_2CO_3, CsOH or Na_2CO_3as a base and tetraethylammonium bromide (TEAB) as catalyst in benzene has been employed. Selective synthesis of monosubstituted p-tert-butylthiacalixarene using K_2CO_3or CsOH as base has been elaborated. Unprecedented alkylation cyclization as well as arene oxidation by using of Na_2CO_3as a base for alkylation of p-tert-butylthiacalix[4]arene under PTC conditions led to the synthesis of two new p-tert-butylthiacalix[4]arene derivatives with heterocyclic bridging rings. The structures of the newly synthesized compounds were characterized by different spectroscopy methods IR, ^{1}H NMR, ^{13} CNMR, and single crystal X-ray diffraction.

HETEROCYCLES, 92 (6) (2016) 1085-1094

Fabrication and applications of potentiometric sensors based on p-tert-butylthiacalix[4]arene comprising two triazole rings ionophore for silver ion detection

Omran A. Omran[1,4,*], Fadl A. Elgendy[2], Ayman Nafady[3,4,*]
[1]*College of Science in Zulfi, Majmaah University, Zulfi 11932, Saudi Arabia,*
[2]*Chemistry Department, College of Science, Qassim University, Saudi Arabia*
[3]*Department of Chemistry, College of Science, King Saud University, Riyadh, Saudi Arabia*
[4]*Chemistry Department, Faculty of Science, Sohag University, Sohag 82524, Egypt*

This work describes the fabrication and applications of potentiometric silver-selective sensors, based on the use of a newly synthesized p-tert-butylthiacalix[4]arenecomprising two triazole rings, as a novel neutral ionophore in plasticized poly(vinyl chloride) (PVC) membranes. The effect of lipophilic anionic additives on the voltammetric responses of the sensors was investigated in details. The constructed sensors exhibited a Nernstian behavior with 53 ± 0.9 mV per decade change in Ag+activity over the range from $7.0x10^{-6}$to $8.0x10^{-3}$, with a repetitive detection limit of 0.421 µg ml^{-1}. Moreover, the effect of lipophilic salts, plasticizers and various interfering ions were probed. Importantly, validation of the method is achieved in terms of good performance characteristics, including good selectivity for Ag+over alkali, alkaline earth and transition metal ions (e.g. Na+, K+, Pb^{2+}, Mg^{2+}, Co^{2+},Ni^{2+}, and Cu^{2+}) together with long life span. Other important characteristics such as low detection limit, acceptable accuracy and precision, long term stability, reproducibility were also demonstrated. On the application side, the sensors were utilized for facile potentiometric measurements of iodide ions (I^-) over the concentration range of 0.749 to 856 µg $ml^{-1}$and also employed for probing sequential titration of some importantly relevant anions (e.g. Cl^-, Br^-, I^-, SCN^- and N^{-3}). Significantly, sequential binding of these anions with Ag+cations produces sharp stepwise titration curves with consecutive end point breaks at the equivalent points.
Int. J. Electrochem. Sci., 11 (2016) 4729 - 4742

Electrochemical behavior of antioxidants: Part 3. Electrochemical studies of caffeic Acid-DNA interaction and DNA/carbon nanotube biosensor for DNA damage and protection

Refat Abdel-Hamid, Emad F. Newair
Department of Chemistry, Faculty of Science, University of Sohag, 82524 Sohag, Egypt

Multi-walled carbon nanotubes-modified glassy carbon electrode biosensor was used for electrochemical studies of caffeic acid-dsDNA interaction in phosphate buffer solution at pH 2.12. Caffeic acid, CAF, shows a well-defined cyclic voltammetric wave. Its anodic peak current decreases and the peak potential shifts positively on the addition of dsDNA. This behavior was ascribed to an interaction of CAF with dsDNA giving CAF-dsDNA complex by intercalative binding mode. The apparent binding constant of CAF-dsDNA complex was determined using amperometric titrations. The oxidative damage caused to DNA was detected using the biosensor. The damage caused by the reactive oxygen species, hydroxyl radical (.-OH) generated by the Fenton system on the DNA-biosensor was detected. It was found that CAF has the capability of scavenging the hydroxide radical and protecting the DNA immobilized on the GCE surface.
Arab. J. Chem., 9 (3) (2016) 365-370

11 April, 2017

Synthesis and Reactivity of Enaminones: Synthesis of Some 1,3,4- Thiadiazole Linked to Pyrazole, Pyridine, Benzimidazolopyrimidine, Pyrazolopyrimidine, Pyrazolotriazine and Triazolotriazine Derivatives

Mohamed A. Raslan[1*], Omran A. Omran[2,3]
[1]*Chemistry Department, Faculty of Science, Aswan University, 81528 Aswan, Egypt*
[2]*Chemistry Department, Faculty of Science, Sohag University, 82524 Sohag, Egypt*
[3]*College of Science in Zulfi, Majmaah University, 1712, 11932, Al Majmaah, Saudi Arabia*

1,3,4-Thiadiazole-enaminone (**6**) was synthesized via reaction of the benzamide (**5**) with DMF-DMA. The simple thiadiazole-enaminone (**6**) was used as a synthetic precursor for the synthesis of a wide variety of new heterocyclic compounds, including the 5-substituted-1,3,4-thiadiazole derivatives (**7**), (**8**), (**16**), (**17**) and (**18**), which were obtained via reactions of (**6**) with nitrogen nucleophiles. Also, reactions of enaminone (**6**) with carbon nucleophiles afforded the respective 1,3,4-thiadiazoles (**10a**,**10b**). Diazotization of the benzamide (**20**) with the heteroaromatic amine salts gave the hydrazone derivatives (**21**) and (**22**). Cyclization of the latter hydrazones yielded the corresponding pyrazolotriazine and 1,2,4-triazolotriazine derivatives (**23**) and (**24**), respectively. All newly synthesized compounds were elucidated by considering the data of both elemental and spectral analysis.

J. Heterocyclic Chem., 53 (2016) 1121-1128

N,N,N-Triethylethanaminium 5,11,17,23-tetra-tert-butyl-25 [(ethoxycarbonyl)methoxy]-26,28-dihy-droxy-27-oxido-2,8,14,20 tetrathiacalix[4]arene: a molecular salt

Joel T. Mague,[1] Mehmet Akkurt, [2] Shaaban K. Mohamed,[3,4] Omran A. Omran[5], Mustafa R. Albayati[6*]
[1]*Department of Chemistry, Tulane University, New Orleans, LA 70118, USA,*
[2]*Department of Physics, Faculty of Sciences, Erciyes University, 38039 Kayseri, Turkey,*
[3]*Chemistry and Environmental Division, Manchester Metropolitan University, England,*
[4]*Chemistry Department, Faculty of Science, Minia University, 61519 El-Minia, Egypt*
[5]*Chemistry Department, Faculty of Science, Sohag University, Sohag 82524, Egypt*
[6]*Kirkuk University, College of Science, Department of Chemistry, Kirkuk, Iraq*

In the title molecular salt, $C_8H_{20}N^1.C_{44}H_{53}O_6S_4$, the conformation of the anionictetrathiacalix[4]arene, which is cone-shaped, is primarilydetermined byintramolecular O-H···O hydrogen bonds. There are also short intramolecularC-H···O contacts present. The guest species do not sit within the bowl of thecalixarene. One of the t-butyl groups in the anion is disordered over two sets ofsites with refined occupancies of 0.706 (6) and 0.294 (6). Atoms of both cationsare equally disordered over centers of symmetry. In the crystal, extensive O-H···O and C-H···O hydrogen bonds and weak O-H···S interactions link thethiacalixarene anions and tetraethylammoniumcations, forming a three- dimensional network.

IUCrData 1 (9) (2016) x161465-3

N,N,N-Triethylethanaminium 5,11,17,23-tetra-tert-butyl-25-cyanomethoxy-26,28-dihydroxy-27-oxido- 2,8,14,20-tetrathiacalix[4]arene: a molecular salt

Omran A. Omran,[1,2]* Joel T. Mague,3 Shaaban K. Mohamed,[4,5] Mehmet Akkurt[6], Alaa F. Mohamed[7]

[1]*Medical Laboratory Department, College of Science, Majmaah University, Saudi Arabia*
[2]*Chemistry Department, Faculty of Science, Sohag University, 82524 Sohag, Egypt*
[3]*Department of Chemistry, Tulane University, New Orleans, LA70118,USA*
[4]*Chemistry and Environmental Division, Manchester Metropolitan University, England*
[5]*Chemistry Department, Faculty of Science, Minia University, 61519El-Minia, Egypt*
[6]*Department of Physics, Faculty of Sciences, Erciyes University, 38039Kayseri, Turkey*
[7]*National Organization for Drug Control and Research, Giza, Egypt*

In the title molecular salt, $C_8H_{20}N^1C_{42}H_{48}NO_4S_4$, the conformation of the anionic tetrathiacalix[4]arene, which is cone-shaped, is primarily determined by intramolecular O-H···O hydrogen bonds. There are also intramolecular C-H···O short contacts present. In the crystal, the anions (A) and cations (C) are linked by C-H···O and C-H···S hydrogen bonds, forming -A-C-A-C- chains along [001]. The chains are linked via C-H···N cyano hydrogen bonds, forming ribbons along[001].

IUCrData 1 (1) (2016) x160115-14

Synthesis and antibacterial activity of some new 4-anilino-5-phenyl-4*H*-1,2,4-triazole-3-thiol derivatives

Abd El-Badih A.G. Ghattas, Hassan M. Moustafa, Elsayed A. A. Hassanein, Bahgat R. M. Hussein
Chemistry Department, Faculty of Science, Sohag University, Sohag, Egypt

4-Anilino-5-phenyl-4H-1,2,4-triazole-3-thiol (**1**) reacted with formaldehyde and different amines to give Mannich bases $\mathbf{2}_{\mathbf{a-i}}$. Treatment of compound **1** with formaldehyde afforded the corresponding 2-hydroxymethyl derivative **3**, which upon its reaction with thionyl chloride yielded the corresponding chloromethyl derivative **4**. Treatment of compound **4** with some thiols gave the corresponding sulfides$\mathbf{5}_{\mathbf{a-f}}$. The ring closure reaction of chloromethyl derivative **4** with hydrazinehydrate, phenyl hydrazine, hydroxylamine, urea and thiourea afforded triazolo-, oxadiazolo- and triazinotriazoles**6-10**, respectively.

Arabian Journal of Chemistry 9 (2016) S1654-S1659

Cobalt(III)-porphyrin complex (CoTCPP) as an efficient and recyclable homogeneous catalyst for the synthesis of tryptanthrinin aqueous media

Mahmoud Abd El Aleem Ali Ali El-Remaily, O. M. Elhady
Department of Chemistry, Faculty of Science, Sohag University, 82524 Sohag, Egypt

The water soluble cobalt(III) porphyrin complex (CoTCPP) was employed as an efficient catalyst for thesynthesis of the biologically active natural product tryptanthrin. The reaction proceeded under mildconditions in aqueous media at room temperature from various isatoic anhydride and isatin derivatives.The advantages of these reactions were excellent yields, short reaction times and a recoverable catalyst.
Tetrahedron Letters 57 (2016) 435-437

A robust synthesis and characterization of superparamagnetic $CoFe_2O_4$ nanoparticles as an efficient and reusable catalyst for green synthesis of some heterocyclic rings

Mahmoud Abd El Aleem Ali El-Remaily*, Ahmed M. Abu-Dief, Rafat M. El-Khatib
Department of Chemistry, Faculty of Science, Sohag University, 82524 Sohag, Egypt

A robust synthesis for magnetic $CoFe_2O_4$ nanoparticles via a hydrothermal technique was investigated. The prepared magnetic nanoparticles were characterized using powder X-ray diffraction, scanning, transmission and high-resolution transmission electron microscopies, energy-dispersive X-ray and infrared spectroscopies, thermogravimetric analysis and vibrating sample magnetometry. Based on the obtained data, the prepared powder was composed of ultrafine particles in nanometer size range with highly homogeneous spherical shape and elemental composition. Moreover, the prepared magnetic $CoFe_2O_4$ nanoparticles were used as an efficient catalyst for green synthesis of tetrahydropyridines and pyrrole derivatives in excellent yields, with easy work-up and purification of products by non-chromatographic methods. The catalyst can be recovered for subsequent reactions and reused without any appreciable loss of activity.
Appl. Organometal. Chem., 30 (2016) 1022-1029

Synthesis and Antimicrobial Screening of Fused Heterocyclic Pyridines

Mahmoud A. A. El-Remaily, O. M. Elhady,* Eman M. M. Abdel-Raheem
Chemistry Department, Faculty of Science, Sohag University, Sohag 82524, Egypt

In an attempt to find a new class of antimicrobial agents, a series of pyridoxazepine, pyridothiazepine,triazepine, naphthyridine, pyridopyrimidine, and other related products containing pyridine moiety were synthesized via the reaction of 2-amino-6-chloro-3,5-dicyanopyridine 1 with nucleophilic chemical reagents.These compounds were screened for cytotoxicity and their antimicrobial activity. Most of products showedinhibitory effect.
J. Heterocyclic Chem., (2016)

Divinyl Sulfone Cross-Linked b-Cyclodextrin Polymer as Newand Effective Corrosion Inhibitor for Zn Anode in 3.5 M KOH

Hany M. Abd El-Lateef and Mahmoud Abd El Aleem Ali AliElremaily
Department of Chemistry, Faculty of Science, Sohag University, Sohag, Egypt

The inhibition behavior of the divinylsulfonecross-linked b-cyclodextrin polymer (βCDS-P) in 3.5 MKOH in the temperature range 25-55 °C on Zn anode wasstudied using weight loss, potentiodynamic polarizationand electrochemical impedance spectroscopy measurements. Results showed that, the inhibition efficiencyincreased with the increase in the concentration of inhibitorand the best inhibitor efficiency was reached with250 ppm. The results also showed that the inhibition efficiency decreased with the increase in temperature. Theinhibition was assumed to occur via adsorption of βCDS-Pon the Zn surface which could be approximated by Langmuir adsorption isotherm model. On the other hand, thecorrosion potential (Ecorr) slightly shifted to more negativevalues. This indicated that the presence of the inhibitor hada positive effect on charge efficiency and self-discharge.X-ray spectroscopy analysis (EDX) and scanning electronmicroscopy observations confirmed the presence of a goodprotective film on the Zn surface.
Trans Indian Inst Met. 69 (9) (2016) 1783-1792

Epichlorohydrin cross-linked β-cyclodextrin:an environmental method for the synthesis of 2-arylbenzothiazoles derivatives in water

Mahmoud Abd El Aleem Ali Ali El-Remaily, Ahmed M. M. Soliman
Department of Chemistry, Faculty of Science, Sohag University, Sohag, Egypt

In the present study, we report an environmentally benign synthesis of 2-arylbenzothiazoles derivatives from o-aminothiophenoland aldehydes in aqueous medium using β-cyclodextrin polymeras a catalyst and air as an oxidant. The polymer showed excellentcatalytic activity, recovered, reused six times, and the catalyst efficiency remained unchanged. This suggests that the catalyst is anefficient and green catalyst for the synthesis of 2-arylbenzothiazolesderivatives and the obtained results could be promising for industrialsynthesis of 2-arylbenzothiazoles derivatives.
Journal of Sulfur Chemistry, 37 (1) (2016) 70-79

Synthesis and in vitro Antibacterial Activity of Some Novel Fused Pyridopyrimidine Derivatives

Mahmoud Abd El Aleem Ali Ali El-Remaily,* O. M. El Hady, H. Salah Abo Zaid, E. M. M. Abd El-Raheem
Chemistry Department, Faculty of Science, Sohag University, Sohag 82524, Egypt

Pyridopyrimidine derivatives 2, 5 and 7-9 were furnished by the reaction of compound 1 with a variety of reagents, namely, formic acid, acetic anhydride, phenyl isothiocyanate, phenyl isocyanate, carbon disulfide, acetamide and thioacetamide, which in turn were treated with hydrazine to give pyrazolopyridopyrimidine derivatives 4, 6 and 11-13. The potency of the results as antibacterial agents has been evaluated. Most ofthe tested products showed a highly inhibition zone against the two bacterial strains. All compounds have been characterized based on their IR, 1H-NMR and Mass spectra.
J. Heterocyclic Chem., 53 (2016) 1304

Design, Synthesis and Hypolipidemic Activity of Novel Hydrazones of Nicotinic acid Hydrazide

Moustafa O. Aboelez[1,2], Omar M. Elhady[3], Montaser S. A. Shaykoon[4], Mai E.Shoman[1], Sanaa A. Ahmed[5], Gamal ElDin A. Abuo-Rahma*,[1]

[1]Department of Medicinal Chemistry, Faculty of Pharmacy, Minia University, Minia, Egypt
[2]Department of Pharmaceutical Chemistry, Faculty of Pharmacy, Sohag University, Egypt
[3]Department of Chemistry, Faculty of Science, Sohag University, Sohag, 82524-Egypt
[4]Department of Pharmaceutical Chemistry, Faculty of Pharmacy, Al-Azhar University, Assiut, Egypt
[5]Department of Pharmacology, Faculty of Medicine, Sohag University, Sohag, 82524-Egypt

Synthesis of novel N-acyl hydrazones of nicotinic acid hydrazide via condensation of nicotinic acid hydrazide **3** with the corresponding aldehydes **1, 2** are described. Their hypolipidemic activities were evaluated in high cholesterol diet fed rat model. The hydrazones were found to decrease the levels of serum total cholesterol, LDL cholesterol and triglycerides in hyperlipidemic rats to a greater degree than the reference gemfibrozil.
J. Pharm. Appl. Chem., 2 (3) (201 6) 147-151

Mimic Analogues and their Toxicological Aspects on *Spodoptera littoralis* (Boisd.)

[1]M. T. M. El-Wassimy, [2]Erian. S. Mansour, [1]Omar M. Elhady, [2]Ali M. Drar

[1]Chemistry Department, Faculty of Science, Sohag University, Egypt
[2]Plant Protection Research Institute, Agriculture Research Center, Dokki, Giza, Egypt

Various mimic analogues were synthesized by the reaction of acid chlorides with tertiary butyl hydrazine hydrochloride, The synthesized compounds were identified by their spectral analyses. The preliminary bioassays indicated that all compounds showed moderate insecticidal activities against cotton leaf worm spodoptera littoralis (Boisd.) which study the susceptibility of laboratory of 2nd and 4th instar larvae of the cotton leaf worm Spodoptera littoralis (Boisd). Five concentration levels (600, 300, 150, 75 and 37.5 ppm) were applied on the fresh plant food to the newly molted (2nd and 4th) instar larvae.
Middle East J. Appl. Sci., 6(1) (2016)

Synthesis of Novel Fused Heterocycles Based on 6-Amino-4-phenyl-2-thioxo-1,2-dihydropyridine-3,5-dicarbonitrile

H. Abdel-Ghany, A. M. El-Sayed, A. A. Amer, A. M. Ahmed
Chemistry Department, Faculty of Science, Sohag University, Sohag, Egypt

Under phase transfer catalysis conditions, 6-amino-4-phenyl-2-thioxo-1,2-dihydropyridine-3,5-dicarbonitrile (1) was allowed to react with halo compounds, acrylonitrile, chloroacetyl chloride, ethyl cyanoacetate, formamide, triethylorthoformate, or formic acid to give new derivatives of fused pyridines 2-22, respectively. Acetylation of compound 1 using acetic anhydride afforded product 23, which in turn underwent intramolecular cyclization in pyridine to give the corresponding pyrido[2,3-d]pyrimidine 24.

J. Heterocyclic Chem., 53 (2016) 2013

Synthesis, structure elucidation, biological screening, molecular modeling and DNA binding of some Cu(II) chelates incorporating imines derived from amino acids

Laila H. Abdel-Rahman, Ahmed M. Abu-Dief*, Mohammed Ismael, Mounir A.A. Mohamed, Nahla Ali Hashem
Chemistry Department, Faculty of Science, Sohag University, Sohag 82524, Egypt

Three tridentate Schiff bases amino acids were prepared by direct condensation of 3-methoxysalicylaldehyde (MS) or 4-diethylaminosalicylaldehyde (DS) with a-amino acid ligands [Lphenylalanine (P), L-histidine (H) and DL-tryptophan (T)]. The prepared Schiff bases amino acids were investigated by melting points, elemental analysis, 1HNMR and 13CNMR, IR, UV-Vis spectra, conductivity and magnetic measurements analyses. Subsequently, copper was introduced and Cu(II) complexes formed. These complexes were analyzed by thermal and elemental analyses and further investigated by FT-IR and UV/Vis spectroscopies. The experimental results indicating that all Cu(II) complexes contain hydrated water molecules (except DSPCu complex) and don't contain coordinated water molecules. The kinetic and thermal parameters were extracted from the thermal data using Coast and Redfern method. The molar conductance values of the Schiff base amino acid ligands and their Cu(II) complexes were relatively low, showing that these compounds have non-electrolytic nature. Magnetic susceptibility measurements showed the diamagnetic nature of the Schiff base amino acid ligands and paramagnetic nature of their complexes. Additionally, a spectrophotometric method was determined to extract their stability constants. It was found that the complexes possess 1:2 (M:L) stoichiometry. The results suggested that 3-methoxysalicylaldehyde and 4-diethylamino-salicylaldehyde amino acid Schiff bases behave as monobasic tridentate ONO ligands and coordinate Cu(II) ions in octahedral geometry according to the general formula [Cu(HL)2]$nH2O. To further understanding the structural and electronic properties of these complexes, Density Functional Theory (DFT) calculations were employed and provided a satisfactory description. The optimized structures of MST Schiff base ligand and its complex were calculated using DFT. The antimicrobial activity of the Schiff base ligands and their complexes were screened against some types of bacteria such as Bacillus subtilis (ve), Escherichia coli (_ve) and Micrococcus luteus (ve) and some types of fungi such as Asperagillus niger, Candida glabrata and Saccharomyces cerevisiae. The results of these studies indicated that the metal complexes exhibit a stronger antibacterial and antifungal efficiency compared to their corresponding ligands. The complexes were screened for antiviral activity against a panel of DNA and RNA viruses. Minimum cytotoxic and minimum virus inhibitory concentrations of these complexes were determined. The mode of interaction between complexes and CT-DNA was monitored using absorption spectra, viscosity measurements and gel electrophoreses.

J. Mol. Struct., 1103 (2016) 232-244

A Biocatalytic Aza-Achmatowicz Reaction

Fernández-Fueyo E.[1], Younes S. H. H.[1,2], Van Rootselaar S.[3], Aben R. W. M.[3], Renirie R.[4], Wever R.[5], Holtmann D.[6], Rutjes F. P. J. T.[3], Hollmann, F.[1]
[1]Department of Biotechnology, Delft University of Technology, Delft, Netherlands
[2]Department of Chemistry, Faculty of Sciences, Sohag University, Sohag, Egypt
[3]Institute for Molecules and Materials, Radboud University, Nijmegen, Netherlands
[4]IVAM UvA BV, Plantage Muidergracht 24, Amsterdam, Netherlands
[5]Van't Hoff Institute for Molecular Sciences (HIMS), Faculty of Science, University of Amsterdam, Science Park 904, Amsterdam, Netherlands
[6]DECHEMA Research Institute, Theodor-Heuss-Allee 25, Frankfurt am Main, Germany

A catalytic, enzyme-initiated (aza-) Achmatowicz reaction is presented. The involvement of a robust vanadium-dependent peroxidase from Curvularia inaequalis allows the simple use of H_2O_2 and catalytic amounts of bromide.
ACS Catalysis, 6(9) (2016) 5904-5907

4-Toluenesulfonamide as a Building Block for Synthesis of Novel Triazepines, Pyrimidines, and Azoles.

A. Khodairy, Ali M. Ali, M. T. El-Wassimy
Chemistry Department, Faculty of Science, Sohag University, Sohag, Egypt

N-{(E)-(dimethylamino)methylidenearbamothioyl}-4-toluenesulfonamide (2) was obtained by reaction of N-carbamothioyl-4toluenesulfonamide (1) with dimethylformamide dimethylacetal or alternatively by the reaction of 1-(dimethylamino)methylidenethiourea with tosyl chloride. Compound 2 was reacted with substituted anilines to yield anilinomethylidine derivatives 3a, 3b, 3c, 3d, 3e, 3f, 3g. Treatment of 3a, 3b, 3c, 3d, 3e, 3f, 3g with phenacyl bromide gave triazepines 4a, 4b, 4c, 4d, 4e, 4f, 4gand imidazoles 5a, 5b, 5c, 5d, 5e, 5f, 5g. Esterification of compound 3e afforded ester derivative 6, which was subjected to react with hydrazine to yield hydrazide derivative 7. Oxadiazole 8 was obtained by reaction of 7 with CS_2/KOH. Compound 3e was treated with o-aminophenol or o-aminothiophenol to give benzazoles 9a, 9b. N-(Diaminomethylidene)-4 toluenesulfonamide (10) reacted with enaminones to yield pyrimidines 11, 12, 13, respectively. The structures of the compounds were elucidated by elemental and spectral analyses. Some selected compounds were screened for their in vitro antifungal activity. In general, the newly synthesized compounds showed good antifungal activity.
J. Heterocyclic Chem.,53 (2016) 1544-1553

Synthesis of 3-Pyrazolyl-1,2,4-Triazoles via One-Pot Multicomponent Reaction in Phosphoric Acid

Amer A. A., Moustafa A. H.
Chemistry Department, Faculty of Science, Sohag University, Sohag, Egypt

A high-yielding synthetic route towards pyrazolyl-[1,2,4]triazole derivatives has been developed via one-pot multicomponent reaction of polyfunctionalized triazoles, DMF-DMA, acetophenone, ethyl cyanoacetate, and/or 3-oxo-3-phenylpropanenitrile in ortho-phosphoric acid (85%). In the same manner, a new series of 2-triazolyl-tetrahydro-indazol-4-ones and pyrazolo[3,4-d]pyrimidines has been synthesized by reaction of triazoles, DMF-DMA and 1,3-cyclohexanediones and/or barbituric acid, respectively. The same products were prepared a classical manner via reaction of triazoles with the corresponding enaminones in ortho-phosphoric acid (85%).
Synlett, 27(11) (2016) 1703-1706

Triclinic and monoclinic polymorphs of meso-(E,E)-1,1'-[1,2-bis(4-chlorophenyl)ethane-1,2-diyl]bis(phenyldiazene): The high-yield synthesis of an unexpected product, concomitant polymorphism and configurational disorder

Mohamed S. K.[1,2], Younes S. H. H.[3], Abdel-Raheem E. M. M.[3], Horton P. N.[4], Akkurt M.[5], Glidewell C.[6]
[1]Chemistry and Environmental Division, Manchester Metropolitan University, UK
[2]Chemistry Department, Faculty of Science, Mini University, El-Minia, Egypt
[3]Chemistry Department, Faculty of Science, Sohag University, Sohag, Egypt
[4]School of Chemistry, University of Southampton, Highfield, Southampton, UK
[5]Department of Physics, Faculty of Sciences, Erciyes University, Kayseri, Turkey
[6]School of Chemistry, University of St.Andrews, Fife, United Kingdom

Pyrazolidine-3,5-diones and their derivatives exhibit a wide range of biological activities. Seeking to explore the effect of combining a hydrocarbyl ring substituent, as present in sulfinpyrazone (used to treat gout), with a chlorinated aryl ring, as present in muzolimine (a diuretic), we explored the reaction between 1-phenylpyrazolidine-3,5-dione and 4-chlorobenzaldehyde under mildly basic conditions in the expectation of producing the simple condensation product 4-(4-chlorobenzylidene)-1-phenylpyrazolidine-3,5-dione. However, the reaction product proved to be meso-(E,E)-1,1'-[1,2-bis(4-chlorophenyl)ethane-1,2-diyl]bis (phenyldiazene), $C_{26}H_{20}Cl_2N_4$, and a tentative mechanism is proposed. Crystallization from ethanol produces two concomitant polymorphs, i.e. a triclinic form, (I), in the space group P, and a monoclinic form, (II), in the space group C2/c. In both polymorphs, the molecules lie across centres of inversion, but in (II), the molecules are subject to whole-molecule disorder equivalent to configurational disorder with occupancies of 0.6021(19) and 0.3979(19). There are no hydrogen bonds in the crystal structure of polymorph (I), but the molecules of polymorph (II) are linked by C-H···π(arene) hydrogen bonds into complex chains, which are further linked into sheets by C-H···N interactions.
Acta Crystallographica Section C: Structural Chemistry, 72 (2016) 57-62

New Heterocyclic Compounds Derived from 4,6-Diamino-3-cyano-2-methylthiopyridine and their Biological Activity

Ghattas A. E.-B. A. G., Khodairy A., Moustafa H. M., Hussein B. R. M.
Department of Chemistry, Faculty of Science, Sohag University, Sohag, Egypt

Treatment of 4,6-diamino-3-cyano-2-methylthiopyridine (1) with aqueous KOH or hydrazine hydrate afforded the corresponding nicotinamide 2 and pyrazolo[3,4-b]pyridine 3, respectively. Reaction of compound 1 with bromine, sulfuryl chloride, formaldehyde, or aromatic diazonium salts gave 5-bromopyridine 4, 5-chloropyridine 5, dipyridylmethane 6, and azo dyes 7, 8, 9, 10, respectively. Compound 1 reacted with diketones to yield the corresponding butenylamino derivative 11 and amides 12, 13, 14, 15, respectively. Treatment of butanamide 13 with diazonium salts or a mixture of urea and aromatic aldehyde in the presence of drops of HCl as a catalyst yielded the corresponding arylhydrazones 16, 17, 18, 19, pyrimidines 20, 21, 22, 23, 24, and 1,8-naphthyridine 25, respectively. The potency of the results as anti-inflammatory and antifungal agents have been evaluated. The compounds have been characterized based on their spectral and elemental analysis.

***Journal of Heterocyclic Chemistry*, 5 (2016)**

Functionalization of Magnetic Nano Particles: Synthesis, Characterization and Their Application in Water Purification

Ahmed M. Abu-Dief[1, 2], Samar Kamel Hamdan[2]
[1]Departamento de Quimica Organica e Inorganica, Faculad de Quimica, Universdad de Oviedo, Oviedo, Spain, [2]Chemistry Department, Faculty of Science, Sohag University, Sohag, Egypt

Contamination of fresh and marine sediments and water environments by oil spills, urban runoffs, industrial and domestic effluents is demonstrating to be of critical concern as the presence of contaminants affects aquatic organisms and can quickly disperse to large as highlighted by the recent Gulf oil spill disaster. Polycyclic aromatic hydrocarbons (PAHs), Poly chlorinated biphenyls (PCBs), dichlorodiphenyltrichloroethane (DDT) and heavy metals like mercury, lead and manganese are among the ubiquitous trace contaminants of marine and freshwater systems. Presence of these contaminants raise concerns as small quantities of the organic chemicals have been displayed to be carcinogenic to mammals and can pose a prohibition to both human health and the aquatic biota. Innovative operations for treating wastewater containing heavy metals often include technologies for reduction of toxicity. Nanotechnology has rampaged plethora of scientific and technological fields; environmental safety is no exception. One of the most promising and well developed environmental applications of nanotechnology has been in water remediation and treatment where different nanomaterials can help purify water meanwhile different mechanisms including adsorption of heavy metals and other pollutants, removal and inactivation of pathogens and diversion of toxic materials into less toxic compounds. Today nanoparticles, nanomembrane and nanopowder used for revelation and removal of chemical and biological substances include metals (e.g. Cadmium, copper, lead, mercury, nickel, zinc), nutrients (e.g. Phosphate, ammonia, nitrate and nitrite), cyanide, organics, algae (e.g. cyanobacterial toxins) viruses, bacteria, parasites and antibiotics. By tracing these technological advances to the physicochemical properties of nanomaterials, the present review outlines recent development in nanotechnology for wastewater treatment. The discussion covers candidate synthesis of magnetic nanomaterials (MNPs), properties and their mechanisms in water purification.

Am. J. Nanosci., 2 (3) (2016) 26-40

4-Hydroxy-1-phenylquinolin-2(1H)-one in One-pot Synthesis of Pyrimidoquinolines and Related Compounds under Microwave Irradiation and Conventional Conditions

Mourad A.-F. E.[1], Amer A. A.[2], El-Shaieb K. M.[1], Ali A. M.[2], Aly A. A.[1]
[1]*Department of Chemistry, Faculty of Science, Minia University, El-Minia, Egypt*
[2]*Department of Chemistry, Faculty of Science, Sohag University, Sohag, Egypt*

Biginelli condensation reactions of 4-hydroxy-1-phenylquinolin-2(1H)-one, aryl aldehydes and urea, or thiourea, 5-amino-1H-1,2,4-triazole, or 2-amine-1H-benzimidazole (9) under microwave irradiation afforded the corresponding pyrimido[5,4-c]quinolin-5-one derivatives in high yields. One-pot synthesis of 2H-pyrano[3,2-c]quinolines is also reported.
© 2015 HeteroCorporation.
J. Heterocyclic Chem., 53(2) (2016) 383-388

Synthesis of novel coumarin derivatives based on 6-aminocoumarin, kinetic inspection of base hydrolysis, and spectrophotometric tracer of intermediate progress

Abd Allah O. A. E. A., Nassr L. A.-M. E.
Department of Organic Chemistry, Faculty of Science Sohag University Sohag 82524 Egypt

The importance of 6-aminocoumarin, d-glucose, and ethyl cyanoacetate in pharmaceutical field was documented in literatures. Therefore, 6-aminocoumarin was reacted with single and double molarity of d-glucose forming Schiff's base and bis-compound derivatives. Also, it was reacted with CS_2 in phase transfer catalysis condition producing dithiocarbamate, which was used as an intermediate for the preparation of fused and polyfused derivatives. Additionally, it was reacted with dicarbonyl compounds via the condensation reaction to give the polycarbonyl derivatives. 6-Aminocoumarin was reacted with ethyl cyanoacetate via the addition and condensation reaction mechanisms; the effect of the side chains at the stability of some of these coumarins has been recorded. The kinetics of the base hydrolysis of 6-aminocoumarin and some of its derivatives was studied spectrophotometrically in aqueous medium at 298 K under pseudo-first-order conditions ($[OH^-] >> [Compound]$). The suggested general rate equation can be given as: Rate = $\{k_1 + k_2 [OH^-]\}$ [complex]. The reasonable mechanism suggested that the investigated reaction proceeded via the formation of an intermediate and the ring opening of the formed intermediate was the rate determining step. This is the first time in which the kinetics of the formation and decay of the intermediate were followed (at $[OH^-] \leq 3.5 \times 10^{-2}$ mol dm^{-3}).
Monatshefte fur Chemie, 147(4) (2016) 735-747

Porous $LaFeO_3$/Silica Nanocomposites via Sol-Gel Mixing Involving Citric Acid

Khalil K. M. S.[1] , Elhamdy W. A.[1], Said A. E.-A. A.[2], Elsamahy A. A.[1]
[1] *Chemistry Department, Faculty of Science, Sohag University, Sohag, Egypt*
[2] *Chemistry Department, Faculty of Science, Assiut University, Assiut, Egypt*

A series of 10, 20 and 30% (w/w) La_2O_3-Fe_2O_3/silica composites were synthesized by mixing of La-Fe citrate complex gels with spherical silica sols. This was followed by calcination of the formed xerogel at 550 °C and 750 °C for 3 h. The materials were characterized by XRD, simultaneous thermal analyses (TGA-DTA), FTIR, N_2 gas adsorption/desorption isotherms at −196 °C, and TEM techniques. Results indicated complete decomposition of the precursor complex upon calcination and development of porous composites with high surface area. However, processing of the La-Fe citrate complex gel or the silica precursors without mixing led to formation of $LaFeO_3$ perovskite oxide type and silica with very low surface area amounting to 4 and 11 m^2/g, respectively. Thus the process led to the formation of nanosized amorphous-like $LaFeO_3$ phase (as a shell) on the surface of the spherical silica particles (core). The enhancement of surface area and porosity of the composites was correlated to the dispersion of La-Fe precursor on the surface of silica sol. The method can be generalized for other mixed oxides.
Colloids and Surfaces A: Physicochemical and Engineering Aspects, 506 (2016) 840-848

Magnetic $NiFe_2O_4$ nanoparticles: efficient, heterogeneous and reusable catalyst for synthesis of acetylferrocene chalcones and their anti-tumour activity

Ahmed M. Abu-Dief[1,2], Ibrahim F. Nassar[2,3], Wafaa H. Elsayed[4]
[1]*Department of Chemistry, Faculty of Science, Sohag University, Sohag 82524, Egypt*
[2]*Departamento de Quimica Organica e Inorganica, Faculad de Quimica, Universdad de Oviedo, 33006, Oviedo, Spain*
[3]*Faculty of Specific Education, Ain Shams University, Cairo, Egypt*
[4]*Faculty of Science and Arts Turaif for Girls, Northern Border University, Saudi Arabia*

A robust synthesis of magnetic $NiFe_2O_4$ nanoparticles via a hydrothermal technique was investigated. The prepared magnetic $NiFe_2O_4$ nanoparticles were characterized using powder X-ray diffraction (XRD), scanning electron microscopy, transmission electron microscopy (TEM), high-resolution TEM, energy-dispersive X-ray spectroscopy, thermogravimetric analysis, infrared spectroscopy and vibrating sample magnetometry. XRD and TEM analyses confirmed the formation of single-phase ultrafine nickel ferrite nanoparticles with highly homogeneous cubic shape and elemental composition. Moreover, the prepared magnetic $NiFe_2O_4$ nanoparticles were used as an efficient, cheap and eco-friendly catalyst for the Claisen-Schmidt condensation reaction between acetylferrocene and various aldehydes (aromatic and/or heterocyclic) yielding acetylferrocene chalcones in excellent yields, with easy work-up and reduced reaction time. The products were purified via crystallization. The structures of the produced compounds were elucidated using various spectroscopic analyses (^{1}H NMR, ^{13}C NMR, GC-MS). The catalyst is readily recovered by simple magnetic decantation and can be recycled several times with no discernible loss of catalytic activity. Furthermore, the prepared chalcone derivatives were evaluated for their anti-tumour activity against three human tumour cell lines, namely HCT116 (colon cancer), MCF7 (breast cancer) and HEPG2 (liver cancer), and showed a good activity against colon cancer.
Appl. Organometal. Chem. 30 (2016) 917-923

Some new nano-sized Fe(II), Cd(II) and Zn(II) Schiff base complexes as precursor for metal oxides: Sonochemical synthesis, characterization, DNA interaction, in vitro antimicrobial and anticancer activities

Laila H. Abdel-Rahman, Ahmed M. Abu-Dief*, Rafat M. El-Khatib, Shimaa Mahdy Abdel-Fatah

Chemistry Department, Faculty of Science, Sohag University, 82534 Sohag, Egypt

The complexes of Fe(II), Cd(II) and Zn(II) with Schiff base derived from 2-amino-3-hydroxypyridine and 3-methoxysalicylaldehyde have been prepared. Melting points, decomposition temperatures, Elemental analyses, TGA, conductance measurements, infrared (IR) and UV-Visible spectrophotometric studies were utilized in characterizing the compounds. The UV-Visible spectrophotometric analysis revealed 1:1 (metal-ligand) stoichiometry for the three complexes. In addition to, the prepared complexes have been used as precursors for preparing their corresponding metal oxides nanoparticles via thermal decomposition. The structures of the nano-sized complexes and their metal oxides were characterized by X-ray powder diffraction and transmittance electron microscopy. Moreover, the prepared Schiff base ligand, its complexes and their corresponding nano-sized metal oxides have been screened in vitro for their antibacterial activity against three bacteria, gram-positive (Microccus luteus) and gram-negative (Escherichia coli, Serratia marcescence) and three strains of fungus. The metal chelates were shown to possess more antimicrobial activity than the free Schiff-base chelate and their nano-sized metal oxides have the highest activity. The binding behaviors of the complexes to calf thymus DNA have been investigated by absorption spectra, viscosity mensuration and gel electrophoresis. The DNA binding constants reveal that all these complexes interact with DNA through intercalative binding mode. Furthermore, the cytotoxic activity of the prepared Schiff base complexes on human colon carcinoma cells, (HCT-116 cell line) and hepatic cellular carcinoma cells, (HepG-2) showed potent cytotoxicity effect against growth of carcinoma cells compared to the clinically used Vinblastine standard.

Bioorg. Chem. 69(2016) 140-152

Some New Nano-sized Mononuclear Cu(II) Schiff Base Complexes: Design, Characterization, Molecular Modeling and Catalytic Potentials in Benzyl Alcohol Oxidation

Laila H. Abdel-Rahman[1], Ahmed M. Abu-Dief[1], Mohamed Shaker S. Adam[1,2], Samar Kamel Hamdan[1]

[1]Chemistry Department, Faculty of Science, Sohag University, Sohag 82534, Egypt

[2]Department of Chemistry, College of Science, King Faisal University, P.O. Box 380, Al Hufuf, 31982 Al Hassa, Saudi Arabia

In the present contribution, some novel Cu(II) complexes were synthesized from tri- and tetradentate imine ligands. All the prepared compounds were elucidated by different physicochemical methods. Density Functional Theory calculations were carried out to explain the equilibrium geometry of the bsisnph and npisnph ligands and their Cu(II) complexes. Interaction of the synthesized ligands with Cu(II) affords nano-sized particles via TEM. The catalytic potentials of the prepared complexes has been tested within the oxidation of benzyl alcohol using an environmental friendly terminal oxidant, i.e. H2O2. The effect of various parameters, e.g. solvents, temperature and amount of catalyst was investigated. A mechanistic pathway of the catalytic oxidation was tentatively described and discussed.

Catal. Lett. 146 (2016) 1373-1396

Artificial Macrocycles by Ugi Reaction and Passerini Ring Closure

Abdelraheem E. M. M.[1,2], Kurpiewska K.[3], Kalinowska-Tluścik J.[3], Dömling A.[1]
[1]*Department of Drug Design, University of Groningen, A. Deusinglaan 1, Groningen, Netherlands*
[2]*Chemistry Department, Faculty of Science, Sohag University, Sohag, Egypt*
[3]*Faculty of Chemistry, Jagiellonian University, 3 Ingardena Street, Kraków, Poland*

Artificial macrocycles can be convergently synthesized by a sequence of an Ugi multicomponent reaction (MCR) followed by an intramolecular Passerini MCR used to close the macrocycle. Significantly, in this work, the first intramolecular macrocyclization through a Passerini reaction is described. We describe 21 macrocycles of a size of 15-20. The resulting macrocyclic depsipeptides are model compounds for natural products and could find applications in drug discovery.
J. Org. Chem., 81(19) (2016) 8789-8795

Some new nano-sized Cr(III), Fe(II), Co(II), and Ni(II) complexes incorporating 2-((E)-(pyridine-2-ylimino) methyl) napthalen-1-olligand: Structural characterization, electrochemical, antioxidant, antimicrobial, antiviral assessment and DNA interaction

Laila H. Abdel-Rahman, Ahmed M. Abu-Dief [*], Emad F. Newair, Samar Kamel Hamdan
Chemistry Department, Faculty of Science, Sohag University, 82534 Sohag, Egypt

To estimate the biological preference of synthetic small drugs towards DNA target, new metal based chemotherapeutic agents of nano-sized Cr(III), Fe(II), Co(II) and Ni(II) Schiff base complexes having N,N,O donor system were synthesized and thoroughly characterized by physic-chemical techniques. The redox behavior of the Cr(III), Fe(II) and Co(II) complex was investigated by electrochemical method using cyclic voltammetry. IR results proven that the tridentate binding of Schiff base ligand with metal center during complexation reflects the proposed structure. Magnetic and spectroscopic data give support to octahedral geometry for Cr(III) and Fe(II) complexes and tetrahedral geometry for Ni(II) and Co(II) complexes. The activation thermodynamic parameters, such as, E*, ΔH*, ΔS* and ΔG* are calculated using Coats-Redfern method by analyzing the TGA data. The particle size of the investigated metal complexes was estimated by TEM. In addition to, the interaction of the nanosized complexes with CT-DNA was estimated by electronic absorption, viscosity and gel electrophoresis. These techniques revealed that the complexes could bind to CT-DNA through intercalation mode. Moreover, the in vitro cytotoxic and antiviral activities of the nanosized complexes were checked against Herpes Simplex virus and Tobacco Mosaic viruses. Moreover, investigation of antioxidant activities of the new nanosized compounds was done by ABTS assay. Among the compounds tested, Fe(II) complex showed the strongest potent radical scavenging activity with percent of 58.60%. Furthermore, the antimicrobial bustle of the prepared compounds was screened against different types of bacteria and fungi and the results showthat all metal complexes have superior activity than its free ligand.
J. Photochem. Photobio. B. 160 (2016) 18-31

New Cd(II), Mn(II) and Ag(I) Schiff Base Complexes : Synthesis, Characterization, DNA Binding and Antimicrobial Activity

Laila H. Abdel-Rahman[1], Ahmed M. Abu-Dief[*1], Rafat M. El-Khatib[1], Shimaa Mahdy Abdel-Fatah[1], Amin Abdou Seleem[2]
[1]*Chemistry Department, Faculty of Science, Sohag University, 82534, Egypt*
[2]*Zoology Department, Faculty of Science, Sohag University, 82534 Sohag, Egypt*

Some Cd (II), Mn (II) and Ag (I) complexes derived from Schiff base ligand, obtained by the condensation of 4-Nitrobenzaldehyde and 2-amino-3-hydroxypyridine were synthesized. The complexes were characterized by elemental analysis, molar conductivity, magnetic susceptibility, IR, UV-Vis spectral data and thermal analysis. The complexes were found to be non-electrolytic in nature depending on value of molar conductance. From the spectral data, an octahedral geometry has been approached for all the complexes except Ag (I) complex which is tetrahedral. Moreover, the metal complexes have been tested for their antibacterial and antifungal activity. Furthermore, DNA interaction of these complexes was tempted by using Electronic spectra, viscosity measurements and gel electrophoresis. The experimental results indicated that the investigated complexes could associate with DNA via intercalative mode and showed a different DNA binding activity.
Int. J. Nano. Chem. 2(3) (2016) 83-91

Nano Sized Moringa oleifera an Effective Strategy for Pb(II) ions Removal from Aqueous Solution

Laila H. Abdel-Rahman[1], Ahmed M. Abu-Dief[1*], M. A. Abd- El Sayed[2], Mallak Megalea Zikry[2]
[1]*Chemistry Department, Faculty of Science, Sohag University, 82534 Sohag, Egypt*
[2]*Medicinal and Aromatic Plants Researches Department, Horticulture Research Institute (HRI), Agri. Res. Center (ARC), Giza, Egypt*

Nano-sized *Moringa oleifera* is considered an effective biosorbent with high surface area from agricultural waste, low coast and environment-friendly which can be used for removal of Pb2+ from waste water. Thus our study stem to investigate the ability of natural nano-sized biosorbents for removing very toxic Pb2+ ions from aqueous solution. The investigated biosorbent (*Moringa oleifera*) was characterized by FTIR, SEM, TEM, XRD and EDX techniques. Moreover, the influence of pH, temperature, adsorbent dosage, contact time and initial metal ion concentration on adsorption process were investigated. The maximum biosorption capacities (qm) of Pb2+ ions by *Moringa oleifera* was 37.9 mg/g. The lowest biosorption was observed (61.4%) for Pb2+ ions at pH 2.0 while the highest one (94.36%) at pH 5. The optimum contact time for the adsorption process was found to be at 60 minutes. The amount of Pb2+ ions adsorbed increases with increasing in initial metal ion concentration. Moreover, biosorption capacity (qe) and removal efficiency of Pb2+ ions solutions increase as temperature increases. FT-IR data indicated that the adsorption of metal ions occurs on the surface of *Moringa oleifera* powder as the main functional groups that are responsible for metal ions binding are involved in the process. Furthermore, Thermodynamic studies confirmed that the biosorption process was endothermic and the positive value of ΔG° is quite common when an ion-exchange mechanism applies in the biosorption. The Positive value of ΔS° suggested an increase in randomness during the biosorption. The kinetics study of sorption indicates that the pseudo secondorder model provides better correlation of the sorption data (R2=0.99) than the pseudo first-order model (R2 = 0.91), confirming the chemisorption of metal ions solutions on *Moringa oleifera.* The Freundlich isotherm has agood fit with the experimental data (R2 close to 1) compared to Langmuir isotherm (R2=0.99). This study shows that *Moringa oleifera* are available, low cost, effective and environment friendlly biosorbent for the removal of Pb2+ ions from aqueous environment.
Chemistry and Materials Research 8, No.4 (2016)

Effect of chromium substitution on the structural and magnetic properties of nanocrystalline zinc ferrite

Ahmed M. Abu-Dief[1,2,3 *], Mohammed S.M. Abdelbaky[2], David Martínez-Blanco[3], Zakariae Amghouz[4], Santigo García-Granda[2]

[1]Chemistry Department, Faculty of Science, Sohag University, 82524 Sohag, Egypt
[2]Department of Physical and Analytical Chemistry, University of Oviedo-CINN, 33006 Oviedo,Spain
[3]Department of Organic and Inorganic Chemistry, University of Oviedo-CINN, 33006 Oviedo, Spain
[4]Scientific and Technical Services, University of Oviedo-CINN, 33006 Oviedo, Spain

Single-phase Cr doped zinc ferrites have been synthesized by hydrothermal method. The crystal structure, microstructure, crystallite size and distribution, composition and magnetic properties of the synthesized nanoparticles were determined using X-ray powder diffraction, electron microscopies and vibrating sample magnetometry. Powders are composed of ultrafine spherical nanoparticles with a highly homogeneous elemental composition. The nanoparticles have partially inversed cubic spinel structure with average crystallite size below 10 nm. Superparamagnetic behavior is observed at high temperature while ferrimagnetic ordering and surface spin canting is reported at 5 K. Substitution of Fe with Cr ions controls both structural and magnetic parameters.

Mater. Chem. Phy. 174 (2016) 164-171

Sonochemical synthesis, DNA binding, antimicrobial evaluation and in vitro anticancer activity of three new nano-sized Cu(II), Co(II) and Ni(II) chelates based on tri-dentate NOO imine ligands as precursors for metal oxides

Laila H. Abdel-Rahman, Ahmed M. Abu-Dief*, Rafat M. El-Khatib, Shimaa Mahdy Abdel-Fatah
Chemistry Department, Faculty of Science, Sohag University, 82534, Egypt

Three new nano sized Cu(II), Co(II) and Ni(II) complexes of imine ligand derived from the condensation of 2-amino-3-hydroxypyridine and 3-methoxysalicylaldehyde have been prepared and investigated using various chemical techniques such as NMR, elemental analysis, molar conductance, IR, electronic spectra, TGA and magnetic moment measurements. The obtained chemical analysis data showed that the synthesis of 1:1 (metal:ligand) ratio and octahedral geometry was proposed on the basis of magnetic moment and spectral data studies except the Cu(II) complex which is tetrahedral geometry. Nano-sized particles of the investigated complexes were prepared by sonochemistry method. Furthermore, metal oxides nanoparticles were gained by calcination of the prepared corresponding complexes at 500 °C and their structures were characterized by powder x-ray and transmittance electron microscopy.Moreover, the free ligand, its complexes and their metal oxides have been checked in vitro against a number of bacteria and fungi in order to assess their antimicrobial activities. In addition to that, DNA binding of the prepared complexeswas tested by many routes such as electronic spectra, viscosity and gel electrophoresis. The results showed that the investigated complexes could bind to DNA via an intercalative mode. The cytotoxicity of the Schiff base complexes on human colon carcinoma cells, (HCT-116 cell line) and Breast carcinoma cells, (MCF-7 cell line) showed potent cytotoxicity effect against growth of carcinoma cells compared to the clinically used Vinblastine standard.

J. Photochem. Photobio. B. 162 (2016) 298-308

Removal of Toxic Pb(II) Ions from Aqueous Solution by Nano Sized Flamboyant Pod (*Delonix regia*)

Laila H Abdel-Rahman[1], Badriah SF Al-Farhan[2], Ahmed M Abu-Dief[1,3], Mallak Megalea Zikry[4]
[1]*Chemistry Department, Sohag University, 82534 Sohag, Egypt*
[2]*Chemistry Department, King Khalid University, 61321 Abha, Saudi Arabia*
[3]*Department of organic chemistry and inorganic chemistry, relevant Faculty of Chemistry, University of Oviedo, 33006, Oviedo, Spain*
[4]*Medicinal and Aromatic Plants Researches Department, Horticulture Research Institute (HRI), Agriculture Research Center (ARC), Giza, Egypt*

The removing of toxic heavy metals from aqueous solution by agricultural biosorbents was investigated by studying the effect of nano sized (*Delonix regia*) and chemically modified biosorbent citric acid *Delonix regia* (CADR) for removing of Pb^{2+} ions. TEM, XRD and EDS, FT-IR, SEM methods were used for characterizing the biosorbent (*Delonix regia*). The effect of contact time, pH, temperature, dosage of biosorbent, and Pb2+ ion concentration on adsorption process were studied. The maximum biosorption capacities (qm) of Pb^{2+} by *Delonix regia* biosorbent was 43.62 mg/g. The highest R. E was (93.5%) at pH 5. FT-IR method showed that the adsorption of metal ions occurs by functional groups on the surface of *Delonixregia* powder. The biosorption process was endothermic from thermodynamic parameters. The pseudo second-order model more fit (R2=0.999) than the pseudo first-order model (R^2=0.985) from studying the kinetic parameters. The experimental data fit with Freundlich isotherm (R2 close to 1). This results indicated that *Delonix regia i*s available agricultural, low cost and environment friendly biosorbent for removing the Pb^{2+} ions.
Arch. Chem. Res. 1 (1) (2016) 3

One-Pot Multicomponent Synthesis of Novel 2 Tosyloxyphenyl-pyrans under Green and Conventional Condition with Anti-inflammatory Activity

Khodairy A. [1], Ali A. M. [1], Aboelez M. O. [2], El-Wassimy M. T. [1]
[1]*Department of Organic Chemistry, Faculty of Science Sohag University Sohag 82524 Egypt*
[2]*Department of Pharmaceutical Medicinal Chemistry, Faculty of Pharmacy Sohag University Egypt*

A mild, efficient, and environmentally green protocol for the synthesis of 2-tosyloxyphenylpyran derivatives 3, 4, 5, 6, 7, 8, 9, 10, 11 via reaction of 2-tosyloxybenzaldehyde (1) with malononitrile and some ketonic reagents in one-pot, three component reaction within few minutes under stirring in methanol in presence of ammonium hydroxide solution or ultrasonic irradiation. On the other hand, the same products 3, 4, 5, 6, 7, 8, 9, 10, 11 were obtained by traditional method, on treatment of 2-tosyloxybenzilidinemalononitrile (2) with the same ketonic reagents in refluxing ethanol in presence of TEA. 2-Tosyloxyphenylpyranopyrazoles 12 and 13 were obtained via treatment of compound 1 with malononitrile, hydrazine hydrate or phenyl hydrazine and ethyl acetoacetate, in one-pot, multicomponent reaction (MCRs). The structures of the new compounds were elucidated by elemental and spectral analyses. The newly synthesized compounds showed promising anti-inflammatory activity
Journal of Heterocyclic Chemistry, 53 (2016)

Reactivity tracers of the hydrolysis of Fe(II)-bis(salicylidene) complexes: Initial - transition states analysis and enhanced impact of tensides on the kinetic trends

Lobna Abddel-Mohsen E. Nassr
Chemistry Department, Faculty of Science, Sohag University, P.O. Box., Sohag, Egypt

The kinetics of the acid hydrolysis reaction of Fe(II)-bis(salicylidene) complexes were followed under pseudo-first-order conditions ($[H^+] >> [complex]$) at 298 K. The ligands of the studied azomethine complexes were derived from the condensation of salicylaldehyde with different five α-amino acids. The hydrolysis reactions were studied in acidic medium at different ratios (v/v) of aqua-organic mixtures. The decrease in the dielectric constant values of the reaction mixture enhances the reactivity of the reaction. The transfer chemical potentials of the initial and transition states (IS-TS) from water into mixed solvents were determined from the solubility measurements combined with the kinetic data. Nonlinear plots of $\log k_{obs}$ versus $1/D$ (the reciprocal of the dielectric constant) suggest the influence of the solvation of IS-TS on the reaction reactivity. Furthermore, the acid hydrolysis reactions were screened in the presence of different concentrations of cationic and anionic tensides. The addition of surfactants to the reaction mixture accelerates the reaction reactivity. The obtained kinetic data were used to determine the values of $\delta_m \Delta G^{\#}$ (the change in the activation barrier) for the studied complexes when transferred from "water to various ratios (v/v) of water-co-organic binary mixtures" and from "water to water containing different [surfactant]." It was found that the reactivity of the acid hydrolysis reaction was controlled by the hydrophobicity of the studied chelates.
International Journal of Chemical Kinetics, 48(2) (2016) 61-71

Oxidation efficiencies of high spin Fe(II)-azo amino acid complexes by potassium peroxydisulfate. Initial state-transition state solvation effects

M. S. S. Adam[1,2], U. El-Ayaan[1,3], A. D. M. Mohamad[2,4]
[1]*Department of Chemistry, College of Science, King Faisal University, Al Hassa, Saudi Arabia*
[2]*Department of Chemistry, Faculty of Science, Sohag University, Sohag 82534, Egypt*
[3]*Department of Chemistry, Faculty of Science, Mansoura University, Mansoura 35516, Egypt*
[4]*Department of Chemistry, Faculty of Science, Northern Boarders University, Arar, Saudi Arabia*

Synthesis of four iron(II)-azo amino acid complexes (**1-4**) carried out by direct mixing of *N*,*N*-diethylamino-4-nitrosoaniline, amino acids (alanine, histidine, tryptophan or phenylalanine) and Fe(II) ions in aqueous-methanol media with general formula $[Fe^{II}L_2(H_2O)_2]Cl_2 \cdot nH_2O$, where L is azo amino acid ligands. Azo ligands act as bidentate ligands and coordinate to Fe(II) ions through O-carboxylic and N-azo groups. Complexes **1-4** are characterized by IR, UV-visible spectra, thermogravimetric analyses (TGA) and conductance measurements. Kinetics of **1-4** oxidation by peroxydisulfate ions are studied spectrophotometrically in an aqueous media and in various aqueous-methanol binary mixtures at 25 ºC. Kinetics of the oxidation followed pseudo first order reaction $k_{obs} = (k_2[S_2O_8^{2-}])[complex]$. Reactivity trends and their rate constants are discussed in terms of polarity, hydrophobicity of **1-4**, and solvation effect of methanol. The effect of methanol ratios on the oxidation reaction is analyzed into initial (*is*) and transition state (*ts*) components. The decrease in the rate constant of the **1-4** oxidation, as the ratio of methanol increases, is predominantly caused by the effect of methanol on the initial state (*ts*) or by an increase in the free energy difference between *is* and *ts*.
Journal of Solution Chemistry, 45 (2016) 772-790

Pyrido-anellated 1,3-azaphospholes-current state and future challenges

M. S. S. Adam[1,2], M. Ghalib[1,3], G. J. Palm[4], P. G. Jones[5], J. W. Heinicke[1]

[1]Institut für Biochemie, Ernst-Moritz-Arndt-Universität Greifswald, Felix-Hausdor.-Str. 4, 17487 Greifswald, Germany, [2]Chemistry Department, Faculty of Science, Sohag University, Sohag-82524, Egypt, [3]Chemistry Department, University of Hodeidah, Hodaidah, Yemen, [4]Institut fur Biochemie (Molekulare Strukturbiologie), Ernst-Moritz-Arndt-Universitat Greifswald, Greifswald, Germany, [5]Institut für Anorganische und Analytische Chemie, Technische Universität Braunschweig, Hagenring 30, 38106 Braunschweig, German

A short overview of the syntheses, properties and some reactions of pyrido-anellated 1,3-azaphospholes is presented. Except for 2-phosphaindolizines, which have been intensively studied with respect to syntheses, electrophilic substitution and cycloadditions, this is a class of compound that has still been only sparingly investigated. Preliminary results and hints as to possible perspectives are included to encourage further research on these novel P,N hybrid ligands.

Phosphorus, Sulfur and Silicon, 191(3) (2016) 548-557

3*H*-1,3-Azaphospholo[4,5-*b*]pyridines - novel heterocyclic P,N-bridging or hybrid ligands: Synthesis and first d^8-transition metal complexes

M. S. S. Adam[1,2], M. K. Kindermann[1], P. G. Jones[3], J. W. Heinicke[1]

[1]Institut für Biochemie, Ernst-Moritz-Arndt-Universität Greifswald, Felix-Hausdor.-Str. 4, 17487 Greifswald, Germany

[2]Chemistry Department, Faculty of Science, Sohag University, Sohag-82524, Egypt

[3]Institut für Anorganische und Analytische Chemie, Technische Universität Braunschweig, Hagenring 30, 38106 Braunschweig, Germany.

The first 3*H*-1,3-azaphospholo-pyridines **2a-c** were synthesized as racemic mixtures in modest to medium yield by the reaction of *N*-(2-chloropyrid-3-yl)-trimethylacetimidoyl chloride **1** with $RPLi_2$ (R = Ph, *n*-Bu, *i*-Bu), generated from RPH_2 and BuLi in THF at -70 °C, and studied with respect to their suitability as ligands (L) in transition metal complexes. Reactions of **2a** with group 6 metal(0) pentacarbonyls led to P-coordinated $LM(CO)_5$ complexes **3a-5a** (Cr, Mo, W) and the reaction of **2c** with (norbornadiene)-$Mo(CO)_4$ surprisingly to **4c**. $[Rh(1,5\text{-}COD)Cl]_2$ and **2a,b**, in metal/ligand ratio 1 : 1, furnished LRh(1,5-COD)Cl complexes **6a,b** with P-coordination, **6b** accompanied by a minor contamination by the *bis*-coordinated $L[Rh(COD)Cl]_2$ complex **7b**. Reactions of **2a,b** with $[(allyl)PdCl]_2$ proceeded in THF with dismutation of *N*-coordinated (allyl)PdCl and formed with **2a** a labile crude product $[(\mathbf{2a})\{(allyl)PdCl\}_{1.2}(PdCl_2)_{0.8}]\cdot C_4H_8O$, with the composition close to L[Pd(allyl)Cl]$PdCl_2$ THF (**8a**·THF), which converted during crystallization to **9a**, whereas **2b** directly formed the *N*,*N*'-$PdCl_2$-bridged *bis*[LPd(allyl)chloride] complex **9b**. Conversion of **2b** with equimolar amounts of $Pd(CH_3CN)_2Cl_2$ in THF, or Na_2PdCl_4 in methanol, gave rise to the dimeric *P*,*N*-bridging complex **10b**. Crystal structure analyses of **6a** (rac), **9b**·2$CDCl_3$ (meso), **10b**·4.5THF and **10b**·2D_6-acetone (rac) provided detailed structural information. **10b**, but more efficiently complexes formed in situ from **2a,b** and $Pd_2(DBA)$ or $Pd(OAc)_2$, catalysed the arylamination of 2-bromopyridine with 2,4,6-trimethylaniline.

Dalton Transactions, 45 (2016) 2261-2272

Voltammetric determination of polyphenolic content in pomegranate juice using a poly(gallic acid)/multiwalled carbon nanotube modified electrode

Abdel-Hamid, R.; Newair, E.F.
Chemistry Department, Faculty of Science, Sohag University, Sohag 82524, Egypt

A simple and sensitive poly(gallic acid)/multiwalled carbon nanotube modified glassy carbon electrode (PGA/MWCNT/GCE) electrochemical sensor was prepared for direct determination of the total phenolic content (TPC) as gallic acid equivalent. The GCE working electrode was electrochemically modified and characterized using scanning electron microscope (SEM), cyclic voltammetry (CV), chronoamperometry and chronocoulometry. It was found that gallic acid (GA) exhibits a superior electrochemical response on the PGA/MWCNT/GCE sensor in comparison with bare GCE. The results reveal that a PGA/MWCNT/GCE sensor can remarkably enhance the electro-oxidation signal of GA as well as shift the peak potentials towards less positive potential values. The dependence of peak current on accumulation potential, accumulation time and pH were investigated by square-wave voltammetry (SWV) to optimize the experimental conditions for the determination of GA. Using the optimized conditions, the sensor responded linearly to a GA concentration throughout the range of 4.97×10^{-6} to 3.38×10^{-5} M with a detection limit of 3.22×10^{-6} M (S/N = 3). The fabricated sensor shows good selectivity, stability, repeatability and (101%) recovery. The sensor was successfully utilized for the determination of total phenolic content in fresh pomegranate juice without interference of ascorbic acid, fructose, potassium nitrate and barbituric acid. The obtained data were compared with the standard Folin-Ciocalteu spectrophotometric results.

***Beilstein Journal of Nanotechnology*, *7* (2016) 1104 -1112**

Mechanism of Chicoric Acid Electrochemical Oxidation and Identification of Oxidation Products by Liquid Chromatography and Mass Spectrometry

Newair, E.F., Abdel-Hamid, R. Paul A. Kilmartin
Chemistry Department, Faculty of Science, Sohag University, Sohag 82524, Egypt

Electrochemical oxidation of chicoric acid (ChA) was investigated using cyclic voltammetry and chronoamperometry at a glassy carbon electrode. Chicoric acid generates single quasi-reversible redox wave in cyclic voltammetry over a wide pH range, and an ECECdimerization mechanism is proposed. Effect of glutathione (GSH) on the electrochemical oxidation of chicoric acid (ChA) was investigated in Britton-Robinson buffer solution. Ultra-high performance liquid chromatography (UPLC) coupled with mass spectrometry (MS) was used to show that the naturally occurring chicoric acid (ChA) underwent an electrochemical oxidation in the presence of glutathione (GSH) to form mono-, bi-, tri-, and four-glutathione conjugates of chicoric acid and a mono-glutathione conjugate of a chicoric acid dimer. The obtained results are useful for understanding and predicting the oxidative degradation pathway of chicoric acid.

Electroanalysis, 28 (2016) 1-12

Electroanalytical Determination of Luteolin in Peanut Hulls Using Carbon Black Modified Glassy Carbon Electrode

Newair E. F., Abdel-Hamid R., François Garcia
Chemistry Department, Faculty of Science, Sohag University, Sohag 82524, Egypt

The main objective of this research was to develop a simple and sensitive electrochemical method for determination of trace-level of luteolin using vulcan carbon black (VCB) modified glassy carbon electrode (GCE). Compared with the bare GCE, the VCB/GCE exhibits higher electrocatalytic ability toward luteolin oxidation. This is due to the large surface-to-volume ratio of the carbon black together with the good conductivity. The results illustrated that the oxidative peak currents increased linearly with the concentration of luteolin in the range of 2.40 x 10^{-9} to 5.14 x 10^{-8} M, with a detection limit of 2.21 x 10 M (S/N = 3). Moreover, the analytical performance of the sensor was successfully applied for the determination of luteolin in peanut hulls as a real sample with satisfactory results.
Brazilian Journal of Analytical Chemistry, 4 (2016) 38-47

Synthesis and evaluation of novel series of Schiff base cationic surfactants as corrosion inhibitors for carbon steel in acidic/chloride media: experimental and theoretical investigations

Hany M. Abd El-Lateef [*1] Ahmed H. Tantawy[2]
[1]*Chemistry Department, Faculty of Science, Sohag University, 82524 Sohag, Egypt*
[2]*Chemistry Department, Faculty of Science, Benha University, 13518 Benha, Egypt*

A new family of Schiffbase cationic surfactants (CSSB) having various alkyl chain lengths were prepared and their chemical structure was elucidated by using different spectroscopic techniques (FTIR, 13 C-NMR and 1 H-NMR). The surface activity parameters of the prepared surfactants were measured to set the adsorption and micellization characteristics at the water/air interface. The corrosion inhibition capability of these surfactants was investigated on a carbon steel surface in 3.5% NaCl+0.5 M HCl solutions at different temperatures (30-60 °C) by potentiodynamic polarization and electrochemical impedance spectroscopy measurements. The results revealed that CSSB compounds inhibited corrosion of carbon steel in the investigated acidic chloride containing environment. It was found that the inhibition efficiency increases with an increase in inhibitor concentrations and decreases with increasing temperature. Polarization data indicated that the investigated compounds act as mixed-type inhibitors, and the adsorption isotherm basically obeys the Langmuir isotherm. The corrosion inhibition mechanism was discussed based on the potential of zero charge value. An SEM/EDX studies confirmed that CSSB inhibitors could form films by adsorption on the carbon steel surface. The theoretical predictions exhibit good agreement with empirical results.
RSC Adv., 6 (2016) 8681-8700

Corrosion protection of mild steel by coating with TiO_2 thin films co- doped with NiO and ZrO_2 in acidic chloride environments

Mai M. Khalaf,Hany M. Abd El-Lateef*
Chemistry Department, Faculty of Science, Sohag University, Sohag 82524, Egypt

A series of TiO_2 thin films co-doped with NiO and ZrO_2 coatings was prepared by sol-gel and dip-coating techniques for the corrosion protection of mild steel substrates. The crystalline phase, morphology and composition of the coatings were achieved by X-ray diffraction (XRD), scanning electron microscopy (SEM), transmission electron microscopy (TEM), energy dispersive X-ray spectroscopy (EDAX) and fourier transform infrared spectroscopy (FTIR). Texture properties of prepared coated samples were investigated by N_2 adsorption- desorption isotherms. The corrosion protection performance was investigated in 3.5% NaCl +1.0 M HCl solution by electrochemical impedance spectroscopy and potentiodynamic measurements. Results show that, the prepared coatings offer good anti-corrosion protection to mild steel in the studied acidic chloride solution, with the degree of protection depending on number of coating layers (thickness) and co-dopant content in the coatings. SEM/EDAX investigations reinforce the possibility of protecting mild steel against corrosion through the formation of a protective layer of NiO/TiO_2 and co-doped $NiO-ZrO_2/TiO_2$ using coatings.

Materials Chemistry and Physics 177 (2016) 250-265

Empirical and Theoretical Calculations for Corrosion Inhibition of Carbon Steel C1018 in Acidic Solutions Using Some Selected Fatty Acid Surfactants

Hany M. Abd El-Lateef*[1], Mohamed Ismael[1], Ahmed H. Tantawy[2]
[1]Chemistry Department, Faculty of Science, Sohag University, 82524 Sohag, Egypt
[2]Chemistry Department, Faculty of science, Benha University, 13518Benha, Egypt

Three different surfactants based on fatty acids (octanoic, tridecanoic and oleic) and ethylenediamine were synthesized and their chemical structures were confirmed by FT-IR, ^{1}H-NMR and ^{13}C-NMR spectroscopy. The surface-active properties of the prepared surfactants were determined by using interfacial tension.The synthesized surfactants were evaluated as corrosion inhibitors for carbon steel in a solution of 0.50 M HCl at 40 ºC. Potentiodynamic polarization, linear polarization resistance corrosion rate and electrochemical impedance spectroscopy measurements were used for this study. Experimental results showed that, the inhibition efficiency increases with increasing the surfactant concentration, getting maximum inhibition efficiency ranged between 97.10 and 99.61% at 400 ppm. Potentiodynamic polarization curves showed that, the three compounds act as mixed type. The adsorption of investigated surfactants obeyed the Langmuir adsorption isotherm, and the thermodynamic parameters were calculated and discussed. Obvious correlation was found between the corrosion inhibition efficiency and the quantum chemical parameters. The obtained theoretical results have been adapted with the experimental data.

Zeitschrift für Physikalische Chemie (2016)

Empirical and quantum chemical studies on the corrosion inhibition performance of some novel synthesized cationic gemini surfactants on carbon steel pipelines in acid pickling processes

Hany M. Abd El-Lateef[1]*, Mohamed A. Abo-Riya[2], Ahmed H. Tantawy[2]
[1]*Chemistry Department, Faculty of Science, Sohag University, 82524 Sohag, Egypt*
[2]*Chemistry Department, Faculty of science, Benha University, 13518Benha, Egypt*

Three novel cationic gemini surfactants were synthesized and their effect on the corrosion of carbon steel in 15% HCl solution was investigated using weight loss, electrochemical impedance spectroscopy, potentiodynamic polarization, surface analysis (SEM and EDX) and quantum chemical methods. The surface parameters of the synthesized surfactants were calculated from the surface tension and conductivity measurements The results revealed that the prepared surfactants were effectively inhibited the carbon steel corrosion in 15% HCl. Analysis of polarization data indicates that all surfactants act as mixed type inhibitors. The inhibitors adsorption on the metal surface obeyed Langmuir isotherm. The correlation between empirical and theoretical results was discussed.
Corrosion Science 108 (2016) 94-110

Modification of Hematite Photoanode with Cobalt Based Oxygen Evolution Catalyst via Bifunctional Linker Approach for EfficientWater Splitting

Amira Y. Ahmed, Mahmoud G. Ahmed, Tarek A. Kandiel
Department of Chemistry, Faculty of Science, Sohag University,

The modification of hematite photoanode with cheap, scalable, and efficient oxygen evolution catalyst is an essential step for its practical application for solar fuel production. In this paper, a simple and water-based method has been developed for the modification of hematite surface with cobalt based oxygen evolution catalyst using 3-aminopropionic acid (APA) as a bifunctional linker. APA exists in an aqueous solution at pH 6.1 in zwitterionic form and thus it has a positive charge on the protonated amino group and a negative charge on the carboxylate group. The carboxylate groups of APA molecules can thus interact with the protonated surface hydroxyl groups of hematite whereas the amino groups tether the cobalt ions. The hematite photoanodes were characterized by X-ray diffraction, scanning electron microscopy, X-ray photoelectron spectroscopy, infrared spectroscopy and inductively coupled plasma optical emission spectroscopy. The photoelectrochemical measurements indicated that Co/APA-hematite photoanode exhibit 3.8-, 3.2-, and 2-fold higher photocurrent at 1.23 V vs RHE than bare, Co-, and CoPi-hematite photoanodes, respectively. Moreover, the onset potential of photoelectrochemical water oxidation on Co/APA-hematite photoanode is cathodically shifted by 290 mV in comparison to that obtained on bare hematite photoanode. This finding has been explained by measuring the transient photocurrent and intensity modulated photocurrent spectroscopy responses. On the basis of these measurements, it was found that the rate constant of electron transfer at Co/APA-hematite photoanode/liquid interface is higher than that measured for bare and CoPi-hematite photoelectrodes. This explains the higher photoelectrochemical activity of Co/APA-hematite photoanode and reflects on the potential application of this simple approach for the modification of different metal oxide photoelectrodes with cobalt-based oxygen evolution catalyst.
The Journal of Physical Chemistry C, 120 (2016) 23415-23420

Solvent-induced deposition of Cu-Ga-In-S nanocrystals onto a titanium dioxide surface for visible-light-driven photocatalytic hydrogen production

Tarek A. Kandiel[1,2], Kazuhiro Takanabe[1]
[1] *Division of Physical Sciences and Engineering, KAUST Catalysis Center (KCC), King Abdullah University of Science and Technology (KAUST), Thuwal, Saudi Arabia*
[2]*Department of Chemistry, Faculty of Science, Sohag University*

In this paper, copper-gallium-indium-sulfide (CGIS) nanocrystals with different Ga/In ratios, i.e., $CuGa_xIn_5$-xS_8, where x = 0-5, were synthesized and investigated for visible-light-driven hydrogen (H_2) evolution from aqueous solutions that contain sulfide/sulfite ions. The synthesized CGIS nanocrystals were characterized by diffuse reflectance spectroscopy (DRS), X-ray diffraction (XRD), transmission electron microscopy (TEM), and photoluminescence spectroscopy (PL). With 1.0 wt.% Ru as a co-catalyst, the H_2evolution rate on $CuGa_2In_3S_8$ (CGIS hereafter) showed the highest activity. The CGIS nanocrystals were deposited onto a TiO_2 surface via a unique solvent-induced deposition method. The CGIS/TiO_2 photocatalyst showed comparable activity to that obtained using bare CGIS nanocrystals when the photocatalyst amount was sufficient in the photoreactor system, suggesting that TiO_2 remains intact in terms of photocatalytic activity. The quantity of CGIS nanocrystals, however, required to achieve the rate-plateau condition at saturation was much lower in the presence of TiO_2. The enhanced activities at low CGIS loadings observed in the presence of TiO_2 were explained by the improved dispersion of the powder suspension and optical path in the photoreactor. This TiO_2 supported photocatalyst lowers the required amount of CGIS, which is beneficial from an economic point of view.
Applied Catalysis B: Environmental, 184 (2016) 264-269

TiO_2(B)/anatase heterostructure nanofibers decorated with anatase nanoparticles as efficient photocatalysts for methanol oxidation

Tarek A. Kandiel[1], Amira Y. Ahmed[1], Detlef Bahnemann[2,3]
[1]*Department of Chemistry, Faculty of Science, Sohag University*
[2]*Photocatalysis and Nanotechnology Research Unit, Institut für Technische Chemie, Leibniz Universität Hannover, Callinstrasse 3, Hannover, Germany*
[3]*Laboratory for Nanocomposite Materials, Department of Photonics, Faculty of Physics, Saint-Petersburg State University, Ulianovskaia Street 3, Peterhof, Saint Petersburg, Russian Federation*

TiO_2(B) nanofibres, TiO_2(B)/anatase heterostructure nanofibres, TiO_2(B)/anatase heterostructure nanofibres decorated with anatase nanoparticles, and thermally highly stable anatase TiO_2 nanorods have been prepared by hydrothermal treatment of TiO_2P25 in aqueous NaOH solution followed by controlled ion-exchange and thermal annealing processes. The obtained TiO_2 nanomaterials were characterized by x-ray diffraction, scanning electron microscopy, transmission electron microscopy, diffuse reflectance spectroscopy, electrochemical impedance spectroscopy, and nitrogen adsorption. The photocatalytic activities of the prepared materials were quantified by measuring the photocatalytic methanol oxidation under UV-vis illumination. The results indicated that TiO_2(B)/anatase heterostructure nanofibres decorated with anatase nanoparticles (84% anatase and 16% TiO_2(B)) exhibit 3.5-fold higher photocatalytic activity towards methanol oxidation than TiO_2(B) nanofibres and anatase TiO_2 nanorods. These nanofibres even showed higher photocatalytic activity than TiO_2 P25. This is explained by a better separation of the photogenerated charge carriers and, most likely, by the facile interfacial charge transfer between TiO_2(B) and anatase structures as confirmed by impedance spectroscopy measurements.
Journal of Molecular Catalysis A: Chemical, 425 (2016) 50-60

Visible light driven hydrogen evolution with a noble metal free $CuGa_2In_3S_8$ nanoparticle system in water

Tarek A. Kandiel, Georgina A. M. Hutton, Erwin Reisner
Department of Chemistry, University of Cambridge, Cambridge, UK

$CuGa_2In_3S_8$ (CGIS) nanoparticles were synthesised by a hot-injection method and rendered water dispersible by modification with the hydrophilic ligand 3-mercaptopropionic acid (MPA). The CGIS nanoparticles were characterised by X-ray diffraction, transmission electron microscopy, X-ray photoelectron, diffuse reflectance and infrared spectroscopy as well as inductively coupled plasma optical emission spectroscopy. Photocatalytic H_2 production using the MPA modified CGIS nanoparticles and a nickel salt under visible light irradiation was achieved from acidic solution (pH 2.6) with ascorbic acid as a sacrificial electron donor. Previously, CGIS required the presence of a precious metal co-catalyst and sulfide ions as a sacrificial reagent in alkaline solution to display photocatalytic activity for H_2 generation. In the reported system, visible light irradiation of the MPA modified CGIS nanoparticles with a Ni salt displayed even superior sacrificial H_2 evolution activity than when employing the precious metals Pt, Rh and Ru. An external quantum efficiency of more than 12% was achieved at λ = 540 nm, which is almost twice that previously reported for CGIS nanoparticles in the presence of a noble metal co-catalyst and sulfide ions as an electron donor.

Catalysis Science & Technology, 6 (2016) 6536-6541

Photocatalytic hydrogen production from biomass-derived compounds: A case study of citric acid

Ayad F. Alkaim, Tarek A. Kandiel, Ralf Dillert, Detlef W. Bahnemann
[1]*Institut für Technische Chemie, Leibniz Universität Hannover, Hannover, Germany*
[2]*Department of Chemistry, College of Science for Women, Babylon University, Hilla, Iraq*
[3]*Department of Chemistry, Faculty of Science, Sohag University, Sohag, Egypt*
[4]*Laboratory for Nanocomposite Materials, Department of Photonics, Faculty of Physics, Saint-Petersburg State University, Saint-Petersburg, Russian Federation*

Highly crystalline anatase TiO_2 nanoparticles with high BET surface area have been synthesized by thermal hydrolysis of titanium(IV) bis(ammoniumlactato) dihydroxide aqueous solutions. The photocatalytic H_2 production from aqueous citric acid (CA) solutions over Pt-loaded TiO_2 has been investigated under different experimental conditions, that is, different CA concentration, temperature, light intensity, and pH of Pt/TiO_2 suspension. For comparison, the photocatalytic dehydrogenation of triethanolamine (TEA) has also been investigated. The highest H_2 production rates were obtained at pH 3 and 9 for CA and TEA, respectively. This behavior is readily explained by the adsorption characteristic of the employed reagent on the surface of the charged TiO_2. The effect of the photocatalyst loading and the light intensity on the H_2 production rate showed the same behavior in the case of CA and TEA evincing that these parameters are catalyst dependent. The apparent activation energies have been determined to be 13.5 ± 1.8 and 14.7 ± 1.6 kJ mol^{-1} for CA and TEA, respectively, indicating the existence of an activation energy barrier in a photocatalytic process which can be attributed to the desorption of adsorbed products.

Environmental Technology, 37 (2016) 2687-2693

Photo and electrical peculiarities of the nanostructured glass/ITO/AAO and glass/ITO/CdS systems

Sh. O. Eminov[1], D. B. Tagiyev[2], A. Sh. Aliyev[2], N. Sh. Soltanova[2], J. A. Guliyev[1], Kh. D. Jalilova[1], N. J. Ismayilov[1], I. S. Hasanov[1], A. A. Rajabli[1], G. Kh. Mamedova[1], I. I. Gurbanov[1], Mahmoud Elrouby[*3]

[1]*Institute of Physics, Azerbaijan National Academy of Sciences, H.Javid Ave., 1143 Baku, Azerbaijan*
[2]*Institute of Catalysis and Inorganic Chemistry, Azerbaijan National Academy of Sciences, H.Javid Ave., 131,1143 Baku, Azerbaijan*
[3]*Chemistry Department, Faculty of Science, Sohag University, Sohag 82524, Egypt*

The systems of indium tin oxide (ITO)/nano-porous anodized aluminum oxide Al2O3 (AAO) and ITO/CdS nano-structured were fabricated on transparent glass substrates by using radio frequency magnetron sputtering and electrochemical deposition. The glass/ITO/AAO samples were transparent for visible light that make them useful and efficient for PV solar cell applications. The effect of annealing on optical and electrical properties of ITO thin films has been studied. It is found that the transparency of the ITO films is directly proportional to the oxygen content of the plasma in the sputtering chamber and increased with annealing temperature, while the sheet resistance is inversely proportional to the annealing. In this work, it is found that the electrochemically fabricated CdS thin films nanostructure of a thickness of 200-500 nm is transparent and well absorbs the light over the wavelength wide ranged from 450 to 800 nm. Raman spectrum of CdS thin film obtained via backscattering geometry exhibits relatively sharp crystal-like peaks at 300 and 600 cm^{-1}. The full width at half maximum value FWHM of Raman peak at the 300 nm is 40 cm^{-1}.

Journal of Materials Science: Materials in Electronics 27 (2016) 9853-9860

Self-assembly of porous copper oxide hierarchical nanostructures for selective determinations of glucose and ascorbic acid

Bahaa G. Mahmoud, Mohamed Khairy, Farouk A. Rashwan, Christopher W. Foster, Craig E. Banks

Chemistry Department, Faculty of Science, Sohag University, Sohag 82524, Egypt

The simple design of CuO micro-/nanostructures has recently attracted tremendous interest particularly for the enzyme-less sensing of biological molecules due to their intrinsic electronic and catalytic properties. Consequently attention has been directed to the development of new CuO nanomaterials that have multi-interdisciplinary applications. Herein, we report for the first time the fabrication of hierarchical porous CuO micro-/nanostructures with flower- and hollow sphere-like morphology via a facile hydrothermal method. Our experimental findings clarify that the source of the copper-ions effectively control the assembly of CuO nano-building blocks via the one-step hydrolysis of $[Cu(NH_3)_4(H_2O)_2]SO_4$ and $[Cu(NH_3)_4(H_2O)_2]Cl_2$ precursors, which produce hollow sphere and flower-like morphologies for sensitive and selective determination of ascorbic acid and glucose, respectively. Moreover, such unique properties of macro-/mesoporous CuO with defined dimensions and topologies offer minimized diffusive resistance for the dispersion of active sites. The best performance of the glucose and ascorbic sensor can be obtained at +0.55 V in 0.1 M sodium hydroxide solution. The as-prepared CuO modified (drop-casted) screen-printed electrodes (SPE) exhibit a fast electroactive response with high sensitivity within a wide concentration range of glucose and ascorbic acid in real samples. Significantly, the anion dependent approach might be used to control effectively the expansion and features of other metal oxide micro-/nanostructures

RSC Adv., 6 (2016) 14474-14482

Electrochemical Fabrication and Characterization of Corrosion-Resistant, Ternary, Lead-Based Alloys as a New Material for Steel Surface Protection

A. Sh. Aliyev[1], H. M. Tahirli[1], Mahmoud Elrouby*[2], N. Sh. Soltanova[1], D. B. Tagiev[1]
[1]*Institute of Physics, Azerbaijan National Academy of Sciences, H.Javid Ave., 1143 Baku, Azerbaijan*
[2]*Chemistry Department, Faculty of Science, Sohag University, Sohag 82524, Egypt*

This article presents the study of the synthesis of the ternary Pb-Sb-Te alloy on the stainless steel substrate via an electrochemical method. The corrosion resistance of the electrodeposited alloy has been investigated via subjecting the electro-synthesized alloy to a corrosive medium containing sulfide ions; this medium is similar to the petroleum refining environment. The resulting film of the electrodeposited alloy was analyzed by the scanning electron microscope, energy-dispersive X-ray analysis, and X-ray diffraction to determine the morphology and the phase structure of the electrodeposited film. It was found that the electrodeposited Pb-Sb-Te alloy thin film is a multiphase composition. The obtained data reveal that the most corrosion-resistant phase is the $PbSb_2Te_4$ alloy..
Metallurgical and Materials Transactions B 47 (2016) 2072-2078

Revealing the mechanism, degradation pathways and kinetics of UV_{254nm} /H_2O_2-baseddegradation of model active sunscreen ingredient PBSA

Wael H. M. Abdelraheem[1, 2], Xuexiang He[2, 3], Zanaty R. Komy[1], Nabawia M. Ismail[1], Dionysios D. Dionysiou[2, 3]
[1]*Chemistry Department, Faculty of Science, Sohag University, Sohag 82524, Egypt*
[2]*Environmental Engineering and Science Program, University of Cincinnati, Cincinnati, Ohio, US*
[3]*NIREAS-International Water Research Center, University of Cyprus, Nicosia, 1678, Cyprus*

Transformation byproducts and pathways for the degradation of 2-phenylbenzimidazole-5-sulfonic acid (PBSA), a widely used organic active sunscreen agent, by UV_{254nm}/H_2O_2advanced oxidation process (AOP) were elucidated by mass spectrometry. Fourteen byproducts were identified, including environmentally hazardous benzamide (BD) and benzamidine (BZD). Beside of aromatic ring opening, desulfonation (−80 Da) and hydroxylation (+16 Da) were also two main reaction pathways. Degradation kinetics were compared with two PBSA structurally related compounds 2-phenylimidazole (2-PIZ) and benzimidazole (BZ) to estimate the application feasibility of the studied AOP. No apparent photolysis was noticed while the degradation of 1 μM pollutants in the presence of 1 mM H_2O_2 followed *pseudo-first-order* kinetics, with their observed rate constant (k_{obs}) in the order of 2-PIZ > PBSA > BZ > BD > BZD, which is consistent with their respective *second-order* rate constant with hydroxyl radical. However, at high pollutant and oxidant concentrations, i.e., 50 μM and 5 mM, respectively, light attenuation contributed significantly to the change in k_{obs} in the following manner, 2-PIZ ~ BZ > PBSA ~ BD > BZD. SO_4^{2-} and NH_4^+ were the major inorganic mineral ions monitored in this study. Release of SO_4^{2-} from PBSA degradation system reached 70% at 190 min. At the same time interval, NH_4^+ were ⩽50% for all pollutants studied. Ultimate mineralization of PBSA, 2-PIZ, BZ, BD and BZD in terms of %TOC at 190 min was found to be 23%, 38%, 45%, 57% and 62%, respectively. UV/H_2O_2 was shown to be efficient for the removal of organic sunscreen agents from water, however, special care toward the formation of environmentally hazardous byproducts should be considered.
Chemical Engineering Journal, 288 (2016) 824-833

A natural clayey adsorbent for selective removal of lead from aqueous solutions

Ali Sdiri, Mohamed Khairy, Samir Bouaziz, Sherif El-Safty
Chemistry Department, Faculty of Science, Sohag University, Sohag 82524, Egypt

Natural clay minerals are an inherently colorless class of materials, which have long been known for their versatility as adsorbents due to their interchange capacity, large catalytic support, great surface area, and low cost. Herein, we have reported the use of natural clay, collected from the Gabes area, southern Tunisia (Early Cretaceous) for selectively capturing of lead ions from aqueous environments. Our results showed that natural clay samples were mainly composed of silica, alumina, iron and magnesium oxides. Adsorption data showed that the studied clay samples preferably removed substantial amounts of lead ions from water. The removal efficiency of lead ions was about 86.4 mg/g of clay and followed pseudo-second-order kinetics. More than 95% of the total adsorptive capacity occurred within 30 min. These results suggest the Early Cretaceous clays, Tunisia, turned out to be an effective natural adsorbent for capturing of lead ions from aqueous environment.
Applied Clay Science 126 (2016) 89-97

Ceria-zirconia modified MnOx catalysts for gaseous elemental mercury oxidation and adsorption

Deshetti Jampaiah,[ab] Samuel J. Ippolito,[b] Ylias M. Sabri,[b] James Tardio,[b] P. R. Selvakannan,[b] Ayman Nafady,[cd] Benjaram M. Reddy[*a], Suresh K. Bhargava[*b]
[a]*RMIT-IICT Joint Research Centre, CSIR-Indian Institute of Chemical Technology, Uppal Road, Hyderabad - 500 607, India*
[b]*Centre for Advanced Materials & Industrial Chemistry (CAMIC), School of Applied Sciences, RMIT University, GPO BOX 2476, Melbourne-3001, Australia*
[c]*Chemistry Department, College of Science, King Saud University, Riyadh, Saudi Arabia*
[d]*Chemistry Department, Faculty of Science, Sohag University, Sohag 82524, Egypt*

A series of MnO_x/CeO_2 (Mn/Ce), MnO_x/ZrO_2 (Mn/Zr), and $MnO_x/Ce_{0.75}Zr_{0.25}O_2$ (Mn/CZ) catalysts prepared by an impregnation method were tested for their ability to catalyse the oxidation of Hg0 at relatively low temperature (423 K). Various characterization techniques, namely, Brunauer-Emmett-Teller (BET) surface area analysis, X-ray diffraction (XRD), Raman spectroscopy (RS), X-ray photoelectron spectroscopy (XPS), and H_2-temperature programmed reduction (H_2-TPR) were employed to understand the structural, surface, and redox properties of the prepared catalysts. Specific aspects of the catalysis of Hg0 oxidation that were investigated included the influence of MnO_x loading (5, 15, and 25%) and the influence of HCl and O_2. Among the catalysts tested, the 15Mn/CZ catalyst achieved the best Hg^0 oxidation performance (~83% conversion of Hg^0 to Hg^{2+}) in the presence of HCl and O_2. The higher activity of the 15Mn/CZ catalyst was most likely due to the presence of more oxygen vacancies, enhanced $Mn^{4+}/Mn^{4+} + Mn^{3+} + Mn^{2+}$ ratio and more surface adsorbed oxygen, which were proved by XRD, BET, Raman, and XPS. H_2-TPR results also show that the strong interaction between the $Ce_{0.75}Zr_{0.25}O_2$ support and MnO_x improved the redox properties significantly as compared to pure CeO_2 and ZrO_2 supported MnO_x catalysts.
Catal. Sci. Technol., 6 (2016) 1792-1803

Natural betanin dye extracted from bougainvillea flowers for the naked-eye detection of copper ions in water samples

Mohamed Khairy, Mohamed Ismael, Rafat M. El-Khatib, Mostafa Abdelnaeemb, Mariam Khalaf
Chemistry Department, Faculty of Science, Sohag University, Sohag 82524, Egypt

We introduce the concept of water-soluble natural dye (betanin) as a novel colorimetric sensor for the naked eye detection of copper ions in water samples. Such simple, green, fast, selective and low-cost colorimetric determination of Cu^{2+} ions would definitely enhance the environmental and economic benefits of this alternative form of synthetic chelating agent

Anal. Methods, 8 (2016) 977-4982

The Path Towards Healthier Societies, Environments & Economies: A Broader Perspective for Sustainable Engineered Nanomaterials

Thabet Tolaymat[1], Wael Abdelraheem[2,3,4], Amro El Badawy[2], Dionysios D. Dionysiou[4], Ash M. Genaidy[2]
[1]*U.S. Environmental Protection Agency, Office of Research and Development, Cincinnati, Ohio, USA*
[2]*Worldtek Inc, Cincinnati, Ohio 45249, USA*
[3]*Chemistry Department, Faculty of Science, Sohag University, Sohag 82524, Egypt*
[4]*Sustainable Solution Laboratory, Department of Biomedical, Chemical and Environmental Engineering, University of Cincinnati, Cincinnati, Ohio 45221, USA*

Economic value is no longer adequate by itself as a proxy for the value-added benefits (VAB) assumed to be generated by emerging technologies such as engineered nanomaterials (ENMs). This study was conducted to explore the potential to establish an integrated sociotechnical framework with the end goal to assess whether or not ENMs and nano-enabled products contribute VAB. Based on the research in this study, it is suggested that all stakeholders in the larger society-environment-economy (SEE) system should develop an understanding of the multiple interrelationships within and between the diverse constituents along the particle lifecycle trajectory to capture their influence on the system benefit and risk outcomes. Furthermore, the sociotechnical framework establishes an additional three-step process: (1) at the pre-design stage, the test of VAB should be assessed using an expert panel representing the different segments of SEE, the social principles of design are detailed and customized to the needs of ENMs and nano-enabled products, and an economic appraisal is conducted to justify the VAB on material grounds; (2) at the design stage, the technical principles should be examined and detailed to ensure the compatibility of stakeholder needs; and (3) an iterative adaptive cycle should be conducted to re-examine the sociotechnical principles on a periodic basis. Within this context, ENMs are considered sustainable when (a) the conditions of VAB and minimal risk elements are satisfied in a sequential order, with VAB demonstrated at the pre-design stage, then at the design stage ENMs posing no harm greater than minimal levels to the SEE constituents; and (b) ENMs and nano-enabled products are bounded by a finite time limit. In addition, to reach the conditions of sustainability, the role of all SEE stakeholders should be broadened (e.g., regulatory agencies should transform their roles from not only the control of risks of negative implications, but also the establishment of positive implications as well)

Clean Technologies and Environmental Policy, 18(2016) 2279-2291

Evaluation of serum cortisol, growth and thyroid hormones and its relation with lipolysis in non-diabetic obese and diabetic obese subjects attending Sohag Governorate, Egypt

Ali Taha A. Hassan[1], Hossam El-Din M. Omar[2], Nagwa M. Elsawi[3]*, Amira M. Ahmed[3]
[1]*Department of Internal Medicine, Faculty of Medicine, Sohag University, Egypt*
[2]*Zoology Department, Faculty of Science, Assiut University, Assiut 71516, Egypt*
[3]*Department of Chemistry, Faculty of Sience, Sohage University, Sohage 82524, Egypt*

The study aim to estimate the level of some hormones and free fatty acids which have a role in metabolic processes and its relation to obesity and diabetes 2 type. Cortisol, growth and thyroid hormones were determined by ELISA in serum of 85 subjectes including 30 controls, 31 non-diabetic obese and 24 obese diabetic. Obesity is described according to BMI. Blood pressure and glucose level were measured for all participants. Free fatty acids (FFAs) analysis was performed by gas chromatography technique. Hormonal assays were performed by ELISA methods Results: Blood levels of cortisol in non-diabetic obese subjects was non-significantly decreased compared to control group, while in obese diabetic group increased significantly compared to non-diabetic obese subjects. Growth hormone in both non-diabetic obese and obese diabetic groups was decreased compared to controls. Thyroid hormones T3 and T4 showed a non-significant decrease in non-diabetic obese subjects compared to control group, however, increased significantly in obese diabetic group compared to nondiabetic obese group. Blood FFAs showed various changes in unsaturated and saturated among the three groups. In conclusion, the present study found that changes in the levels of cortisol, growth hormone and thyroid hormones were correlated with BMI and the level of FFAs in serum.

GARJMMS, 5 (4) (2016) 96-102

Preferential synthesis of highly conducting Tl(TCNQ) phase II nanorod networks via electrochemically driven TCNQ/Tl(TCNQ) solid-solid phase transformation

Nafady, A.[ab] , Sabri, Y.M.[c], Kandjani, A.E.[c], Alsalme, A.M.[a], Bond, A.M.[d], Bhargava, S.[c]
[a] Department of Chemistry, College, King Saud, Riyadh, Saudi Arabia
[b] Department of Chemistry, Faculty of Science, Sohag University, Sohag, Egypt
[c] Centre for Advanced Materials and Industrial Chemistry (CAMIC), School of Applied Sciences, RMIT University, GPO Box 2476 V, Melbourne, VIC, Australia
[d] School of Chemistry, Monash University, Clayton, VIC, Australia

Facile synthesis and characterization of the highly conducting, thermodynamically favored, Tl(TCNQ) phase II microrods/nanorods onto conducting (glassy carbon (GC)) and semiconducting (indium tin oxide (ITO)) surfaces have been accomplished via redox-based transformation of 7,7,8,8-tetracynoquinodimethane (TCNQ) microcrystals. This electrochemically irreversible process involves the one-electron reduction of surface-confined solid TCNQ into $TCNQ^{\cdot -}$ with concomitant incorporation of the $Tl^{+}_{(aq)}$ cation, from the bulk solution, at the triple-phase boundary, GC or ITO $\left| (TCNQ_{(s)}/TCNQ^{\cdot -}{}_{(s)}) \right| Tl^{+}_{(aq)}$, through a nucleation/growth mechanism. Consistent with the conceptually related M(TCNQ) systems ($M^{+} = Li^{+}$, Na^{+}, K^{+}, Ag^{+}, and Cu^{+}), the TCNQ/Tl(TCNQ) interconversion is strongly dependent upon scan rate, $Tl^{+}_{(aq)}$ electrolyte concentration, and the method of attaching solid TCNQ onto the electrode surface. Spectroscopic (infrared (IR) and Raman), microscopic (scanning electron microscopy (SEM)), and surface science (X-ray photoelectron spectroscopy (XPS), energy-dispersive X-ray (EDX), and X-ray diffraction (XRD)) characterization of the electrochemically synthesized material revealed formation of pure Tl(TCNQ) phase II. Importantly, the generic solid-state electrochemical approach used in this study not only offers facile protocol for controllable and preferential synthesis of Tl(TCNQ) phase II but also provides access to fabricate and tune the morphology to yield microrod/nanorod networks.

Journal of Solid State Electrochemistry, 20 (12) (2016) 3303-3314

Potentiometric and computational studies of Cobalt, nickel and copper complexes with bipyridyl and dl-2-amino-N-hydroxy-n-butanamide in aqueous solution

Laila H. Abdel Rahman, Badriah S.F Al Farhan, Mohamed Ismael
Chemistry Department, Faculty of Science, Sohag University, 82524 Sohag, Egypt

Equilibrium investigations of Co^{2+}, Ni^{2+}, Cu^{2+} complexes with mixed-ligand of 2,2'-bipyridyl (bipy) and Dl-2-amino N-hydroxy-n-butanamide (ahbt) were performed by potentiometric pH titrations in aqueous solution at room temperature and I = 0.5 mol/dm3 KCl. The obtained data were analyzed using the HYPERQUAD program. The results showed that the complexes has the molecular formula of $[M(bipy)(H2ahbt)]^{3+}$, $[M(bipy)(Hahbt)]^{2+}$, $[M(bipy)(ahbt)]^{1+}$ and $[M(bipy)(ahbt)H_{-1}]$. In the $[M(bipy)(ahbt)]^{1+}$ species, the complexes were stabilized by forming five-member ring through the donation of the amino and hydroxomate nitrogens (Namino, Nhydroxom.) of ahbt and the two nitrogen atoms of bipy in the square planar geometry of the complex in basic solution. In the acidic and neutral solutions, protonated ahbt coordinates to $[M(bipy)]^{2+}$ by the hydroxomate group forming a five- member ring with (O, O) donor atoms. In addition, 3D-structural geometry and electronic structures of Cu complexes were predicted using quantum mechanics calculations.
Arab J. Phys. Chem, 3 (1) (2016) 10-16

Ascorbic Acid Assisted Synthesis of Cobalt Oxide Nanostructures, Their Electrochemical Sensing Application for the Sensitive Determination of Hydrazine

Tahira A.[a], Nafady, A.[bc], Baloach Q.[a], Q.[a], Sirajuddin[d], Sherazi, S.T.H.[d], Shaikh, T.[d], Arain, M.[a], Willander, M.[e], Ibupoto, Z.H.[a]
[a]*Dr. M.A. Kazi Institute of Chemistry, University of Sindh, Jamshoro, Pakistan*
[b]*Department of Chemistry, College of Science, King Saud University, Riyadh, Saudi Arabia*
[c]*Chemistry Department, Faculty of Science, Sohag University, Sohâg, Egypt*
[d]*National Centre of Excellence in Analytical Chemistry, University of Sindh, Jamshoro, Pakistan*
[e]*Department of Science and Technology, Linkoping University, Campus Norrkoping, Sweden*

This study describes, the synthesis of cobalt oxide nanostructures using ascorbic acid as a growth directing agent by the hydrothermal method. Ascorbic acid is used for the first time for the synthesis of cobalt oxide nanostructures and a unique morphology is prepared in the present study. The cobalt oxide nanostructures were characterized by scanning electron microcopy, x-ray diffraction, and x-ray photoelectron spectroscopy techniques. These analytical techniques demonstrated well defined morphology, good crystalline quality, and high purity of as prepared cobalt oxide nanostructures. The glassy carbon electrode was modified with cobalt oxide nanostructures for the development of a sensitive and selective electrochemical hydrazine sensor. The developed hydrazine sensor exhibits a linear range of 2-24 μM. The sensitivity and limit of detection of presented hydrazine sensors are 12,734 μA/mM/cm^2 and 0.1 μM respectively. The developed hydrazine sensor is highly selective, stable, and reproducible. The proposed sensor is successfully applied for the detection of hydrazine from different water samples. The present study provides the development of an alternative tool for the reliable monitoring of hydrazine from environmental and biological samples.
Journal of Electronic Materials, 45 (7) (2016) 3695-3701

The synthesis of new nanostructures of CuO using ascorbic acid as growth directing agent and their sensitive electrochemical detection of hydrazine

Tahira A.[a], Nafady A.[bc], Arain M.[a], Sirajuddind[d], Sherazi S. T. H.[d], Shaikh T.[d], Baloach Q.[a], Willander M.[e], Ibupoto Z. H.[a]

[a]*Dr. M. A. Kazi Institute of Chemistry, University of Sindh, Jamshoro, Pakistan*
[b]*Department of Chemistry, College of Science, King Saud University, Riyadh, Saudi Arabia*
[c]*Chemistry Department, Faculty of Science, Sohag University, Sohag, Egypt*
[d]*National Centre of Excellence in Analytical Chemistry, University of Sindh, Jamshoro, Pakistan*
[e]*Department of Science and Technology, Campus Norrkoping, Linkoping University, Sweden*

In this research work, ascorbic acid is used as a template for the growth of new nanostructures of copper oxide (CuO) by hydrothermal method. The use of ascorbic acid played a significant role in controlling the morphological features of CuO nanostructures as well as its properties. CuO nanostructures were characterized by scanning electron microscopy (SEM) and X-ray diffraction (XRD) techniques. As prepared CuO nanostructures exhibited well define morphology and good crystalline properties. The unique properties possessed by CuO nanostructures are exploited for the construction of sensitive hydrazine sensor by modifying the glassy carbon electrode. As synthesized CuO nanostructures showed excellent electrocatalytic properties toward the oxidation of hydrazine. The cyclic voltammetry and amperometric techniques were used for the measurement of electrochemical response of the modified electrode in the determination of hydrazine. The oxidative current rises linearly with successive injection of hydrazine on the surface of CuO modified electrode for the concentration range of 2 μM to 24 μM and detection limit for the developed sensor was estimated to be 0.02 μM at a signal-to-noise ratio of 3(S/N = 3). The sensitivity was found to be 12405 μA/mM/cm^2 for the proposed sensor. The proposed sensor device is stable, selective, sensitive and reproducible. The oxidation mechanics of hydrazine on the surface of new CuO nanostructures is also described. The presented sensor has high potential for the determination of hydrazine from real water samples that is also explored in the present study and the obtained results are accurate.

Sensor Letters, 14 (6) (2016) 611-615

Copper Oxide Microstructures with Hemisphere Pineapple Morphology for Selective Amperometric Determination of Vitamin C (L-ascorbic Acid) in Human Fluids

Mohamed Khairy, Bahaa G. Mahmoud
Chemistry Department, Faculty of Science, Sohag University, Sohag, Egypt

Control over morphology, surface composition and porosity of nanostructured metal oxides play a significant role in designing a selective and sensitive electrochemical sensor. Herein, we explore a simple synthesis route for control fabrication of porous CuO hemisphere pineapple-like morphology without using any structure directing agents. The results show that, CuO hemispheres are consisting of self-assembled porous nanoneedles. The as-prepared CuO hemispheres were simply drop-casted onto graphite screen-printed electrodes (CuO-SPEs). Then, it was tested for determination of ascorbic acid in Britton Robinson (B. R.) buffer of pH 7.4. Interestingly, the CuO-SPE provides robust, sensitive, fast response and selective enzyme-less ascorbic acid sensor. These superior features allowed efficient, costless, stable, and precise non-enzymatic detection of ascorbic acid in urine samples avoiding interferences and enhancing the accuracy of urinalysis examination.

Electroanalysis 28 (2016) 606-2612

Simpler and highly sensitive enzyme-free sensing of urea via NiO nanostructures modified electrode

Arain, M.[a], Nafady, A.[bc], Sirajuddin[d] , Ibupoto, Z.H.[a], Hussain Sherazi, S.T.[d], Shaikh, T.[d], Khan, H.[e], Alsalme, A.[b], Niaz, A.[f], Willander, M.[g]

[a]Dr. M. A. Kazi Institute of Chemistry, University of Sindh, Jamshoro, Pakistan
[b]Department of Chemistry, College of Science, King Saud University, Riyadh, Saudi Arabia
[c]Chemistry Department, Faculty of Science, Sohag University, Sohag, Egypt
[d]National Centre of Excellence in Analytical Chemistry, University of Sindh, Jamshoro, Pakistan
[e]Department of Chemistry, Islamia College University, Peshawar, KPK, Pakistan
[f]Department of Chemistry, Bannu University of Science and Technology, Pakistan
[g]Department of Science and Technology, Linkoping University Campus Norrkoping, Sweden

In this study, NiO nanostructures were synthesized via a hydrothermal process using ascorbic acid as doping agent in the presence of ammonia. As prepared nanostructures were characterized using Scanning Electron Microscopy (SEM), X-Ray Diffraction (XRD), Brunauer-Emmett-Teller (BET) specific surface area analysis, and thermogravimetric analysis (TGA). These analyses showed that these nanostructures are in the form of cotton-like porous material and crystalline in nature. Furthermore, the average size of these NiO crystallites was estimated to be 3.8 nm. These nanostructures were investigated for their potential to be a highly sensitive and selective enzyme-free sensor for detection of urea after immobilizing on a glassy carbon electrode (GCE) using 0.1% Nafion as binder. The response of this as developed amperometric sensor was linear in the range of 100-1100 μM urea with a R^2 value of 0.990 and limit of detection (LOD) of 10 μM. The sensor responded negligibly to various interfering species including glucose, uric acid, and ascorbic acid. This sensor was applied successfully for determining urea in real water samples such as mineral water, tap water, and river water with acceptable recovery.

RSC Advances, 6 (45) (2016) 39001-39006

Cefuroxime derived copper nanoparticles and their application as a colorimetric sensor for trace level detection of picric acid

Hussain M.[a], Nafady A.[bc], Sirajuddin[a] , Hussain Sherazi, S.T.[a], Shah, M.R.[d], Alsalme, A.[b], Kalhoro, M.S.[e], Mahesar, S.A.[a], Siddiqui, S.[a]

[a]National Centre of Excellence in Analytical Chemistry, University of Sindh, Jamshoro, Pakistan
[b]Department of Chemistry, College of Science, King Saud University, Riyadh, Saudi Arabia
[c]Chemistry Department, Faculty of Science, Sohag University, Sohag, Egypt
[d]International Centre for Chemical and Biological Sciences, HEJ Research Institute, Chemistry University of Karachi, Karachi, Pakistan
[e]Department of Physics, University of Sindh, Jamshoro, Pakistan

Picric acid (PA) is an explosive material often used in explosive tools, destructive weapons and nuclear technology. In this work we demonstrate a simple, novel and efficient wet chemical protocol for fabricating copper nanoparticles using cefuroxime drug as a protecting agent. Cefuroxime functionalized copper nanoparticles (Cefu-CuNPs) were initially confirmed and characterized via UV-Visible (UV-Vis) spectroscopy. Surface interaction between cefuroxime and copper nanoparticles was investigated by Fourier transform infrared (FTIR) spectroscopy while their shapes and size were observed via Atomic Force Microscopy (AFM) where an average size of 30.3 ± 2 nm was recorded. As-synthesized Cefu-CuNPs were used as a colorimetric sensor for detection of picric acid. Cefu-CuNPs demonstrated highly sensitive and selective colorimetric detection of picric acid in the linear range of 1.0-20 μM based on increase in intensity with an R2 value of 0.995 determined by UV-Vis spectroscopy measurements. The resulting sensor is highly economical, simple compared to other sensors and sensitive to detect picric acid with a detection limit as low as 38 nM. The sensor can be successfully employed for picric acid detection in real water samples. © (2016) The Royal Society of Chemistry.

RSC Advances, 6 (86) (2016) 82882-82889

Design and control of Lewis acid sites in Sn-substituted microporous architectures

Khaled M. H. Mohammed,*[abc] Arunabhiram Chutia,[ab] June Callison,[ab] Peter P. Wells,[ab] Emma K. Gibson,[ab] Andrew M. Beale,[ab] C. Richard A. Catlow[abd], Robert Raja[*e]

[a]UK Catalysis Hub, Research Complex at Harwell (RCaH), Rutherford Appleton Laboratory, Harwell
[b]Department of Chemistry, University College London, 20 Gordon Street, London, UK
[c]Chemistry Department, Faculty of Science, Sohag University, Sohag, Egypt
[d]Cardiff Catalysis Institute, School of Chemistry, Cardiff University, Cardiff
[e]School of Chemistry, University of Southampton, Southampton, UK

Monometallic and bimetallic tin-containing framework architectures have been prepared by hydrothermal methods. Structural and spectroscopic techniques were used to probe the nature of the solid-acid sites, at the molecular level, using a combination of XRD, DR UV-Vis, solid state MAS NMR (119Sn, 27Al and 31P) and XAFS. The nature and strength of the solid-acid sites were experimentally probed by FT-IR spectroscopy using CD3CN as a probe molecule. To elucidate further the local-structure, the structural characteristics of the Sn sites were probed using DFT calculations, with a view to rationalising the experimental findings. These detailed structural and spectroscopic studies revealed the presence of multiple Sn environments, with the monometallic SnAlPO-5 catalyst displaying a greater number of tetrahedral Sn(IV) active centres. These framework Sn(IV) centres generated strong Lewis acid sites, when compared with their bimetallic Co-Sn analogue, thereby affording attractive possibilities for modulating catalytic reactivity.
J. Mater. Chem. A, 4 (2016) 5706-5712

Effect of phosphoric acid concentration on conductivity of anodic passive film formed on surface of lead-indium alloy

Abdel-Rahman El-Sayed, Hossnia S. Mohran, Hoda Abdel Shafy Shilkamy
Department of Chemistry, Faculty of Science, Sohag University, Sohag 82524, Egypt

The addition of phosphoric acid into sulfuric acid solution is mentioned to be helpful in the reduction of sulfation after deep discharge of lead-acid battery. The anodic behavior of Pb and Pb-In alloys was studied in pure phosphoric acid and sulfuric acid containing various concentrations of phosphoric. The electrochemical measurements were performed using potentiodynamic, potentiostatic and cyclic voltammetric techniques. The composition and morphology of passive layer formed on the surfaces of Pb and Pb-In alloys were characterized by X-ray diffraction (XRD), energy dispersive X-ray spectroscopy analysis (EDX) and scanning electron microscopy (SEM). The potentiodynamic study shows that the passive current density increases with increasing the indium content in the alloy in the examined solutions. The addition of 0.1 mol/L H_3PO_4 into the electrolyte is more effective to decrease the thickness of passive film on the surface of alloys containing higher indium content (10% and 15%). The XRD, EDX and SEM data reveal that the formation of $PbSO_4$ and PbO on the surface decreases with increasing the indium level in the alloy and is completely prevented at higher indium content (15%) in mixed acid.
Trans. Nonferrous Met. Soc. China, 26 (3) (2016) 882-894

Iminophosphoranes in Heterocyclic Synthesis: A FacileSynthesis of Pyrido[4,3-D]Pyrimidine andPyrido [4,3D][1,3]Oxazine Derivatives viaIntermolecularaza-Wittig Reactions

Omran A. Omran,[1,2] Samia M. Sayed,[3], Mohamed A. Raslan[3*]
[1]*Chemistry Department, Faculty of Science, Sohag University, 82524, Egypt*
[2]*College of Science in Zulfi, P. O. Box 1712, Majmaah University, 11932 Saudi Arabia*
[3]*Chemistry Department, Faculty of Science, Aswan University, 81528 Aswan, Egypt*

A novel series of pyrido[4,3-d]pyrimidine and pyrido[4,3-d][1,3]oxazine derivatives were synthesized via tandem aza-Wittig and annulation reactions with the corresponding iminophosphoranes, aromatic isocyanate, and amines. All newly synthesized compounds were elucidated by considering the data of both elemental and spectral analysis.
J. Heterocyclic Chem., 00, 00 (2016).

Designing CuO_x Nanoparticle-Decorated CeO_2 Nanocubes for Catalytic Soot Oxidation: Role of the Nanointerface in the Catalytic Performance of Heterostructured Nanomaterials

Putla Sudarsanam†, Brendan Hillary†, Baithy Mallesham‡, Bolla Govinda Rao‡, Mohamad Hassan Amin†, Ayman Nafady§‖, Ali M. Alsalme§, B. Mahipal Reddy‡, Suresh K. Bhargava*†
†Centre for Advanced Materials and Industrial Chemistry (CAMIC), School of Applied Sciences, RMIT University, Melbourne, Victoria 3001, Australia
‡Inorganic and Physical Chemistry Division, Council of Scientific and Industrial Research (CSIR)−Indian Institute of Chemical Technology, Uppal Road, Hyderabad, Telangana 500 007, India
§Chemistry Department, College of Science, King Saud University, Riyadh 12372, Saudi Arabia
‖Chemistry Department, Faculty of Science, Sohag University, Sohag 11432, Egypt

This work investigates the structure-activity properties of CuOx-decorated CeO_2 nanocubes with a meticulous scrutiny on the role of the CuO_x/CeO_2 nanointerface in the catalytic oxidation of diesel soot, a critical environmental problem all over the world. For this, a systematic characterization of the materials has been undertaken using transmission electron microscopy (TEM), transmission electron microscopy-energy-dispersive X-ray spectroscopy (TEM-EDS), high-angle annular dark-field-scanning transmission electron microscopy (HAADF-STEM), scanning transmission electron microscopy-electron energy loss spectroscopy (STEM-EELS), X-ray diffraction (XRD), Raman, N_2 adsorption-desorption, and X-ray photoelectron spectroscopy (XPS) techniques. The TEM images show the formation of nanosized CeO_2 cubes (∼25 nm) and CuO_x nanoparticles (∼8.5 nm). The TEM-EDS elemental mapping images reveal the uniform decoration of CuOx nanoparticles on CeO_2 nanocubes. The XPS and Raman studies show that the decoration of CuO_x on CeO_2 nanocubes leads to improved structural defects, such as higher concentrations of Ce3+ ions and abundant oxygen vacancies. It was found that CuO_x-decorated CeO_2 nanocubes efficiently catalyze soot oxidation at a much lower temperature (T_{50} = 646 K, temperature at which 50% soot conversion is achieved) compared to that of pristine CeO_2 nanocubes (T_{50} = 725 K) under tight contact conditions. Similarly, a huge 91 K difference in the T_{50} values of CuO_x/CeO_2 (T_{50} = 744 K) and pristine CeO_2 (T_{50} = 835 K) was found in the loose-contact soot oxidation studies. The superior catalytic performance of CuO_x-decorated CeO_2 nanocubes is mainly attributed to the improved redox efficiency of CeO_2 at the nanointerface sites of CuO_x-CeO_2, as evidenced by Ce M5,4 EELS analysis, supported by XRD, Raman, and XPS studies, a clear proof for the role of nanointerfaces in the performance of heterostructured nanocatalysts.
Langmuir, 32 (9) (2016) 2208-2215

Effect of preparation conditions on structural and catalytic properties of lithium zirconate

Katabathini Narasimharao[a], Tarek T. Ali[a,b]
[a]*Department of Chemistry, Faculty of Science, King Abdulaziz University, P.O. Box 80203, Jeddah 21589, Kingdom of Saudi Arabia*
[b]*Chemistry Department, Faculty of Science, Sohag University, P.O. Box 82524, Sohag, Egypt*

Inorganic (inorg) and organic (org) routes with acid (A) and base (B) hydrolyzing agents were utilized to synthesize lithium zirconate (LiZr) nanomaterials. The effect exerted by the nature of hydrolyzing agent and synthesis route on the morphology and structural properties of the samples was studied by X-ray diffraction, Raman spectroscopy, TEM, SEM, XPS, N_2-adsorption and CO_2-TPD techniques. The characterization results revealed that LiZr-org-B sample prepared using organic base possessed hollow nanospheres which are composed of small platelets; in contrast, LiZr-inorg-B sample prepared using inorganic base showed nanotubular structure due to more alkaline nature of the inorganic precursors. Additionally, LiZr-org samples possessed different textural characteristics and basic properties. LiZr-org samples, in particular LiZr-org-B showed relatively high surface area, uniform micro pores, and more number of basic sites as well as high catalytic activities in transesterification of tributyrin with methanol than LiZr-inorg samples. LiZr-org-B sample is stable and showed excellent reusability for more than five cycles without any loss of activity in transesterification reaction.
Ceramics International, 42 (1B) (2016) 1318-1331

In situ spectroscopic investigations of MoO_x/Fe_2O_3 catalysts for the selective oxidation of methanol

Catherine Brookes,[*ab] Michael Bowker,[ab] Emma K. Gibson,[ac] Diego Gianolio,[d] Khaled M. H. Mohammed,[ace] Stephen Parry,[d] Scott M. Rogers,[ac] Ian P. Silverwood[ac], Peter P. Wells[*ac]
[a]UK Catalysis Hub, Research Complex at Harwell, Rutherford Appleton Laboratory, Harwell, UK
[b]Cardiff Catalysis Institute, School of Chemistry, Cardiff University, Park Place, Cardiff, UK
[c]Department of Chemistry, University College London, 20 Gordon St., London, UK
[d]Diamond Light Source, Harwell Science and Innovation Campus, Didcot, UK
[e]Chemistry Department, Faculty of Science, Sohag University, Sohag, Egypt

Multicomponent oxide shell@core catalysts have been prepared, affording overlayers of MoO_x on Fe_2O_3. This design approach allows bulk characterization techniques, such as X-ray Absorption Fine Structure (XAFS), to provide surface sensitive information. Coupling this approach with in situ methodologies provides insights during crucial catalytic processes. Calcination studies were followed by a combination of XAFS and Raman, and demonstrate that amorphous multi-layers of MoO_x are first converted to MoO_3 before formation of $Fe_2(MoO_4)_3$. However, a single overlayer of Oh Mo units remains at the surface at all times. In situ catalysis studies during formaldehyde production identified that Mo^{6+} was present throughout, confirming that gas phase oxygen transfer to molybdenum is rapid under reaction conditions. Reduction studies in the presence of MeOH resulted in the formation of reduced Mo-Mo clusters with a bonding distance of 2.6 Å. It is proposed that the presence of the clusters indicates that the selective conversion of MeOH to formaldehyde requires multiple Mo sites.
Catal. Sci. Technol., 6 (2016) 722-730

Electrochemical behaviour of antioxidants: Part 2. Electrochemical oxidation mechanism of quercetin at glassy carbon electrode modified with multi-wall carbon nanotubes

Refat Abdel-Hamid, Emad F. Newair
Department of Chemistry, Faculty of Science, University of Sohag, 82524 Sohag, Egypt

Electrochemical oxidation mechanism of quercetin was investigated at glassy carbon electrode modified with multi-wall carbon nanotubes in aqueous 0.2 M phosphate solutions with different pHs. The investigation was carried out using cyclic voltammetry, double potential step chronoamperometric and chronocoulometric techniques. It was found that the oxidation mechanism proceeds in sequential steps, related with the five-hydroxyl groups in the three aromatic rings. The mechanism was proposed to be an ECEC, first-order kinetics. The proposed mechanism was confirmed on comparing the digital simulated cyclic voltammetric responses with the experimental ones. The electrode homogeneous and heterogeneous kinetic parameters of electrode reaction are estimated from the simulated data. Moreover, quercetin molecules adsorb on the electrode surface.
Arab. J. Chem., 9 (3) (2016) 350-356

Evaluation of copper speciation in the extract of Eichhornia crassipes using reverse and forward/CLE voltammetric titrations

Wael H.M. Abdelraheem, Mostafa K.M. Rabia, Nabawia M. Ismail
Department of Chemistry, Faculty of Science, University of Sohag, 82524 Sohag, Egypt

Reverse and forward titrations coupled with the competitive ligand equilibration (CLE) technique were, for the first time, used to investigate the chemical organic speciation of copper ions in an aqueous extract of Eichhornia crassipes (E.C) plant growing in Egypt. Salicylaldoxime (SA) was used as the competitive ligand. Two samples were collected from huge submerged masses in the Nile water at Sohag and Mansura cities. In this study the concentration of the natural complexing ligands (CLn) and their conditional stability constants with copper (View the MathML sourceKCuLn′) in the aqueous extract were determined by linear and nonlinear modeling. Reverse titration resulted in two classes of copper complexation (CuL1 and CuL2) in both samples. The strongest class, CuL1, is predominant in Sohag-sample with average logView the MathML sourceKCuL1′ and CL1 of 15.66 and 435.5 nM, respectively, and also dominated in the Mansura-sample with average 16.77 and 162 nM, respectively. The second class (CuL2) is minor in both samples. For comparison, forward titration was performed for the Sohag-sample. The results indicated that reverse titration showed a breakthrough ability to detect, for the first time, different types of metal complexation present in equilibrium in the aqueous extracts of biological samples. Moreover, the presence of E.C in Nile water is so useful in transforming free Cu ions to less toxic forms by organic complexation.
Arab. J. Chem., 9 (2016) S1670-S1678

Photocatalytic degradation of p-nitrophenol in aqueous suspension by using Graphene/ZrO_2 catalysts

Basahel, Sulaiman N.; Mokhtar, Mohamed; Alsharaeh, Edreese H.; Ali, Tarek T.; Mahmoud, Hatem A.; Narasimharao, Katabathini
Chemistry Department, Faculty of Science Sohag University Sohag, Egypt

A series of reduced graphene oxide (rGO) supported zirconia (ZrO2) nanocomposites with 1, 2 and 5 wt.% GO were synthesized using the sol-gel technique. The reduced graphene oxide/zirconia composites were characterized by X-ray powder diffraction (XRD), Raman spectroscopy, scanning electron microscopy (SEM) high resolution transmission electron microscopy (HRTEM), ultravioletvisible (UV-Vis) and, X-ray photoelectron spectroscopy (XPS), and N2 adsorption and desorption measurements. The photocatalytic performance of the prepared samples was evaluated by monitoring the degradation of p-nitrophenol in aqueous suspension under UV illumination. The photocatalytic activity is strongly affected by the concentration of graphene in the ZrO2. The band gap values calculated from the Kubelka-Munk method showed a pronounced decrease upon increasing the amount of GO from 3.05 eV for pure ZrO2 to 2.77 eV for 5 wt.% rGO/ZrO2. Graphene serves as a good electron collector and transporter that effectively hindered the recombination of photo-generated electron-hole pairs resulting in high performance of photocatalytic degradation of p-nitrophenol.
Nanoscience and Nanotechnology Letters, 8 (5) (2016) 448-457

Physico-chemical and catalytic properties of mesoporous CuO-ZrO_2 catalysts

Sulaiman N. Basahel[1], Mohamed Mokhtar[1], Edreese H. Alsharaeh[2], Tarek T. Ali[1,3,*], Hatem A. Mahmoud[3,4], Katabathini Narasimharao[1,*]
[1]Chemistry Department, Faculty of Science, King Abdulaziz University, Jeddah 21589, Saudi Arabia
[2]Chemistry Department, College of Science & General Studies, Alfaisal University, Saudi Arabia
[3]Chemistry Department, Faculty of Science, Sohag University, Sohag, P.O. Box 82524, Egypt
[4]Chemistry Department, College of Science, University of Hail, Hail 81451, Saudi Arabia

Mesoporous CuO-ZrO_2 catalysts were prepared and calcined at 500 °C. The performance of the synthesized catalysts for benzylation of benzene using benzyl chloride was studied. The bare support (macroporous ZrO_2) offered 45% benzyl chloride conversion after reaction time of 10 h at 75 °C. Significant increase in benzyl chloride conversion (98%) was observed after CuO loading (10 wt. %) on porous ZrO_2 support. The conversion was decreased to 80% with increase of CuO loading to 20 wt.%. Different characterization techniques (XRD, Raman, diffuse reflectance UV-vis, N_2-physisorption, H_2-TPR, XPS and acidity measurements) were used to evaluate physico-chemical properties of CuO-ZrO_2 catalysts; the results showed that the surface and structural characteristics of the ZrO_2 phase as well as the interaction between CuO-ZrO_2 species depend strongly on the CuO content. The results also indicated that ZrO_2 support was comprised of monoclinic and tetragonal phases with macropores. An increase of the volume of monoclinic ZrO_2 phase was observed after impregnation of 10 wt. % of CuO; however, stabilization of tetragonal ZrO_2 phase was noticed after loading of 20 wt.% CuO. The presence of low-angle XRD peaks indicates that mesoscopic order is preserved in the calcined CuO-ZrO_2 catalysts. XRD reflections due to CuO phase were not observed in case of 10 wt.% CuO supported ZrO_2 sample; in contrast, the presence of crystalline CuO phase was observed in 20 wt.% CuO supported ZrO_2 sample. The mesoporous 10 wt.% CuO supported ZrO_2 catalyst showed stable catalytic activity for several reaction cycles. The observed high catalytic activity of this catalyst could be attributed to the presence of a higher number of dispersed interactive CuO (Cu^{2+}-O-Zr^{4+}) species, easy reducibility, and greater degree of accessible surface Lewis acid sites.
Catalysts, 6(4) (2016) 57

Sol-gel Derived Mixed Oxide Zirconia: Titania Green Heterogeneous Catalysts and Their Performance in Acridine Derivatives Synthesis

Mai M. Khalaf, Antar A. Abdelhamid

Chemistry Department, Faculty of Science Sohag University Sohag, Egypt

Various zirconia content in ZrO_2-TiO_2 mixed oxide catalysts (x = 5, 10, 20 ZrO_2 wt%) were synthesized by cost-effective sol-gel process and characterized by different techniques, i.e. XRD diffraction patterns, TG-DTA analyses, FTIR spectroscopy, N_2 adsorption/desorption measurements, and TEM microscope. The investigation of the acidic/basic properties was studied by means of FTIR spectroscopy using pyridine as an adsorbed molecule. Characterization estimates exhibit that the deposition by ZrO_2 improves the surface properties of TiO_2 structures and increase the TiO_2 surface area up to 92 m^2/g. TEM results affirmed the homogeneous distribution of ZrO_2 particles on the surface of TiO_2 of particle size in the range of 12-17 nm. The performance of the prepared zirconia-titania catalysts with different concentration ratios in acridine derivates synthesis from hydroxyl-benzaldehyde was studied. The results of catalytic test reveal that, the activity of ZrO_2-TiO_2 catalysts was significantly enhanced by depositing an optimum amount ratio of ZrO2 reach to 10 % to raise the yield to 95, 97 and 99 %. This can be attributed to the higher its surface area and its performance as basic site catalyst in the studied test.

Catalysis Letters, 146 (3) (2016) 645-655

Synergistic effect of polyethylene glycols and rare earth Ce^{4+} on the corrosion inhibition of carbon steel in sulfuric acid solution: electrochemical, computational, and surface morphology studies

Hany M. Abd El-Lateef

Chemistry Department, Faculty of Science Sohag University Sohag, Egypt

The inhibition effect of two selected polyethylene glycols (PEGs) with different molecular weight and the synergistic effect with rare earth Ce^{4+} ions on corrosion of carbon steel in 0.1 M H_2SO_4 solution has been investigated by using electrochemical measurements, scanning electron microscopy, and quantum chemical calculations. The inhibition efficiency (Z%) increased with increasing PEG concentration and molecular weight and decreased with increasing temperature. The adsorption of the PEGs obeyed the Langmuir adsorption isotherm. Potentiodynamic polarization studies showed that the PEGs were mixed-type inhibitors of corrosion by H_2SO_4. The results reveal that incorporation of PEGs with Ce^{4+} ions improved the inhibition performance. The Z% value for the PEGs in combination with Ce^{4+} was higher than the sum of the Z% values for the individual PEGs and Ce^{4+} ions, confirming a synergistic effect. Some quantum chemical parameters were calculated to corroborate the experimental results.

Research on Chemical Intermediates, 42 (4) (2016) 3219-3240

Physical-chemical study for the treatment of Iron and Manganese in ground water

M. K. Moustsfa[1], M. A. Hussien[2], M.E. Mohamed[1], A.A. Mohamed[2]
[1]Department of Chemistry, Faculty of science, Sohage University, Egypt
[2]Department of Chemistry, Faculty of Science, Port Said University, Egypt

Underground drinking water treatment is one of the hardest types of treatment because the difficulty to control on the water source, which is an underground water source and due to the high salt content of solid dissolved (TDS) which arrive in Egypt to approximately 1000 parts per million. Iron and manganese form the most famous elements of bilateral parity in drinking underground water. We show in this study physico-chemical ways for treatment of iron and manganese in ground water.
Intternattiionall Journall of Chemiicall and Natturall Sciience, 4 (4) (2016) 442-446

Physico-Chemical Studies on Treatment of some Divalent Elements in Ground Water

M. K. Moustsfa[1], M. A. Hussien[2], M.E. Mohamed[1], A.A. Mohamed[2]
[1]Department of Chemistry, Faculty of science, Sohage University, Egypt
[2]Department of Chemistry, Faculty of Science, Port Said University, Egypt

When there is no surface water we must think in use groundwater, but groundwater need treatment, Treatment of underground water one of the most difficult treatment methods, that because under groundwater contain high amount of total dissolved salts(TDS), and there is great difficulty in control the source of underground water, iron and manganese from the famous divalent elements in groundwater, the Egyptian standard for the concentration of iron is (0.3 ppm) and for manganese is (0.4 ppm) the increase in concentration for iron and manganese case change in the taste of water and sometimes effect on the human health. We will show in this study physical, chemical study for treatment of iron and manganese in groundwater.
Global Journal of HUMAN-SOCIAL SCIENCE: B, 16 (3) (2016) 1-5

Botany Department
قسم النبات

Botany

Botany Department
قسم النبات

Cyanobacterial Toxins in Water Sources and Their Impacts on Human Health

Z. Mohamed
Department of Botany and Microbiology, Sohag University, Sohag, Egypt

Cyanobacteria are a group of phytoplankton of marine and freshwaters. The accelerated eutrophication of water sources by agricultural and industrial run-off has increased the occurrence and intensity of cyanobacterial blooms. They are of particular concern because of their production for potent hepato-, neuro-, and dermatoxins, being hazardous to human health. Dissemination of knowledge about cyanobacteria and their cyanotoxins assists water supply authorities in developing monitoring and management plans, and provides the public with appropriate information to avoid exposure to these toxins. This chapter provides a broad overview and up-to-date information on cyanobacteria and their toxins in terms of their occurrence, chemical and toxicological characteristics, fate in the environment, guideline limits, and effective treatment techniques to remove these toxins from drinking water. Future research directions were also suggested to fill knowledge and research gaps, and advance the abilities of utilities and water treatment plant designers to deal with these toxins.

In A. McKeown, & G. Bugyi (Eds.), ***Impact of Water Pollution on Human Health and Environmental Sustainability*** **(2016) 120-149. Hershey, PA: IGI Global**

Breakthrough of *Oscillatoria limnetica* and microcystin toxins into drinking water treatment plants - Examples from the Nile River, Egypt

Mohamed Z. A.
Department of Botany and Microbiology, Sohag University, Sohag, Egypt

The presence of cyanobacteria and their toxins (cyanotoxins) in processed drinking water may pose a health risk to humans and animals. The efficiency of conventional drinking water treatment processes (coagulation, flocculation, rapid sand filtration and disinfection) in removing cyanobacteria and cyanotoxins varies across different countries and depends on the composition of cyanobacteria and cyanotoxins prevailing in the water source. Most treatment studies have primarily been on the removal efficiency for unicellular *Microcystis* spp., with little information about the removal efficiency for filamentous cyanobacteria. This study investigates the efficiency of conventional drinking water treatment processes for the removal of the filamentous cyanobacterium, *Oscillatoria limnetica,* dominating the source water (Nile River) phytoplankton in seven Egyptian drinking water treatment plants (DWTPs). The study was conducted in May 2013. The filamentous O. *limnetica* was present at high cell densities (660-1 877 cells/mL) and produced microcystin (MC) cyanotoxin concentrations of up to 877 $\mu g.g^{-1}$, as determined by enzyme-linked immunosorbent assay (ELISA). Results also showed that conventional treatment methods removed most phytoplankton cells, but were ineffective for complete removal of O. *limnetica*. Furthermore, coagulation led to cell lysis and subsequent microcystin release. *Microcystins* were not effectively removed and remained at high concentrations (0.37-3.8 $\mu g\text{-}L^{-1}$) in final treated water, exceeding the WHO limit of 1 $\mu g\text{-}L^{-1}$. This study recommends regular monitoring and proper treatment optimization for removing cyanobacteria and their cyanotoxins in DWTPs using conventional methods.

Water SA., 42 (1) (2016) 161-165

Harmful cyanobacteria and their cyanotoxins in Egyptian fresh waters-state of knowledge and research needs

Mohamed Z. A.
Department of Botany and Microbiology, Faculty of Science, Sohag University, Sohag, Egypt

Cyanobacterial blooms have increased in freshwater ecosystems worldwide in the last century, mostly resulting from eutrophication and climate change. These blooms represent serious threats to environmental and human health because of the production of harmful metabolites, called cyanotoxins. Like many countries, Egypt has been plagued with cyanobacterial blooms in most water sources, including the Nile River, irrigation canals, lakes and fishponds. However, the data about cyanotoxins produced in these blooms are limited. Only two types of cyanotoxins, *Microcystins* and *Cylindrospermopsin*, have been identified and characterized, mainly from *Microcystis* and *Cylindrospermopsis* blooms. The data revealed the presence of microcystins in raw and treated drinking waters at concentrations (0.05–3.8 μg l^{-1}), exceeding the WHO limit (1 μg l^{-1}) in some drinking water treatment plants. In addition, Nile tilapia *Oreochromis niloticus* caught from ponds containing heavy cyanobacterial blooms have accumulated considerable amounts of cyanotoxins in their edible tissues. The data presented here could be the catalyst for the establishment of a monitoring and management program for harmful cyanobacteria and their cyanotoxins in Egyptian fresh waters. This review also elucidates the important research gaps and possible avenues for future research on cyanobacterial blooms and cyanotoxins in Egypt.
African Journal of Aquatic Science 41 (4) (2016) 361-368.

Occurrence of toxic cyanobacteria and microcystin toxin in domestic water storage reservoirs, Egypt

Mohamed Z. A., Deyab M. A., Abou-Dobara M. I., El-Raghi W. M.
[a]*Department of Botany and Microbiology, Faculty of Science, Sohag University, Sohag, Egypt*
[b]*Botany Department, Faculty of Science, Damietta University, Damietta, Egypt*

Residents in many developing countries store treated drinking water in tanks or reservoirs because of intermittent and infrequent water supplies. Many studies have focused on bacterial contamination of domestic reservoir waters, the cyanobacterial and algal contamination is largely unexplored. Therefore, the present study investigates toxic cyanobacteria and their microcystin (MC) toxins in some domestic water storage reservoirs in Egypt as an example for developing countries. Three phytoplankton groups including cyanobacteria, green algae and diatoms were found in domestic reservoirs. Among these species, the toxic cyanobacterium *Microcystis aeruginosa* had the highest cell density during warm months (4.2-5.92 cells × 10^6 L^{-1}). This cell density increased along the time, indicating that environmental conditions in these reservoirs promoted the proliferation of this species. Intra- and extracellular MCs were also detected in reservoir waters at concentrations of 3.5-40 and 1-7.6 μg L^{-1}, respectively, exceeding the WHO guideline limit of 1 μg L^{-1} for these toxins in drinking water. Heterotrophic bacteria were found in association with cyanobacteria in reservoir waters. The study suggests that treated-water storage reservoirs should be monitored for the presence of toxic cyanobacteria to protect the public from exposure to their potent toxins.
Journal of Water Supply: Research and Technology - AQUA, 65 (5) (2016) 431-440

Photosynthesis, antioxidant status and gas-exchange are altered by glyphosate application in peanut leaves

Radwan D. E. M. , Fayez K. A.

[a]*Plant Physiology Laboratory, Botany Department, Faculty of Science, Sohag University, Egypt*

[b]*Biology Department, Faculty of Science, Jazan University, Jazan, Saudi Arabia*

Glyphosate herbicide caused oxidative stress and exhibited negative effects on photosynthesis and gas exchange of peanut [*Arachis hypogaea* L. cv. Giza (G) 5 and 6] leaves. We demonstrated that glyphosate caused various morphological symptoms, such as chlorosis, yellowing, and appearance of curly edges in leaves treated with high doses of herbicide in both cultivars; however, the G5 cultivar was more sensitive and showed severer symptoms. Glyphosate lowered photosynthesis and reduced contents of pigments and proteins as well as free amino acids in both cultivars. The gas-exchange parameters, such as photosynthetic (P_N) and transpiration rate (E), were highly altered by the glyphosate application. For example, P_N and E were reduced by 65 and 61%, respectively, in G5 treated with high dose of glyphosate compared with control. Antioxidant enzymes, such as peroxidase, catalase, ascorbate peroxidase, and superoxide dismutase were induced by both low and high concentrations in the glyphosate-treated leaves. Moreover, the level of lipid peroxidation, indicated by a malondialdehyde content, as well as the hydrogen peroxide content increased in the glyphosate-treated leaves. However, an increase in total antioxidant activity was detected in leaves and this reflected changes in the antioxidant status and accumulation of antioxidants as a defense mechanism against glyphosate toxicity in peanut.

Photosynthetica, 54 (2) (2016) 307-316

Impact of greenhouse environmental factors and fungicide Trinol (triadimend) treatment on berry leaves infected with powdery mildew (*Uncinula necator* (Schwein.) Burrill: Role of host antioxidant systems against pathogen infection

Khalaf A Fayez[1, 2], Yassin M Al-Sodany[1, 3]*, Alaa Abouzaid[4]

[1]*Biology Department, Faculty of Science, Taif University, Taif, KSA*

[2]*Botany Department, Faculty of Science, South Valley University, Sohag, Egypt*

[3]*Botany Department, Faculty of Science, Kafr El-Sheikh University, Kafr El-Sheikh, Egypt*

[4]*Botany Department, Faculty of Science, Tanta University, Tanta, Egypt*

Unfavorable environmental conditions such as temperature and humidity within greenhouse enhanced powdery mildew (*Uncinula necator*) fungal plant disease on black mulberry (*Morus nigra*). The initial symptoms of powdery mildew were appeared on leaves as light green to yellow spots associated with leaf chlorosis. As the disease progresses, the spots get larger due to formation of large numbers of spores. With late fungus infection, the chlorosis and necrosis of leaves were observed. Ultramicroscopic examination (SEM) of infected leaves showed a colonization of fungus on leaves. In response to Trinol (triadimend) fungicide, the fungus growth on plant leaves was strongly inhibited. Physiological activities of healthy plants, fungal infected plants as well as that infected with fungus and sprayed with fungicide were investigated. Photosynthetic pigments, that affect the efficiency of photosynthesis in higher plants, showed a high sensitivity with powdery mildew infection. Fungus infected leaves that sprayed with Trinol fungicide had more contents of photosynthetic pigments compared to those of infected and healthy plants. Soluble carbohydrate contents of infected leaves and that sprayed with the fungicide were significantly increased compared with that of healthy one. Soluble protein contents of infected leaves significantly increased in response to fungicide spraying. The response of infected plants and fungicide treated plants stimulated own defense systems for against pathogen infection. The results confirmed a reduction in *U. necator* infected berry due to application of Trinolfungicide.

Research Journal of Pharmaceutical, Biological and Chemical Sciences, 7 (2016) 3058-3072

Isolation of *Bdellovibrio* sp. from Wastewater and Their Potential Application in Control of *Salmonella paratyphi* in Water

El-Shanshoury A. E.-R. R.[ab], Abo-Amer A. E.[cd] , Alzahrani O. M.[a]

[a]*Department of Biotechnology, Faculty of Science, University of Taif, Taif, Saudi Arabia*
[b]*Unit of Bacteriology, Department of Botany, Faculty of Science Tanta University, Tanta, Egypt*
[c]*Division of Microbiology, Department of Biology, Faculty of Science, Univ. of Taif, Saudi Arabia*
[d]*Division of Microbiology, Department of Botany, Faculty of Science, Sohag University, Sohag, Egypt*

The problem of the increasing resistance of bacteria to conventional antibiotics gives the bacteria *Bdellovibrio* a great utility as a potential alternative source of antibiotics. Therefore, the preliminary goal of the present study was isolation and identification of antibiotic-resistant bacteria used as prey organisms for isolated *Bdellovibrio* sp., by xylose lysine desoxycholate (XLD) agar from different types of water in the Taif area, Saudi Arabia, and also to investigate water quality. Four antibiotic-resistant isolates of Salmonella sp. which were susceptible to *Bdellovibrio* were identified by morphological, biochemical and 16S rRNA characterization as *Salmonella paratyphi*. Seventeen strains of *Bdellovibrio* sp. were isolated from sewage wastewater using isolated *S. paratyphi* as prey bacteria by a double-layer plate. Only one of them causing a large plaque after 48 h of incubation at 37°C was designated *Bdellovibrio* AOA12. The shape of *Bdellovibrio* was confirmed by morphological characterization and electron microscopy. The kinetic lysis of the *Bdellovibrio* as predator to four isolates of antibiotic-resistant *Salmonella paratyphi* as prey organisms was demonstrated. The results suggest that it may be possible to utilize *Bdellovibrio* to control antibiotic-resistant *S. paratyphi* in water

Geomicrobiology Journal, 33 (10) (2016) 886-893

Mycobiota of Oil-Contaminated Soil Samples and Their Abilities for Dibenzothiophene Desulfurization

Gherbawy Y.[ab], El-Deeb B.[ac], Hazzani A. A.[d], Maher A.[ef], Shehata A.[d]

[a]*Department of Biology, Faculty of Science, Taif University, Taif, Saudi Arabia*
[b]*Department of Botany, Faculty of Science, South Valley University, Qena, Egypt*
[c]*Department of Botany, Faculty of Science, Sohag University, Sohag, Egypt*
[d]*Department of Botany & Microbiology, College of Science, King Saud University, Saudi Arabia*
[e]*Faculty of Medical Applied Science, Tarabah Branch, Taif University, Saudi Arabia*
[f]*Chlamydia Unit, Animal Health Research Institute, Dokki, Giza, Egypt*

High sulfur content of crude oil leads to poor quality of oil products and many other negative consequences such as corrosion, catalyst poisoning and environmental pollution. Saudi Arabia is seeking to reduce sulfur content in diesel and gasoline to 10 ppm and to lower benzene content in gasoline to 1%. Biotechnological processes such as biodesulfurization can be considered an alternative or complement to conventional oil refining technologies. So, the objective of the present project is to isolate and identify endogenous fungal isolates capable of oil biodesulfurization. From 60 oil-contaminated soil samples collected from Saudi Arabia, 15 species belonged to 9 fungal genera were collected and identified morphologically and with ITS sequencing. Members of *Aspergillus*, *Penicillium* and Fusarium were the most prevalent in the investigated samples. Among the collected fungal species, only *Stachybotrys bisbyiisolates* were able to utilize dibenzothiophene (DBT) as the sole sulfur source. *Stachybotrys bisbyi* TUSb1 could desulfurize 99% of the DBT (0.3 mM) as the sulfur source by a co-metabolism reaction with other carbon sources through the same pathway as 4S (involves sequential oxidation of the sulfur part and cleaving of the C–S bonds), and produced 2-hydroxy biphenyl (2-HBP) during 7 days of incubation at 30°C and 180 rpm. *Stachybotrys bisbyi* TUSb1 showed broad specificity for removing sulfur in different sulfur-containing compounds. © 2016 Taylor & Francis Group, LLC.

Geomicrobiology Journal, 33 (7) (2016) 618-624

The genus Lolia from freshwater habitats in Egypt with one new species

Abdel-Aziz F. A.
Department of Botany and Microbiology, of Sohag University, Sohag, Egypt

A new species of Lolia and the sexual morph of L. aquatica are described, with illustrations, from decayed submerged wood in the River Nile, Egypt. Molecular phylogenetic analyses of partial SSU and LSU rDNA sequence data place the sexual morph of L. aquatica and the new species, L. dictyospora in a monophyletic clade, distant from the closely related fungi in the freshwater family Lindgomycetaceae. Pairwise LSU rDNA sequence alignment of the sexual/asexual morphs of L. aquatica are 99% similar. Lolia species are characterized by pseudothecial or stromatic, immersed to erumpent, dark-brown to black, coriaceous to sub-carbonaceous ascomata, cylindric-clavate, bitunicate, fissitunicate, short pedicellate asci, yellow to reddish-brown, phragmo- or dictyospores, surrounded by prominent gelatinous sheath. Lolia species are phylogenetically distant from the closely related genera: Leptosphaeria (Leptosphaeriaceae) and Massariosphaeria (Pleosporales incert. sed.). Lolia differs from Leptosphaeria in having a prominent large gelatinous ascospore sheath, while this is absent in Leptosphaeria species. Lolia differs from Massariosphaeria in having smaller ascospores and fewer transverse septa. Based on molecular data and morphology, a new species, Lolia dictyospora, is established. © 2016 Magnolia Press.
Phytotaxa, 267 (4) (2016) 279-288

Comparative anatomy of stems and leaves of plectranthus L. (Lamiaceae) in Saudi Arabia and systematic implications

Khalik, K.N.A., Karakish, E.A.
*Biology Department, **Faculty** of Applied **Science**, Umm Al-Qura University, Mecca, Saudi Arabia*

A comparative anatomical study of the Plectranthus species growing in Saudi Arabia by using light microscopy method in order to evaluate their diagnostic value for systematic studies. Macro- and micromorphological characters, including stem, leaf, petiole anatomical, and trichome structures are presented. Descriptions of stem shape in cross-section, epidermal cell shape, cortex, pith, vascular bundles, leaf shape in cross-section, mesophyll, types and distribution of trichomes are presented. Taxonomic phylogenetic implications of stem, leaf, and trichomes anatomical micromorphology are also discussed in comparison with the available gross morphological and molecular data. Results of the present study offer useful data for evaluating the taxonomy of Plectranthus both at subgeneric and sectional levels. Moreover, our results indicate some degree of similarity among the species of subgenus Germanea and support the monophyly of this subgenus. A remarkable result from this study was identifying P. arabicus with distinctive characters and suggesting that it should be treated as a separate subgenus. Likewise, distinguishing differences between closely related endemic species P. asirensis and P. hijazensis are offered, and should be conserved as a different subgenus. A key for the identification of the investigated taxa based on studied characters is provided. Microsc. Res. Tech. 79:583–594, 2016.
Microscopy Research and Technique, 79 (7) (2016) 583-594

Two new species of Kallichroma (Bionectriaceae, Hypocreales) from Saudi Arabian mangroves

Abdel-Wahab M. A., Bahkali A. H., Jones E. B. G., Elgorban A. M., Abdel-Aziz F. A., Hodhod M. S., Al-Hebshi M.O.

Department of Botany and Microbiology, College of Science, King Saud University, Saudi Arabia
Department of Botany and Microbiology, Faculty of Science, Sohag University, Sohag 82524, Egypt

During an ongoing study of marine fungi in Saudi Arabia, two undescribed Kallichroma species were recorded from decayed intertidal wood of Avicennia marina from two mangrove stands along the Red Sea coast and the Arabian Gulf coast in Saudi Arabia. Kallichroma asperum sp. nov. is characterized by rough ascospores cell walls surrounded by a granular sheath. Kallichroma ellipsoideum sp. nov. is characterized by its small sized hyaline ascomata, asci and ascospores. Both new species have 3 or 8-spored asci and perithecoid or confluent ascomata with large, globose papillae. Phylogenetic analyses of the combined SSU and LSU rDNA sequences placed the two new species in the family Bionectriaceae. © 2016 Magnolia Press.

Phytotaxa, 260 (1) (2016) 66-74

Two new cheirosporous asexual taxa (Dictyosporiaceae, Pleosporales, Dothideomycetes) from freshwater habitats in Egypt

Abdel-Aziz FA

Department of Botany and Microbiology, Faculty of Science, Sohag University, Sohag 82524, Egypt

Two new cheirosporous asexual taxa (Dictyosporiaceae, Pleosporales, Dothideomycetes) from freshwater habitats in Egypt. Mycosphere 7(4), 448–457, Doi 10.5943/mycosphere/7/4/5 Abstract Cheirosporium vesiculare and Dictyosporium palmae spp. nov. were collected from submerged wood in the River Nile, Sohag, Egypt. Cheirosporium vesiculare is characterized by macronematous conidiophores, and non-complanate conidia, that are circular in vertical view with seven rows arranged in six peripheral rows and one in the center. Conidia are equipped with 2 to 5 balloon-like large appendages with long necks that penetrate through the peripheral rows and connect to the central row. Phylogenetic analyses of LSU sequence data place C. vesiculare in a monophyletic clade with C. triseriale in the family Dictyosporiaceae. Dictyosporium palmae is distinguished from the previously described species by its different conidial dimensions and the variable shapes of the gelatinous conidial appendages. Phylogenetic analyses of LSU sequence data place D. palmae in Dictyosporium sensu sticto in a clade with D. digitatum and D. stellatum with high statistical support.

Mycosphere, 7 (4) (2016) 448-457

Seed morphology and surface microstructure of the genus 'Plectranthus' L. (Lamiaceae) in Arabian Peninsula highlighting on their systematic implications

Khalik, Kadry Abdel

Seed coat morphology of 13 species of Plectranthus L. in Arabian Peninsula was comparatively examined using scanning and light microscopy methods. The diagnostic values for systematic were studies. Macro- and micro-morphological characteristics, including seed shape, colour, size, seed surface, epidermal cell shape, anticlinal boundaries, and periclinal cell wall are presented. Descriptions of seed size, shape, colour, surface, and seed coat types are summarised for the genus. Taxonomic phylogenetic implications of the seed coat micromorphology are also discussed in comparison with the available gross morphological and molecular data. Results of the seed character analyses offered useful data for evaluating the taxonomy of plectranthus both on subgeneric and sectional levels. Monophyly of both subgenus Burnatastrum (Briq) Codd, and Germanea (Benth.) Briq. is also supported here. The remarkable result of this study was to identify P. arabicus as a separate group. The results suggested that it should be treated as a separate subgenus because of having reddish-brown colour seeds and flat-to-convex periclinal cell wall which is distinguishable from the rest of the species. Likewise, the endemic species of P. asirensis, P. ovatus, and P. hijazensis group and P. hyemalis and P. hadiensis group should be homogeneous groups. A key for the identification of the investigated taxa based on seed characters is also provided here

Australian Journal of Crop Science, 10 (2016) 1222-1231

Growth and Physiological Response of Some Cultivated Species Under Allelopathic Stress of Calotropis Procera (Aiton)

A. A. El-Khatib[1], N. A. Barakat[2], Heba Nazeir[3]
[1]Botany Department, Faculty of Science, Sohag University, Egypt
[2]Botany Department, Faculty of Science, Minia University, Egypt

The present work through light on the role of allelopathic potential of Calotropis procera on some growth and physiological parameters of three cultivated crops. The selected species, namely; cucumber, tomato, and wheat were grown in a pot experiment under six different concentrations of aqueous leaf extract ranged from 0 % to 50 % (w/v) with 10 % intervals for one month after seedling stage. The data obtained revealed a significant reduction in shoot and root length, which was higher in the root than shoot and the inhibition rate among studied species were in the order of tomato>cucumber>wheat. The plant fresh and dry weight showed a significant inhibition in both tomato and wheat and a nonsignificant and especially at low concentration. The species response was in the order of tomato>cucumber>wheat and tomato>wheat>cucumber for fresh and dry weight respectively. A variety of responses in the pigment content in which tomato>cucumber>wheat and wheat>cucumber >tomato for chlorophyll and carotenoids respectively. Allelopathic stress stimulates the accumulation of study metabolites soluble proteins, amino acids and proline by the same manner in all target species wheat>cucumber >tomato except for soluble carbohydrates; cucumber>wheat> tomato. These data may confirm the response of wheat to the allelopathic stress of Calitropis procera was lower than tomato and cucumber were in between, and the target species tend to accumulate these metabolites as an adaptive strategy to alleviate the allelochemical stress of Calitropis procera

Applied Science Reports, 14 (2016) 237-246

A new species of Plectranthus (Lamiaceae) from Saudi Arabia

Khalik K. Abdel

[a]*Department of Biology, Faculty of Applied Science, Umm Al-Qura University, Makkah, Saudi Arabia*

Plectranthus hijazensis Abdel Khalik (Lamiaceae) is described as a new species from Al-Baha Province in Saudi Arabia. Information given on the new species includes a taxonomic description and its affinity to Plectranthus asirensis L. A key to Plectranthus species of Saudi Arabia is provided, and the relationships of the species and the relevant morphological characters, particularly seed, pollen grains, trichomes, and anatomy of stem and leaf, are discussed. A distribution map of the new species and related species is provided

Turkish Journal of Botany, 40 (5) (2016) 506-513

Evaluation of silver nanoparticles for the control of Phragmidium species in vitro and taif'rose rust disease in field

Gado E. A. M.[ab], El-Deeb B.[ac], Ali, E. F.[ad], Mostafa N. Y.[ef], Bazaid S.A.[a]

[a]*Department of Biology, Faculty of Science, Taif University, P.O. Box: 888, Taif, Saudi Arabia*

[b]*Plant Pathol.Dept., Fac. Agric., Ain Shams Univ., Egypt*

Rose rust caused by Phragmediumsp is one of the most important diseases adversely affecting its yield in Saudia Arabia. In this study, Identity of the causal agent fungus was confirmed by LSU rDNA sequencing and identified as Phragmidiummucronatum. Also, the present study is focused on the extracellular synthesis of silver nanoparticles (AgNPs) using culture supernatant of an agriculturally important bacterium, Proteus maribials and demonstrates its effective application for the management of rust disease in rose. The biosynthesis of AgNPs by Proteus maribials was monitored by UV-visible spectrum that showed the surface plasmon resonance (SPR) peak at 406 nm, an important characteristic of AgNPs. Further characterization of synthesized AgNPs carried out using the X-ray diffraction (XRD), transmission electron microscope (TM) and FTIR spectroscopy, respectively. The AgNPs were spherical in shape with size range of ~10 to 20 nm. The XRD analysis confirmed successful biosynthesis and crystalline nature of AgNPs. The AgNPs exhibited strong antifungal activity against P. mucro, the rust disease pathogen of rose. Interestingly, all concentrations of AgNPs (0.25, o.5 and 1 mM) used displayed a strong inhibition of urediospore germination, 3.05, 2.2, and 1.1% respectively, whereas in the absence of AgNPs, urediospore germination was 62.32 %. The results were further tested under field conditions, where application of AgNPs significantly reduced P.mucronatuminfection in rose plants. The averages of disease severity were reduced from 3.6 in non-sprayed plants to 1.06 % in case of spraying with AgNPs (1mM). In summary, our findings represent the efficient application of AgNPs in rust disease management, therefore, it is recommended to consider biological synthesized silver nanoparticles in further studies for possible controlling of rose rust disease.

Research Journal of Pharmaceutical, Biological and Chemical Sciences, 7 (3) (2016) 886-896

Diagnosis of pulmonary tuberculosis and detection of resistance to rifampin and isoniazid through direct molecular methods in stool samples

Al Yousef S. A.[a], Ali AbdelRahim K. A.[bc], Ahmed A. O.[d], Almaary K. S.[b], Mohamed A. M. A.[a]

Background. Tuberculosis (TB) is an infectious disease that is caused by Mycobacterium tuberculosis (M.tb). TB has high morbidity and mortality around the world. Objective. To evaluate molecularbased methods performed directly on stool samples for the diagnosis of pulmonary tuberculosis (PTB) and to determine the susceptibility to Rifampicin (RMP) and Isoniazid (INH). Study design. This is a descriptive study evaluating the performance of the PCR-based method for direct PTB diagnosis and to determine the susceptibility of RMP and INH using stool samples from PTB patients. The study was conducted between March 2011 and March 2014. Methods. Three stool samples and three sputum samples (n=300 stool and 300 sputum) were collected from 100 PTB patients (75 pretreatment and 25 follow up). Stool samples (n=60) were also collected from 20 healthy individuals to serve as controls. DNA was extracted from stool samples using Chelex®-100. PTB was diagnosed using a Genekam® kit. RMP and INH susceptibility testing was performed using the Genotype MTBDRplus® assay. The sputum Lowenstein Jensen (LJ) culture and agar proportion method (PM) of drug susceptibility testing for INH and RMP were considered to be the gold standard methods for comparing the results of the molecular methods. Results. The Genekam kit showed 100% sensitivity and 95.24% specificity for diagnosing new patients and showed 100% sensitivity and 80% specificity for follow-up patients. The Genotype MTBDR-plus assay showed 86.4% and 100% sensitivity and 98.1% and 97.8% specificity for determining INH and RMP sensitivity, respectively, in newly diagnosed patients and 85.7% and 94.4% sensitivity and specificity, respectively, for both INH and RMP in follow-up patients. Conclusion. Molecular-based methods are promising techniques for the diagnosis and susceptibility testing of PTB when the ease of sample collection and the speed of diagnosis are taken into consideration. However, they are not as useful for assessing follow-up patients

Annals of Clinical and Laboratory Science, 46 (6) (2016) 616-621

Antimicrobial activity of silver and gold nanoparticles biosynthesized using ginger extract

El-Deeb B.[ac], Elhariry H.[ad], Mostafa N. Y.[be]

[a]Department of Biology, Faculty of Science, Taif University, P.O. Box: 888, Taif, Saudi Arabia

[b]of Chemistry, Faculty of Science, Taif University, P.O. Box: 888, Taif, Saudi Arabia

Biofabricated metal nanoparticles is under exploration due to wide biomedical applications and research interest in nanotechnology. Biosynthesis of silver and gold nanoparticles was achieved by reduction of silver nitrate ($AgNO_3$) and chloroauric acid ($HAuCl_4$), respectively, using ginger rhizome (Zingiber officinale) extract. The biosynthesized silver (AgNPs) and gold (AuNPs) nanoparticles were characterized by using UV-Vis spectroscopy and TEM. The UV-vis spectrum showed maximum absorption peak at 450 and 547 nm corresponding to the plasmon absorbance of AgNPs and AuNPs, respectively. The AgNPs were generally found to be spherical in shape with diameter of 5-50 nm, whereas AuNPs were found to be in the range of 5-35 nm. The antibacterial potential of the biosynthesized nanoparticles was measured by the Kirby-Bauer method against 5 Gram-negative and 5 Gram-positive bacteria. AuNPs did not show any inhibition potential. However, AgNPs showed antimicrobial activity against, except Bacillus cereus TUB8, which observed complete resistance to AgNPs and 1 µg oxacillin. AgNPs displayed synergistic improving effect when it was combined with oxacillin (1 µg) or tetracycline (30 µg) in ready to use disks. In conclusion, Ginger rhizome water extract could be considered as a potential bioreductant for the synthesis of AgNPs and AuNPs. AgNPs showed high antimicrobial potential against Gram-positive and Gram-negative bacteria. For the antibiotic resistant bacteria, the combination of antibiotics with AgNPs could improve its susceptibility to these antibiotics. © 2010 RJPBCS.

Research Journal of Pharmaceutical, Biological and Chemical Sciences, 7 (30 (2016) 1085-1091

11 April, 2017

A Systematic Revision of the Genus Plectranthus L. (Lamiaceae) in Saudi Arabia Based on Morphological, Palynological, and Micromorphological Characters of Trichomes

Kadry N. Abdel Khalik[1,2]
[1]Department of Biology, Faculty of Applied Science, Umm Al-Qura University, Makkah, KSA
[2]Botany Department, Faculty of Science, Sohag University, Sohag, Egypt

This study aims to investigate the morphology and ultrastructure characters of pollen grains and trichomes in order to evaluate their systematic value of these characters in specific and intraspecific separation of the Saudi Arabian Plectranthus species. A critical systematic revision of 7 species of Plectranthus (Lamiaceae) in Saudi Arabia was conducted by means of numerical analyses based on thirty-one morphological characters, including vegetative parts, seeds, pollen grains, and trichomes. Macro- and micro-morphological characters, including seed and pollen shape, size, coat sculpture, trichome structure, were studied. It reveals the presence of seven species, including two endemic species. The pollen grains were zonocolpate, hexacolpate, prolate to subprolate. Three types of exine ornamentation were recognized. Also, two trichome types could be distinguished and classified into glandular and non-glandular. The glandular trichomes could be distinguished as peltate, capitate and digitiform. The eglandular trichomes were single, uniseriate, multicellular. Pollen and trichome characters were found to be valuable, while seed characters presented only minor taxonomic value. On the basis of UPGMA clustering analysis four branches and clusters were distinguished. The results offer useful data for evaluating the taxonomy of Plectranthus both at subgeneric and sectional levels. Our results indicated some degree of similarity among the species of subgenus Burnatastrum. Plectranthus arabicus is considered as a separate group and may be treated as separate subgenus. Furthermore, the endemic species Plectranthus asirensis and Plectranthus hijazensis constitute a monophyletic group and there are close relationships between this group and Plectranthus tenuiflorus. A key for the identification of the investigated taxa based on studied characters is provided

American Journal of Plant Sciences, 7 (10) (2016) 1429-1444

Recommendations for competing sexual-asexually typified generic names in Sordariomycetes (except Diaporthales, Hypocreales, and Magnaporthales)

Réblová M., Miller, A.N., Rossman, A.Y., Seifert, K.A., Crous, P.W., Hawksworth, D.L., Abdel-Wahab, M.A., Cannon, P.F., Daranagama, D.A., Wilhelm De Beer, Z., Huang, S.-K., Hyde, K.D., Jayawardena, R., Jaklitsch, W., Gareth Jones, E.B., Ju, Y.-M., Judith, C, Maharachchikumbura S.S.N., Pang, K.-L., Petrini, L.E., Raja, H.A., Romero, A.I., Shearer, C., Senanayake, I.C., Voglmayr, H., Weir, B.S.,Wijayawarden, N.N.

With the advance to one scientific name for each fungal species, the generic names in the class Sordariomycetes typified by sexual and asexual morphs are evaluated based on their type species to determine if they compete with each other for use or protection. Recommendations are made for which of the competing generic names should be used based on criteria such as priority, number of potential names changes, and frequency of use. Some recommendations for wellknown genera include Arthrinium over Apiospora, Colletotrichum over Glomerella, Menispora over Zignoëlla, Microdochium over Monographella, Nigrospora over Khuskia, and Plectosphaerella over Plectosporium. All competing generic names are listed in a table of recommended names along with the required action. If priority is not accorded to sexually typified generic names after 2017, only four names would require formal protection: Chaetosphaerella over Oedemium, Diatrype over Libertella, Microdochium over Monographella, and Phaeoacremonium over Romellia and Togninia. Concerning species in the recommended genera, one replacement name (Xylaria benjaminii nom. nov.) is introduced, and the following new combinations are made: Arthrinium sinense, Chloridium caesium, C. chloroconium, C. gonytrichii, Corollospora marina, C. parvula, C. ramulosa, Juncigena fruticosae, Melanospora simplex, Seimatosporium massarina, Sporoschisma daemonoropis, S. taitense, Torpedospora mangrovei, Xylaria penicilliopsis, and X. termiticola combs. nov

IMA Fungus, 7 (1) (2016) 131-153

Families of Sordariomycetes

Maharachchikumbura S.S.N., Hyde K.D., Jones E.B.G., McKenzie E.H.C., Bhat J.D., Dayarathne M.C., Huang S.K., Norphanphoun C., Senanayake I.C., Perera R.H., Shang Q.J., Xiao Y., D'souza M.J., Hongsanan S., Jayawardena R.S., Daranagama D., Konta S., Goonasekara I.D., Zhuang W.Y., Jeewon R., Alan J. L. Phillips, Abdel-Wahab M.A., Al-SadiAli A.M., Bahkali A.H., Boonmee S., Boonyuen N., Cheewangkoon R., Asha J. Dissanayake Jichuan Kang Qi-Rui Li, Liu J.K., Liu X.Z., Liu Z.Y., Luangsa-ard J.J., Pang K.L., Phookamsak R., Promputtha I., Suetrong S., Stadler M., Wen T., Wijayawardene N.N.

Sordariomycetes is one of the largest classes of Ascomycota that comprises a highly diverse range of fungi characterized mainly by perithecial ascomata and inoperculate unitunicate asci. The class includes many important plant pathogens, as well as endophytes, saprobes, epiphytes, coprophilous and fungicolous, lichenized or lichenicolous taxa. They occur in terrestrial, freshwater and marine habitats worldwide. This paper reviews the 107 families of the class Sordariomycetes and provides a modified backbone tree based on phylogenetic analysis of four combined loci, with a maximum five representative taxa from each family, where available. This paper brings together for the first time, since Barrs' 1990 Prodromus, descriptions, notes on the history, and plates or illustrations of type or representative taxa of each family, a list of accepted genera, including asexual genera and a key to these taxa of Sordariomycetes. Delineation of taxa is supported where possible by molecular data. The outline is based on literature to the end of 2015 and the Sordariomycetes now comprises six subclasses, 32 orders, 105 families and 1331 genera. The family Obryzaceae and Pleurotremataceae are excluded from the class

Fungal Diversity, 79 (1) (2016) 1-317.

Freshwater fungi from the River Nile, Sohag, Egypt

Abdel-Aziz F A

Department of Botany and Microbiology, Faculty of Science, Sohag University, Sohag 82524, Egypt

This study represents the first published data of freshwater fungi from the River Nile in Egypt. Knowledge concerning the geographic distribution of freshwater ascomycetes and their asexual morphs in Egypt and in the Middle East is limited. Ninety-nine taxa representing 42 sexual ascomycetes, 55 asexual taxa and two basidiomycetes were identified from 959 fungal collections recorded from 400 submerged samples. Samples were randomly collected from the River Nile, in Sohag, Egypt in the winter and summer between December 2010 and August 2014. Fifty-eight taxa (22 sexual ascomycetes and 36 asexual taxa) were collected during winter, while 60 taxa (25 sexual ascomycetes, 33 asexual taxa and two basidiomycetes) were collected in summer season. Of the 99 taxa recorded, 50 are new records for Egypt, including five new genera and 30 new species., Three new genera and ten new species were described in previous articles. Fungi recorded from the two seasons were markedly different, with only 19 species common to both winter and summer collections. Asexual fungi dominated the fungal community during the two seasons. Taxonomical placements of 33 species were confirmed by molecular data based on LSU and SSU rDNA genes. Lolia aquatica (14.2%) was the dominant fungus in both winter and summer collections. Other dominant fungi were: Ceratorhiza sp. (19.5 %) and Limnoperdon sp. (13 %). These two basidiomycetes were the most common taxa in the summer, while they were absent in the winter. Common fungi were Coleophoma emperti (9.2 %), Zopfiella latipes (8 %), Discosporium tremuloides (5.5 %), Trematophoma lignicola (5.5 %) and Ophioceras commune (5 %). Specious genera recorded from the two seasons were Dictyosporium (6 species), Monodictys-like (3 species), Aniptodera (3 species), Lolia (3 species), Podospora (3 species), Zopfiella (3 species), and two species belong to each of the following genera: Achaetomium, Annulatascus, Lentithecium, Linocarpon, Cirrenalia, Ciliochora, Coleophoma, Colletogloeum, Clohesyomyces, Periconia, Pseudorobillarda and Stagonospora. Key words – asexual fungi – coelomycetes – fungal diversity – fungal ecology – phylogeny

Mycosphere, 7 (6) (2016) 741-756

Mycotoxins production by Aspergillus ostianus Wehmer and using phytochemicals as control agent

Saber S M[1], Youssef M S[1], Arafa R F[2], Hassane A M A[2]

[1]*Botany Department, Faculty of Science, Sohag University, Egypt*

[2]*Botany and Microbiology Department, Faculty of Science, Al-Azhar University, Assiut*

Aspergillus ostianus Wehmer was a new record to the Mycological Laboratories in Egypt, isolated form cabbage seeds and tested for aflatoxins and ochratoxin A production. Aflatoxins B1 and G1 and ochratoxin A were demonstrated in the crude extracts of Aspergillus ostianus cultivated on different media for mycotoxins production. Both of essential oil and ethanol extract of clove were tested in order to control Aspergillus ostianus. The minimum inhibitory concentration (MIC) was 46.77 and 500 mg/ml for essential oil and ethanol extract, respectively. Also, qualitative phytochemical screening of the extracts and their chemical components using GC/MS analysis were determined. Keywords Aflatoxins, ochratoxin A, Aspergillus ostianus, clove extracts, GC/MS analysis.

Journal of Scientific and Engineering Research, 3 (2) 2016 198-213

Differential tolerance to high salt with regard to cell growth and superoxide dismutase (SOD) activity in calluses of the halophyte Suaeda maritima from Japan and Egypt

Elsayed Mohamed, Ryuya Matsuda, Ahmed A El-khatib, Katsuaki Takechi, Hiroyoshi Takano, Susumu Takio

Faculty of Science, Sohag University, Sohag, 82524, Egypt

To determine the mechanism of regulation of superoxide dismutase (SOD; EC 1.15.1.1) isozymes in halophytes at the cellular level, we isolated calluses from Suaeda maritima plants native to Japan and Egypt. Calluses from Egyptian S. maritima could grow in a high salt medium (~400 mM NaCl), whereas Japanese S. maritima calluses could not. The expression characteristics of SOD isozyme genes encoding two CuZn-SOD proteins, two Mn-SOD proteins, and one Fe-SOD protein in the two callus lines were analyzed. All SOD isozyme genes expressed in leaves were also expressed in both callus lines grown in normal medium and their expression levels were not affected by high salt. In-gel SOD activity assay after native-polyacrylamide gel electrophoresis revealed that both callus lines possessed a CuZn-SOD and an Fe-SOD as major SOD isozymes in normal medium. When calluses were grown on high salt medium, both SOD isozyme activities were decreased in Japanese calluses, while they were stable or slightly increased in Egyptian calluses. When calluses were incubated in normal medium with excess copper (Cu, ~100 μM), callus growth of both callus lines was less affected. In excess Cu, CuZn-SOD activity was greatly increased in both callus lines, while Fe-SOD activity was decreased in Japanese calluses and was stable in Egyptian calluses. Since both Fe-SOD and CuZn-SOD activities exhibited a positive association with growth tolerance to high salt, they may play a role in salt tolerance in callus cells. In addition, our results indicate that the Fe-SOD activity contributes to copper stress tolerance.

Plant Omics Journal, 9 (2016) 81-89

Fungal diversity notes 253-366: taxonomic and phylogenetic contributions to fungal taxa

Li GJ, Hyde KD, Zhao RL, Hongsanan S, Abdel-Aziz FA, Abdel-Wahab MA, Alvarado P, Alves-Silva G, Ammirati JF, Ariyawansa HA, Baghela A, Bahkali AH, Beug M, Bhat DJ, Dimitar Bojantchev D, Boonpratuang T, Bulgakov TS, Camporesi E, Boro MC, Ceska O, Chakraborty D, Chen JJ, Chethana KWT, Chomnunti P, Consiglio G, Cui BK, Dai DQ, Dai YC, Daranagama DA, Das K, Dayarathne MC, De Crop E, De Oliveira RJV, de Souza CAF, de Souza JI, Dentinger BTM, Dissanayake AJ, Doilom M, Drechsler-Santos ER, Ghobad- Nejhad M, Gilmore SP, Góes-Neto A, Gorczak M, Haitjema CH, Hapuarachchi KK, Hashimoto A, He MQ, Henske JK, Hirayama K, Iribarren MJ, Jayasiri SC, Jayawardena RS, Sun Jeong Jeon, Gustavo H Jerônimo, Ana L Jesus, EB Gareth Jones, Ji Chuan Kang, Karunarathna SC, Kirk PM, Konta S, Kuhnert E, Langer E, Lee HS, Lee HB, Li WJ, Li XH, Liimatainen K, Lima DX, Lin CG, Liu JK, Liu XZ, Liu ZY, Luangsaard JJ, Lücking R, Lumbsch HT, Lumyong S, Leaño EM, Marano AV, Matsumura M, McKenzie EHC, Mongkolsamrit S, Mortimer PE, Nguyen TTT, Niskanen T, Norphanphoun C, O'Malley MA, Parnmen S, Pawłowska J, Perera RH, Phookamsak R, Phukhamsakda C, Pires-Zottarelli CLA, Raspé O, Reck MA, Rocha SCO, de Santiago ALCMA, Senanayake IC, Setti L, Shang QJ, Singh SK, Sir EB, Solomon KV, Song J, Srikitikulchai P, Stadler M, Suetrong S, Takahashi H, Takahashi T, Tanaka K, Tang LP, Thambugala KM, Thanakitpipattana D, Theodorou MK, Thongbai B, Thummarukcharoen T, Tian Q, Tibpromma S, Verbeken A, Vizzini A, Vlasák J, Voigt K, Wanasinghe DN, Wang Y, Weerakoon G, Wen HA, Wen TC, Wijayawardene NN, Wongkanoun S, Wrzosek M, Xiao YP, Xu JC, Yan JY, Yang J, Yang SD, Hu Y, Zhang JF, Zhao J, Zhou LW, Peršoh D, Phillips AJL, Maharachchikumbura SSN

Notes on 113 fungal taxa are compiled in this paper, including 11 new genera, 89 new species, one new subspecies, three new combinations and seven reference specimens. A wide geographic and taxonomic range of fungal taxa are detailed. In the Ascomycota the new genera Angustospora (Testudinaceae), Camporesia (Xylariaceae), Clematidis, Crassiparies (Pleosporales genera incertae sedis), Farasanispora, Longiostiolum (Pleosporales genera incertae sedis), Multilocularia (Parabambusicolaceae), Neophaeocryptopus (Dothideaceae), Parameliola (Pleosporales genera incertae sedis), and Towyspora (Lentitheciaceae) are introduced. Newly introduced species are Angustospora nilensis, Aniptodera aquibella, Annulohypoxylon albidiscum, Astrocystis thailandica, Camporesia sambuci, Clematidis italica, Colletotrichum menispermi, C. quinquefoliae, Comoclathris pimpinellae, Crassiparies quadrisporus, Cytospora salicicola, Diatrype thailandica, Dothiorella rhamni, Durotheca macrostroma, Farasanispora avicenniae, Halorosellinia rhizophorae, Humicola koreana, Hypoxylon lilloi, Kirschsteiniothelia tectonae, Lindgomyces okinawaensis, Longiostiolum tectonae, Lophiostoma pseudoarmatisporum, Moelleriella phukhiaoensis, M. pongdueatensis, Mucoharknessia anthoxanthi, Multilocularia bambusae, Multiseptospora thysanolaenae, Neophaeocryptopus cytisi, Ocellularia arachchigei, O. ratnapurensis, Ochronectria thailandica, Ophiocordyceps karstii, Parameliola acaciae, P. dimocarpi, Parastagonospora cumpignensis, Pseudodidymosphaeria phlei, Polyplosphaeria thailandica, Pseudolachnella brevifusiformis, Psiloglonium macrosporum, Rhabdodiscus albodenticulatus, Rosellinia chiangmaiensis, Saccothecium rubi, Seimatosporium pseudocornii, S. pseudorosae, Sigarispora ononidis and Towyspora aestuari. New combinations are provided for Eutiarosporella dactylidis (sexual morph described and illustrated) and Pseudocamarosporium pini. Descriptions, illustrations and / or reference specimens are designated for Aposphaeria corallinolutea, Cryptovalsa ampelina, Dothiorella vidmadera, Ophiocordyceps formosana, Petrakia echinata, Phragmoporthe conformis and Pseudocamarosporium pini. The new species of Basidiomycota are Agaricus coccyginus, A. luteofibrillosus, Amanita atrobrunnea, A. digitosa, A. gleocystidiosa, A. pyriformis, A. strobilipes, Bondarzewia tibetica, Cortinarius alborsericeus, C. badioflavidus, C. dentigratus, C. duboisensis, C. fragrantissimus, C. roseobasilis, C. vinaceobrunneus, C. vinaceogrisescens, C. wahkiacus, Cyanoboletus hymenoglutinosus, Fomitiporia atlantica, F. subtilissima, Ganoderma wuzhishanensis, Inonotus shoreicola, Lactifluus armeniacus, L. ramipilosus, Leccinum indoaurantiacum, Musumecia alpina, M. sardoa, Russula amethystina subp. tengii and R. wangii are introduced. Descriptions, illustrations, notes and / or reference specimens are designated for Clarkeinda trachodes, Dentocorticium ussuricum, Galzinia longibasidia, Lentinus stuppeus and Leptocorticium tenellum. The other new genera, species new combinations are Anaeromyces robustus, Neocallimastix californiae and Piromyces finnis from Neocallimastigomycota, Phytophthora estuarina, P. rhizophorae, Salispina, S. intermedia, S. lobata and S. spinosa from Oomycota, and Absidia stercoraria, Gongronella orasabula, Mortierella calciphila, Mucor caatinguensis, M. koreanus, M. merdicola and Rhizopus koreanus in Zygomycota.

Fungal Diversity 78: 1-237

Fungal diversity notes 367-492: taxonomic and phylogenetic contributions to fungal taxa

Kevin D. Hyde, Sinang Hongsanan, Rajesh Jeewon , D. Jayarama Bhat, Eric H. C. McKenzie, E. B. Gareth Jones, Rungtiwa Phookamsak, Hiran A. Ariyawansa, Ali H. Bahkali, Saranyaphat Boonmee, Qi Zhao, Faten A .Abdel-Aziz, Mohamed A. Abdel-Wahab, Supharat Banmai, Putarak Chomnunti, Bao-Kai Cui, Dinushani A. Daranagama, Kanad Das, Monika C. Dayarathne, Nimali I. de Silva, Asha J. Dissanayake, Mingkwan Doilom , Anusha H. Ekanayaka, Tatiana Baptista Gibertoni, Aristóteles Góes-Neto , Shi-Ke Huang, Subashini C. Jayasiri, Ruvishika S. Jayawardena, Sirinapa Konta, Hyang Burm Lee, Wen-Jing Li, Chuan-Gen Lin, Jian-Kui Liu, Yong-Zhong Lu, Zong-Long Luo, Ishara S. Manawasinghe, Patinjareveettil Manimohan, Ausana Mapook, Tuula Niskanen, Chada Norphanphoun, Moslem Papizadeh, Rekhani H. Perera, Chayanard Phukhamsakda, Christian Richter, André L. C. M. A. de Santiago, E. Ricardo Drechsler-Santos, Indunil C Senanayake, Kazuaki Tanaka, T. M. D. S. Tennakoon, Kasun M. Thambugala, Qing Tian, Saowaluck Tibpromma, Benjarong Thongbai, Alfredo Vizzini, Dhanushka N. Wanasinghe, Nalin N. Wijayawardene, Haixia Wu, Jing Yang, Xiang-Yu Zeng, Huang Zhang, Jin-Feng Zhang, Timur S. Bulgakov, Erio Camporesi, Mohammad A. Amoozegar, Lidia Silva Araujo-Neta, Joseph F. Ammirati, Abhishek Baghela, R. P. Bhatt, Dimitar Bojantchev, Bart Buyck, Gladstone Alves da Silva, Catarina Letícia Ferreira de Lima, Rafael José Vilela de Oliveira, Carlos Alberto Fragoso de Souza, Yu-Cheng Dai, Bálint Dima, T.T. Duong, Enrico Ercole, Fernando Mafalda-Freire, Aniket Ghosh, Akira Hashimoto, Sutakorn Kamolhan, Ji-Chuan Kang, Samantha C. Karunarathna, Thilini Chethana, Paul M. Kirk, Ilkka Kytövuori, Angela Lantieri, Kare Liimatainen, Zuo Yi Liu, Xing-Zhong Liu, Robert Lücking, Gianfranco Medardi, Peter E. Mortimer, Thi Thuong Thuong Nguyen, K. N. Anil Raj, Mateus A. Reck, Saisamorn Lumyong, Seyed Abolhassan Shahzadeh-Fazeli, Marc Stadler, Mohammad Reza Soudi, Hong-Yan Su, Takumasa Takahashi, Narumon Tangthirasunun, Priyanka Uniyal, Yong Wang, Ting Chi Wen, Jian-Chu Xu ,Zhongkai Zhang, Yongchan Zhao, Jun-Liang Zhou, Lin Zhu, Itthayakorn Promputtha, Saisamorn Lumyong

This is a continuity of a series of taxonomic papers where materials are examined, described and novel combinations are proposed where necessary to improve our traditional species concepts and provide updates on their classification. In addition to extensive morphological descriptions and appropriate asexual and sexual connections, DNA sequence data are also analysed from concatenated datasets (rDNA, TEF-α, RBP2 and β-Tubulin) to infer phylogenetic relationships and substantiate systematic position of taxa within appropriate ranks. Wherever new species or combinations are being proposed, we apply an integrative approach (morphological and molecular data as well as ecological features wherever applicable). Notes on 125 fungal taxa are compiled in this paper, including eight new genera, 101 new species, two new combinations, one neotype, four reference specimens, new host or distribution records for eight species and one alternative morphs. The new genera introduced in this paper are *Alloarthopyrenia*, *Arundellina*, *Camarosporioides*, *Neomassaria*, *Neomassarina*, *Neotruncatella*, *Paracapsulospora* and *Pseudophaeosphaeria*. The new species are *Alfaria spartii*, *Alloarthopyrenia italica*, *Anthostomella ravenna*, *An. thailandica*, *Arthrinium paraphaeospermum*, *Arundellina typhae*, *Aspergillus koreanus*, *Asterina cynometrae*, *Bertiella ellipsoidea*, *Blastophorum aquaticum*, *Cainia globosa*, *Camarosporioides phragmitis*, *Ceramothyrium menglunense*, *Chaetosphaeronema achilleae*, *Chlamydotubeufia helicospora*, *Ciliochorella phanericola*, *Clavulinopsis aurantiaca*, *Colletotrichum insertae*, *Comoclathris italica*, *Coronophora myricoides*, *Cortinarius fulvescentoideus*, *Co. nymphatus*, *Co. pseudobulliardioides*, *Co. tenuifulvescens*, *Cunninghamella gigacellularis*, *Cyathus pyristriatus*, *Cytospora cotini*, *Dematiopleospora alliariae*, *De. cirsii*, *Diaporthe aseana*, *Di. garethjonesii*, *Distoseptispora multiseptata*, *Dis. tectonae*, *Dis. tectonigena*, *Dothiora buxi*, *Emericellopsis persica*, *Gloniopsis calami*, *Helicoma guttulatum*, *Helvella floriforma*, *H. oblongispora*, *Hermatomyces subiculosa*, *Juncaceicola italica*, *Lactarius dirkii*, *Lentithecium unicellulare*, *Le. voraginesporum*, *Leptosphaeria cirsii*, *Leptosphaeria irregularis*, *Leptospora galii*, *Le. thailandica*, *Lindgomyces pseudomadisonensis*, *Lophiotrema bambusae*, *Lo. fallopiae*, *Meliola citri-maximae*, *Minimelanolocus submersus*, *Montagnula cirsii*, *Mortierella fluviae*, *Muriphaeosphaeria ambrosiae*, *Neodidymelliopsis ranunculi*, *Neomassaria fabacearum*, *Neomassarina thailandica*, *Neomicrosphaeropsis cytisi*, *Neo. cytisinus*, *Neo. minima*, *Neopestalotiopsis cocoës*, *Neopestalotiopsis musae*, *Neoroussoella lenispora*, *Neotorula submersa*, *Neotruncatella endophytica*, *Nodulosphaeria italica*, *Occultibambusa aquatica*, *Oc. chiangraiensis*, *Ophiocordyceps hemisphaerica*, *Op. lacrimoidis*, *Paracapsulospora metroxyli*, *Pestalotiopsis sequoiae*, *Peziza fruticosa*, *Pleurotrema thailandica*, *Poaceicola arundinis*, *Polyporus mangshanensis*, *Pseudocoleophoma typhicola*, *Pseudodictyosporium thailandica*, *Pseudophaeosphaeria rubi*, *Purpureocillium sodanum*, *Ramariopsis atlantica*, *Rhodocybe griseoaurantia*, *Rh. indica*, *Rh. luteobrunnea*, *Russula indoalba*, *Ru. pseudoamoenicolor*, *Sporidesmium aquaticivaginatum*, *Sp. olivaceoconidium*, *Sp. pyriformatum*, *Stagonospora forlicesenensis*, *Stagonosporopsis centaureae*, *Terriera thailandica*, *Trematheia arundicola*, *Tr. guiyangensis*, *Trichomerium bambusae*, *Tubeufia hyalospora*, *Tu. Roseohelicospora* and *Wojnowicia italica*. New combinations are given for *Hermatomyces mirum* and *Pallidocercospora thailandica*. A neotype is proposed for *Cortinarius fulvescens*. Reference specimens are given for *Aquaphila albicans*, *Leptospora rubella*, *Platychora ulmi* and *Meliola pseudosasae*, while new host or distribution records are provided for *Diaporthe eres*, *Di. siamensis*, *Di. foeniculina*, *Dothiorella iranica*, *Do. sarmentorum*, *Do. vidmadera*, *Helvella tinta* and *Vaginatispora fuckelii*, with full taxonomic details. An asexual state is also reported for the first time in *Neoacanthostigma septoconstrictum*. This paper contributes to a more comprehensive update and improved identification of many ascomycetes and basiodiomycetes.

Fungal Diversity 80: 1-270

Zoology

11 April, 2017

Cistrome Analysis of Glucocorticoid Receptor Activity in Bronchial Epithelial Cells Defines Novel Mechanisms of Steroid Efficacy

Vineela Kadiyala[1,*] Sarah K. Sasse[1,*] M. Omar Altonsy,[1] Tzu L. Phang,[2] and Anthony N. Gerber[1,2]

[1]*National Jewish Health, Denver, Colorado,* [2]*University of Colorado, Denver, Colorado*

Glucocorticoids (GCs), which act by inducing the glucocorticoid receptor (GR) to regulate gene expression, are the primary therapy used to achieve long-term asthma control and are also used to treat asthma exacerbations, even among patients who exhibit relative baseline GC resistance. We hypothesized that analysis of the airway epithelial cistromes of GR, p65 (a component of the inflammatory nuclear factor [NF]-κB transcription factor complex), and RNA polymerase II (RNAP2) would provide new mechanistic insights into how GCs function in asthma. We performed chromatin immunoprecipitation and high-content sequencing (ChIP-seq) to determine genome-wide occupancy of GR, p65, and RNAP2 in BEAS-2B cells treated with vehicle, dexamethasone (dex, a potent GR agonist), tumor necrosis factor (TNF, which rapidly induces NF-κB activity), and a combination of dex and TNF. We identified thousands of genomic regions that are occupied by GR, p65 and RNAP2 in Beas-2B cells. GR and p65 co-occupancy resulted in surprisingly varied effects on RNAP2 occupancy at associated genes. GR was able to either antagonize or enhance the primary effects of TNF on RNAP2 occupancy and gene expression in a target-specific fashion. Through identifying genes in which RNAP2 occupancy was increased by both dex and TNF individually, with combinatorial treatment preserving or further enhancing RNAP2 levels, we defined novel, induced, antiinflammatory effectors of GCs in the airway, including TNFAIP3 and TNIP1. Taken together, our data strongly refute the long-standing model in which antagonism of NF-κB by GCs in the airway has been primarily attributed to GR tethering with NF-κB and reducing its activity. Instead, coinduction of shared antiinflammatory targets of GR and NF-κB is now also implicated in mediating beneficial effects of GCs in asthma. These data have important implications for current models of steroid-resistant airway disease.

Ann Am Thorac Soc., 13(Suppl 1) (2016) S103.

Diallyl disulfide protects against rectal cancer in vivo model of male rabbits: II-Analysis of histological and cytogenetic variations

Tito N. Habib1*, Mohammed O. Altonsy1, Soheir A. Abd El-Raheem2 and Yassmin R. Bakeer

[1]*Molecular Genetics Laboratory, Zoology Department, Faculty of Science, Sohag Univ., Sohag, Egypt*

[2]*Animal Physiology Laboratory, Zoology Department, Faculty of Science, Sohag Univ., Sohag, Egypt*

The present work was conducted to perform a short-term comparative analysis and evaluate the anti-neoplastic effects of diallyl disulfide on rectal carcinogenicity via histopathological changes, chromosomal aberrations, and mitotic index induced by 1,2-dimethylhydrazine on male rabbits (Orectolagus cuniculus). The histological changes that can be seen microscopically showed that 1,2-dimethylhydrazine at the suggested dose (20 mg/kg) produced significant alterations in rectal mucosa of 1,2-dimethylhydrazine group. The presence of dysplasia was regarded as an early histopathological changes in the precursor lesions of rectal cancer. Three varieties of intrachromosomal instability were detected, deletions (1p12, 15q23, 21q14), duplications (5q14; 13q23, 14q21) and ring (X) chromosome with a highly significant increase ($P<0.05$) in comparison with control. Such aberrations were markedly inclined in 1,2- dimethylhydrazine group after treatment by diallyl disulfide and the pretreated group that received diallyl disulfide prior to 1,2-dimethylhydrazine injection with a significant decrease ($P<0.01$). Mitotic index ranged from 46, 22, 17, and 18% to 20% in 1,2-dimethylhydrazine, 1,2- dimethylhydrazine +diallyl disulfide, diallyl disulfide, control, and pretreated diallyl disulfide +1,2- dimethylhydrazine groups, respectively. Examination of 1,2-dimethylhydrazine group showed that it caused neoplastic changes with cytogenetic abnormality identified by hematoxylin and eosin staining and G-banding analysis, respectively. Such changes were similar to those seen in human sporadic colorectal carcinogenesis.

Journal of Cancer Research and Experimental Oncology, 8 (1) (2016) 1-14

Survivin as a Novel Biomarker in the Pathogenesis of Acne Vulgaris and Its Correlation to Insulin-Like Growth Factor-I

Hanan A. Assaf,[1] Wafaa M. Abdel-Maged,[1] Bakheet E. M. Elsadek,[2] Mohammed H. Hassan,[3] Mohamed A. Adly,[4] and Soher A. Ali[1]

[1]Department of Dermatology, Faculty of Medicine, Sohag University, P.O. Box 82524, Sohag, Egypt
[2]Department of Biochemistry and Molecular Biology, Faculty of Pharmacy, Al-Azhar University, Assiut Branch, P.O. Box 71524, Assiut, Egypt
[3]Department of Biochemistry and Molecular Biology, Qena Faculty of Medicine, South Valley University, P.O. Box 83523, Qena, Egypt
[4]Department of Zoology, Faculty of Science, Sohag University, P.O. Box 82524, Sohag, Egypt

Survivin, a member of the inhibitor of apoptosis protein family, has an important role in cell cycle regulation. Insulin-like growth factor-I (IGF-I) is a polypeptide hormone with wide range of biologic effects including stimulation of lipogenesis in sebaceous glands. Their overexpression in some fibrotic disorders suggests a possible implication of both IGF-I and survivin in the pathogenesis of acne and/or acne scars. The current study aimed to assess and correlate serum levels of IGF-I and survivin in patients with active acne vulgaris and postinflammatory acne scars and to evaluate their lesional expressions in comparison to healthy controls. Serum IGF-I and survivin were estimated using commercially available ELISA kits and their tissues expressions were investigated using Western blotting. Our findings suggest that IGF-I and survivin could play potential roles in the pathogenesis of active acne vulgaris and more importantly in postinflammatory acne scars with significant positive correlation coefficient between serum levels of IGF-I and survivin which support IGF-I-/PI3K-/AKT-mediated downregulation of nuclear expression of FoxO transcription factors resulting in enhanced survivin expression.

Disease Markers Volume 2016, (2016) Article ID 7040312- 8

Effects of seasonal acclimatization on temperature-dependence of cardiac excitability in the roach, Rutilus rutilus

A. Badr1,2*, M.F. El-Sayed[2] and M. Vornanen1

[1]Department of Environmental and Biosciences, Faculty of Science and Forestry, University of Eastern Finland, Joensuu, Finland
[2]Department of Zoology, Faculty of Science, Sohag University, Sohag, Egypt

Temperature-sensitivity of electrical excitability is a potential limiting factor for performance level and thermal tolerance of excitable tissues in ectothermic animals. In order to test whether rate and rhythm of the heart acclimatize to seasonal temperature changes, thermal sensitivity of cardiac excitation in a eurythermal teleost, the roach (Rutilus rutilus), was examined. Excitability of the heart was determined from in vivo electrocardiograms and in vitro microelectrode recordings of action potentials (APs) from winter (WiR) and summer (SuR) roach acclimated to 4°C and 18°C, respectively. Under heat ramps (3°C/h), starting from the acclimatization temperatures of the fish, heart rate (HR) increased to the maximum value of 78±5 beats/min (at 19.8±0.5°C) and 150±7 beats/min (at 28.1±0.5°C) for WiR and SuR, respectively, and then declined in both groups. Below 20°C HR was significantly higher in WiR than SuR ($P<0.05$) indicating positive thermal compensation. Cardiac arrhythmias appeared with rising temperature as missing QRS complexes, increase in variability of HR, episodes of atrial tachycardia, ventricular bradycardia and complete cessation of the heartbeat (asystole) in both WiR and SuR. Unlike WiR, atrial APs of SuR had a distinct early repolarization phase, which appeared as shorter duration of atrial AP at 10% and 20% repolarization levels in comparison to WiR ($P<0.05$). In contrast, seasonal acclimatization had only subtle effects on ventricular AP characteristics. Plasticity of cardiac excitation appears to be necessary for seasonal improvements in performance level and thermal resilience of the roach heart.

J Exp Biol 219 (2016) 1495-1505

11 April, 2017

Establishment of hepatitis model in rat liver induced by injecting extracted DNA: Histopathological study

Ahmed S. Ibraheem*, Mohamed F. El-Sayed, Heba A. Khalil
Zoology Department, Faculty of Science, Sohag University, Egypt

Chronic inflammatory liver diseases can be induced by viral infections, toxic-metabolic factors and/or autoimmune mechanisms. Inflammation or viral infection results in hepatocyte damage or cell lyses which cause DNA or other cell nuclear materials to be released by hepatocytes to serve as auto-antigens that participate in auto-immune hepatitis. Those released cellular materials will be exposed to the immune system before phagocytosis by Kupffer cells. In this study, injecting rats with extracted DNA combined with CFA resulted in hepatitis cellular symptoms. Plasma globulin was increased and liver function enzymes were higher in plasma and lower in liver tissues compared to CFA and control groups. The inflammation was indicated histologically by the presence of active Kupffer cells, it led to irregularly shaped hepatic lobule, pyknotic cells, vacuolated nucleus and infiltration of liver parenchyma with lymphocytes. Vacuolation of the cells with fatty degeneration and necrotic hepatocytes also, was recorded. It is clear that using cell nuclear materials can induce inflammation that has some hepatitis identity.
The Journal of Basic & Applied Zoology, 77 (2016) 102-111

Ameliorative effect of antioxidants (vitamins C and E) against abamectin toxicity in liver, kidney and testis of male albino rats

B. Wilson Magdy a, F. El_sayed Mohamed b,*, A. Seleem Amin b, S. Sarhan Rana
[a]*Agliculture Research Center, Doki, Egypt*
[b]*Zoology Department, Faculty of Science, Sohag University, Egypt*

This study evaluated the effect of vitamins C and E as antioxidants on the physiological and histopathological changes induced by abamectin pesticide in liver, kidney and testis of male albino rats. Thirty male albino rats were divided into five groups of 6 rats each. First group served as control, while the second group received 10 mg/kg b.wt of abamectin orally, the third group received abamectin daily and 160 mg/kg b.wt of vitamin C two times per week. The fourth group received abamectin daily plus 50 mg/kg b.wt of vitamin E two times per week, while the fifth group received abamectin daily plus vitamins C and E two times per week. The experiment was conducted for six weeks. Abamectin was found to induce, hepato renal and testicular toxicity in rats, since the biochemical parameter of liver function (i.e. alanine amino transferase (ALT), aspartame amino transferase (AST), acid phosphatase (AP), glucose, total protein, albumin) and kidney function (i.e. creatinine, urea, uric acid, cholesterol and triglycerides) were highly affected. These effects were demonstrated by histopathological examination of liver, kidney and testis tissues. These observations were much reduced in the vitamin-treated groups. In conclusion, it appears that vitamins C and E, or in combination (as antioxidants) ameliorate the hepato-renal and testicular toxicity of abamectin, but are not completely protective, especially in liver tissue.
The Journal of Basic & Applied Zoology, 77 (2016) 69-82

Single or combined cadmium and aluminum intoxication of mice liver and kidney with possible effect of zinc

Ahmed S. Ibraheem, Amin A. Seleem, Mohamed F. El-Sayed, Basma H. Hamad
Zoology Department, Faculty of Science, Sohag University, Egypt

In this study, we planned to test toxic effects of cadmium, aluminum either alone or combined with each other on sensitive organs as kidney and liver. The cadmium alone decreased the animal's body weight. Meanwhile, aluminum did not affect the changes in body weight of cadmium treated animals; adding the zinc significantly reduced the loss of body weight. Serum creatinine and urea were significantly lower in treated group than in control group. Cadmium aluminum or combination of them resulted in a significant increase in serum GPT and GOT activity. Zinc did not prevent the changes caused by aluminum, however, the changes resulted by cadmium intoxication were almost healed or ameliorated by zinc. Treating with Zn alone resulted in drastic effects on kidney tissues more than either cadmium or aluminum. Treating with cadmium or aluminum resulted in infiltration of the liver parenchyma with lymphocytes, fibrosis, micro vesicular steatosis of the hepatocytes for both and appearance of many phagocytic cells, pyknotic cells and vacuolation for cadmium. Combined cadmium and aluminum treatment resulted in less damage than cadmium alone with exception of fatty degeneration. Unexpectedly, zinc induced acute cell vacuolation and steatosis. Cadmium and aluminum combined together did not worsen the situation as expected but was less damaging than cadmium alone, which suggests a possible synergistic effect of combination. Meanwhile, zinc failed to protect kidney from aluminum intoxication, which strengthens the suggestion of two different pathways of cadmium and aluminum intoxication. This finding meant that cadmium is more hepatotoxic than aluminum.

The Journal of Basic & Applied Zoology, 77 (2016) 91-101

Comparative histopathological and histochemical abnormalities induced by the posterior salivary gland and ink sac extracts of Octopus vulgaris into mice

Alaa Y. Moustafa and Aziz waad
Zoology Department, Faculty of Science, Sohag University, Egypt

Octopus vulgaris is of great importance for humans as a food resource and in fishery. The present study gave the first new insight about the comparative histopathological and histochemical impacts of oral administration of a single dose (25 mg/kg) of the posterior salivary gland (PSG) and ink sac (IS) extracts of O. vulgaris in mice. Histopathologically, the changes in the liver of PSG and IS extracts administrated mice were lymphocyte aggregations, cytoplasmic vacuolar degeneration and enlargement and congestion of hepatic portal veins. The changes caused by the PSG extract were more than those of the IS extract. In the treated spleen, IS extract showed higher impacts more than the PSG extract and occurred as lymphocyte aggregations, red pulp infiltration, increase of megakaryocytes number and mild distortion in the follicle shape. PSG and IS extracts exerted similar impacts in the ileum which detected as villi hyperplasia, epithelial and lamina propria degeneration, epithelial detachment and lymphocytes infiltration. Histochemically, IS extract increased hepatic collagenous fibers more than PSG extract especially after 7 days of administration. Both extracts reduced the liver general carbohydrates and illealmucopolysaccharide biosynthesis. PSG and IS extracts exerted significant elevation in alanine aminotransferase (ALT) and aspartate aminotransferase (AST) enzymes. Hematological studies after PSG administration revealed a significant increase in leukocytic count, and platelets and a significant decrease in lymphocytes and granulocytes. However, IS extract caused a significant increase in platelets. The present data could introduce new information about the toxicity of these extracts especially in the countries which depend on O. vulgaris ink in their food.

The Journal of Basic & Applied Zoology, 77 (2016) 23-36.

Immunotoxicity of acid secretion produced by *Berthellinacitrina* (Mollusca: Heterobranchia) in mice spleen: Histological and Immunohistochemical study

Aziz Awaad and Alaa Y. Moustafa
Zoology Department, Faculty of Science, Sohag University, Egypt

Acid secretion containing sulfuric and hydrochloric acids is a fascinating defensive phenomenon within many groups of marine organisms. This study aimed to investigate the mice spleen histology and immunotoxicity using skin acid secretion (SAS) of the sea slug Berthellinacitrina after oral administration. The spleen showed atrophy in the white pulp, decrease in the splenocytes density, megakaryocytes cytoplasmic degeneration as well as inflammatory cells infiltrations. The white and red pulp splenocytes number decreased time-dependently in the treated spleens. Additionally, the size of the megakaryocytes increased as compared with the control. The administration with SAS increased the number of the IgA+ cells aggregation in the splenic red pulp. Furthermore, after 7 days of the administration, large number of dispersed IgA+ cells were distributed in splenic parenchyma. The IgA+ cells numbers increased time-dependently as compared with those in the control. The aggregation sizes and number of the F4/80+cell in the splenic red pulp were increased. Furthermore the F4/80+cells numbers increased time-dependently as compared with those in the control. The UEAI+ cells were found as free cells but not in aggregations in the control splenic red pulp. Contradictory to the number of IgA+ cells and F4/80+cells the number of the UEAI+ cells decreased time-dependently after administration with SAS. Hematologically, abnormal numbers of WBCs different cells were observed after administration with SAS. This study provides new insight about the toxicity of a marine extract may be used in natural products industry or medical applications.

Acta Histo chemical, 118 (2016) 596-605

A review of the genus Berthellina (Mollusca: Heterobranchia: Pleurobranchidae) in the Red Sea based on molecular and anatomical data

Alaa Y. Moustafa &Haleh Golestani & Ángel Valdés
[1]*Department of Zoology, Faculty of Science, Sohag University, Sohag 82524, Egypt*
[2]*Department of Biological Sciences, California State Polytechnic University, 3801 West Temple Avenue, Pomona, CA 91768, USA*

The genus Berthellina Gardiner 1936 (Mollusca:Heterobranchia: Nudipleura) is a circumtropical group of pleurobranchid sea slugs including species with uniform coloration patterns, varying from yellow and orange to red. Thesystematics of Berthellina is in need of a revision for many areas of the world, particularly in the Indo-West Pacific region, where more than one species seem to occur. In this paper, we examined specimens of three color morphs collected from the Egyptian coast of the Red Sea. Based on sequence data from two mitochondrial genes, cytochrome c oxidase I(COI) and 16S ribosomal RNA (16S), as well as the nuclear histone 3 (H3) gene, and using phylogenetic and species delimitation approaches, we determined that two species of Berthellina co-occur in the Egyptian coast of the Red Sea. Molecular phylogenies and a revision of the literature confirmed that B. citrina is the correct name for the orange and yellow color morphs, whereas the red color morph is most likely B. delicata. Morphological and anatomical data corroborated the molecular results. This paper constitutes the first record of B. delicata from the Red Sea. Further molecular phylogenetic studies are necessary to provide a comprehensive phylogeny for Berthellina and resolve outstanding questions on the identification and distribution of most species.

Marine Biodiversity, (2016) 1-14

Reproductive Cycle, Gametogenesis and Embryonic Development of *Nitiateretiuscula* (Bivaliva : Unionidae), from the River Nile, at Sohag Governorate, Egypt

Fathey E. Soliman; Alaa Y. Moustafa[#]; Tarek G. Ismail and Olfat T. Mohamed
Zoology Department, Faculty of Science, Sohag University, Egypt

The present study dealt with the description of the reproductive and gametogenic cycles and the embryonic development of the freshwater mussel *Nitiateretiuscula* from the River Nile. Macro and micro-anatomy showed that the present species is dioceous and gonadosomatic indices showed that the species is semiannual and had two gonadal growth periods, a short period of gonadal growth from January to March and a long period from April to August. Visceral indices revealed a reciprocal relationship with the gonadosomatic indices of both the two sexes. The recorded sex ratio of females to males was (1.5: 1). The oogenesis displayed five developmental stages; oogonia, previtellogenic oocytes, vitellogenic oocytes, late vitellogenic oocytes and mature ova. Also, spermatogenesis illustrated five developmental stages: spermatogonia, primary spermatocytes, and secondary spermatocytes, spermatids; which clustered to form sperm morula and finally metamorphosed to spermatozoa. Within the gills of females (marsupia), brooding of embryos was occurred till the formation of glochidia larvae. The unfertilized eggs were released from the gonads with distinct germinal vesicle. The fertilized eggs had two polar bodies and a fertilization cone. Successive cleavages were observed. Spiral cleavage, non-ciliated blastula and D-shaped larvae were recorded.
Egypt. J. Zool., 66 (2016) 115-138

Drosophila melanogaster as a suitable in vivo model to determine potential side effects of nanomaterials: A review

Alaraby M[1,2], Annangi B[1], Marcos R[1,3], Hernández A[1,3]
[1]Grup de Mutagènesi, Departament de Genètica i de Microbiologia, Facultat de Biociències, Universitat Autònoma de Barcelona , Campus de Bellaterra , Cerdanyola del Vallès , Spain
[2]Zoology Department, Faculty of Sciences , Sohag University , Sohag , Egypt
[3]CIBER Epidemiología y Salud Pública , ISCIII , Madrid , Spain.

Despite being a relatively new field, nanoscience has been in the forefront among many scientific areas. Nanoparticle materials (NM) present interesting physicochemical characteristics not necessarily found in their bulky forms, and alterations in their size or coating markedly modify their physical, chemical, and biological properties. Due to these novel properties there is a general trend to exploit these NM in several fields of science, particularly in medicine and industry. The increased presence of NM in the environment warrants evaluation of potential harmful effects in order to protect both environment and human exposed populations. Although in vitro approaches are commonly used to determine potential adverse effects of NM, in vivo studies generate data expected to be more relevant for risk assessment. As an in vivo model Drosophila melanogaster was previously found to possess reliable utility in determining the biological effects of NM, and thus its usage increased markedly over the last few years. The aims of this review are to present a comprehensive overview of all apparent studies carried out with NM and Drosophila, to attain a clear and comprehensive picture of the potential risk of NM exposure to health, and to demonstrate the advantages of using Drosophila in nanotoxicological investigations.
J Toxicol Environ Health B Crit Rev., 19(2) (2016) 65-104

New insights in the acute toxic/genotoxic effects of CuO nanoparticles in the in vivo Drosophila model

Alaraby M [1,2], Hernández A [1,3], Marcos R [1,3].

[1]*Grup De Mutagènesi, Departament De Genètica I De Microbiologia, Facultat De Biociències , Universitat Autònoma De Barcelona , Barcelona , Spain*

[2]*Zoology Department, Faculty of Sciences , Sohag University , Sohag , Egypt*

[3]*CIBER Epidemiología Y Salud Pública, ISCIII , Madrid , Spain*

Metal oxide nanoparticles are highly reactive from the biological point of view and, for this reason, it exists important reservations in regard human health impact. We used Drosophila as a promising in vivo model to diagnose the biological effects of copper oxide nanoparticles (CuO-NPs). Due to the potential role of ions release the effects of CuO-NPs were compared with those induced by copper sulfate, CuSO4. A wide battery of approaches has been used including toxicity, cell and body internalization, induction of reactive oxygen species (ROS) as well as changes in gene expression, related to both general stress and alterations in the intestinal barrier, and genotoxicity. The obtained results show that CuO-NPs have the ability to be distributed inside midgut cells and translocate to the general body compartment (internal hemolymph) interacting with hemocytes. Its exposure leads to reduced larval growth, decreased flies viability, delaying their emergency periods, especially at higher doses (2 and 10 mM). Moreover, deregulation of stress genes including antioxidant genes, and genes involved in wound healing were also observed. In this point it should be emphasized the novelty of using genes such as Duox, Upd3, PPO2, and Hml to determine injury on the intestinal barrier. On the other hand, CuO-NPs had non-genotoxic potential, in agreement with their inability to increase ROS production. In general dissolved copper produced higher toxic/genotoxic effects than those induced by CuO-NPs which would indicate that copper ions alone are more important in inducing harmful effects than copper nanoparticles itself.

Nanotoxicology. 10 (6) (2016) 749-60

Impact of nematode helminthes on metal concentrations in the muscles of Koshar fish, Epinephelussummana, in Jeddah, Saudi Arabia

A.H. Hassan [a,b] ,* ,N.A. Al-Zanbagia ,E.A [a]. Al-Nabatic [c]

[a]*Biology Department, Science College, King Abdulaziz University, Jeddah, Saudi Arabia*

[b] *Zoology Department, Faculty of Science, Sohag University, Sohag, Egypt*

[c] *Biology Department, Science College, Taibah University, Medina, Saudi Arabia*

The aim of the present study was to determine the impact of nematode parasites on the metal balance of the Koshar fish Epinephelussummana. A total of 102 fish were randomly collected from the Red Sea, Jeddah coast, during the period of March to September 2014. The element concentrations in the infected and non-infected fish were analyzed using flame atomic absorption spectrometry.Nematodes were collected and described from fish liver, intestine, stomach and gonads.The results showed that intestinal and stomach nematodes caused significant decreases in both magnesium and lead and insignificant decreases in iron and calcium compared to non-infected fish.There were significant increases in potassium and sodium and insignificant increases in zinc and copper in fish infected with intestinal and stomach nematodes. Most elements significantly decreased in fish infected with gonadal nematodes, with the exception of magnesium and lead, which insignificantly decreased in comparison to healthy fish. Adult nematode infection in marine fish is considered to be a biological indicator for heavy metal pollution, and its presence can minimize the bioaccumulation of heavy metals in fish tissue and organs.

The Journal of Basic & Applied Zoology, 74 (2016) 56-61

11 April, 2017

Buccal deformities in chironomid larvae (Diptera: Chironomidae) as an indicator Risk Assessment and Anthropogenic stresses of pollution in fresh water of the River Nile, Sohag Governorate, Egypt. Available from

Fatma K. Adham[2], Azza M. Khedre[1], Tarek G. Ismail[1], Mohamed El Araby[1], Shahenda , A.A[2]. Abu ElEla, Wael M. ElSayed[2]

[1]*Zoology Department, Faculty of Science, Sohag University, Sohag, Egypt*
[2]*Zoology Department, Faculty of Science, Cairo University, Sohag, Egypt*

Mouth parts deformities in chironomid larvae are considered as indicators of environmental stress in aquatic systems caused by water and sediment pollution such as heavy metals, pesticides as well as organic contamination. Fourth instar chironomid larvae were collected from two sites (SI and SII) located in the River Nile, Sohag Governorate, Egypt. The chironomid community of the two SI and SII was dominated by Dicrotendipesnilophilus (Diptera: Chironomidae). The percentage numbers of chironomid larvae with deformed mouthparts were 29% (SI) and 14% (SII). Although there were no significant differences in the sediment metal concentrations between the two sites, significant differences were recorded among the metal concentrations of iron (Fe), zinc (Zn) and copper (Cu). Moreover, the present results revealed that some physicochemical parameters played an important role in increasing the mouthparts abnormalities.

Journal of Biodiversity and Environmental Sciences (JBES). *Vol. 8, No. 6, p.37-48, 2016*

Histopathological study on rodent small intestine infected with an adult tapeworm, *Hymenolepis diminuta* recorded at Sohag, Egypt

Ramadan S. A., Hassan A. H., Asran A. A., Abd Elgwad E. F.
Department of Zoology, Faculty of Science, Sohag University, Egypt

Rodents play a significant role in public health, Chiefly due to their role as carriers or reservoirs of microbes and parasites of zoonotic importance. The main objective of the present study was to make a histopathological study on the small intestine of rodents infected with an adult tapeworm, *Hymenolepisdiminuta*collected from two sites at Sohag, Egypt. The study revealed that The infection percentages of the present rodent with the adult tapeworm *Hymenolepisdiminuta*were (12% females) and (16% males) and (12% females) and (8% males) in first and second sites, respectively. Histopathologically, the lumina of the present rodent intestine contained tapeworm. Presence of the tapeworm in lumina of the infected rodent intestine lead to excessive mucin secretion in luminal debris. Some intestinal villi appeared blunt and reduced in height. The intestinal muscularis layers were thickened. Moreover, inflammatory cells infiltration in the connective tissue core of the villi and crypts were observed. Erosion and adhesion of the tip of villi were observed in the intestine. The proliferating activity of the enterocytes was evidently increased and mitotic figures were observed not only in the intestinal crypts but also in the epithelium covering the middle third of the villi. Crypts and villi hyperplasia of intestine were observed.

Journal of Environmental studies 15 **(2016)** ***11-18***

Histopathological changes of rodent liver infected with a larval cestodes recorded at Sohag, Egypt

Ramadan S. A., Hassan A. H., Asran A. A., Abd Elgwad E. F.
Department of Zoology, Faculty of Science, Sohag University

Rodents are important in many ecosystems because they reproduce rapidly, and can function as food source for predators, mechanisms for seed dispersal and as diseases vectors. Rodents may act as reservoir hosts for important human parasitic diseases. The present study was focused on histopathological changes of rodent liver infected with a larval cestodes recorded at two locations situated at Sohag, Egypt. This study reported infection rate of 56% and 32% for rodents at the two locations, respectively. The study also showed that the incidence in females is higher than in males in the second location compared with that of the first location. Microscope examinations of the liver tissue sections revealed a wall cyst of larval cestode, *Cysticercusfasciolaris*in parenchyma consists of two compressed layers of highly proliferative fibrous connective tissue and inflammatory cells mainly lymphocytes. Inflammatory reaction was seen in the hepatic parenchyma around the cyst. Also, there are dilatation and congestion in the central and portal veins and infiltration of the liver parenchyma with inflammatory cells. The hepatocytes in the central and portal areas showed fatty degenerative changes. While, in the portal area the histological tissue of the liver showed microvesicularsteatosis and edematous infiltration. Signs of inflammation including sinusoid widening and prominent kupffer cells were noted.
Rec. 10 Feb, 2016 Accept. 12 Mar, 2016

Effect of maternal caffeine and retinoic acid intake on liverduring pre- and postnatal development of mice, musmusculus

Fakhr El-Din M. Lashein*, Amin A. Seleem and Abeer A. Ahmed
Zoology Department, Faculty of Science, Sohag University, Sohag, Egypt

The present study was conducted to evaluate the effect of caffeine and retinoic acid as the active metabolite form of vitamin Aon the liver at pre- and postnatal periods of development. In either the pre- or the postnatal period of study, caffeine was ableto perturb carbohydrates, increase calcium and decrease iron those accompanied with down regulated expression of TGFβ2in hepatic tissue as compared to control. Treatment with retinoic acid at both doses in the present study either separate orcombined with caffeine upregulate calcium against suppression of iron. Moreover, TGFβ2 show biphasic that severely downregulated during gestation and extended to express intranuclear at postnatal in liver tissue. Decreased iron overload of liver withconcomitant down regulation of TGFβ2 expression represent the most important points of this study that protect the liver ofyoung age from oxidative damage and suppress the gene-dependent extracellular matrix deposition. These data may contributeto the therapeutic uses of these substances in preventing the progression of liver damage in hepatitis diseases.
International Journal of Pure and Applied Zoology, *4 (2) (2016) 189-202*

Effect of verapamil on some of the pro- and apoptotic factors during prenatal retinaldifferentiation of mice, Musmusculus

Amin AbdouSeleem*, Fakhr El-Din M. Lashein
Zoology Department, Faculty of Science, Sohag University, Sohag, Egypt

The present study was conducted to evaluate the effect of caffeine and retinoic acid either separately or in combination on the skeleton of the developing embryos of mice. Pregnant females were treated with either caffeine or retinoic acid at the onset of organogenesis (7th day of gestation). At morphological level no abnormalities in either caffeine or retinoic acid in the developing embryos at 14th day of gestation whose mothers' were administered caffeine (2 mg/100 g b.w.) or those of the mothers' treated with retinoic acid up to 4 mg/kg b.w. during the onset of the second trimester of pregnancy were observed. However, dose-dependent retinoic acid treatment initiates chondrocyte vacuolation, depression of PAS+ve intracellular inclusions and depression of nuclear fluorescence that were concomitant with downregulation of TGFb2 expression in the perichondrium of the developing vertebrae. Co-administration of caffeine was found to ameliorate the effects of 2 mg/kg b.w. rather than 4 mg/kg b.w. of retinoic acid treatment. At the 18th day of gestation the uterine horns appeared normal without any signs of fetoresorption in all treatments. However, the effect of both caffeine (2 mg/100 g b.w) and retinoic acid at both doses (2, 4 mg/kg b.w) in Alizarin Red stain of wholemount revealed minor phalange deformation of the developing limbs either separately or in combined treatments.
The Journal of Basic & Applied Zoology, 75 (2016) 28–35

Effect of caffeine and retinoic acid on skeletonof mice embryos

Fakhr El-Din M. Lashein*, Amin A. Seleem, Abeer A. Ahmed
Zoology Department, Faculty of Science, Sohag University, Sohag, Egypt

The present study was conducted to evaluate the effect of caffeine and retinoic acid either separately or in combination on the skeleton of the developing embryos of mice. Pregnant females were treated with either caffeine or retinoic acid at the onset of organogenesis (7th day of gestation). At morphological level no abnormalities in either caffeine or retinoic acid in the developing embryos at 14th day of gestation whose mothers' were administered caffeine (2 mg/100 g b.w.) or those of the mothers' treated with retinoic acid up to 4 mg/kg b.w. during the onset of the second trimester of pregnancy were observed. However, dose-dependent retinoic acid treatment initiates chondrocyte vacuolation, depression of PAS+ve intracellular inclusions and depression of nuclear fluorescence that were concomitant with downregulation of TGFb2 expression in the perichondrium of the developing vertebrae. Co-administration of caffeine was found to ameliorate the effects of 2 mg/kg b.w. rather than 4 mg/kg b.w. of retinoic acid treatment. At the 18th day of gestation the uterine horns appeared normal without any signs of fetoresorption in all treatments. However, the effect of both caffeine (2 mg/100 g b.w) and retinoic acid at both doses (2, 4 mg/kg b.w) in Alizarin Red stain of wholemount revealed minor phalange deformation of the developing limbs either separately or in combined treatments.
The Journal of Basic & Applied Zoology, 75 (2016), 36-45

Geology

Carbonate platform facies development of the Turonian Wata Formation in central and eastern Sinai, Egypt

Khalifa, M. A.[a], Farouk, S.[b], Hassan, A. M.[c]
[a]Geology Determent, Menoufia University, Shiben El Kom, Egypt, [b]Exploration Determent, Egyptian Petroleum Research Institute, Nasr City, Egypt, [c]Geology Determent, Sohag University, Sohag, Egypt

The Wata carbonate platform in central and eastern Sinai show a clear pattern of evolutionary development during sedimentation. Three facies are recognized in the carbonate platform. Inner-platform in the south, inter-platform basin in the middle, and outer-platform in the northwest. Such classification was probably performed by the effect of Syrian Arc System that culminated during Turonian in Sinai. Inner-platform includes fining-upward cycles, each begins with packstone, followed by wackestone and capped by lime-mudstone or claystone or molluscan bioclastic wackestone at the base capped by sandy oolitic packstone or dolostone. The dominant faunal associations are molluscs, and echinoids. Inter-platform basin occurs north of inner-platform and extends northwest-southeast direction and comprises fining-upward cycles, each of which begins with bioclastic ostracodal packstone, calcisphere packstone, bioclastic packstone, capped by wackestone and lime-mudstone The faunal association includes, sponge spines, ostracodes, molluscan debris and calcispheres. They were deposited in shoal marine and barrier. The outer-platform occurs at Gebel Giddi and extended northwestwards. The lithofacies are entirely represented by calcisphere wackestone/packstone, with a reduced thickness of 20 m.
Journal of African Earth Sciences, 124 (2016) 126-138

New simulation technique to estimate the hydrocarbon type for the two untested members of Belayim Formation in the absence of pressure data, Badri Field, Gulf of Suez, Egypt

Abudeif, A.M.[a], Attia, M.M.[a], Radwan, A.E.[b]
[a]Geology Department, Sohag University, Sohag, Egypt
[b]Gulf of Suez Petroleum Company, Cairo, Egypt

Determination of the fluid type in a reservoir is considered one of the main essential purposes of the formation evaluation processes. Badri Field, located in the southern part of the Gulf of Suez, is one of the most prolific areas in the Gulf of Suez. Presence of sandstone streaks in Sidri and Baba members within Belayim Formation in some wells within this field of relatively high resistivity signature in electric logs is the main reason to investigate its petrophysical parameters, to delineate the main characterization of these sands, and to evaluate their ability for hydrocarbon accumulation and production. This study aims to estimate the fluid types in these two untested members, especially that they are sandwiched between two productive sandstone zones, Kareem Formation and Hammam Faraun Member. The fluid type can be determined using formation pressure and pressure gradient, which play a great role to differentiate between the different formations' fluids (oil, gas, and water). Because of absence of pressure data in the studied wells, a new simulation technique was applied using well logging crossplot responses in the different hydrocarbon types (oil and/or gas), which were tested before to estimate the fluid type in the untested two studied zones. These include density-neutron, sonic-neutron, M-N, and matrix identification (MID) crossplots. This can be performed by correlation of the crossplot responses in the two productive sandstone zones: Kareem Formation and Hammam Faraun Member versus the untested studied sandstone zones of Sidri and Baba members, depending on the similarities and the differences between the crossplot responses or signatures in the oil and gas fluids. The results of this approach revealed that the most fluid type in BDR-A8 and BDR-B9 wells is gas in Baba and Sidri zones and oil in the BDR-A9 well for Baba zone.
Arabian Journal of Geosciences, 9 (2016) 218

Natural and human-induced sinkhole hazards in Saudi Arabia: distribution, investigation, causes and impacts

Ahmed M. Youssef [1,2] & Hasan M. Al-Harbi [1] & Francisco Gutiérrez [3] & Yasser A. Zabramwi [1] & Ali B. Bulkhi [1] & Saeed A. Zahrani [1] & Alaa M. Bahamil [1] & Ahmed J. Zahrani [4] & Zaam A. Otaibi [4] & Bosy A. El-Haddad [2]

[1]*Geological Hazards Department, Applied Geology Sector, Saudi Geological Survey, Jeddah, KSA*
[2]*Geology Department, Faculty of Science, Sohag University, Sohag, Egypt*
[3]*Earth Sciences Department, University of Zaragoza, Zaragoza, Spain*
[4]*Geophysical Survey Department, Saudi Geological Survey Jeddah, KSA*

Approximately 60 % of the 2,150,000 km^2 area of Saudi Arabia is underlain by soluble sediments (carbonate and evaporite rock formations, salt diapirs, sabkha deposits). Despite its hyper-arid climate, a wide variety of recent sinkholes have been reported in numerous areas, involving significant property losses. Human activities, most notably groundwater extraction, have induced unstable conditions on pre-existing cavities. This work provides an overview of the sinkhole hazard in Saudi Arabia, a scarcely explored topic. It identifies the main karst formations and the distribution of the most problematic sinkhole areas, illustrated through several case studies covering the wide spectrum of subsidence mechanisms. Some of the main investigation methods are presented through selected examples, including remote sensing, trenching and geophysics. Based on the available data, the main causal factors are identified and further actions that should be undertaken to better assess and manage the risk are discussed.

Hydrogeol J, 24 (2016) 625–644.

Petrophysical and petrographic evaluation of Sidri Member of Belayim Formation, Badri field, Gulf of Suez, Egypt

Abudeif A. M.[a] , Attia M. M.[a], Radwan A. E.[b]

[a]*Sohag University, Faculty of Science, Geology Department, Sohag, Egypt*
[b]*Exploration Department, Geological Operations and Petrophysics Division, GUPCO, Egypt*

Presence of sandstone streaks in Sidri Member within Belayim Formation that lies between two productive zones; Kareem Formation and Hammam Faraun Member, was the main reason to perform this study. It may represent a good hydrocarbon reservoir and will be added to the Egyptian oil production in some wells of Badri field. This Member has high resistivity signature on Electric-logs responses which attracted the attention to investigate its occurrence in the field, to delineate its distribution all-over the area, to evaluate the petrographic and petrophysical characteristics and to evaluate its productivity. Petrographic and petrophysical analyses of these sand zones were undertaken using thin section samples. The electric logs and subsurface geologic data was used to evaluate the main reservoir characteristics of the Sidri sandstone such as lithology, cementation, shale volume, porosity (Φ), effective porosity (Φ_{eff}), estimated permeability (K), fluid saturation, fluid type and Net pay thickness.This study revealed that, Sidri sandstone facies was classified into two mainly sandy facies; blocky sandy facies which located at the northern part of the field and streaky sandy facies at the southern area of the field. These two facies are separated by shaley facies. Some wells were studied to represent the two sandy facies in Sidri Member and these sand intervals have not been tested yet. These sands consist of quartz grains with grey and pink feldspars as accessory minerals, with siliceous and calcareous cementation, with good porosity. Petrophysical evaluation of this sand unit indicated that it is hydrocarbon bearing formation in three wells and water bearing one in other wells. Electrical logs analysis (Resistivity, Density-Neutron, Sonic and Gamma-Ray) revealed that The volume of shale in this sandstone, the effective porosity, the water saturation, the estimated permeability, the hydrocarbon saturation, and the net-pay thickness are varying from 9 to 13%, 19%-22%, 26%-34%, 200 and 600 mD, 66 and 74%, 20-35 feet respectively. The fluid types are oil, gas and water.

Journal of African Earth Sciences, 115 (2016) 108-120

Human-Induced Geo-Hazards in the Kingdom of Saudi Arabia: Distribution, Investigation, Causes and Impacts

Ahmed M. Youssef [1, 2], Hasan M. Al-Harbi [1], Yasser A. Zabramwi[1], Bosy A. El-Haddad[2]
[1] Geological Hazards Department, Applied Geology Sector, Saudi Geological Survey, Jeddah, Kingdom of Saudi Arabia, [2] Geology Department, Faculty of Science, Sohag University, Egypt

Different types of geological hazards are induced by human activities in the Kingdom of Saudi Arabia (KSA). These geological hazards include land subsidence and earth fissures, sinkholes, expansive soils, and flash floods. A wide variety of recent geological hazards have been reported in several areas, causing significant human and property losses. Human activities, most notably groundwater extraction, infrastructure development, and agricultural activities, have induced unstable conditions. This chapter provides an overview of the human-induced geological hazard in the KSA, mainly earth fissures and sinkhole, which represent a scarcely explored topic. This work identifies the main types of human-induced geological-hazard formations, distribution, causes, and impacts, illustrated through several case studies in the KSA.
Geohazards Caused by Human Activity, Chapter 3 (2016) 37-61

Comparison of four kernel functions used in support vector machines for landslide susceptibility mapping: a case study at Suichuan area (China)

Hong H.[ab], Pradhan B.[cd], Bui D. T.[e], Xu C.[a], Youssef A. M.[f], Chen W.[g]
[a]Key Laboratory of Active Tectonics and Volcano, Institute of Geology, China Earthquake Administration, Beijing, [b]Jiangxi Provincial Meteorological Observatory, Jiangxi Meteorological Bureau, Nanchang, China, [c]Department of Civil Engineering, Geospatial Information Science Research Center (GISRC), Faculty of Engineering, University Putra Malaysia, Selangor Darul Ehsan, Malaysia, [d]Department of Energy and Mineral Resources Engineering, Choongmu-gwan, Sejong University, Seoul, Republic of Korea, [e]Geographic Information System group, Department of Business Administration and Computer S cience, University College of Southeast Norway, Bø i Telemark, Norway, [f]Department of Geology, Faculty of Science, Sohag University, Sohag, Egypt, [g]College of Geology & Environment, Xi'an University of Science and Technology, Xi'an, Chin

Suichuan is a mountainous area at the Jiangxi province in Central China, where rainfall-induced landslides occur frequently. The purpose of this study is to assess landslide susceptibility of this region using support vector machine (SVM) with four kernel functions: polynomial (PL), radial basis function (RBF), sigmoid (SIG), and linear (LN). A total of 178 landslides were used to accomplish this approach, of which, 125 (70%) landslides were randomly selected for training the landslide susceptibility models, whereas the remaining 53 (30%) were used for the model validation. Fifteen landslide conditioning factors were considered including slope-angle, altitude, slope-aspect, topographic wetness index (TWI), sediment transport index (STI), stream power index (SPI), plan curvature, profile curvature, distance to rivers, distance to faults, distance to roads, precipitation, landuse, normalized difference vegetation index (NDVI), and lithology. Using the training dataset, nine landslide susceptibility models for the Suichuan area were constructed with the four kernel functions. To evaluate the performance of these models, the receiver-operating characteristic curve (ROC) and area under the curve (AUC) were used. Using the training dataset, AUC values for the SVM-PL models with six degrees PL function (1–6) are 0.715, 0.801, 0.856, 0.891, 0.919, 0.953, respectively, and for the SVM-RBF model, the SVM-SIG model, and the SVM-LN model are 0.716, 0.741, and 0.740, respectively. Using the validation dataset, AUC values for the SVM-PL models with six degrees PL function (1–6) are 0.738, 0.730, 0.683, 0.648, 0.608, and 0.598, respectively, and for the SVM-RBF model, the SVM-SIG model, and the SVM-LN model are 0.716, 0.741, and 0.740, respectively. Our results suggested that the SVM-RBF model is the most suitable for landslide susceptibility assessment for the study area
Geomatics, Natural Hazards and Risk,7 (2016) 1-26.

Landslide susceptibility mapping using random forest, boosted regression tree, classification and regression tree, and general linear models and comparison of their performance at Wadi Tayyah Basin, Asir Region, Saudi Arabia

Youssef, A.M.[ab] , Pourghasemi, H.R.[c] , Pourtaghi, Z.S.[d], Al-Katheeri, M.M.[b]

[a]Geology Department, Faculty of Science, Sohag University, Sohag, Egypt, [b]Geological Hazards Department, Applied Geology Sector, Saudi Geological Survey, Saudi Arabia, [c]Department of Natural Resources and Environmental Engineering, College of Agriculture, Shiraz University, Shiraz, [d]Department of Environment Management Engineering, College of Natural Resources, Yazd University, Yazd, Iran

The purpose of the current study is to produce landslide susceptibility maps using different data mining models. Four modeling techniques, namely random forest (RF), boosted regression tree (BRT), classification and regression tree (CART), and general linear (GLM) are used, and their results are compared for landslides susceptibility mapping at the Wadi Tayyah Basin, Asir Region, Saudi Arabia. Landslide locations were identified and mapped from the interpretation of different data types, including high-resolution satellite images, topographic maps, historical records, and extensive field surveys. In total, 125 landslide locations were mapped using ArcGIS 10.2, and the locations were divided into two groups; training (70 %) and validating (25 %), respectively. Eleven layers of landslide-conditioning factors were prepared, including slope aspect, altitude, distance from faults, lithology, plan curvature, profile curvature, rainfall, distance from streams, distance from roads, slope angle, and land use. The relationships between the landslide-conditioning factors and the landslide inventory map were calculated using the mentioned 32 models (RF, BRT, CART, and generalized additive (GAM)). The models' results were compared with landslide locations, which were not used during the models' training. The receiver operating characteristics (ROC), including the area under the curve (AUC), was used to assess the accuracy of the models. The success (training data) and prediction (validation data) rate curves were calculated. The results showed that the AUC for success rates are 0.783 (78.3 %), 0.958 (95.8 %), 0.816 (81.6 %), and 0.821 (82.1 %) for RF, BRT, CART, and GLM models, respectively. The prediction rates are 0.812 (81.2 %), 0.856 (85.6 %), 0.862 (86.2 %), and 0.769 (76.9 %) for RF, BRT, CART, and GLM models, respectively. Subsequently, landslide susceptibility maps were divided into four classes, including low, moderate, high, and very high susceptibility. The results revealed that the RF, BRT, CART, and GLM models produced reasonable accuracy in landslide susceptibility mapping. The outcome maps would be useful for general planned development activities in the future, such as choosing new urban areas and infrastructural activities, as well as for environmental protection.

Landslides,Volume 13 (2016) 839-856.

Debris flow impact assessment along the Al-Raith Road, Kingdom of Saudi Arabia, using remote sensing data and field investigations

Youssef, A.M.[ab], Al-Kathery, M.[b], Pradhan, B.[c] , El-Sahly, T.[b]

[a]Geology Department, Sohag University, Sohag, Egypt

[b]Geological Hazards Department, Applied Geology Sector, Saudi Geological Survey, Saudi Arabia

[c]Department of Civil Engineering, Geospatial Information Science Research Center (GISRC), University Putra Malaysia (UPM), Serdang, Malaysia

Jizan mountainous areas in Kingdom of Saudi Arabia are suffering from a variety of slope failures. Most of these failures happen due to heavy rainfalls from time to time. These landslides include rock topples, rockslides, debris flow, and some combination of these which affected many roads, highways, and buildings. The Al-Raith Road is one of these roads connecting Red Sea coast cities with Asir and Al-Hasher areas. The length of this road reaches about 45 km and it has been exposed to landslides during each heavy rain storm. One of these events happened in 24 August 2013, which caused huge debris flows that cut and damaged the road. The current research aims to evaluate the debris flow assessment along this highway using remote sensing data and field studies. According to the detailed analysis of geological and geomorphological maps, as well as field investigation, it is evident that the debris flow materials are mainly related to the different types of landslides. These landslides included rock topples which are frequently observed along the side walls of the channels (flexture which occur in foliated rocks and block which occurs in massive rocks), rock sliding (planner failures) where many rock joints and shear zones dip towards the channel, and rockfalls. Debris range in their size from up to 2 m in diameter to fine materials less than 2 mm. These materials can be easily moved with water causing a risk to vehicles, roads, and housing in the area. Field study indicated that these debris channels especially at the lower part have been reactivated several times in the past. Finally, suitable solutions have been suggested to these critical sites to minimize and/or avoid the debris flow hazards in the future.

Geomatics, Natural Hazards and Risk, 7 (2016) 620-638

Analysis on causes of flash flood in Jeddah city (Kingdom of Saudi Arabia) of 2009 and 2011 using multi-sensor remote sensing data and GIS

Youssef A. M.[ab], Sefry S. A.[a], Pradhan B.[c] , Alfadail E. A.[a]
[a]*Geological Hazards Department, Applied Geology Sector, Saudi Geological Survey, Saudi Arabia*
[b]*Geology Department, Faculty of Science, Sohag University, Sohag, Egypt*
[c]*Department of Civil Engineering, Geospatial Information Science Research Center (GISRC), Faculty of Engineering, University Putra Malaysia, Serdang, Malaysia*

The Jeddah city is located in a coastal plain area, in the middle of the western side of the Kingdom of Saudi Arabia, bounded by the Red Sea to the west and mountains to the east. Jeddah city receives rainfall runoff from the foothills through different drainage pathways (wadis). During intense rainfall events, runoff flows westward from the hills and mountains towards the Red Sea, causing flash floods in the urban areas along the pathways of these wadis. Two major flash flood events occurred in Jeddah city during 20 November 2009 - January 2011. These events were characterized by rainfall precipitation values of 70 and 111 mm, respectively. Each flash flood event has duration of three hours. The impact of these two flood events have been disastrous causing extensive flooding that killed 113 people in 2009 and damaged infrastructure and property (more than 10,000 homes and 17,000 vehicles). This study deals with the analysis of the different factors that caused these flash flood events. The results indicate that the causes of these floods are related to a number of factors which play as a major contribution to the worsening of the flood disaster. These factors were classified into the following: geomorphological features, anthropogenic activities (urban changes), network and catchment factors, and rainfall and climatic changes factors. The climatic changes have a major impact on the rainfall intensity and will appear more in the future. Other factors related to the wadis tributaries are narrow passes, and high slope of the wadi has additional impacts in the flash floods in the area. The anthropogenic activities include the proliferation of slums and construction in the valleys coupled with the lack of suitable water streams to accommodate the amount of water flowing and the presence of dirt led to the direction of flow.
Geomatics, Natural Hazards and Risk, 7 (2016) 1018-1042

Effect of water–rock interaction processes on the hydrogeochemistry of groundwater west of Sohag area, Egypt

Redwan M., Abdel Moneim A. A., Amra M. A.
Geology Department, Sohag University, Sohag, Egypt

Groundwater is used intensively for land reclamations and domestic purposes in new reclaimed areas west of the Nile Valley in Sohag Governorate, Upper Egypt as it is the only source of water in the area. Twenty-six groundwater samples are collected to evaluate the hydrochemical characteristics and the impact of water–rock interaction on the chemistry of groundwater using classical geochemical and statistical tools. The total dissolved solids (TDS) are ranging between fresh and saline water (530–4,850 ppm). The distribution of the major ions is the order of $Na^+ > Ca^{2+} > Mg^{2+} > K^+$ and $Cl^- > SO_4^{2-} > HCO_3^-$. The entire samples belong to a shallow meteoric source as indicated by the meteoric genesis index. Ionic abundance plot of alkalis with $Ca^{2+} + Mg^{2+}$ is suggestive of mix type trends of concentrations. Two groundwater zones are identified in the area using the cluster analysis; the first zone contains high TDS (mean 2,157.7 ppm) while the second zone is characterized by relatively low TDS values (mean 1,003.1 ppm). Gibbs ratio's showed that two main processes prevailed, chemical weathering, hydrolysis, and ion-exchange of rock-forming minerals, especially the silicates (middle and southern parts) and evaporation and subsequent crystallization of gypsum and halite (northern part). This is also proved by the hydrochemical signatures and correlation relationships of the different elements. The obtained results revealed that about 53.8 % of the samples are suitable for drinking purposes. The combination of hydrogeochemical and clustering tools is effective in identifying and evaluating the water–rock interaction processes on the chemistry of groundwater.
Arabian Journal of Geosciences, 9 (2016) 1-14.

Flash flood susceptibility assessment in Jeddah city (Kingdom of Saudi Arabia) using bivariate and multivariate statistical models

Youssef, A.M.[ab], Pradhan, B.[c] , Sefry, S.A.[a]

[a]*Geological Hazards Department, Applied Geology Sector, Saudi Geological Survey, Saudi Arabia*
[b]*Geology Department, Sohag University, Sohag, Egypt*
[c]*Department of Civil Engineering, Geospatial Information Science Research Center (GISRC), University Putra Malaysia (UPM), Serdang, Malaysia*

The city of Jeddah (Saudi Arabia) has experienced two catastrophic flash flood events in 2009 and 2011. These flood events had catastrophic effect on human lives and livelihoods around the wadi Muraikh, wadi Qus, wadi Methweb, and wadi Ghulail in which 113 people were dead and with 10,000 houses and 17,000 vehicles were damaged. Thus, a comprehensive flood management is required. The flood management requires information on different aspects such as the hydrological, geotechnical, environmental, social, and economic aspects of flooding. Flood susceptibility mapping for any area helps the decision makers to understand the flood trends and can aid in appropriate planning and flood prevention. In this study, two models were used for the generation of flood susceptibility maps for the Jeddah region. The first model includes bivariate probability analysis (frequency ratio), and the second model uses the multivariate analysis. For the multivariate model, the acquired weights of the FR model were entered into the logistic regression model to evaluate the correlation between flood occurrence and each related factor. This integration will overcome some of the weakness of the logistic regression, and the performance the LR will be enhanced. A flood inventory map was prepared with a total of 127 flood locations. These flood locations were extracted from different sources including field investigation and high-resolution satellite image (IKONOS 1 m). These flood locations were randomly split into two groups, one dataset representing 70 % was used for training the models, and the remaining 30 % was used for models validation. Various independent flood-related factors such as slope, elevation, curvature, geology, landuse, soil drain, and distance from streams were included. The impact of each independent flood-related factors on flooding was evaluated by analyzing each independent factor with the historical flood inventory data. The training and validation datasets were used to evaluate the flood susceptibility maps using the success and the prediction rate methods. The results of the accuracy assessment showed a success rate of 90.4 and 91.6 % and a prediction rate of 89.6 and 91.3 % for FR and ensemble FR and LR models, respectively. In addition, a comparison has been made between real flood events in 2009 and the resultant susceptibility maps. Hence, it is concluded that the FR and ensemble Fr and LR models can provide an acceptable accuracy in the prediction of flood susceptibility in the Saudi Arabia. Our findings indicated that these flood susceptibility maps can assist planners, decision makers, and other agencies to deal with the flood management and planning in the area.

Environmental Earth Sciences, 75 (2016) 1-16.

Using Na/K Ratios to Identify the Potential Impacts of Sewage Effluent on Groundwater Quality in Sohag, Egypt

Redwan M., Abdel Moneim A.A.

Geology Department, Faculty of Science, Sohag University, Sohag, Egypt

Improper disposal of wastewater is an important source of groundwater contamination, as it poses serious threats to the environment and human health. In this case study, 18 groundwater and 3 sewage effluent samples were collected from the area adjacent to a wastewater treatment plant in Sohag, Egypt. These samples were subjected to detailed chemical and bacteriological analyses to quantify the potential impact of sewage effluent on the groundwater quality using geochemical indicators. The groundwater aquifer in the study area is represented by the highly permeable Qena Sands that are composed of sands and gravels. The bacteriological analyses indicated the presence of fecal coliform in groundwater at wells nearby the wastewater ponds and farm lands. NH_4 concentration of the contaminated groundwater samples ranged from 0.36 to 5.70 mg/L (78% of the samples > 1.20 mg/L) and the NH_4 in the non-impacted samples ranged from 0.40 to 2.23 mg/L (22% > 1.20 mg/L). Variations in NH_4 concentrations are due to the transformation processes occurring in the aquifer. The groundwater samples were categorized based on the Na/K ratio into two classes. The first class shows the Na/K ratios vary from 2.52 to 12.19 for sewage effluent and contaminated samples, while in the second class they range from 12.85 to 31.60 for non-impacted samples. As a result, the Na/K ratio in combination with other chemical and microbiological indicators is a useful screening tool for assessing possible sewage influence on shallow groundwater from shallow wells.

Groundwater Monitoring and Remediation, 36 (2016) 62-70

Factors controlling groundwater hydrogeochemistry in the area west of Tahta, Sohag, Upper Egypt

Redwan, M. , Abdel Moneim, A. A.
Geology Department, Faculty of Science, Sohag University, Sohag, Egypt

Groundwater quality suffers from various degradation mechanisms such as extensive urbanization, agricultural and industrial activities in many developing countries. This study was carried out to identify the factors responsible for the change in the hydrogeochemistry of groundwater in the area west of Tahta, Sohag, Upper Egypt. The Piper diagrams show the predominance of Na–Cl (75%) with minor Ca–Na–HCO_3 and Ca–Cl water-types. The equiline diagrams and ionic ratios show the dominance of $Ca^{2+} + Mg^{2+}$ over $Na^+ + K^+$ and $HCO_3^- + SO_4^{2-}$ over Cl^- suggesting silicate minerals dissolution and reverse ion exchange reactions Results of Gibb's diagram revealed that the chemical budget of the groundwater in this area is mainly derived from water–rock interaction and evaporation-crystallization dominances. The R-mode factor analysis applied to quantify the chemical characteristics of groundwater and the anthropogenic impacts that affect groundwater quality, revealed that the Pliocene clays are the major sources of Cl^- and Na^+ in the groundwater due to silicate minerals dissolution and ion exchange reactions and, Ca^{2+} and Mg^{2+} are mainly from dissolution of carbonates and silicate minerals abundant in the Pleistocene Qena Formation lithologies. Higher concentration of SO_4^{2-} at the newly reclaimed lands may be due to the effect of rainfall, addition of potassium sulfates fertilizers to the agricultural soils and gypsum-anhydrite dissolution. The results of this study suggest that the R-mode factor analysis combined with the geological–hydrogeological analyses of the aquifer is useful in recognizing the geochemical trends and identifying the anthropogenic sources affecting the groundwater quality.
Journal of African Earth Sciences, 118 (2016) 328-338

Landslide susceptibility maps using different probabilistic and bivariate statistical models and comparison of their performance at Wadi Itwad Basin, Asir Region, Saudi Arabia

Youssef, A.M.[b], Pourghasemi, H.R.[c], El-Haddad, B.A.[a], Dhahry, B.K.[b]
[a]*Geology Department, Sohag University, Sohag, Egypt*
[b]*Geological Hazards Department, Applied Geology Sector, Saudi Geological Survey, Saudi Arabia*
[c]*Department of Natural Resources and Environment, College of Agriculture, Shiraz University, Iran*

The purpose of the current study is to produce landslide susceptibility maps using different probabilistic and bivariate statistical approaches; namely, frequency ratio (FR), weights-of-evidence (WofE), index-of-entropy (IofE), and Dempster–Shafer (DS) models, at Wadi Itwad, Asir region, in the southwestern part of Saudi Arabia. Landslide locations were identified and mapped from interpretation of high-resolution satellite images, historical records, and extensive field surveys. In total, 326 landslide locations were mapped using ArcGIS and divided into two groups; 75 % and 25 % of landslide locations were used for training and validation of models, respectively. Twelve layers of landslide-related factors were prepared, including altitude, slope degree, slope length, topography wetness index, curvature, slope aspect, distance from lineaments, distance from roads, distance from streams, lithology, rainfall, and normalized difference vegetation index. The relationships between the landslide-related factors and the landslide inventory map were calculated using different statistical models (FR, WofE, IofE, and DS). The model results were verified with landslide locations, which were not used during the model training. In addition, receiver operating characteristic curves were applied, and area under the curve (AUC) was calculated for the different susceptibility maps using the success (training data) and prediction (validation data) rate curves. The results showed that the AUC for success rates are 0.813, 0.815, 0.800, and 0.777, while the prediction rates are 0.95, 0.952, 0.946, and 0.934 for FR, WofE, IofE, and DS models, respectively. Subsequently, landslide susceptibility maps were divided into five susceptibility classes, including very low, low, moderate, high, and very high. Additionally, the percentage of training and validating landslides locations in high and very high landslide susceptibility classes in each map were calculated. The results revealed that the FR, WofE, IofE, and DS models produced reasonable accuracy. The outcomes will be useful for future general planned development activities and environmental protection.
Bulletin of Engineering Geology and the Environment, 75 (2016) 63-87

Seasonal variation and enrichment of metals in sediments of Rosetta branch, Nile River, Egypt

Redwan M.[a], Elhaddad E.[b]
[a]*Geology Dept., Faculty of Science, Sohag University, Sohag, Egypt*
[b]*National Institute of Oceanography and Fisheries, Cairo, Egypt*

This study investigated heavy metal pollution in sediments of the Rosetta branch of the River Nile of Egypt to quantify the toxic distribution potential of metals into the surrounding environment. Sediment samples were collected at 9 sites during in four seasons. Organic matter and total metal concentrations were determined using loss on ignition and inductively coupled plasma spectrometry, respectively. Principal component analysis has been applied to evaluate the metal sources and the relationships between metals in sediments. Metal concentrations showed the following order: winter > autumn > spring > summer. Mean concentrations of Cu, Zn, Cd, and Pb in sediments were above the average background value of metals in shale. Pb and Cd showed higher enrichment during all seasons at stations N3/N4, Zn at stations N1 to N4, and Cu at stations N6/N8. The variations in heavy metal total concentration and organic matter are due to different input sources, physico-chemical conditions, and adsorption/precipitation/redox conditions in sediments. Mean values of Geo-accumulation index (Igeo) for Fe, Mn, and Cu were below 0 which were classified as unpolluted during spring, summer, and autumn, except Cu increased from unpolluted to moderately polluted during winter. Igeo values for Cd, Pb, and Zn increased from unpolluted–moderately polluted to highly–very highly polluted during autumn and winter. Pollution Load Index was recorded in highest values during winter, especially at Fuwwah/Basioun and in lowest values during summer at after the Edfina Barrage/before Kafer El-Zayat due to industrial/human activities. Both natural and anthropogenic sources contributed to the metal accumulations in sediments, and industrial, agricultural, and municipal sewage effluents discharged from non-point sources may be the main anthropogenic sources for metals in the Rosetta branch.
Environmental Monitoring and Assessment, 188 (2016) 1-12

Groundwater Management at West El-Minia Desert Area, Egypt Using Numerical Modeling

Ahmed A. Abdel Moneim[1], José Paulino Fernández-Álvarez[2], Elsayed M. Abu El Ella[3], Ahmed M. Masoud[1]
[1]*Geology Department, Faculty of Science, Sohag University, Sohag, Egypt*
[2]*Hydro-Geophysics and NDT Modeling Unit, Polytechnic School of Mieres, University of Oviedo, Mieres, Spain,* [3]*Geology Department, Faculty of Science, Assiut University, Assiut, Egypt*

Water shortage is the main problem facing any development in Egypt especially in the desert lands. River Nile is considered the main source of water in Egypt but its water covers only the area of flood plain where its tributaries do not reach to the desert. The desert fringes, west of El-Minia governorate, Egypt, are areas of natural expansion for agricultural, industrial, and civil activities. This implies an increasing demand for groundwater. A numerical groundwater model is one of the main tools used for assessment of the resource potential and prediction of future impact under different circumstances and stresses. In this paper, a transient groundwater flow model in the desert district west of El-Minia, Egypt, was developed. The conceptual model was built by analyzing the hydrogeological data and previous work. Steady state model of year 1990 was used to investigate and calibrate the parameters such as hydraulic conductivities, recharge and conductance of the surface water streams. The storage coefficients are calibrated by the transient model based on the available data observed from 1990 to 2013, which provides insights to understand the behavior of groundwater system in Quaternary Aquifer and to predict spatial-temporal distributions of groundwater levels and groundwater flow in responding to extraction of water. The calibrated transient model will be used to predict the impacts of desert development schemes and water resources management schemes on groundwater in the study area.
Journal of Geoscience and Environment Protection, 4 (2016) 66-76

Experimental study on the utilization of dune sands as a construction material in the area between Jeddah and Mecca, Western Saudi Arabia

Abu Seif E.-S. S.[ab], Sonbul A. R.[a], Hakami B. A. H.[a], El-Sawy E.K.[ac]
[a]*Faculty of Earth Sciences, King Abdulaziz University, Jeddah, Saudi Arabia*
[b]*Geology Department, Faculty of Science, Sohag University, P.O. Box 82524, Sohag, Egypt*
[c]*Geology Department, Faculty of Science, Al-Azhar University (Assiut Branch), Assiut, Egypt*

Due to the arid continental climatic conditions, about 37 % of Saudi Arabia is covered by desert sands. These sands are mostly dynamic and cause environmental problems. However, these huge quantities of dune sands are considered important natural resources of fine aggregate construction materials. The studied dune sands are predominantly coarse, medium and fine sands with average percentages of 2.4, 19.97 and 76.28 %, respectively, with scarce percents of silt and clay-size particles (around 1 %). The fineness modulus (FM) values of these sands vary from 0.98 to 1.02. Therefore, it is necessary to improve their gradation and textural characters by adding well-graded, crushed fine aggregates to produce an acceptable level of gradation. Mineralogically, the studied dune sands are mainly composed of quartz (88 %), feldspars (9 %) and a negligible amount of carbonates (2.2 %). The workability and compressive strength values of both cement mortar and concrete of the studied dune sands were found to decrease abruptly at dune sand contents >50 %. Finally, the studied dune sands are acceptable as fine aggregates for both concrete and mortar when they do not exceed 50 % of the total volume of fine aggregates at a constant mix ratio of 2:1:3 (water:cement:fine aggregates) and 1:2:4:6 (water:cement:fine aggregates: coarse aggregates), respectively, for cement mortar and concrete.

Bulletin of Engineering Geology and the Environment, 75 (2016) 1007-1022

Evaluation of geotechnical properties of Cretaceous sandstone, Western Desert, Egypt

Seif E.-S. S. A.[ab]
[a]*King Abdul Aziz University, Jeddah, Saudi Arabia*
[b]*Geology Department, Sohag University, P.O. Box. 82524, Sohag, Egypt*

The Western Desert, Egypt, mostly covered by clastic sedimentary rocks ranging in age from Lower Cretaceous to the Quaternary. Taref Formation of Nubian Group constitutes one of Cretaceous succession; it consists mainly of yellowish, pale red, pink, and white massive and cross-bedded sandstone in fining-upward cyclic manner. The petrographical parameters and mechanical properties of these clastic rocks must be integrated to better understand their geotechnical behavior. Mineralogically, it composes quartz, feldspars, and rock fragments, with an average value of 97.9, 1.2, and 0.9 %, respectively. Accordingly, Taref Sandstone can be classified as quartz arenite. The roundness of grains are dominated by sub-angular, sub-rounded, angular, rounded, very angular, and well rounded with an average value of 36, 25, 17, 9, 7, and 6 %. Its dry density (γd, g/cm^3) varies from 1.65 to 1.87 g/cm^3 that indicates Taref Sandstone classified as dense-very dense sandstone. Porosity (n%) ranges from 9.41 to 13.59 % that means that it ranges from medium to high porous sandstone. The dry uniaxial unconfined compressive strength (UCS_{dry}) and point load strength index (IS_{50}) values indicated that its compressive strength rages from moderately strength to very high strength and both of them are closely related. The porosity (n%) of Taref Sandstone has a significant correlation with mostly its physical and mechanical properties of the studied sandstone. Through matching correlation data among these parameters, it was clearly indicated that both porosity (n%) and dry density (γd) had been considered as the major parameters influencing other physical and mechanical properties of the studied Cretaceous sandstone samples.

Arabian Journal of Geosciences, 9 (2016) 9:299

Geochemistry and spatial distribution of selected heavy metals in surface soil of Sohag, Egypt: a multivariate statistical and GIS approach

Ali M. H.[a], Mustafa A.-R. A.[b], El-Sheikh A. A.[a]
[a]*Geology Department, Faculty of Science, Sohag University, Sohag, Egypt*
[b]*Soil and Water Department, Faculty of Agriculture, Sohag University, Sohag, Egypt*

In this study, selected heavy metals were estimated in surface soil samples of Sohag, Egypt, with the aim to characterize their accumulation patterns. Median concentrations of Cd, Co, Cr, Cu, Fe, Mn, Ni, Pb and Zn were 0.89, 39, 162, 74, 72,000, 1434, 72, 25 and 164 μg g^{-1}, respectively. The higher average concentrations of these HMs compared with corresponding concentrations in average shale suggesting their anthropogenic inputs. Application of principal component analysis and cluster analysis successfully grouped the investigated HMs according to their anthropogenic or geogenic origin. The uncontrolled excessive application of agrochemical products, wastewater irrigation, industrial and urbanization emissions are significant contributors for elevated concentrations of Cd, Cu, Zn, Cd and Pb in the agricultural surface soil, whereas Ni, Mn, Co and Fe amounts are controlled by parent material influences. Chromium was found to exhibit a mixed source in the study cultivated system. Geographical information system (GIS) techniques were used to illustrate the spatial distribution trends of the investigated elements. Integration of GIS mapping and multivariate statistical analysis identified locations affected by the major polluting sources responsible for HMs concentrations in the study area (i.e., hotspot areas). In addition, this study provides a reliable approach for HMs source apportionment in the area using APCS–MLR receptor model. The present work is important to document the status of HM pollution and offer baseline data for the future research in the study region

Environmental Earth Sciences, 75 (2016) 75:1257

Genesis and petrology of Late Neoproterozoic pegmatites and aplites associated with the taba metamorphic complex in southern Sinai, Egypt

Abdelfadil K. M.[a], Asimow P. D.[b], Azer M. K.[bc], Gahlan H. A.[de]
[a]*Geology Department, Sohag University, Sohag, Egypt*
[b]*Division of Geological & Planetary Sciences, California Institute of Technology, Pasadena, CA,US*
[c]*Geological Sciences Department, National Research Centre, 12622-Dokki, Cairo, Egypt*
[d]*Department of Geology and Geophysics, College of Science, King Saud University, Riyadh, SA*
[e]*Geology Department, Assiut University, Assiut, Egypt*

We present new field, petrographical, mineralogical and geochemical data from late Neoproterozoic pegmatites and aplites in southern Sinai, Egypt, at the northernmost limit of the Arabian-Nubian Shield. The pegmatites cross-cut host rocks in the Taba Metamorphic Complex (TMC) with sharp contacts and are divided into massive and zoned pegmatites. Massive pegmatites are the most common and form veins, dykes and masses of variable dimensions; strikes range mainly from E-W through NW-SE to N-S. Mineralogically, the massive pegmatites are divided into K-feldspar-rich and albite-rich groups. Zoned pegmatites occur as lenses of variable dimensions, featuring a quartz core, an intermediate zone rich in K-feldspars and an outer finer-grained zone rich in albite. All compositions are highly evolved and display geochemical characteristics of post-collisional A-type granites: high SiO_2, Na_2O+K_2O, FeO*/MgO, Ga/Al, Zr, Nb, Ga and Y alongside low CaO, MgO, Ba and Sr. They are rich in Rare Earth Elements (REE) and have extreme negative Eu anomalies (Eu/Eu*= 0.03-0.09). A genetic linkage between the pegmatites, aplites and alkali granite is confirmed by their common mild alkaline affinity and many other geochemical characteristics. These pegmatites and aplites represent the last small fraction of liquid remaining after extensive crystallization of granitic magma, injected along the foliation and into fractures of the host metamorphic rocks. The extensional tectonic regime and shallow depth of emplacement are consistent with a post-collisional environment.

Geologica Acta, 14 (2016) 219-235